

UNIVERSITÉ DU QUÉBEC À MONTRÉAL

SOIL-VEGETATION-ATMOSPHERE INTERACTION IN THE BOREAL  
FOREST ECOSYSTEM IN EASTERN CANADA

THESIS

PRESENTED

AS A PARTIAL REQUIREMENT OF

DOCTORATE IN SCIENCES DE L'ENVIRONNEMENT

BY

SHALINI OOGATHOO

FEBRUARY 2021

UNIVERSITÉ DU QUÉBEC À MONTRÉAL

INTERACTION SOL-VÉGÉTATION-ATMOSPHÈRE DANS L'ÉCOSYSTÈME  
DE LA FORÊT BORÉALE DE L'EST DU CANADA

THÈSE

PRÉSENTÉE

COMME EXIGENCE PARTIELLE

DOCTORAT EN SCIENCES DE L'ENVIRONNEMENT

PAR

SHALINI OOGATHOO

FÉVRIER 2021

UNIVERSITÉ DU QUÉBEC À MONTRÉAL  
Service des bibliothèques

Avertissement

La diffusion de cette thèse se fait dans le respect des droits de son auteur, qui a signé le formulaire *Autorisation de reproduire et de diffuser un travail de recherche de cycles supérieurs* (SDU-522 – Rév.10-2015). Cette autorisation stipule que «conformément à l'article 11 du Règlement no 8 des études de cycles supérieurs, [l'auteur] concède à l'Université du Québec à Montréal une licence non exclusive d'utilisation et de publication de la totalité ou d'une partie importante de [son] travail de recherche pour des fins pédagogiques et non commerciales. Plus précisément, [l'auteur] autorise l'Université du Québec à Montréal à reproduire, diffuser, prêter, distribuer ou vendre des copies de [son] travail de recherche à des fins non commerciales sur quelque support que ce soit, y compris l'Internet. Cette licence et cette autorisation n'entraînent pas une renonciation de [la] part [de l'auteur] à [ses] droits moraux ni à [ses] droits de propriété intellectuelle. Sauf entente contraire, [l'auteur] conserve la liberté de diffuser et de commercialiser ou non ce travail dont [il] possède un exemplaire.»

## REMERCIEMENTS

Je tiens à débiter ma thèse en remerciant les personnes qui m'ont soutenu pendant toute la durée de mon doctorat. Je souhaite d'abord remercier grandement mon directeur Daniel Houle, qui m'a donné l'opportunité de faire ce doctorat, pour sa supervision continue, et aussi pour son expertise, sa présence et disponibilité et de répondre à toutes mes questions et doutes pendant toute la durée de mon doctorat. J'aimerais aussi remercier grandement mon co-directeur, Daniel Kneeshaw, pour son expertise, ses conseils et ses questions qui me poussent à réfléchir au delà. J'aimerais aussi ajouter la gentillesse, la générosité et l'encouragement continu de mes deux directeurs m'ont aidé beaucoup à terminer ce doctorat.

Un grand remerciement à Louis Duchesne, qui m'a fourni toutes les données et informations pertinentes utilisées dans mon projet de doctorat, et aussi pour ses conseils sur les analyses statistiques et le logiciel R, et pour les révisions de mes trois chapitres. J'aimerais aussi remercier Richard Harvey pour ces conseils sur l'utilisation de CLASS et à Travis Logan pour son aide sur l'extraction des données au début de mon doctorat. Un remerciement au personnel d' Ouranos (Mourad et Romy) pour leur aide technique et à Marco Alves pour ses conseils sur CLASS et le logiciel R au début de mon doctorat. Un remerciement également à Christine Guillerme pour son aide au niveau administratif à UQAM. J'aimerais aussi remercier mon amie Stéphanie Gladu et tous les amis dans le labo de Daniel Kneeshaw qui m'ont soutenu pendant mes dernières années de doctorat. Finalement, un grand remerciement à ma fille Mishti pour sa patience pendant toute la durée de mon doctorat.

## AVANT-PROPOS

La présente recherche fait partie d'une plus grande question de recherche sur la sécheresse dans la forêt boréale, conçu par Dr Daniel Houle (Professeur associé à UQAM) et Dr Daniel Kneeshaw (Professeur à UQAM) et financé par le MFFP, Ouranos et MITACS. De fait, la problématique est de mieux comprendre le lien entre le contenu en eau et la transpiration durant la saison de croissance et des épisodes de sécheresse dans des peuplements forestiers boréaux situés dans la province du Québec, au Canada.

Cette thèse de doctorat est formée de cinq chapitres rédigés en anglais (trois sous forme d'articles scientifiques) sur l'interaction du sol-végétation-atmosphère dans la forêt boréale. Ces trois articles sont mes contributions originales pour ma thèse de doctorat en sciences de l'environnement à Université du Québec à Montréal.

Chapitre I et V sont l'introduction générale et la conclusion générale de ma thèse, respectivement. Les chapitres II, III et IV sont les trois articles suivants.

Le premier article est intitulé: « PERFORMANCE EVALUATION AND SENSITIVITY ANALYSES USING THE CANADIAN LAND SURFACE SCHEME (CLASS) FOR THE SIMULATION OF SOIL TEMPERATURE AND SOIL WATER IN THE BOREAL FOREST OF EASTERN CANADA ». Les coauteurs sont Daniel Houle, Louis Duchesne, et Daniel Kneeshaw. Cet article sera soumis sous peu à la revue *Journal of Hydrology*.

Le deuxième article est intitulé : « VAPOUR PRESSURE DEFICIT AND SOLAR RADIATION ARE THE MAJOR DRIVERS OF TRANSPIRATION OF BALSAM FIR AND BLACK SPRUCE TREE SPECIES IN HUMID BOREAL REGIONS, EVEN DURING A SHORT-TERM DROUGHT ». Les coauteurs sont Daniel Houle, Louis Duchesne et Daniel Kneeshaw. Cet article est publié dans la revue *Agricultural and Forest Meteorology*.

Le troisième article est intitulé : « TREE TRANSPIRATION WELL SIMULATED BY THE CANADIAN LAND SURFACE SCHEME (CLASS) BUT NOT DURING DROUGHT ». Les coauteurs sont Daniel Houle, Louis Duchesne, et Daniel Kneeshaw. Cet article est soumis à la revue *Journal of Hydrology*.

Daniel Houle, Daniel Kneeshaw et moi-même avons conçu les projets de même que leurs approches méthodologiques. Louis Duchesne a collaboré à la collection de toutes les données de mesure et des informations pertinentes sur les deux sites d'étude. J'ai fait toutes les simulations avec le modèle CLASS et toutes les analyses statistiques. J'ai aussi rédigé les trois articles, l'introduction générale et la conclusion générale. Pendant toute la durée de mon doctorat, Louis Duchesne a fourni des informations pour combler des manquements pour simuler le modèle et les analyses statistiques. Il m'avait aussi conseillé sur l'utilisation de certaines applications d'analyse sur le logiciel R. Richard Harvey m'a aussi conseillé plusieurs fois sur le modèle CLASS, sur le fonctionnement et la limitation du modèle. De plus, mes directeurs, Daniel Houle et Daniel Kneeshaw, ont commenté et suggéré plusieurs fois sur le contenu de ma thèse pour l'améliorer. Ils ont aussi corrigé les trois articles et la thèse en générale.

## TABLE DES MATIÈRES

AVANT-PROPOS .....	iv
LISTE DES FIGURES.....	x
LISTE DES TABLEAUX.....	xvi
RÉSUMÉ .....	xviii
ABSTRACT .....	xx
CHAPITRE I GENERAL INTRODUCTION .....	1
1.1 Trees in boreal forest ecosystems .....	1
1.1.1 Annual cycle of stem diameter variation .....	3
1.2 Soil temperature and soil water .....	5
1.3 Transpiration.....	6
1.3.1 Environmental control on transpiration .....	7
1.3.2 Plant physiological control on transpiration .....	8
1.3.3 Measurement of transpiration via sap flow techniques.....	8
1.4 Representation of land surface processes in land surface schemes .....	11
1.4.1 Land surface processes.....	11
1.4.2 Land surface schemes .....	12
1.4.3 Impact of land surface processes in Land Surface Schemes on climate models .....	14
1.5 Objectives of the study .....	16
1.6 Study area – Laflamme and Tirassee.....	17
1.7 References.....	18
CHAPITRE II Performance evaluation and sensitivity analyses using the Canadian Land Surface Scheme (CLASS) for the simulation of soil temperature and soil water in the boreal forest of eastern Canada .....	26

2.1	Résumé .....	27
2.2	Abstract.....	28
2.3	Introduction.....	29
2.4	Methods .....	33
2.4.1	Description of study areas.....	33
2.4.2	Measured data .....	33
2.4.3	Canadian Land Surface Scheme (CLASS) .....	34
2.4.4	Analyses .....	37
2.5	Results .....	41
2.5.1	Soil temperature .....	41
2.5.2	Soil water .....	43
2.5.3	Sensitivity analysis.....	45
2.6	Discussion.....	52
2.6.1	Soil temperature .....	52
2.6.2	Soil water .....	54
2.7	Conclusion.....	56
2.8	Acknowledgements.....	58
2.9	References.....	58
2.10	Supplementary materials .....	64
	<b>CHAPITRE III VAPOUR PRESSURE DEFICIT AND SOLAR RADIATION ARE THE MAJOR DRIVERS OF TRANSPIRATION OF BALSAM FIR AND BLACK SPRUCE TREE SPECIES IN HUMID BOREAL REGIONS, EVEN DURING A SHORT-TERM DROUGHT.....</b>	<b>72</b>
3.1	Résumé .....	73
3.2	Abstract.....	74
3.3	Introduction.....	75
3.4	Materials and methods.....	77
3.4.1	Site description.....	77
3.4.2	Meteorological and soil measurements.....	78
3.4.3	Sap flow & dendrometric data .....	79
3.4.4	Analyses .....	81
3.5	Results .....	84

3.5.1	Impact of environmental variables on sap flow during the growing season	84
3.5.2	Impact of an extreme drought on sap flow in the summer 2012 at the balsam fir site	89
3.6	Discussion	92
3.6.1	Control of sap flow during the growing season	92
3.6.2	The analysis of the 2012 summer drought at the balsam fir site	95
3.7	Conclusion	97
3.8	Acknowledgements	98
3.9	References	98
3.10	Supplementary materials	104
	CHAPITRE IV TREE TRANSPIRATION WELL SIMULATED BY THE CANADIAN LAND SURFACE SCHEME (CLASS) BUT NOT DURING DROUGHT	112
4.1	Résumé	113
4.2	Abstract	114
4.3	Introduction	114
4.4	Materials & methods	118
4.4.1	Description of study area	118
4.4.2	Measured data	118
4.4.3	Canadian Land Surface Scheme (CLASS)	120
4.4.4	Analyses	124
4.5	Results and discussion	125
4.5.1	Transpiration during the rehydration period (prior to growing season)	125
4.5.2	Transpiration during the growing season	128
4.5.3	Transpiration during observed and simulated drought at the balsam fir site	132
4.6	Conclusion	137
4.7	Acknowledgements	137
4.8	References	138
4.9	Supplementary materials	144
	CHAPITRE V GENERAL CONCLUSION	149

5.1	Summary of findings .....	149
5.1.1	Performance and sensitivity analyses of CLASS for the simulation of soil water and soil temperature .....	150
5.1.2	Environmental drivers of transpiration in humid boreal region during growing season and a drought period .....	151
5.1.3	Performance of CLASS for the simulation of transpiration during the rehydration period, the growing season and a drought .....	152
5.2	Limitations and future works.....	154
5.2.1	Field measurement limitations .....	154
5.2.2	Shortcomings of CLASS.....	156
5.3	Concluding remarks.....	157
5.4	References.....	158
	APPENDIX A .....	161
	BIBLIOGRAPHY .....	165

## LISTE DES FIGURES

Figure	Page
1.1 Major forest ecozones across Canada.....	1
1.2 Phenology of stem diameter variation of boreal trees over three years with shrinkage, rehydration and growth illustrated for one of those years.....	3
1.3 Cross sectional views of wood composition .....	4
1.4 Three main sap flow techniques: thermal dissipation (TD); heat field deformation (HFD); and heat pulse velocity (HPV).....	10
1.5 Schematic diagram of CLASS.....	15
1.6 Location of the two study areas (red squares) in the Quebec province, Canada .....	17
2.1 Observations of daily soil water at the three soil profiles (SP1 to SP3) at the black spruce (a) and four soil profiles (SP1 to SP4) in the B and C horizons at the balsam fir (b) sites.....	39
2.2 Observed and simulated daily soil temperature (°C) for the humus layer (top), horizon B (middle) and C (bottom) at the black spruce (observed Ts is mean of 3 soil profiles; a) and balsam fir (observed Ts is mean of 4 soil profiles; b) sites from 2001 to 2016.....	42
2.3 Performance metrics of Kling-Gupta Efficiency (KGE), Pearson's correlation (r), and root mean square error (RMSE) at the black spruce (a) and balsam fir (b) sites for soil temperature for the three soil horizons (Hum, HorB and Horc) for the entire year .....	43

2.4	Observed and simulated daily soil water (%) for horizons B (top) and C (bottom) at the black spruce (a) and balsam fir (b) sites from 2001 to 2016. .....	44
2.5	Performance metrics of Kling-Gupta Efficiency (KGE), Pearson's correlation (r), and root mean square error (RMSE) at black spruce (a) and balsam fir (b) sites for soil liquid water for the two soil horizons (HorB and Horc) for an entire year (Year), winter/spring (DJFMAM) and summer (JJAS) periods.....	45
2.6	Sensitivity analysis of the thickness of the organic layer (TOL; left panel) and of % of sand and % of clay (PSPC; right panel) on multiyear (2001 to 2016) average daily soil temperature (top) and soil liquid water (bottom) at the balsam fir (BF) site. ....	48
2.7	Sensitivity analysis of the drainage parameter (DP; left panel) and of freezing point (FP; right panel) for multiyear (2001 to 2016) average daily soil temperature (top) and soil liquid water (bottom) at the balsam fir site. ....	49
2.8	Taylor diagrams of observations vs simulations of all sensitivity analyses for soil temperature (Ts; left) and soil liquid water ( $\theta$ ; right) for the three soil horizons (Hum, HorB and HorC) at the balsam fir site. ....	50
2.9	Taylor diagrams of observations vs simulations of all sensitivity analyses for soil liquid water ( $\theta$ ) during winter (DJFMAM; left) and summer months (JJAS; right) for the three soil horizons (Hum, HorB and HorC) at the balsam fir site.....	51
2S.1	Observed and simulated daily snow depth (m) at black spruce (a) and balsam fir (b) sites from 2001 to 2016.....	64
2S.2	Sensitivity analysis of thickness of organic matter (TOL; left panel) and of % sand and % clay (PSPC; right panel) on multiyear (2001 to 2016) average daily soil temperature ( $^{\circ}\text{C}$ ; top) and soil liquid water (%; bottom) at black spruce (BS) site. ....	65
2S.3	Sensitivity analysis of drainage parameter (DP; left panel) and of freezing point (FP; right panel) on multiyear (2001 to 2016) average daily soil temperature ( $^{\circ}\text{C}$ ; top) and soil liquid water (%; bottom) at black spruce (BS) site. ....	66

2S.4	Taylor diagrams of observations vs simulations of all sensitivity analyses for soil temperature ( $T_s$ ; left) and soil liquid water ( $\theta$ ; right) for the three soil horizons (Hum, HorB and HorC) at the black spruce site. ....	67
2S.5	Taylor diagrams of observations vs simulations of all sensitivity analyses for soil liquid water ( $\theta$ ) during winter (DJFMAM; left) and summer (JJAS; right) months for the three soil horizons (Hum, HorB and HorC) at the black spruce site.....	68
2S.6	Multiyear (2001 to 2016) average daily soil heat fluxes ( $W\ m^{-2}$ ) entering (positive) & leaving (negative) by thickness of organic layer (TOL; top left), drainage parameter (DP; top right), and freezing point (FP; bottom left) sensitivity analyses at the balsam fir (BF) site; multiyear (2001 to 2016) average daily energy used to melt ice ( $W\ m^{-2}$ ) in snow and soil layers for freezing point sensitivity analysis at the balsam fir (bottom right).....	69
2S.7	Multiyear (2001 to 2016) average frozen soil water (%) by thickness of organic layer (TOL) and freezing point (FP) sensitivity analyses at the balsam (BF) fir site (top and bottom left) and black spruce site (top and bottom right); multiyear (2001 to 2016) average daily snow depth (m) for freezing point sensitivity analysis at balsam fir (middle left) and black spruce (middle right) sites .....	71
3.1	Daily soil water content from 1 <sup>st</sup> May (Julian day 122) to 31 <sup>st</sup> October (Julian day 305) in soil horizons B ( $\theta_{HorB}$ ) and C ( $\theta_{HorC}$ ) at the balsam fir site for the year 2012 (red) and for the average of years 1999 to 2016 (excluding 2012).....	83
3.2	An example of sap flow velocity ( $cm\ h^{-1}$ ; mean of the sun-side and shade-side of each tree) for balsam fir (BF1, BF2 and BF3; top left) and black spruce (BS1, BS2 and BS3; bottom left) together with vapour pressure deficit (VPD, Pa) and solar radiation (Rad, $W\ m^{-2}$ ) for one week in June (peak transpiration period) 2007; hourly mean sap flow velocity (average of the six probes) and hourly mean solar radiation for one-week in June 2007 and one-week in August 2007 for balsam fir (BF; top right) and black spruce (BS; bottom right) .....	85
3.3	Coefficient of determination ( $R^2$ ) between daily sap flow and each environmental variable of the three sample trees at both balsam fir (left) and black spruce (right) site for each studied year. ....	86

3.4	Example of the relationship between daily sap flow (cm/d) and vapour pressure deficit (VPD; kPa) for each probe (sun and shade sides) for balsam fir (BF1 to BF3) and black spruce trees (BS1 to BS3) for the year 2007 using the Gompertz (3 parameters) equation.....	87
3.5	Example of the relationship between daily sap flow (cm/d) and solar radiation (Rad; $W\ m^{-2}$ ) for each probe (sun and shade sides) for balsam fir (BF1 to BF3) and black spruce (BS1 to BS3) for the year 2007 using the sigmoidal (3 parameters) equation.....	88
3.6	Typical hysteresis loop of standardized sap flow velocity ( $SF_{NORM}$ ) data with standardized VPD and Rad on an hourly basis for 2007 for the period from the beginning of the growing season to the end of August.....	89
3.7	Daily sap flow (SF, cm) with stem diameter variation (SDV, mm) for the three balsam fir trees during the growing season (May-Sep) over a year (2012), together with variations in vapour pressure deficit (VPD, kPa), minimum and maximum air temperature ( $T_{min}$ and $T_{max}$ , °C), soil water content (SWC, %) in the B horizon and precipitation (PCP, mm).....	90
3.8	Moving average (15-day) of coefficient of determination ( $R^2$ ; average of the six probes) for the regression between daily sap flow and the main environmental variables (VPD, Rad and SWC) for balsam fir during and one week prior to and after the drought (1 <sup>st</sup> Jul to 4 <sup>th</sup> Aug 2012; highlighted in grey).....	91
3S.1	Total monthly precipitation and its anomalies from 2001 to 2016 (top panel) and daily soil moisture anomalies during growing season (Jun to Aug) from 1999 to 2016 (bottom panel) at the balsam fir site .....	108
3S.2	Diel hysteresis of standardized sap flow velocity ( $SF_{NORM}$ ) with standardized VPD from 2001 to 2013 (excluding 2007 which is shown in the main text) for balsam fir for the period from the beginning of the growing season to the end of August at the balsam fir site. ....	109
3S.3	Diel hysteresis of standardized sap flow velocity ( $SF_{NORM}$ ) with standardized Rad from 2001 to 2013 (excluding 2007 which is shown in the main text) for the period from the beginning of the growing season to the end of August at the balsam fir site.. ....	110

3S.4	Diel hysteresis of standardized sap flow velocity ( $SF_{NORM}$ ) with standardized VPD (top panel) and Rad (bottom panel) from 2006 to 2009 (excluding 2007 which is shown in the main text) for the period from the beginning of the growing season to the end of August at the black spruce site.....	111
4.1	Simulated and observed air temperature within canopy ( $T_{ac}$ - °C; top panel); simulated and observed snow depth (m; 2 <sup>nd</sup> panel); standardized modeled transpiration and standardized observed sapflow velocity (mean $\pm$ 1 SE [grey zone] of three trees; 3 <sup>rd</sup> panel); simulated (liquid and ice) and observed (mean of four pedons) soil water content in the B horizon (%; 4 <sup>th</sup> panel); and simulated and observed (mean of four pedons) soil temperature in the B horizon (°C; bottom panel) at the balsam fir site in 2004 (a) and 2010 (b).....	126
4.2	Simulated and observed snow depth (m) from 2004 to 2013 at the balsam fir site (top) and from 2006 to 2009 at the black spruce site (bottom) .....	128
4.3	Daily standardized modeled transpiration [unitless] and standardized sap flow velocity [-; mean $\pm$ 1 SE (grey zone) of six probes] at the black spruce (a) and balsam fir sites (b) in 2007.. .....	130
4.4	Simple linear regression of standardized modeled transpiration ( $Tr_{SIM\_NORM}$ ) vs standardized observed sap flow velocity ( $SF_{OBS\_NORM}$ , mean of three trees) during the growing period at black spruce (a; 2006 to 2009) and balsam fir (b; 2004 to 2013) sites.. .....	131
4.5	Vapour pressure deficit (VPD, kPa; top panel); standardized modeled transpiration (Sim) and standardized observed sap flow velocity (Obs, mean of six probes; 2 <sup>nd</sup> panel); observed soil water content (%) in the B and C Horizons and precipitation (mm, PCP; 3 <sup>rd</sup> panel); 15-day moving average of regression coefficients between simulated and observed data ( $R^2$ ; bottom panel) at the balsam fir site during the drought (grey shaded area) of 2012 .....	134
4.6	Simulated ice (top panel) and liquid (middle panel) soil water content for the three soil layers (Hum, HorB, HorC) and simulated transpiration (bottom panel) for the first hydrological year of the forced zero-precipitation simulation.. .....	135

4S.1	Daily standardized modeled transpiration [-] and daily standardized sapflow velocity [-; mean $\pm$ 1 SE (grey zone) of six probes] at the balsam fir site from 2004 to 2013 (excluding 2007).....	146
4S.2	Daily standardized modeled transpiration [-] and daily standardized sapflow velocity [-; mean $\pm$ 1 SE (grey zone) of six probes] at the black spruce site .....	147
4S.3	Simulated and observed air temperature within canopy (T <sub>ac</sub> -°C; 1 <sup>st</sup> panel); simulated and observed snow depth (m; 2 <sup>nd</sup> panel); standardized modeled transpiration and standardized observed sapflow velocity (mean of six probes; 3 <sup>rd</sup> panel); simulated (liquid and ice) and observed soil water content in the B horizon (%; 4 <sup>th</sup> panel); and simulated and observed soil temperature in the B horizon (°C; bottom panel) at balsam fir in 2007. ....	148

## LISTE DES TABLEAUX

Tableau	Page
1.1 Climate and main tree species in the boreal forest ecozones of Canada .....	2
2.1 Initialisation parameters used in CLASS.....	37
2.2 Summary of sensitivity analyses carried out at the balsam fir and black spruce sites.....	40
3.1 Description of forest stand characteristics for trees with a DBH > 9.1 cm and the three instrumented trees at the two sites .....	79
3S.1 Description of soil characteristics at the two sites.....	104
3S.2 Regression coefficients of sap flow (daily and half-hourly) between the sun-side and the shade side of the same tree and between trees from the beginning of the growing season to the end of August for each year at the balsam fir site.....	105
3S.3 Regression coefficients of sap flow (daily and half-hourly) between sun-side and shade side of the same tree and between trees from the beginning of the growing season to the end of August for each year at the black spruce site.....	106
3S.4 Mean seasonal regression coefficients (direction of correlation: positive or negative) between daily sap flow and environmental variables for the six probes at the balsam fir and black spruce sites.....	107
3S.5 Characterization of average seasonal radial growth patterns for balsam fir and black spruce for their respective years.....	108

4.1	Initialisation parameters used in the model .....	123
4.2	Regression coefficients ( $R^2$ ) and slopes (b) of the simple linear regressions, Euclidean Distances (ED) and Dynamic Time Warping (DTW) between standardized transpiration and standardized sap flow velocity for multiple years during the rehydration period of balsam fir and black spruce.....	127
4.3	Regression coefficients ( $R^2$ ) and slopes (b) of the simple linear regressions, Euclidean Distances (ED) and Dynamic Time Warping (DTW) between standardized transpiration and standardized sap flow velocity for multiple years during the period without snow from the beginning of the growing season to the end of August of balsam fir and black spruce.....	132

## RÉSUMÉ

L'augmentation de la température de l'air et de l'occurrence des épisodes de sécheresses dans les dernières décennies à travers le monde ont stimulé la recherche sur les processus de surface, leurs interactions avec l'atmosphère, et aussi leurs effets sur les projections climatiques dans le futur. La transpiration est un processus important et la seule composante du cycle hydrologique qui relie les compartiments sols, végétation et atmosphère, les plantes relâchant dans l'atmosphère l'eau extrait du sol. La fiabilité des projections futures de la précipitation et de la température de l'air par les modèles climatiques dépendent de la précision et de l'exactitude de la modélisation de la transpiration par les schémas de surface intégrés à l'intérieur de ces modèles climatiques. Outre les variables climatiques (déficit de pression de vapeur, radiation solaire, température de l'air et vitesse du vent), les variables de la surface terrestre (e.g. contenu en eau et température du sol) ont aussi un effet important sur la transpiration. Tandis que le contenu en eau a un effet direct, la température du sol a un effet indirect à travers son influence sur le contenu en eau liquide du sol, et ceci particulièrement pour la forêt boréale. L'objectif général de ce projet est d'améliorer la compréhension du processus transpiration et des variables sous-jacentes dans un système naturel et à l'intérieur du schéma de surface Canadien (CLASS). L'étude a porté sur deux forêts boréales de l'est du Canada dominée par le sapin baumier et l'épinette noire. Premièrement, les simulations des variables sous-jacentes produites par CLASS, tel que le contenu en eau et la température du sol, ont été étudiées et validé par des mesures in situ à long terme. De plus, des analyses de sensibilité ont été aussi faites pour déterminer la sensibilité du modèle à des paramètres reliés au contenu en eau. Deuxièmement, le contrôle environnemental de la transpiration a été évalué pendant plusieurs saison de croissance ainsi que pendant un épisode de sécheresse dans un milieu naturel, en utilisant le flux de sève mesuré pendant plusieurs saisons de croissance. Troisièmement, le processus de la transpiration a été étudié dans le schéma de surface Canadien et validé avec ces mesures de flux de sève à long terme.

Les résultats montrent que CLASS simule très bien la température du sol et plus ou moins bien le contenu en eau, la qualité des simulations variant selon le site, la saison et l'horizon du sol. Le contenu en eau est grandement sous-estimé pendant l'hiver dans les deux sites malgré que CLASS simule bien les variations saisonnières. Les analyses de sensibilités montrent que l'épaisseur de la couche organique, le pourcentage de sable et d'argile, le drainage et le point de congélation ont eu des effets importants sur le contenu eau. Ceci démontre que ces paramètres sont importants dans le modèle, et

illustre l'importance de leur fidèle représentation dans le modèle pour obtenir des simulations fiables des variables d'étude et des processus qui contrôlent ces variables. L'évaluation du contrôle environnemental de la transpiration dans le système naturel montre que le déficit de pression de vapeur et la radiation solaire sont fortement corrélés aux variations quotidiennes de la transpiration pendant toutes les saisons de croissances étudiées et également pendant l'épisode de sécheresse Juillet 2012 comparé aux autres variables environnementales (température de l'air maximale, précipitation, contenu en eau, température de l'air minimale et vitesse du vent). CLASS simule adéquatement la transpiration pendant toute la période de croissance pour toutes les années d'études, sauf pendant la période de réhydratation (avant le début de croissance), le coup de chaleur et la sécheresse. Pendant la période de réhydratation, CLASS sous-estimait la transpiration, dû à la surestimation de durée de la présence de neige sur le sol dans le modèle. Durant le coup de chaleur et la sécheresse, CLASS surestimait la transpiration, malgré l'augmentation de la température de l'air et la baisse de contenu en eau dans le modèle, respectivement. Ceci montre que le modèle est insensible à la baisse du contenu en eau du sol, et également incapable de reproduire le comportement éco-physiologique des arbres lors d'épisodes climatiques extrêmes. La surestimation de la transpiration dans CLASS, malgré le stress hydrique, mènera à une surestimation de la précipitation par le modèle climatique. Ainsi, dans l'avenir, le modèle régional climatique Canadien (MRCC) aura tendance à sous-estimer le nombre de sécheresses intenses. Cette étude montre que CLASS a des failles importantes au niveau de la représentation du contenu en eau et aussi de la transpiration dans des circonstances particulières. La transpiration et le contenu en eau dans le modèle doivent être améliorés pour augmenter la qualité des projections climatiques, car ils ont des rétroactions directes sur l'atmosphère. Dans cette étude, plusieurs recommandations ont été faites à cet égard.

Mots-clés : contenu en eau, température du sol, transpiration, flux de sève, CLASS, sapin baumier, épinette noire, sécheresse, forêt boréale.

## ABSTRACT

Rising air temperature and the increasing occurrence of drought in the past few decades across the globe have led to an increasing interest in investigating land surface processes, their interactions with the atmosphere, and their impacts on future climate projections. Transpiration is an important land surface process and the only component in the hydrological cycle that links soil-vegetation-atmosphere, via the transport of water from the soil, through the plant, to the atmosphere. Accurate projection of future precipitation and air temperature by climate models depends on the accurate simulation of transpiration by land surface schemes integrated within climate models. In addition to climatic variables (vapour pressure deficit, solar radiation, air temperature, and wind speed), land surface variables (soil water and soil temperature) also have an important impact on transpiration. Soil water has a direct impact while soil temperature has an indirect impact on transpiration through its impact on liquid soil water, particularly in the boreal region. The general objective of this PhD research project is to improve the understanding of the transpiration process and the driving factors in a natural system and in a model: the Canadian Land Surface Scheme (CLASS). This study focused on two boreal forests in eastern Canada, the first dominated by balsam fir and the second by black spruce. First, the simulation of the underlying variables of transpiration, such as soil water content and soil temperature, were studied and validated using long-term *in-situ* measurements. In addition, sensitivity analyses were also performed to determine the model's sensitivity to parameters related to soil water content. Secondly, the environmental control on transpiration was evaluated in a natural system over multiple growing seasons as well as during a drought period, using long-term sap flow measurements. Third, the transpiration process was validated within CLASS, using these same long-term sap flow measurements.

The results showed that CLASS simulated well soil temperature, while the performance of soil water varied with site, season and soil horizon. Despite CLASS greatly underestimating soil water during winter at both sites, the seasonal variation of simulated soil water corresponded well with observations. The sensitivity analyses showed that thickness of organic layer, percentage of sand and percentage of clay, drainage parameter, and freezing point had substantial impacts on soil water. This shows that these parameters are important in the model and their accurate representation in CLASS is crucial in order to obtain reliable simulations of studied variables and linked processes. The evaluation of environmental control on transpiration in the natural system showed that vapour pressure deficit and solar

radiation were the main drivers of transpiration on a daily basis, throughout all growing seasons as well as during the July 2012 drought compared to other environmental variables (maximum air temperature, precipitation, soil water content, minimum air temperature and wind speed). Transpiration was adequately simulated by CLASS during all growing seasons, except during the rehydration period (prior to the growing season), and during heat stress and drought conditions. For the rehydration period, CLASS underestimated transpiration due to overestimating the duration of snow cover on the ground. For heat stress and drought conditions, CLASS overestimated transpiration, despite the increase in air temperature and the decrease in soil water content in the model. This shows the model's insensitivity to the decrease in soil water content as well as its inability to reproduce the eco-physiological behaviour of trees during extreme climatic events. The overestimation of transpiration in CLASS, despite water stress, will result in an overestimation of precipitation by the coupled climate model. Hence, in the future, the Canadian Regional Climate Model (CRCM) will tend to underestimate the frequency of intense drought events. This study showed that CLASS is significantly limited by its representation of soil water content and transpiration in specific conditions. Both transpiration and soil water need to be improved in the model in order to increase the accuracy of climate projections, as they have a direct feedback to the atmosphere. In this study, several recommendations were made in this regard.

Keywords : soil water, soil temperature, transpiration, sap flow, CLASS, balsam fir, black spruce, drought, boreal forest.

## CHAPITRE I

### GENERAL INTRODUCTION

#### 1.1 Trees in boreal forest ecosystems

While more than 100 tree species are found across different ecozones in the Canadian forest, boreal tree species are much less numerous and are located in the taiga plains, boreal cordillera, boreal plains and boreal shield forest ecozones (Johnston, 2009; Figure 1.1). The boreal forest ecozones are composed mostly of white and black spruce, balsam fir and trembling aspen (Table 1.1).

For my PhD research project, black spruce and balsam fir were the tree species studied as they are the two most important commercial species in the region. These are located in the boreal shield forest ecozone, which comprises mostly closed-canopy conifer stands. In general, the boreal ecozones have acidic soils caused by the accumulation of lignin-rich needles in the soil (Tyrrell, 2020) and undergo frequent forest fires and insect outbreaks such as spruce budworm. In addition, unlike other forest ecosystems where there is only expansion of stem diameter annually (except during drought, Sánchez-Costa et al., 2015), boreal trees have a unique annual stem diameter variation based on their climate (cold and long winters and short summers). Trees growing in boreal climate exhibit shrinkage in stem diameter during winter, followed by expansion of stem diameter in the spring (returning to the stem diameter attained the previous year) and further stem expansion during summer.

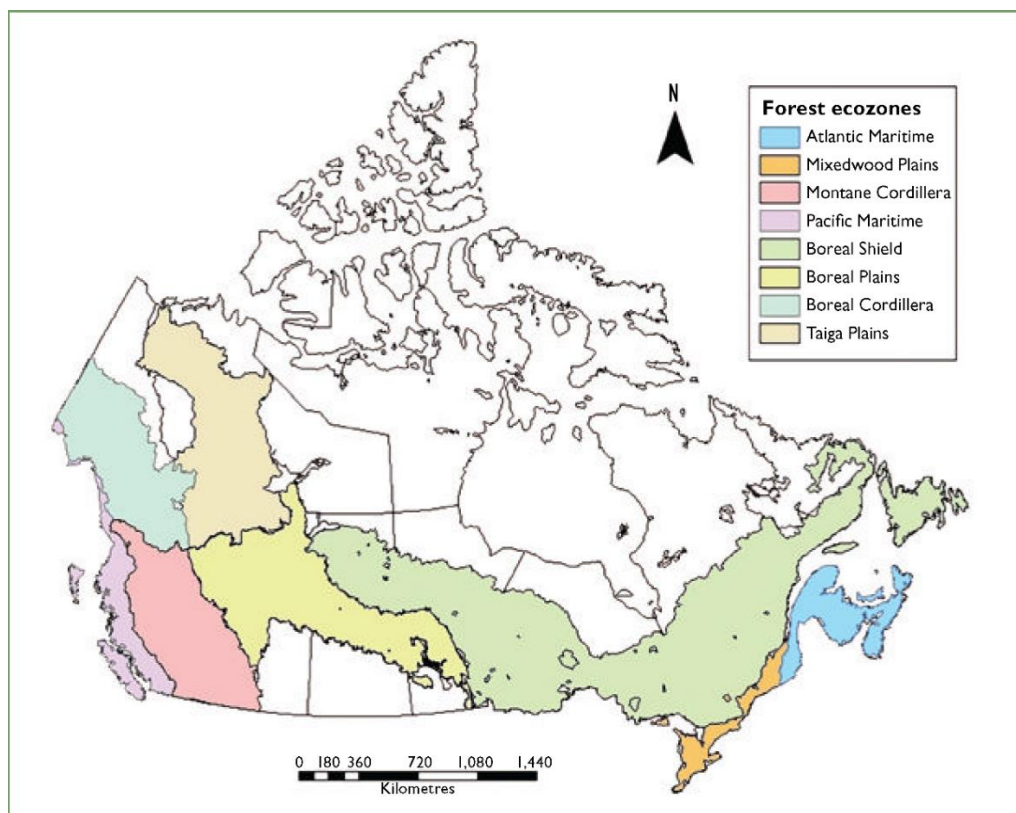


Figure 1.1: Major forest eozones across Canada (Johnston, 2009)

Table 1.1: Climate and main tree species in the boreal forest eozones of Canada (Johnston, 2009)

Forest eozone	Climate	Tree species
Taiga plains	Short and cool summers, long and cold winters	White and black spruce, balsam poplar
Boreal Cordillera		White and black spruce, sub-alpine fir, lodgepole pine, trembling aspen, balsam poplar, white birch
Boreal shields	Short and warm summers, long and cold winters	White and black spruce, balsam fir, tamarack, white birch, trembling aspen, balsam poplar, eastern white cedar, red, white and jack pine.
Boreal plains	Moderately warm summers and cold winters	Jack and lodgepole pine, white and black spruce, balsam fir, tamarack, trembling aspen

### 1.1.1 Annual cycle of stem diameter variation

The annual cycle of stem diameter variation of trees in the boreal region can be classified into three phases: 1) autumn/winter shrinkage/dehydration; 2) spring rehydration; and 3) summer tree growth (wood formation) (Figure 1.2).

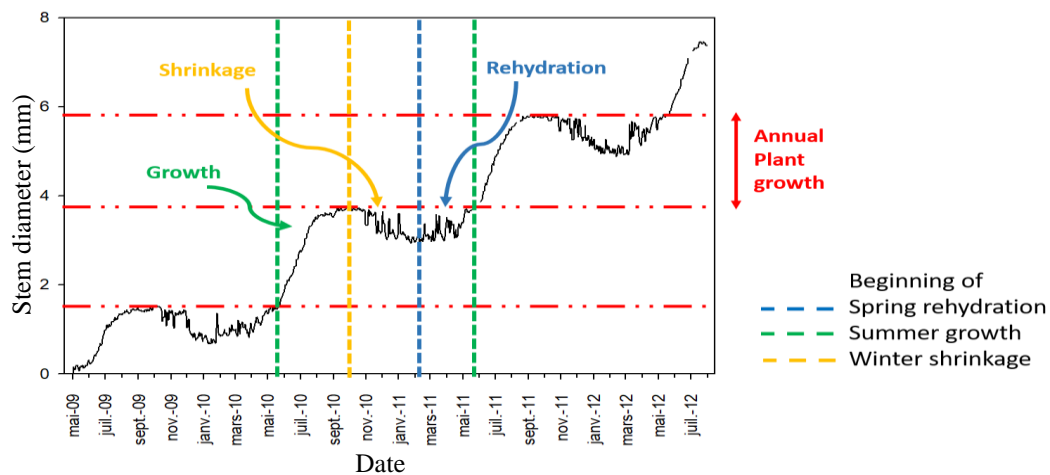


Figure 1.2: Phenology of stem diameter variation of boreal trees over three years with shrinkage, rehydration, and growth illustrated for one of those years

#### 1.1.1.1 Autumn/winter dehydration

During autumn/winter, prior to the rehydration phase, trees normally exhibit stem shrinkage when temperatures are below  $-5\text{ }^{\circ}\text{C}$  due to the dehydration of living cells (cambium, phloem and parenchyma; Figure 1.3) (Zweifel and Hasler, 2000). However, during this period, there are also episodes of stem expansion probably associated with freeze-thaw events. Stem expansion occurs when a potential water gradient is built up once ice has formed in the xylem, thus drawing water from the outer portion of the stem into the xylem (Zweifel and Hasler, 2000). The water drawn in can be stored in the air-filled intercellular spaces of the xylem, as ice or in a liquid state.

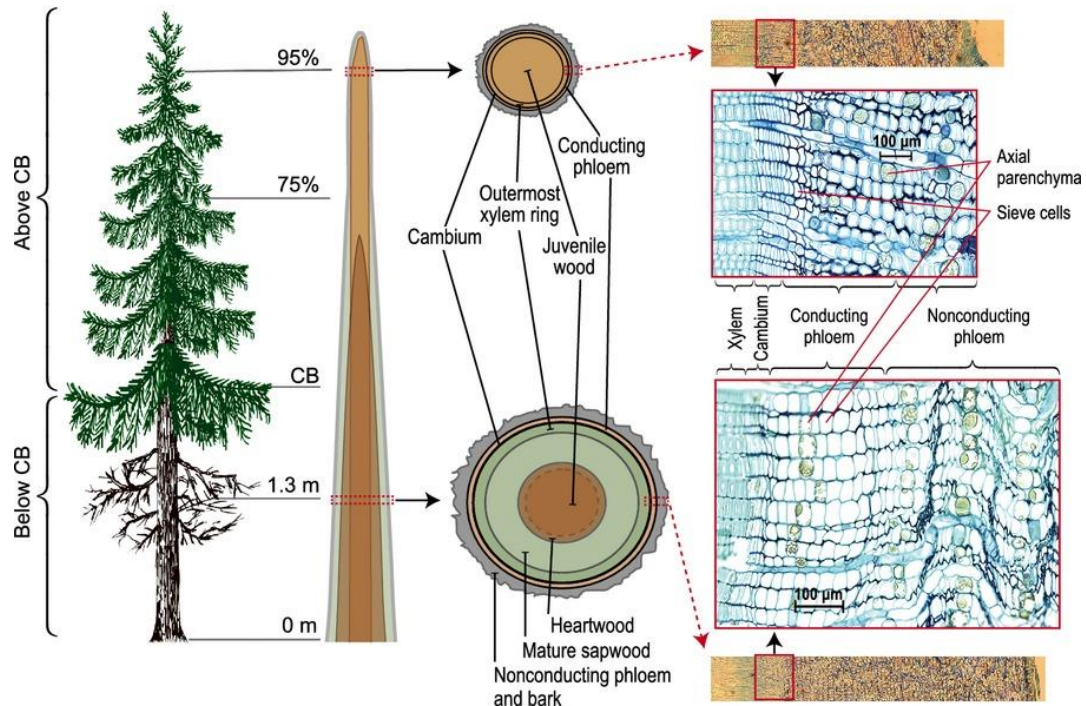


Figure 1.3: Cross-sectional views of wood composition. Reprinted from “Comparison of phloem and xylem hydraulic architecture in *Picea abies* stems” by T. Jyske and T. Hölttä, 2015, *New phytologist*, 205(1), 102-115. CB is base of the living crown

#### 1.1.1.2 Spring rehydration

In the boreal forest, the rehydration phase consists of stem expansion after the cold, dry winter season but there is no new cell production in the cambium (Ziaco et al, 2016). Rehydration is the recharge of the depleted internal stem water stores. The beginning of the rehydration period normally coincides with the beginning of the snowmelt period, while the ending of rehydration period coincides with the initial phase of cambial initiation/wood formation, where the latter in turn depends again on air temperature and date of snowmelt (Turcotte et al., 2009). Since stem radius expansion in the boreal forest might be a consequence of both rehydration and wood formation at the beginning of the growing season, the process causing stem expansion during this transition period may be masked (Mäkinen et al., 2003).

### 1.1.1.3 Tree growth (wood formation period)

In boreal forests, the growing season when wood formation occurs (i.e. production of new xylem cells or xylogenesis) is limited to the period of the year when daily minimum air temperature is above a threshold value (4 - 5 °C) (Rossi et al., 2008). The duration of xylogenesis may range from 3 to 5 months depending on the region and the elevation, whereby it starts after approximately one month of rehydration (Turcotte et al., 2009) and ends around the beginning of September (Rossi et al., 2008). A wider cambial zone and higher cell production throughout the growing season were found to be associated with early snowmelt and high temperature (Vaganov et al., 1999). While soil temperature is not the main driving variable for xylogenesis (as air temperature is the main driving variable; Lupi et al., 2012), it was observed to have an indirect impact on xylogenesis due to the interchange of water between the plant and the soil (Ziaco et al., 2016). In the presence of frozen soil or low soil moisture content, trees may use water stored in the stem (mainly from the sapwood) for photosynthesis (Waring et al., 1979). The amount of xylem stored water varies with tree age and height (Phillips et al., 2003), and basal sapwood area (Goldstein et al., 1998).

## 1.2 Soil temperature and soil water

Global warming in recent decades has resulted in an increase in air and soil temperature (Qian et al., 2011) as well as increased aridity across the globe including western Canada (Dai, 2011; Michaelian et al., 2011), leading to high tree mortality (Allen et al., 2010). In the boreal forest region, despite the fact that soil temperature is not the main factor limiting tree growth compared to air temperature (Lupi et al., 2012), it affects the exchange of liquid water between the soil and the plant (Ziaco et al., 2016). In turn, soil temperature is greatly influenced by air temperature, ground cover (snow or litter),

soil water content, and freezing/melting processes. As for soil water, it is an important variable controlling tree growth, whereby the latter is suppressed under water stress condition. The plant's available water in the soil depends on the intensity, duration and frequency of rainfall, the water holding capacity of the soil and the evaporative demand. The soil water holding capacity itself is a function of soil texture, organic matter and the degree of soil compaction. In the boreal forest region, both soil temperature and soil water are important variables that affect transpiration, which in turn has an important feedback to the climate system.

### 1.3 Transpiration

Kramer (1983) defined transpiration as the 'loss of water in the form of vapor from plants' (Ward and Trimble, 2004). Evapotranspiration is the combined process of transpiration and evaporation that occurs on vegetation-covered land surfaces, whereby evaporation is the loss of water from the soil surface and canopy. In forest ecosystems, the contribution of transpiration is much greater than evaporation (Ward and Trimble, 2004). In a boreal forest, evaporation from the canopy and the forest floor were found to be 20 % and 15 %, respectively, while tree transpiration was found to be 65 % of the total forest evapotranspiration during the growing season (Grelle, et al. 1997).

Evapotranspiration is an important component of the hydrological cycle that links the land surface with the atmosphere. As mentioned by Granier et al. (1996), a strong coupling was found between the forest and the atmosphere, whereby the vertical transfer of water flux to the atmosphere is strongly controlled by the vapour pressure deficit and canopy conductance. However, the impact of environmental variables on transpiration varies with climatic region, tree species (Ewers et al., 2005), and age of trees (Delzon and Loustau, 2005; Ewers et al., 2005). For example, in tropical regions,

the air is warmer and drier, resulting in much higher vapour pressure deficit than in the boreal region. Similarly, the growing season with favourable air temperature is longer (i.e. throughout the year) in the tropical region. These combined conditions (higher vapour pressure deficit and optimum air temperature) lead to higher transpiration in tropical forests than in boreal forests. The intrinsic properties of tree species (iso/anisohydricity of trees) has a great influence on the impact of environmental variables on transpiration, such that isohydric trees stop transpiring much earlier during a drought, while anisohydric trees continue to transpire despite decreasing soil water content (Tardieu and Simmoneau, 1998). In the study of Ewers et al. (2005), younger black spruce trees had greater stomatal control of transpiration compared to older ones (> 70 years) in the Canadian boreal forest. On the other hand, transpiration decreased with age in a maritime pine forest due to decreasing stomatal conductance and leaf area index (Delzon and Loustau, 2005).

### 1.3.1 Environmental control on transpiration

As mentioned earlier, transpiration is controlled by many environmental variables, such as solar radiation, vapour pressure deficit, air temperature, soil water and wind speed. Many studies have been conducted on transpiration to determine the key variables affecting this process. As mentioned in the preceding section, vapour pressure deficit is the physical variable that drives most transpiration followed by solar radiation (Tsuruta et al., 2016; Wang et al., 2017). This being said, contrasting results have been found for the influence of air temperature. Tsuruta et al. (2016) found air temperature to be an important variable in the temperate Japanese cypress forest while Wang et al. (2017) suggested it was less important than other variables in boreal Scots pine forests of Scotland for transpiration. Besides climatic variables, soil water was identified as an important land surface variable for transpiration, but only when rainfall was scarce (Gartner et al., 2009; Wang et al., 2017), implying the presence of a threshold beyond which soil water begins to drive transpiration. According to Lagergren and Lindroth

(2002), a reduction in transpiration begins only after plant available water in the soil drops below 20 %.

### 1.3.2 Plant physiological control on transpiration

Though water stress conditions affect plant physiology, which in extreme drought conditions can lead to mortality, its impact depends on the characteristics of the plant species. Plants have varying stomatal responses to drought, with isohydric plants being more preventive of drought effects and anisohydric plants being more tolerant (Tardieu and Simmoneau, 1998). When isohydric plants reach a severe minimum water potential, they close their stomata to reduce water loss via transpiration and thus protect the xylem from cavitation. However, with the cessation of photosynthesis but the continuation of respiration, there will be depletion of the carbon stores, which in a long drought can lead to death. On the other hand, anisohydric plants keep their stomata open even under water stress conditions, thus maintaining photosynthesis and respiration (Tardieu and Simmoneau, 1998). However, by keeping stomata open, anisohydric plants are more exposed to cavitation that can lead to death of the plant (McDowell et al., 2008). Tree species were found to occur in “a continuum from isohydric to anishohydric behaviors” based on the response of stomata to their leaf water potential (Klein, 2014). Both our study tree species were found to be anisohydric in this humid boreal forest of eastern Canada, with the degree of anisohydricity being greater in black spruce than in balsam fir (unpublished data). A logarithmic model was fitted to the relationship of standardized total conductance versus vapour pressure deficit in order to determine the degree of anisohydricity (smaller slope of the fitted logarithmic model implies higher degree of anisohydricity).

### 1.3.3 Measurement of transpiration via sap flow techniques

While eddy covariance techniques are widely used to measure transpiration at the stand level, transpiration can also be measured using sap flow techniques at the tree level.

There are numerous sap flow techniques that exist, which can be classified into continuous or heat-pulse (Vandegehuchte and Steppe, 2013). Among the continuous sap flow techniques, there are thermal dissipation and heat field deformation techniques, whereby continuous heat is applied to the heater probe. For the heat-pulse technique, there are compensation heat pulse, T<sub>max</sub>, heat ratio, calibrated average gradient, Sapflow+ methods, whereby heat pulse is applied to the heater probe. Among all the sap flow techniques (Figure 1.4), only the heat field deformation (Vandegehuchte and Steppe, 2013) and the recent heat pulse sapflow sensors (East 30 sensors, 2021) measure the radial sapflux density profile. Though each technique has its own advantages and flaws, all of them cause wounds to the tree (Vandegehuchte and Steppe, 2013). Moreover, Steppe et al. (2010) found thermal dissipation, heat field deformation and heat pulse to greatly underestimate sap flux density and recommended carrying out species-specific calibration when using these techniques. Unlike other techniques, thermal dissipation requires a zero flow condition to determine the maximum temperature difference. The zero flow condition is when there is no sap flow in the stem, which occurs during the night for most tree species, except for those having nocturnal transpiration (Kavanagh et al., 2007; Konarska et al., 2016). Our studied species did not exhibit any nocturnal transpiration based on our sap flow data, thus met the zero flow condition. While thermal dissipation measures from low to high sap flows, heat field deformation and Sapflow+ measures reverse, low to high sap flows (Vandegehuchte and Steppe, 2013). The reverse sap flow is the downward movement of sap that occurs mostly at night, for the purpose of hydraulic redistribution in stems (Burgess and Bleby, 2006). Similarly, low flows mostly occur at night (Forster, 2014), thus they are more relevant for species exhibiting nocturnal transpiration. In this study, the thermal dissipation technique is used for the measurement of sap flow. Moreover, in terms of performance, the thermal dissipation technique is comparable to heat field deformation and heat pulse techniques (Steppe et al., 2010).

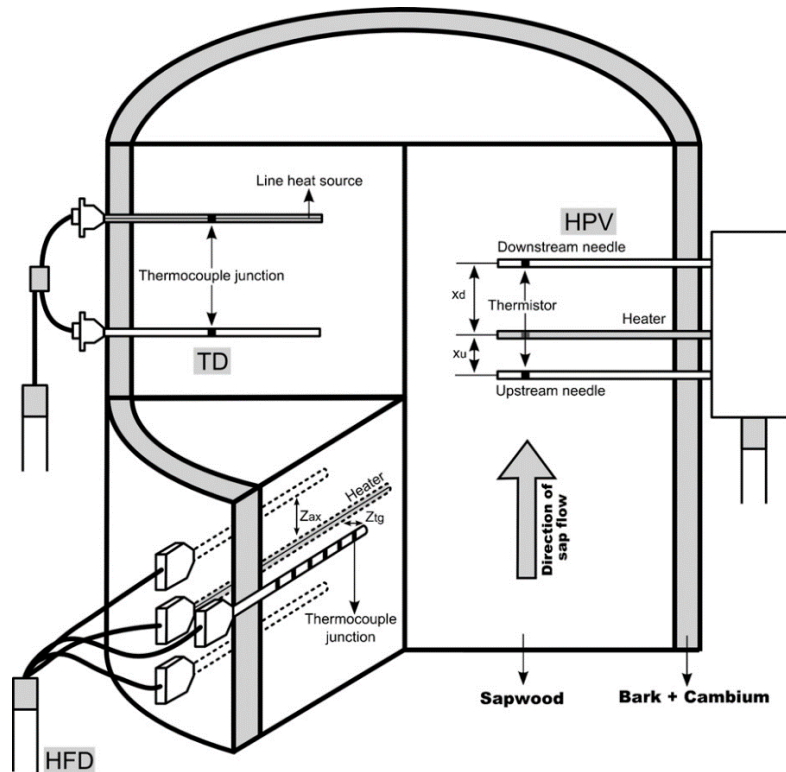


Figure 1.4: Three main sap flow techniques: thermal dissipation (TD); heat field deformation (HFD); and heat pulse velocity (HPV).  $x_d$  and  $x_u$  are the downstream and upstream distance of the needle from the heater.  $Z_{ax}$  and  $Z_{tg}$  are the axial and tangential distance of needle from the heater. Reprinted from “A comparison of sap flux density using thermal dissipation, heat pulse velocity and heat field deformation methods” by K. Steppe, D.J. De Pauw, T.M. Doody and R.O. Teskey, 2010, *Agricultural and Forest Meteorology*, 150(7-8), pp.1046-1056.

Many studies have been carried out using sap flow techniques to determine tree transpiration or canopy conductance (Saugier et al., 1997; Köstner et al., 1998; Granier et al., 2000; Daley and Phillips, 2006; Macfarlane et al., 2010; Jung et al., 2011) or to evaluate the impact of environmental variables on sap flow (Hogg and Hurdle, 1997; Wullschlegel et al., 2000; Lagergren and Lindroth, 2002; Bovard et al., 2005; Wang et al., 2005; Chen et al., 2011; Jonard et al., 2011; van Herk et al., 2011; Patankar et al., 2015; Juice et al., 2016; Wang et al., 2017; Collins et al., 2018). However, most studies on the environmental controls over sap flow have been carried out in the temperate

region. Although a few studies have been conducted in the boreal forest, the study sites were either in dry boreal forests focusing on vapour pressure deficit and air/soil temperature only (Hogg and Hurdle, 1997; van Herk et al., 2011) or in boreal peatlands exhibiting rapid permafrost thaw (Patankar et al., 2015). Those studies conducted in humid boreal regions were on other tree species (Lagergren and Lindroth, 2002; Wang et al., 2017). No studies on the relationship between sap flow and environmental variables have been carried out on dominant boreal species black spruce or balsam fir in cold-humid boreal forests such as those found in eastern Canada.

#### 1.4 Representation of land surface processes in land surface schemes

##### 1.4.1 Land surface processes

Although the land surface accounts for only 29 % of the Earth's surface compared to the ocean, many studies have shown that its impact on the atmosphere is important due to changing surface albedo and heating in contrast to the ocean (Sellers, 1965 in Verstraete and Dickinson, 1986). Surface albedo varies based on the type of surface, with snow having the highest albedo followed by desert, vegetation, dry soil, wet soil, and finally water. Moreover, some of these surface albedos vary seasonally such as snow and deciduous vegetation in winter. Although vegetation surfaces cover at most 20 % of the Earth's surface, they have a complex interaction with the atmosphere compared to flat surfaces like snow, soil and water bodies. As leaf area index (projected area of leaves over a unit of land,  $m^2/m^2$ ) ranges from 1 to 10, the total areal coverage of vegetation may exceed the total surface area of the Earth. Verstraete and Dickinson, 1986.

Interactions between land surface and atmosphere in vegetation-covered areas occur in four ways. Firstly via transpiration, where a large portion of the continental water goes

to the atmosphere as vegetation has the ability to extract water from deeper soil profiles compared to soil evaporation that occurs only from shallow soil layers. Second via its albedo, where a considerable amount of leaf albedo (reflected radiation) in the visible (10-15 %) and near infrared portion (30- 50 %) of the electromagnetic spectrum goes to the atmosphere. Third via heat energy, with higher exchange between the canopy and the atmosphere during both the dry season (as sensible heat) and wet season (as latent heat) compared to bare land surfaces. Fourth via increased vegetation surface roughness, which leads to reduced momentum in the lower atmosphere. Bare soil surfaces are flat, thus have a small surface roughness. On the other hand, vegetation-covered surfaces have irregular heights, and thus have higher surface roughness, leading to a greater interaction with the lower atmosphere and thereby reducing the motion (momentum) of air masses. Overall, compared to the ocean, the land surface exhibits a high spatial and temporal variability in its interaction with the atmosphere. These land-atmosphere interactions (or land surface processes) will in turn have major feedbacks on the climate system. Verstraete and Dickinson, 1986.

#### 1.4.2 Land Surface Schemes

The land surface can be described as “the surface that comprises vegetation, soil and snow, coupled with the way these influence the exchange of energy, water and carbon within the Earth system” (Pitman, 2003). Land surface schemes (LSSs), which numerically represent the hydrosphere, cryosphere, lithosphere and biosphere, are models that were especially designed to work within climate models. Climate models are themselves numerical models that were developed for climate projections as well as to simulate past climate. These climate models, in general, are complex due to the numerous processes and components that represent the entire climate system (Laprise, 2008), with processes being physically-based, empirical or statistical (Dutrieux, 2016). According to Chapin et al. (2000), the land surface - atmosphere coupling is controlled via water and heat exchange from local to regional scales, and via carbon dioxide and

methane at a global scale. As a result, these LSSs within climate models enable us to study the impact of land cover changes, such as deforestation, afforestation or agricultural intensification, on the climate system (Pitman, 2003).

In order to represent land surface processes, numerous LSSs have been built by different research groups with varying levels of complexity across the globe to couple with their climate models. These LSSs range from a simple bucket Model (1<sup>st</sup> generation LSS; Manabe, 1969), to those that add a vegetation layer that computes transpiration using an empirical equation (2<sup>nd</sup> generation LSS; Dickinson et al., 1986; Sellers et al., 1986), and finally to schemes that add a semi-mechanistic photosynthesis model (3<sup>rd</sup> generation LSS; Collatz et al., 1991). The 2<sup>nd</sup> generation LSSs have an empirical approach to the computation of stomatal conductance based on the Jarvis (1976) formulation, where it is controlled by environmental stresses (solar radiation, humidity, air temperature and soil water potential). However, the individual functions of these environmental stresses vary among the various LSSs. Examples of 2<sup>nd</sup> generation LSSs are Biosphere-Atmosphere Transfer scheme (BATS; Dickinson et al., 1986), Simple Biosphere Model (SiB; Sellers et al., 1986), and Canadian Land Surface Scheme (CLASS; Versegny, 1991; Versegny et al., 1993). The 3<sup>rd</sup> generation LSSs use a biochemical approach for stomatal conductance, in which conductance is controlled by the net assimilation rate, partial pressure of carbon dioxide at the leaf surface, and relative humidity/vapour pressure deficit. However, the 3<sup>rd</sup> generation LSSs are more complex in their input data requirements. Examples of 3<sup>rd</sup> generation LSSs are coupled CLASS-Canadian Terrestrial Ecosystem Model (CTEM; Arora, 2003), CSIRO Atmosphere Biosphere Land Exchange (CABLE; Kowalczyk et al., 2006), the Joint UK Land Environment Simulator (JULES; Best et al., 2011), and Community Land Model (CLM; Oleson et al., 2013).

In my study, since my focus is transpiration instead of photosynthesis, CLASS (version 3.6) is used in place of the CLASS-CTEM version. Thus, CLASS, which was built to

be coupled with the Canadian Regional Climate Model (CRCM; Zadra et al., 2008), is used to evaluate soil temperature, soil water and the temporal variation of transpiration. CLASS models the hydrological cycle in a one-dimensional column, at a time step of 30 mins. The model consists of a layer of vegetation, a single snow layer of variable depth and multiple soil layers of varying thicknesses. The vegetation in the model is grouped into four categories: broadleaves, conifers, crops, and grass. Each model grid is divided into four sub-grids based on land cover types: 1) bare soil; 2) soil covered with snow; 3) soil covered with vegetation; 4) and vegetation over snow-covered soil. The energy and mass balances are calculated for each sub-grid and the composite energy and mass balance are determined for each grid by doing a weighted average based on the area occupied by each land cover type (Verseghy, 1991; Verseghy et al., 1993). Figure 1.5 shows the main processes modelled in CLASS, such as evaporation from soil and canopy, transpiration, albedo of snow, ground and canopy, sensible and latent heat flux, infiltration and vertical drainage, interception of water and snow by canopy, etc..

#### 1.4.3 Impact of land surface processes in Land Surface Schemes on climate models

Many studies have shown that the representation of land surface variables and processes in an LSS have considerable impact on climate projections in climate models (Brochu and Laprise, 2007; Roy et al., 2012). Using an LSS coupled with a climate model, simulated regional deforestation resulted in a decrease in evapotranspiration and an increase in surface temperature (Dickinson and Henderson-Sellers, 1988; Brovkin et al. 2009), whilst global-scale deforestation led to a net decrease in Earth's average temperature (Bala et al. 2007) due to an increase in surface albedo in the higher latitudes (Betts, 2000). On the other hand, simulated afforestation in a global climate model in high northern latitudes led to increased transpiration and warming of the arctic region (Swann et al., 2010) due to decreased surface albedo (Betts, 2000).

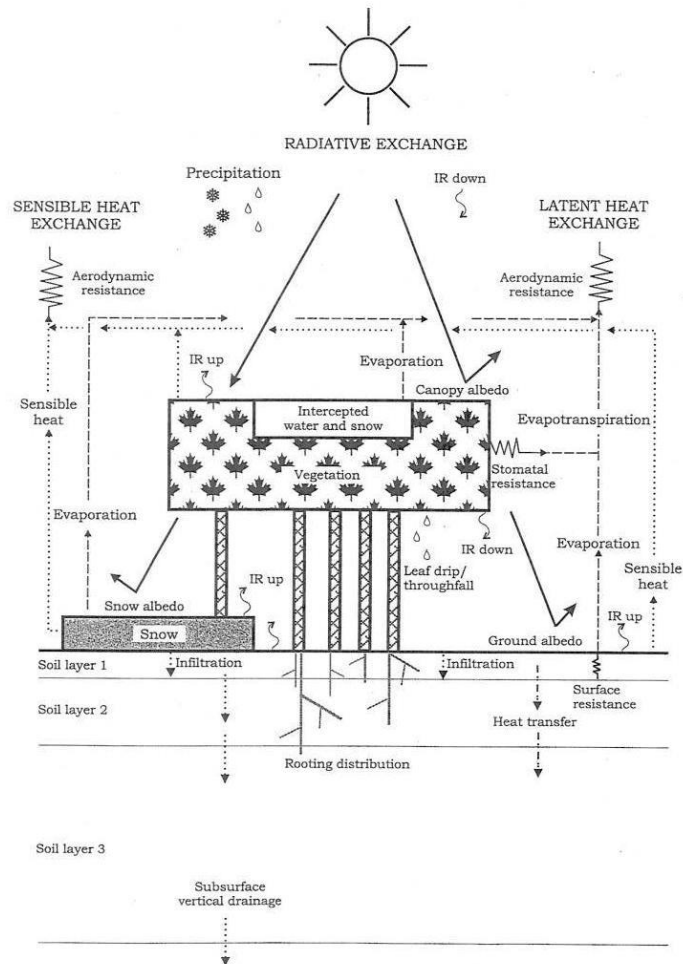


Figure 1.5: Schematic diagram of CLASS. Reprinted from “CLASS–The Canadian land surface scheme (version 3.6)” by D. Verseghy, 2012. *Environment Canada Science and Technology Branch Tech. Rep.*

These findings underscore the importance of forested ecosystems on the climate system via the impact of afforestation/deforestation on both air/surface temperature and transpiration/evapotranspiration. On the other hand, transpiration in LSSs is greatly influenced by soil water (Ukkola et al., 2016). The study of Ukkola et al. (2016) showed that accurate simulation of soil water is crucial for the simulation of latent heat flux and evapotranspiration in LSSs, especially during dry periods, across different

ecosystems (including forests). Furthermore, increasing soil water was found to have positive feedbacks on precipitation in climate models most of the time from global, regional to continental scales (e.g. Schär et al., 1999 in Seneviratne et al., 2010), although in a few exceptions negative feedbacks occurred (Cook et al., 2006).

Thus, in this study, the transpiration process in the CLASS LSS will be evaluated for its performance in the boreal forest ecosystem of eastern Canada. Since in the boreal region, both soil water and soil temperature are important variables that greatly influence transpiration, the simulation of these variables will be assessed using CLASS.

### 1.5 Objectives of the study

The aim of my thesis is to analyse transpiration and its underlying driving environmental variables in a natural system, and to evaluate simulated transpiration and land surface variables (soil water and soil temperature) in a numerical model. The natural system is two humid boreal forests located in Quebec, Canada, while the numerical model is the Canadian Land Surface Scheme (CLASS). This study comprises three phases, where the goal of the first phase is to evaluate the performance of CLASS as well as the model's sensitivity to certain model parameters for simulating the land surface variables soil water and soil temperature over multiple years. The goal of the second phase is to understand the impact of environmental variables on boreal tree sap flow (as a proxy for transpiration) during the growing season and during extreme events such as drought based on long-term observations. The goal of the third phase is to evaluate the performance of CLASS in simulating the temporal evolution of transpiration during tree rehydration and the growing season over multiple years, and a drought period.

## 1.6 Study area - Laflamme and Tirasse

The study area comprises two boreal forests sites situated in two different watersheds, located in the province of Quebec in Canada (Figure 1.6). The first site, the Laflamme watershed, located north of Québec city ( $47^{\circ}19'41''$  N and  $71^{\circ}07'37''$  W), is dominated by balsam fir, with some white spruce and paper birch (Duchesne et al., 2012). The site elevation is 784 m above sea level, with mean annual temperature of  $1.3^{\circ}\text{C}$  and mean annual precipitation of 1300 mm. The forest floor is covered with mosses and lichen. The second site, the Tirasse watershed, located in the wildlife reserve Ashuapmushuan ( $49^{\circ}12'45''$  N and  $73^{\circ}39'00''$  W), consists of black spruce (66.4%) and Jack pine as the dominant vegetation and a thick layer of mosses on the forest floor (Duchesne and Houle, 2006; Houle and Moore, 2008). The site elevation is at 411 m above sea level, with mean annual temperature of  $1.3^{\circ}\text{C}$  and mean annual precipitation of 941 mm.

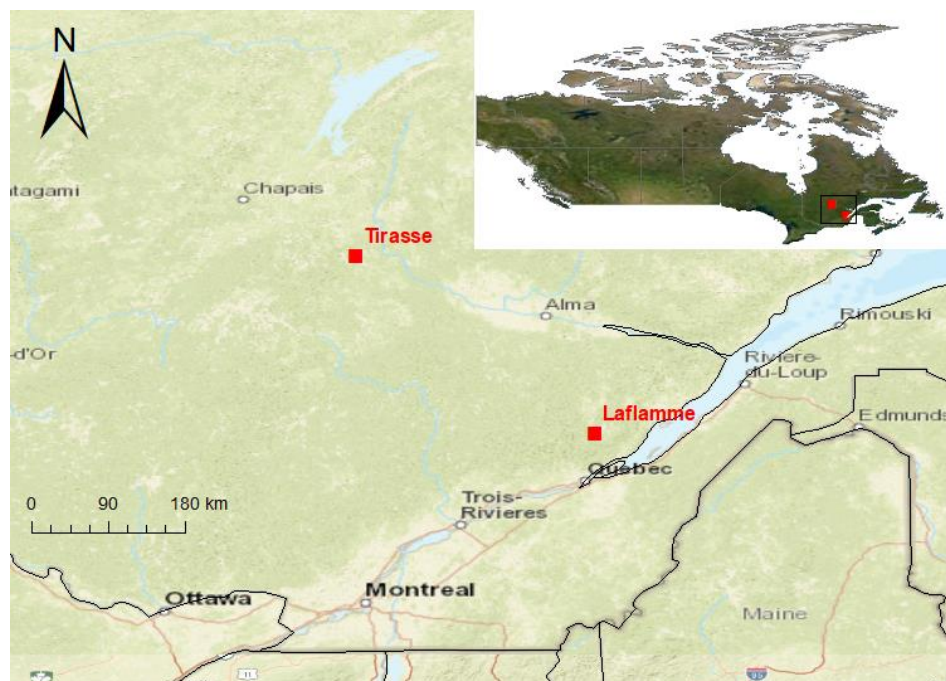


Figure 1.6: Location of the two study areas (red squares) in the Quebec province, Canada.

## 1.7 References

- Allen, C. D., A. K. Macalady, H. Chenchouni, D. Bachelet, N. McDowell, M. Vennetier, T. Kitzberger, A. Rigling, D. D. Breshears, E. H. Hogg, P. Gonzalez, R. Fensham, Z. Zhang, J. Castro, N. Demidova, J.-H. Lim, G. Allard, S. W. Running, A. Semerci and N. Cobb, 2010. A global overview of drought and heat induced tree mortality reveals emerging climate change risks for forests. *Forest Ecology and Management* 259(4): 660-684.
- Arora, V.K., 2003. Simulating energy and carbon fluxes over winter wheat using coupled land surface and terrestrial ecosystem models. *Agricultural and Forest Meteorology*, 118(1-2), pp.21-47.
- Bala, G., Caldeira, K., Wickett, M., Phillips, T.J., Lobell, D.B., Delire, C. and Mirin, A., 2007. Combined climate and carbon-cycle effects of large-scale deforestation. *Proceedings of the National Academy of Sciences*, 104(16), pp.6550-6555.
- Best, M.J., Pryor, M., Clark, D.B., Rooney, G.G., Essery, R.L.H., Ménard, C.B., Edwards, J.M., Hendry, M.A., Porson, A., Gedney, N. and Mercado, L.M., 2011. The Joint UK Land Environment Simulator (JULES), model description– Part 1: energy and water fluxes. *Geoscientific Model Development*, 4(1), pp.677-699.
- Betts, R.A., 2000. Offset of the potential carbon sink from boreal forestation by decreases in surface albedo. *Nature*, 408(6809), pp.187-190.
- Bovard, B.D., Curtis, P.S., Vogel, C.S., Su, H.B., Schmid, H.P., 2005. Environmental controls on sap flow in a northern hardwood forest. *Tree Physiol.* 25 (1), 31–38. <https://doi.org/10.1093/treephys/25.1.31>.
- Brochu, R. and Laprise, R., 2007. Surface water and energy budgets over the Mississippi and Columbia river basins as simulated by two generations of the Canadian Regional Climate Model. *Atmosphere-ocean*, 45(1), pp.19-35.
- Brovkin, V., Raddatz, T., Reick, C.H., Claussen, M. and Gayler, V., 2009. Global biogeophysical interactions between forest and climate. *Geophysical Research Letters*, 36(7).
- Burgess, S.S.O. and Bleby, T.M., 2006. Redistribution of soil water by lateral roots mediated by stem tissues. *Journal of Experimental Botany*, 57(12), pp.3283-3291.
- Chapin iii, F. S., McGuire, A. D., Randerson, J., Pielke Sr, R., Baldocchi, D., Hobbie, S. E., Roulet N., Eugster W., Kasischke E., Rastetter E.B., Zimov S.A., Running, S. W., 2000. Arctic and boreal ecosystems of western North America as

- components of the climate system. *Global Change Biology*, 6(SUPPLEMENT 1), 211-223. doi: 10.1046/j.1365-2486.2000.06022.x
- Chen, L., Zhang, Z., Li, Z., Tang, J., Caldwell, P., Zhang, W., 2011. Biophysical control of whole tree transpiration under an urban environment in Northern China. *J. Hydrol. (Amst.)* 402 (3–4), 388–400 <https://doi.org/10.1016/j.jhydrol.2011.03.034>.
- Collatz GJ, Ball JT, Grivet C, Berry JA. 1991. Physiological and environmental regulation of stomatal conductance, photosynthesis and transpiration: a model that includes a laminar boundary layer. *Agricultural and Forest Meteorology* 54: 107–136.
- Collins, A.R., Burton, A.J., Cavaleri, M.A., 2018. Effects of Experimental Soil Warming and Water Addition on the Transpiration of Mature Sugar Maple. *Ecosystems* 21 (1), 98–111. <https://doi.org/10.1007/s10021-017-0137-9>.
- Cook, B.I., Bonan, G.B. and Levis, S., 2006. Soil moisture feedbacks to precipitation in southern Africa. *Journal of Climate*, 19(17), pp.4198-4206.
- Dai, A., 2011. Characteristics and trends in various forms of the Palmer Drought Severity Index during 1900–2008. *Journal of Geophysical Research: Atmospheres*, 116(D12).
- Daley, M.J., Phillips, N.G., 2006. Interspecific variation in nighttime transpiration and stomatal conductance in a mixed New England deciduous forest. *Tree Physiol.* 26 (4), 411–419.
- Delzon, S. and Loustau, D., 2005. Age-related decline in stand water use: sap flow and transpiration in a pine forest chronosequence. *Agricultural and Forest Meteorology*, 129(3-4), pp.105-119.
- Dickinson, R. E., A. Henderson-Sellers, P. J. Kennedy, M.F. Wilson., 1986. Biosphere-atmosphere transfer scheme (BATS) for the NCAR community climate model Tech Note/TN-275+STR. Nat. Cent. for Atmos.Res., Boulder, Colo.
- Dickinson, R.E. and Henderson-Sellers, A., 1988. Modelling tropical deforestation: A study of GCM land-surface parametrizations. *Quarterly Journal of the Royal Meteorological Society*, 114(480), pp.439-462.
- Duchesne, L. and D. Houle, 2006. Base cation cycling in a pristine watershed of the Canadian boreal forest. *Biogeochemistry* 78(2): 195-216.
- Duchesne, L., Houle, D. and D'Orangeville, L., 2012. Influence of climate on seasonal patterns of stem increment of balsam fir in a boreal forest of Québec, Canada. *Agricultural and forest meteorology*, 162, pp.108-114.

- Dutrieux, P., 2016. Évaluation de simulations du Modèle Régional Canadien du Climat (MRCC5) au-dessus de l'Atlantique Nord. Maîtrise, Université du Québec à Montréal.
- East 30 sensors, 2021. East 30 Sapflow sensors. Available at <[Sap Flow Sensors \(east30sensors.com\)](http://east30sensors.com)> [Accessed 12 February 2021].
- Ewers, B.E., Gower, S.T., Bond-Lamberty, B. and Wang, C.K., 2005. Effects of stand age and tree species on canopy transpiration and average stomatal conductance of boreal forests. *Plant, Cell & Environment*, 28(5), pp.660-678.
- Forster, M.A., 2014. How significant is nocturnal sap flow?. *Tree physiology*, 34(7), pp.757-765.
- Gartner, K., Nadezhdina, N., Englisch, M., Čermak, J. and Leitgeb, E., 2009. Sap flow of birch and Norway spruce during the European heat and drought in summer 2003. *Forest Ecology and Management*, 258(5), pp.590-599.
- Granier, A., P. Biron, N. Bréda, J. Y. Pontailler and B. Saugier, 1996. Transpiration of trees and forest stands: short and long-term monitoring using sapflow methods. *Global Change Biology* 2(3): 265-274.
- Granier, A., Biron, P., Lemoine, D., 2000. Water balance, transpiration and canopy conductance in two beech stands. *Agric. For. Meteorol.* 100 (4), 291–308.
- Grelle, A., Lundberg, A., Lindroth, A., Morén, A.S. and Cienciala, E., 1997. Evaporation components of a boreal forest: variations during the growing season. *Journal of Hydrology*, 197(1-4), pp.70-87.
- Goldstein, G., J. L. Andrade, F. C. Meinzer, N. M. Holbrook, J. Cavelier, P. Jackson and A. Celis, 1998. Stem water storage and diurnal patterns of water use in tropical forest canopy trees. *Plant, Cell & Environment* 21(4): 397-406.
- Jarvis, P.G., 1976. The interpretation of the variations in leaf water potential and stomatal conductance found in canopies in the field. *Philosophical Transactions of the Royal Society of London. B, Biological Sciences*, 273(927), pp.593-610.
- Johnston, M., 2009. *Vulnerability of Canada's tree species to climate change and management options for adaptation: An overview for policy makers and practitioners*. Canadian Council of Forest Ministers.
- Jonard, F., André, F., Ponette, Q., Vincke, C., Jonard, M., 2011. Sap flux density and stomatal conductance of European beech and common oak trees in pure and mixed stands during the summer drought of 2003. *J. Hydrol. (Amst.)* 409 (1–2), 371–381.

- Juice, S.M., Templer, P.H., Phillips, N.G., Ellison, A.M., Pelini, S.L., 2016. Ecosystem warming increases sap flow rates of northern red oak trees. *Ecosphere* 7 (3), e01221. <https://doi.org/10.1002/ecs2.1221>, -n/a.
- Jung, E.Y., Otieno, D., Lee, B., Lim, J.H., Kang, S.K., Schmidt, M.W.T., Tenhunen, J., 2011. Up-scaling to stand transpiration of an Asian temperate mixed-deciduous forest from single tree sapflow measurements. *Plant Ecol.* 212 (3), 383–395. <https://doi.org/10.1007/s11258-010-9829-3>.
- Jyske, T., & Hölttä, T., 2015. Comparison of phloem and xylem hydraulic architecture in *Picea abies* stems. *New phytologist*, 205(1), 102-115.
- Hogg, E.H., Hurdle, P.A., 1997. Sap flow in trembling aspen: implications for stomatal responses to vapor pressure deficit. *Tree Physiol.* 17 (8–9), 501–509. <https://doi.org/10.1093/treephys/17.8-9.501>.
- Houle, D. and J.-D. Moore, 2008. Soil solution, foliar concentrations and tree growth response to 3-year of ammonium-nitrate addition in two boreal forests of Québec, Canada. *Forest Ecology and Management* 255(7): 2049-2060.
- Kavanagh, K. L., R. Pangle and A. D. Schotzko, 2007. Nocturnal transpiration causing disequilibrium between soil and stem predawn water potential in mixed conifer forests of Idaho. *Tree Physiol* 27(4): 621-629.
- Klein, T., 2014. The variability of stomatal sensitivity to leaf water potential across tree species indicates a continuum between isohydric and anisohydric behaviours. *Functional ecology*, 28(6), pp.1313-1320.
- Konarska, J., J. Uddling, B. Holmer, M. Lutz, F. Lindberg, H. Pleijel and S. Thorsson, 2016. Transpiration of urban trees and its cooling effect in a high latitude city. *Int J Biometeorol* 60(1): 159-172.
- Köstner, B., Falge, E.M., Alsheimer, M., Geyer, R., Tenhunen, J.D., 1998. Estimating tree canopy water use via xylem sapflow in an old Norway spruce forest and a comparison with simulation-based canopy transpiration estimates. *Ann. For. Sci.* 55 (1–2), 125–139.
- Kowalczyk, E.A., Wang, Y.P., Law, R.M., Davies, H.L., McGregor, J.L. and Abramowitz, G., 2006. The CSIRO Atmosphere Biosphere Land Exchange (CABLE) model for use in climate models and as an offline model. *CSIRO Marine and Atmospheric Research Paper*, 13, p.42.
- Kramer, P. J., 1983. *Water Relations of Plants*. Academic Press, Inc. Orlando, Fl.
- Lagergren, F. and A. Lindroth, 2002. Transpiration response to soil moisture in pine and spruce trees in Sweden. *Agricultural and Forest Meteorology* 112(2): 67-85.
- Laprise, R., 2008. Regional climate modelling. *J. Comput. Phys.* 227(7): 3641-3666.

- Lupi, C., Morin, H., Deslauriers, A., & Rossi, S., 2012. Xylogenesis in black spruce: Does soil temperature matter? *Tree Physiology*, 32(1), 74-82. doi: 10.1093/treephys/tpr132
- Macfarlane, C., Bond, C., White, D.A., Grigg, A.H., Ogden, G.N., Silberstein, R., 2010. Transpiration and hydraulic traits of old and regrowth eucalypt forest in southwestern Australia. *For. Ecol. Manage.* 260 (1), 96–105.
- Mäkinen, H., P. Nöjd and P. Saranpää, 2003. Seasonal changes in stem radius and production of new tracheids in Norway spruce. *Tree Physiology* 23(14): 959-968.
- Manabe S. 1969. Climate and the ocean circulation: 1, the atmospheric circulation and the hydrology of the Earth's surface. *Monthly Weather Review* 97: 739–805.
- McDowell, N., Pockman, W.T., Allen, C.D., Breshears, D.D., Cobb, N., Kolb, T., Plaut, J., Sperry, J., West, A., Williams, D.G. and Yezzer, E.A., 2008. Mechanisms of plant survival and mortality during drought: why do some plants survive while others succumb to drought?. *New phytologist*, 178(4), pp.719-739.
- Michaelian, M., Hogg, E.H., Hall, R.J. and Arsenault, E., 2011. Massive mortality of aspen following severe drought along the southern edge of the Canadian boreal forest. *Global Change Biology*, 17(6), pp.2084-2094.
- Oleson, K.W., Lawrence, D.M., Bonan, G.B., Drewniak, B., Huang, M., Koven, C.D., Levis, S., Li, F., Riley, W.J., Subin, Z.M. and Swenson, S.C., 2013. Technical description of version 4.5 of the Community Land Model (CLM), NCAR Technical Note: NCAR/TN-503+ STR. *National Center for Atmospheric Research (NCAR), Boulder, CO, USA*, <https://doi.org/10.5065/D6RR1W7M>.
- Patankar, R., Quinton, W.L., Hayashi, M. and Baltzer, J.L., 2015. Sap flow responses to seasonal thaw and permafrost degradation in a subarctic boreal peatland. *Trees*, 29(1), pp.129-142.
- Phillips, N. G., M. G. Ryan, B. J. Bond, N. G. McDowell, T. M. Hinckley and J. Čermák, 2003. Reliance on stored water increases with tree size in three species in the Pacific Northwest. *Tree Physiology* 23(4): 237-245.
- Pitman, A. J., 2003. The evolution of, and revolution in, land surface schemes designed for climate models. *International Journal of Climatology*, 23(5), 479-510. doi: 10.1002/joc.893
- Qian, B., Gregorich, E.G., Gameda, S., Hopkins, D.W. and Wang, X.L., 2011. Observed soil temperature trends associated with climate change in Canada. *Journal of Geophysical Research: Atmospheres*, 116(D2).
- Rossi, S., A. Deslauriers, J. Gričar, J.-W. Seo, C. B. K. Rathgeber, T. Anfodillo, H. Morin, T. Levanic, P. Oven and R. Jalkanen, 2008. Critical temperatures for

- xylogenesis in conifers of cold climates. *Global Ecology and Biogeography* 17(6): 696-707.
- Roy, P., Gachon, P. and Laprise, R., 2012. Assessment of summer extremes and climate variability over the north-east of North America as simulated by the Canadian Regional Climate Model. *International journal of climatology*, 32(11), pp.1615-1627.
- Sánchez-Costa, E., R. Poyatos and S. Sabaté, 2015. Contrasting growth and water use strategies in four co-occurring Mediterranean tree species revealed by concurrent measurements of sap flow and stem diameter variations. *Agricultural and Forest Meteorology* 207: 24-37.
- Saugier, B., Granier, A., Pontailler, J.Y., Dufrene, E., Baldocchi, D.D., 1997. Transpiration of a boreal pine forest measured by branch bag, sap flow and micrometeorological methods. *Tree Physiol.* 17 (8\_9), 511–519.
- Schär, C., Lüthi, D., Beyerle, U. and Heise, E., 1999. The soil–precipitation feedback: A process study with a regional climate model. *Journal of Climate*, 12(3), pp.722-741.
- Sellers W.D., 1965. *Physical Climatology*. The University of Chicago Press, 272 pp.
- Sellers PJ, Mintz Y, Sud YC, Dalcher A. 1986. A Simple Biosphere model (SiB) for use within general circulation models. *Journal of the Atmospheric Sciences* 43: 505–531.
- Seneviratne, S.I., Corti, T., Davin, E.L., Hirschi, M., Jaeger, E.B., Lehner, I., Orlowsky, B. and Teuling, A.J., 2010. Investigating soil moisture–climate interactions in a changing climate: A review. *Earth-Science Reviews*, 99(3-4), pp.125-161.
- Steppe, K., De Pauw, D.J., Doody, T.M. and Teskey, R.O., 2010. A comparison of sap flux density using thermal dissipation, heat pulse velocity and heat field deformation methods. *Agricultural and Forest Meteorology*, 150(7-8), pp.1046-1056.
- Swann, A.L., Fung, I.Y., Levis, S., Bonan, G.B. and Doney, S.C., 2010. Changes in Arctic vegetation amplify high-latitude warming through the greenhouse effect. *Proceedings of the National Academy of Sciences*, 107(4), pp.1295-1300.
- Tardieu, F., & Simonneau, T., 1998. Variability among species of stomatal control under fluctuating soil water status and evaporative demand: modelling isohydric and anisohydric behaviours. *Journal of Experimental Botany*, 419-432.
- Tsuruta, K., Kosugi, Y., Takanashi, S., & Tani, M., 2016. Inter-annual variations and factors controlling evapotranspiration in a temperate Japanese cypress forest. *Hydrological Processes*, 30(26), 5012-5026. doi: 10.1002/hyp.10977

- Turcotte, A., H. Morin, C. Krause, A. Deslauriers and M. Thibeault-Martel, 2009. The timing of spring rehydration and its relation with the onset of wood formation in black spruce. *Agricultural and Forest Meteorology* 149(9): 1403-1409.
- Tyrrell, M., 2020. *Boreal Forest Ecology | Global Forest Atlas*. [online] Globalforestatlas.yale.edu. Available at: <<https://globalforestatlas.yale.edu/boreal-forest/boreal-ecoregions-ecology/boreal-forest-ecology>> [Accessed 28 March 2020].
- Ukkola, A.M., Pitman, A.J., Decker, M., De Kauwe, M.G., Abramowitz, G., Kala, J. and Wang, Y.P., 2016. Modelling evapotranspiration during precipitation deficits: identifying critical processes in a land surface model. *Hydrology and Earth System Sciences*, 20(6), pp.2403-2419.
- Vaganov, E. A., M. K. Hughes, A. V. Kirilyanov, F. H. Schweingruber and P. P. Silkin, 1999. Influence of snowfall and melt timing on tree growth in subarctic Eurasia. *Nature* 400(6740): 149-151.
- Van Herk, I.G., Gower, S.T., Bronson, D.R., Tanner, M.S., 2011. Effects of climate warming on canopy water dynamics of a boreal black spruce plantation. *Can. J. Forest Res.* 41 (2), 217–227.
- Vandegehuchte, M.W. and Steppe, K., 2013. Corrigendum to: Sap-flux density measurement methods: working principles and applicability. *Functional Plant Biology*, 40(10), pp.1088-1088.
- Verseghy, Diana, 2012. CLASS—The Canadian land surface scheme (version 3.6). *Environment Canada Science and Technology Branch Tech. Rep.*
- Verseghy, D. L., 1991. Class—A Canadian land surface scheme for GCMS. I. Soil model. *International Journal of Climatology* 11(2): 111-133.
- Verseghy, D. L., N. A. McFarlane and M. Lazare, 1993. Class—A Canadian land surface scheme for GCMS, II. Vegetation model and coupled runs. *International Journal of Climatology* 13(4): 347-370.
- Verstraete, M. M., & Dickinson, R. E., 1986. Modeling surface processes in atmospheric general circulation models. *Annales Geophysicae, Series B*, 4 B(4), 357-364.
- Wang, K.-Y., Kellomäki, S., Zha, T., Peltola, H., 2005. Annual and seasonal variation of sap flow and conductance of pine trees grown in elevated carbon dioxide and temperature. *J. Exp. Bot.* 56 (409), 155–165.
- Wang, H., Tetzlaff, D., Dick, J. J., & Soulsby, C., 2017. Assessing the environmental controls on Scots pine transpiration and the implications for water partitioning in a boreal headwater catchment. *Agricultural and Forest Meteorology*, 240-241, 58-66. doi: 10.1016/j.agrformet.2017.04.002

- Ward, A. D., & Trimble, S. W., 2004. *Hydrology of Forests, Wetlands, and Cold Climates Environmental Hydrology* (Second ed.). New York: Lewis Publishers.
- Waring, R. H., D. Whitehead and P. G. Jarvis, 1979. The contribution of stored water to transpiration in Scots pine. *Plant, Cell & Environment* 2(4): 309-317.
- Wullschleger, S.D., Wilson, K.B., Hanson, P.J., 2000. Environmental control of whole-plant transpiration, canopy conductance and estimates of the decoupling coefficient for large red maple trees. *Agric. For. Meteorol.* 104 (2), 157–168 [http://dx.doi.org/10.1016/S0168-1923\(00\)00152-0](http://dx.doi.org/10.1016/S0168-1923(00)00152-0).
- Zadra, A., D. Caya, J. Côté, B. Dugas, C. Jones, R. Laprise, K. Winger and L.-P. Caron, 2008. The Next Canadian Regional Climate Model. *La Physique au Canada* 64(2).
- Ziaco, E., F. Biondi, S. Rossi and A. Deslauriers, 2016. Environmental drivers of cambial phenology in Great Basin bristlecone pine. *Tree Physiology* 36(7): 818-831.
- Zweifel, R. and Häsler, R., 2000. Frost-induced reversible shrinkage of bark of mature subalpine conifers. *Agricultural and Forest Meteorology*, 102(4), pp.213-222.

## CHAPITRE II

# PERFORMANCE EVALUATION AND SENSITIVITY ANALYSES USING THE CANADIAN LAND SURFACE SCHEME (CLASS) FOR THE SIMULATION OF SOIL TEMPERATURE AND SOIL WATER IN THE BOREAL FOREST OF EASTERN CANADA

Article écrit par Shalini Oogathoo <sup>1</sup>

et révisé par Daniel Houle <sup>2,3</sup>, Daniel Kneeshaw <sup>1</sup>, Louis Duchesne <sup>2</sup>.

<sup>1</sup> Centre d'Étude de la Forêt, Université du Québec à Montréal, Case Postale 8888,  
Succursale Centre-Ville, Montréal, Quebec H3C 3P8, Canada.

<sup>2</sup> Direction de la Recherche Forestière, Ministère des Forêts, de la Faune et des Parcs du  
Québec, 2700 Einstein, Quebec City, Quebec G1P 3W8, Canada.

<sup>3</sup> Consortium sur la Climatologie Régionale et l'Adaptation aux Changements  
Climatiques (Ouranos), 550 Sherbrooke W, Montréal, Quebec H3A 1B9, Canada.

## 2.1 Résumé

Pour produire des projections réalistes, les modèles climatiques nécessitent une simulation précise de la transpiration. La simulation de la transpiration est affectée directement et indirectement par les valeurs de contenu en eau et de la température du sol, respectivement. Bien que certaines études aient utilisé le Schéma de surface Canadien (CLASS) pour simuler la température du sol et/ou le contenu en eau du sol, elles se sont principalement concentrées sur des écosystèmes autres que la forêt boréale et n'ont pas évalué les deux variables avec une grande résolution temporelle. Dans cette étude, des mesures quotidiennes à long terme de la température du sol et du contenu en eau du sol (2001 à 2016) sont utilisées pour évaluer la performance de CLASS à deux sites situés dans la forêt boréale humide de l'est du Canada. Des analyses de sensibilité ont ensuite été effectuées pour évaluer l'impact de l'épaisseur de la couche organique (TOL), la texture du sol (pourcentage de sable et d'argile, PSPC), le paramètre de drainage (DP) et le point de congélation (FP) sur la température du sol et le contenu en eau du sol. La température du sol a été bien simulée par CLASS, tandis que l'exactitude des simulations de contenu en eau variait selon le site, la saison et l'horizon du sol. Le contenu en eau liquide du sol modélisé a été grandement sous-estimé sur le site de d'épinette noire ( $8.7 \pm 2.4$  dans l'horizon B et  $2 \pm 2.6$  dans l'horizon C) pendant l'hiver, car la température du sol était inférieure à  $0\text{ }^{\circ}\text{C}$  causant l'accumulation de glace dans le sol. Néanmoins, la variation saisonnière correspondait bien aux observations. D'après les analyses de sensibilité, le TOL a eu un effet important sur la température du sol et le contenu en eau du sol. Bien que le PSC n'ait pratiquement aucun effet sur la température du sol, son effet sur le contenu en eau du sol était substantiel. Dans l'analyse DP, la température du sol a augmenté pendant l'été en raison de l'augmentation des flux de chaleur du sol entrants, causés par la simulation irréaliste de l'eau saturée du sol avec la diminution du drainage. La température du sol a augmenté tout au long de l'année et le contenu en eau liquide du sol a augmenté pendant l'hiver avec la

diminution du FP, toutefois le contenu en eau liquide du sol modélisée ne représentait pas bien les observations. En général, la température du sol a été bien simulée par CLASS, sauf pour le gel en hiver. Cependant, la simulation du contenu en eau du sol dans CLASS doit être améliorée. Nos analyses de sensibilité ont montré que même avec la variation des paramètres liés au contenu en eau du sol, ce dernier n'est pas beaucoup amélioré, soulignant ainsi la nécessité de revoir les équations régissant le contenu en eau du sol dans CLASS.

## 2.2 Abstract

Transpiration is a key component of the hydrological cycle, extracting large amounts of water from the soil and releasing it to the atmosphere, thus its accurate representation in models (such as Land Surface Schemes) is extremely important. However, modelled transpiration is affected directly and indirectly by modelled soil water and soil temperature, respectively. While some studies have used the Canadian Land Surface Scheme (CLASS) to simulate soil temperature or/and soil water, they focused mostly on ecosystems other than the boreal forest and did not evaluate both variables on a daily basis. In this study, long-term daily measurements of soil temperature and soil water (2001 to 2016) are used to evaluate the performance of CLASS at two sites in the humid boreal forest of eastern Canada. Subsequently sensitivity analyses were then carried out to evaluate the impact of thickness of organic layer (TOL), soil texture (percentage sand and clay, PSPC), the drainage parameter (DP), and freezing point (FP) on both soil temperature and soil water simulations. Soil temperature was well simulated by CLASS, while simulated values of soil water varied by site, season and soil horizon. Modeled soil liquid water was greatly underestimated at the black spruce site ( $8.7 \pm 2.4$  in horizon B and  $2 \pm 2.6$  in horizon C) during the winter compared to summer as soil temperature was below  $0^{\circ}\text{C}$ . Nevertheless, the seasonal variation corresponded well

with observations. Based on sensitivity analyses, TOL had an important effect on both soil temperature and soil water. Although PSPC had almost no effect on soil temperature, its effect on soil water was substantial. In the DP analysis, soil temperature increased during the summer via increasing incoming soil heat fluxes due to the unrealistic simulation of saturated soil water obtained due to decreasing drainage. Soil temperature increased throughout the year and soil liquid water increased during the winter with decreasing FP, yet, the modelled soil water did not well represent observations. In general, soil temperature was well simulated by CLASS, except for the freezing during winter. However, the simulation of soil water in CLASS requires improvement. Our sensitivity analyses showed that even with variation in the soil water related parameters used, the simulated soil water did not improve much, emphasizing the need to review the equations governing soil water in CLASS.

### 2.3 Introduction

Soil temperature and soil water are two fundamental land surface variables that have important impacts on many processes, especially in forest ecosystems, influencing seed germination (Milbau et al., 2009), nutrient availability via organic matter decomposition and soil mineralisation, nutrient assimilation by trees (Rennenberg et al., 2006), nutrient losses from tree canopies (Houle et al., 2016) and tree growth (Geßler et al., 2004). Soils receive water from the atmosphere via precipitation, but also release water back into the atmosphere via transpiration and soil/canopy evaporation and snow sublimation (Seneviratne et al., 2010). There is a close link between soil temperature and soil water content, the latter influencing the former via freezing and melting during winter/spring, where latent heat energy is released and absorbed, respectively (Subin et al., 2013).

Even though the beginning of the growing season in the boreal forest is driven primarily by air temperature and photoperiod (Rossi et al., 2008; Delpierre et al., 2019; Huang et al., 2020), soil water extraction by boreal trees depends on soil liquid water availability, which in turn depends on soil temperature and freezing point, especially in areas having a thin layer of ground and snow cover. The influence of air temperature on soil temperature is affected by the type of land cover and snow cover (Iijima et al., 2010). Both ground cover (such as organic and litter layers) and snow cover insulate soils, thus minimising temperature extremes. Warmer winter soil temperature due to snow insulation can be carried over into early summer (Gold, 1963; Williams and Smith, 1989), but late snowmelt can cool soils in the early part of the growing season (Jungqvist et al., 2014; D'Orangeville et al., 2016). While snow cover is seasonal, the organic/litter layer is present throughout the year. The organic layer reduces both soil heat loss towards the atmosphere in fall and winter (MacKinney, 1929; Napoly et al., 2017) and soil heat gain from incoming solar radiation in the spring and summer (Bonan and Shugart, 1989).

Different structured and textured soils also influence drainage of water and the ease of water extraction by plants, as well as the freezing point of water in the soil. Fine textured soils (clays) have high porosity with greater capillary water for absorption by plants, while coarse textured soils (e.g. sands) have low porosity with greater gravitational water draining out of the soil column. On the other hand, compacted soil, which normally increases with soil depth, has a reduced soil hydraulic conductivity thereby decreasing soil drainage. As well as influencing soil water, the freezing point is also lowered by the presence of small soil pores (Johnsson and Lundin, 1991), which in turn depends on soil texture, structure and degree of compaction. Liquid water in soil can thus also be found even when sub-freezing soil temperatures are observed.

The simultaneous measurement and simulation of soil temperature and soil water on a daily basis is essential to capture or predict the effect of crucial short-term

meteorological events. These include severe short-duration droughts, or minimum soil water levels critical for growth, or the number of days having extreme high soil temperatures and/or extreme low soil water content during the growing season. The Canadian Land Surface Scheme (CLASS; Verseghy, 1991; Verseghy et al., 1993) is a land surface model developed especially to simulate the exchange of water and heat with the Canadian Regional Climate Model (CRCM). CLASS has been evaluated for its ability to simulate soil temperature (Tilley et al., 1997; Bellisario et al., 2000; Munro et al., 2000; Marchand et al., 2018) and soil water (Wen et al., 1998; Yuan et al., 2007; Dumedah et al., 2011; MacDonald et al., 2016) or both (Luo et al., 2003; Wen et al., 2007; Paquin and Sushama, 2015). However, most of the above-mentioned studies were conducted in wetlands, wooded wetlands, flooded/near-saturation forests, subalpine forest, coastal temperate rainforest, permafrost, tundra, agricultural lands and prairies. Furthermore, these studies only used data measured at weekly (Wen et al., 1998; Munro et al., 2000) or monthly intervals (Paquin and Sushama, 2015) and over short-time periods (Bellisario et al., 2000; Wen et al., 2007; Yuan et al., 2007; Dumedah et al., 2011). Marchand et al. (2018) used a long time-series of soil temperature data but the data were measured only at a 5 cm depth. The exception (Luo et al., 2003) carried out in a boreal forest located in Russia was based on several years (~ 16) of daily measured soil temperature, but had only 1 to 3 measurements of soil water taken every month. The performance of CLASS for long-term simulation of daily soil temperature and water content over many years and at different soil depths has never been evaluated, especially for the boreal forest of Eastern Canada.

As per Ukkola et al. (2016a; 2016b), a misrepresentation of soil temperature and soil water in land surface schemes affects other land surface processes. The latter studies show that accurate simulation of soil water is critical for the simulation of latent heat flux variation and evapotranspiration in LSSs, especially during dry periods. Ukkola et al. (2016a; 2016b) recommended a comprehensive re-assessment of LSSs, especially during extreme events, in order to identify inconsistencies and consequently to improve

hydrological processes in order to accurately simulate soil water. The accurate simulation of soil temperature and soil water in LSSs is a prerequisite for increasing the confidence in the projections of climate models on future extreme events such as drought (Ukkola et al., 2016a). Henceforth, the assessment of LSSs using long-term observations at a smaller temporal resolution is important in order to examine the ability of LSSs to capture the long-term average behaviour as well as extremes in soil temperature and soil water. My first hypothesis of this chapter is that CLASS simulates well both soil temperature and soil water on a daily basis in all seasons (winter and summer) both in magnitude and seasonal variation. Thus, the first objective of this study is to use a long time series of daily soil temperature and soil water measurements to evaluate the performance of CLASS for soil temperature and soil water at a fine temporal scale.

In addition to studies evaluating model performance, sensitivity analyses studies are equally important as they evaluate the robustness and sensitivity of parameters within a model. To date, the few sensitivity analyses studies carried out with CLASS for specific variables have shown that CLASS performs well but is highly sensitive to soil depth and composition, incoming solar radiation and initial soil moisture conditions (Tilley et al., 1997), as well as atmospheric and canopy parameters (Wang et al., 2001; Bartlett et al., 2006; Wang et al., 2016). Our study sites are located in boreal forests where the thickness of the organic (litter) layer, soil texture, soil drainage and freezing point might impact both soil temperature and soil water. My second hypothesis is that CLASS is sensitive to the following model parameters (thickness of organic layer, soil texture and drainage, and freezing point) for the simulation of soil temperature and soil water. Thus, the second objective of this study is to conduct sensitivity analyses to evaluate the effect of the thickness of the organic layer, soil texture, model drainage parameter and freezing point on soil temperature and soil water.

## 2.4 Methods

### 2.4.1 Description of study areas

There are two study sites, where the first one is a balsam fir dominated stand ( $47^{\circ} 19' 41''$  N and  $71^{\circ} 07' 37''$  W) and the second is a black spruce dominated stand ( $49^{\circ} 12' 45''$  N and  $73^{\circ} 39' 00''$  W), both located in the Quebec province in Canada. Their elevations are 784 m and 411 m above sea level, respectively. The mean annual temperature is  $1.3^{\circ}\text{C}$  at both the balsam fir and black spruce sites for the period from 2001 to 2016. The mean annual precipitation is 1300 mm at the balsam fir and 941 mm at the black spruce site for the period 2001 to 2016.

### 2.4.2 Measured data

Climate variables were measured on an hourly basis at both forest sites, which were used as input for CLASS. These climate variables are photosynthetic active radiation (solar radiation in the visible range (400 to 700 nm wavelength) used for photosynthesis) and wind speed measured from a flux tower at 14 m height; air temperature and relative humidity measured at a height of 3.3 m, and precipitation measured at ground level. The snow cover depth was measured close to the instrumented trees with ultrasonic sensors (SR50 type sonic distance sensor, Campbell Scientific inc.). All climate data are available from 1999 to 2016 at the balsam fir site and from 1997 to 2016 at the black spruce site.

Soil water content (CS615, Campbell Scientific, Logan, UT) and soil temperature were measured hourly and averaged on a daily basis in 3 and 4 pedons at the black spruce and balsam fir sites, respectively. Both soil temperature and soil water probes were calibrated prior to installation at their respective soil profiles. The mean values of the soil properties for these pedons were used to parameterise CLASS at each site. For each pedon, measurements were carried out at three depths: 2 cm above the mineral horizon

(humus layer: hum), 22 cm below the mineral soil surface (horizon B: horB) and 81 cm below the mineral soil surface (horizon C: horC). For model validation, all three soil horizons were used for soil temperature whereas only soil horizons B and C were used for soil water content. In this study, the black spruce site has data for 21 years (since 1997) and the balsam fir site has data for 19 years (since 1999). This almost two-decades of daily observations of soil temperature and soil water enables us to study long-term climate variability at a fine temporal resolution, which is not possible with only a few years of daily observations or weekly/monthly observations.

#### 2.4.3 Canadian Land Surface Scheme (CLASS)

The CLASS model was developed by the Canadian Climate Centre to be used in the Canadian Regional Climate Model (CRCM; Zadra et al., 2008). CLASS allows the exchange of water and energy with the atmospheric component of CRCM. CLASS models the hydrological cycle in a one-dimensional column, at a time step of 30 mins. The model consists of a layer of vegetation, a single snow layer of variable depth and multiple soil layers of varying thicknesses. The vegetation in the model is grouped into four categories: broadleaves, conifers, crops, and grass. Each model grid is divided into four sub-grids based on the land cover types: 1) bare soil; 2) soil covered with snow; 3) soil covered with vegetation; 4) and vegetation over snow-covered soil. The energy and mass balances are calculated for each sub-grid and the composite energy and mass balance are determined for each grid by doing a weighted average based on the area occupied by each land cover type (Verseghy, 1991; Verseghy et al., 1993).

In CLASS, porosity and saturated hydraulic conductivity are a function of percentage of sand only, while hydraulic conductivity is a function of porosity, saturated hydraulic conductivity and the Clapp & Hornberger (1978) empirical  $b$  parameter (Verseghy, 2012). The latter in turn, is a function of the percentage of clay (Verseghy, 2012). Thus, infiltration/percolation in CLASS, which is controlled by hydraulic conductivity, depends on the percentage of both sand and clay. However, CLASS incorporates an

additional drainage parameter (XDRAIN) that ranges from 0 (no infiltration/percolation) to 1 (infiltration/percolation based on the hydraulic conductivity of the soil layer) to allow for water flow at the bottom of the soil profile. The final hydraulic conductivity for each soil layer is quantified as the product of the hydraulic conductivity of that layer and the drainage parameter.

#### 2.4.3.1 Model inputs for CLASS

##### 2.4.3.1.1 Climate data

The climate variables required by CLASS are incoming shortwave radiation ( $\text{W m}^{-2}$ ), downwelling longwave radiation ( $\text{W m}^{-2}$ ), precipitation ( $\text{mm s}^{-1}$ ), air temperature ( $^{\circ}\text{C}$ ), specific humidity ( $\text{kg kg}^{-1}$ ), wind speed ( $\text{m s}^{-1}$ ), and atmospheric pressure (Pa) at 30-min intervals. The hourly measured data (incoming shortwave radiation, precipitation, air temperature, and wind speed) were assumed not to vary greatly within an hour, thus each hourly observation was duplicated to obtain two half-hourly observations so as to be compatible with the time-step of the input data required by the CLASS model.

Downwelling longwave radiation ( $R_{ldc}$ ) was estimated using the equation of Sugita and Brutsaert (1993; Eq 2.1), where  $\varepsilon_{ac}$  is atmospheric emissivity under clear skies,  $\sigma$  is the Stefan-Boltzmann constant,  $T_a$  is air temperature in kelvin near the ground.  $\varepsilon_{ac}$  was determined using the equation of Brutsaert (1975; Eq 2.2), where  $\rho_a$  is ambient vapour pressure (hPa),  $a_3$  is 0.98 and  $b_3$  is 0.0687 (Sugita and Brutsaert, 1993).

$$[R_{ldc} = \varepsilon_{ac} \sigma T_a^4] \quad \text{Eq. 2.1}$$

$$\varepsilon_{ac} = a_3 (\rho_a / T_a)^{b_3} \quad \text{Eq. 2.2}$$

Atmospheric pressure ( $P_h$ ) was estimated using the barometric formula (Eq. 2.3), where  $P_0$  is atmospheric pressure at sea level (101.3 kPa),  $m$  is the mass of one molecule

( $0.02896 \text{ kg mol}^{-1}$ ),  $g$  is acceleration due to gravity ( $9.807 \text{ m s}^{-2}$ ),  $h$  is the altitude above sea level (m), and  $R$  is the universal gas constant ( $8.3143 \text{ J mol}^{-1}\text{k}^{-1}$ ).

$$P_h = P_0 \exp^{-mgh/RT} \quad \text{Eq. 2.3}$$

Specific humidity ( $q$ ) was calculated using Eq. 2.4, where  $MR$  is the mixing ratio. The latter was determined using Eq. 2.5, where  $\varepsilon$  is the ratio of molecular weight of water and dry air (0.62198),  $\rho_a$  is actual vapour pressure (Pa) and  $P_h$  is atmospheric pressure. Actual vapour pressure was calculated using Eq. 2.6, where  $RelHum$  is relative humidity (%). The saturation vapour pressure  $\rho_s$  (Pa) was determined using Eq. 2.7, where  $T$  is air temperature in degrees Celsius (Campbell and Norman, 2012).

$$q = MR/(MR + 1) \quad \text{Eq. 2.4}$$

$$MR = \varepsilon(\rho_a/(P_h - \rho_a)) \quad \text{Eq. 2.5}$$

$$\rho_a = \rho_s(RelHum/100) \quad \text{Eq. 2.6}$$

$$\rho_s = 611e^{(17.502T/(T+240.97))} \quad \text{Eq. 2.7}$$

#### 2.4.3.1.2 Initialisation parameters

Initialisation parameters are required to describe vegetation and soil properties (Versegny, 2012). For most of the parameters, default values (Appendix A) for the model were used except for parameters presented in Table 2.1 where measured values were used. The top layer (humus layer) was configured as a peat layer of fibric type (Letts et al., 2000).

Table 2.1: Initialisation parameters used in CLASS

Parameters	Balsam fir	Black spruce
Vegetation properties		
For plant functional type 1 (needleleaf):		
○ Log of roughness length (m)	0.438	0.182
○ Above-ground canopy mass (kg m <sup>-2</sup> )	18.5	14.6
○ Maximum rooting depth (m)	0.81	0.52
Soil properties		
○ Soil permeable depth (m)	1	1
○ Sand (%): horB / horC	69.8 / 83.0	86.9 / 89.0
○ Clay (%): horB / horC	5.5 / 4.1	2.0 / 0.8
○ Organic matter (%) *: horB / horC	3.2 / 0.5	1.7 / 0.3
○ Soil layer thickness (m) hum / horB / horC	0.17 / 0.30 / 0.60	0.13 / 0.30 / 0.60

\* Ouimet and Duchesne, 2005

#### 2.4.4 Analyses

The performance of CLASS was evaluated without calibration for the simulation of soil temperature and soil water on a daily basis. For soil temperature, averages of the soil profiles were used to evaluate the model at both sites (average of 3 soil profiles at the black spruce and an average of 4 soil profiles at the balsam fir site). For soil water, some probes yield temporal variations that were unexpected, mainly due to the development of saturation conditions in the soil profile due to lateral water fluxes. At the black spruce site, soil profiles 2 and 3 had very high soil water throughout the summer in the HorC (near saturation) and a high peak in several years at the beginning of summer in HorB (Figure 2.1). Similarly, for the balsam fir site, there was an

increase/decrease pattern in soil water after some years in soil profiles 2 and 3 in HorB and HorC respectively, while soil profile 1 had a near-saturation soil water content during the summer in HorC. Currently, CLASS is not formulated to simulate lateral soil water fluxes. Thus, at both sites, only the soil profiles having consistent observations in all years of measurement in all soil layers were considered for this study, which are soil profile 1 at the black spruce site and soil profile 4 at the balsam fir site.

Local sensitivity (one-at-a-time method) analyses were carried out in CLASS to evaluate the effect of the thickness of the organic layer (top layer), percentage of sand and percentage of clay, drainage factor, and freezing point on soil temperature and soil water. A problem-oriented approach was adopted for the selection of these specific model parameters in order to improve model simulation for soil temperature and soil water. Table 2.2 summarizes the configuration of these sensitivity analyses, where the model parameters were varied within reasonable ranges that reflect the site characteristics and observations. For the organic matter sensitivity analysis, the type of organic matter was defined as fibric (Verseghy, 2012). The percentage of sand was varied by  $\pm 10$  % from the baseline model configuration for both sites. For clay, the percentage was varied by  $\pm 4$  % from the baseline model configuration at the balsam fir site, but varied from 0 to less than 10 % at the black spruce site. The drainage factor sensitivity analysis was carried out by decreasing the XDRAIN parameter from 1 up to 0.001 to reduce the amount of water draining out of the soil column. While the default freezing point in CLASS is 0 °C, liquid water is in reality still present in soil pores down to a temperature of -6 °C (Verseghy, 1991). Thus, the freezing point was varied from 0 (base scenario) to -6 °C in the freezing point sensitivity analysis in order to evaluate its effect on soil temperature and soil water, especially during the winter/snowmelt period.

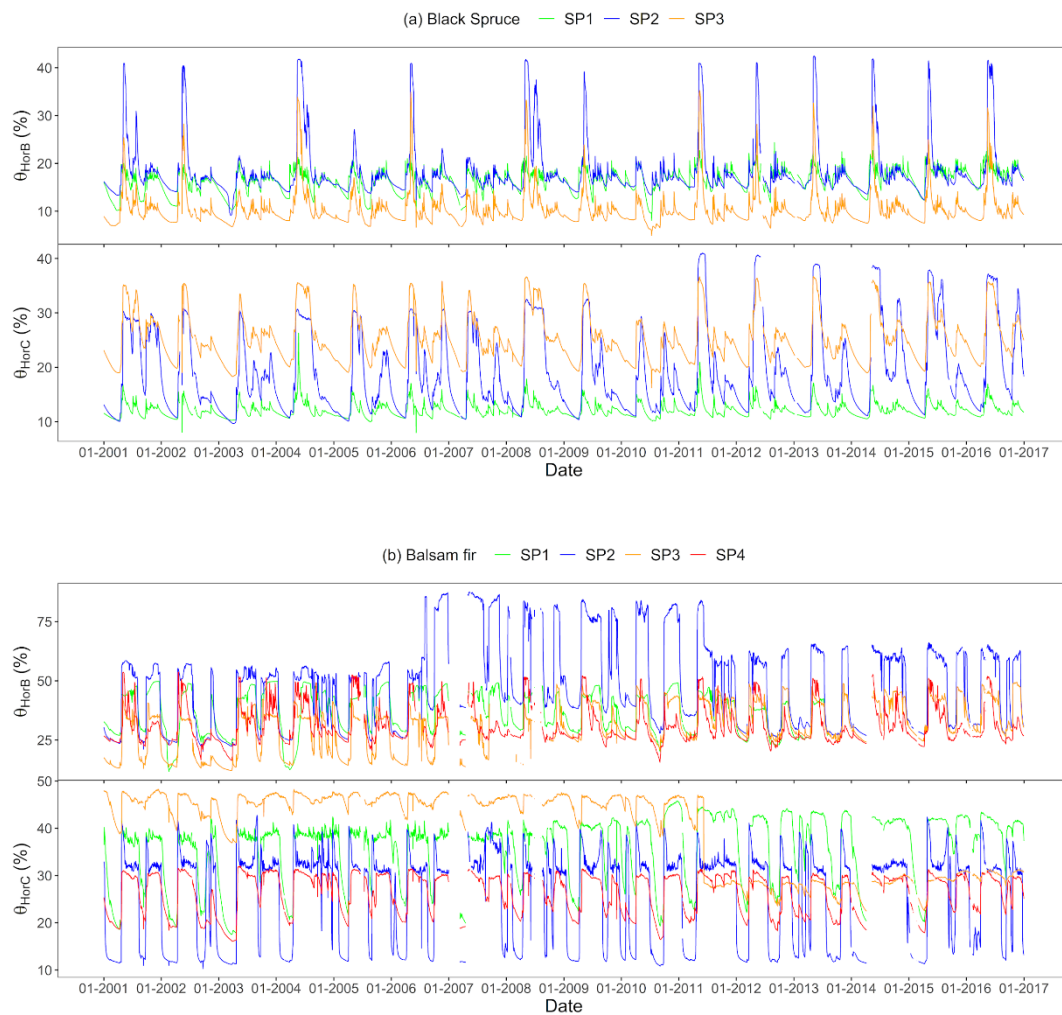


Figure 2.1: Observations of daily soil water at the three soil profiles (SP1 to SP3) at the black spruce (a) and four soil profiles (SP1 to SP4) in the B and C horizons at the balsam fir (b) sites.

Table 2.2: Summary of sensitivity analyses carried out at the balsam fir and black spruce sites

	Black spruce		Balsam fir	
	Baseline	Scenarios	Baseline	Scenarios
Thickness of organic matter (TOL; cm)				
Hum	13	6; 20	17	8; 26
Percentage of sand (PS; %)				
HorB	86.9	77; 97	69.8	60; 80
HorC	89	79; 99	83	73; 93
Percentage of clay (PC; %)				
HorB	2	0; 4; 8	5.5	1.5; 9.5
HorC	0.8	0; 2.8; 6.8	4.1	0.1; 8.1
Drainage parameter, XDRAIN (DP; -)				
	1	0.001; 0.01; 0.1	1	0.001; 0.01; 0.1
Freezing point (FP; °C)				
	0	-2; -4; -6	0	-2; -4; -6

The model was run from August 1999 to 2016 at the balsam fir site and from August 1997 to 2016 at the black spruce site. The model simulation was started in summer (August) at both sites in order to avoid erroneous snow conditions when initialising the model. Moreover, the first 3-5 years (at balsam fir/black spruce sites) were excluded from the analyses for model spin-up and only the years 2001 to 2016 were used for the evaluation. CLASS was found to have a model spin-up time of 2 years and less in a tropical forest (Yang et al., 1995). The purpose of the model spin-up is to allow the model to reach an equilibrium state after model initialisation, especially for the soil moisture content. In this study, the initial conditions set up in CLASS at both sites were taken from an output of the coupled CLASS-CRCM previous simulation (at the two grids where the two sites are located) in order to reduce the model spin-up time

(Cosgrove et al., 2003). The performance of CLASS was evaluated using Pearson correlation ( $r$ ), Kling-Gupta Efficiency (KGE) and root mean square error (RMSE). The KGE was chosen as a performance metric as it is considered to be an improved version of Nash-Sutcliffe Efficiency (Gupta et al., 2009). KGE incorporates correlation, relative variability and bias, whereby the relative variability calculates the variance in the observation compared to the simulation. On the other hand, the bias is the ratio of the simulation mean over the observation mean. For the sensitivity analyses, Taylor diagrams were used to evaluate model performance as they allow for efficient comparison of multiple simulations via three model performance metrics, which are Pearson's correlation coefficient, RMSE and standard deviation. The best model is identified as the one closest to the observation (i.e., the reference point in the x-axis), or the one having the highest Pearson's correlation coefficient and lowest RMSE with a similar standard deviation as the observation.

## 2.5 Results

### 2.5.1 Soil temperature

CLASS simulated very well the annual pattern of soil temperature at both sites, except for some slight overestimations in some years in the HorC layer at the balsam fir site during summer and slight underestimation in all soil layers at the more northern black spruce site during winter (Figures 2.2a and 2.2b). All three performance metrics showed that the model adequately simulates soil temperature, with  $r$  above 0.96 at both sites, KGE values were above 0.69 at the black spruce and above 0.88 at the balsam fir site (Figure 2.3). Model error was very low, with maximum RMSE of 2.27 at the black spruce and 1.26 at the balsam fir site.

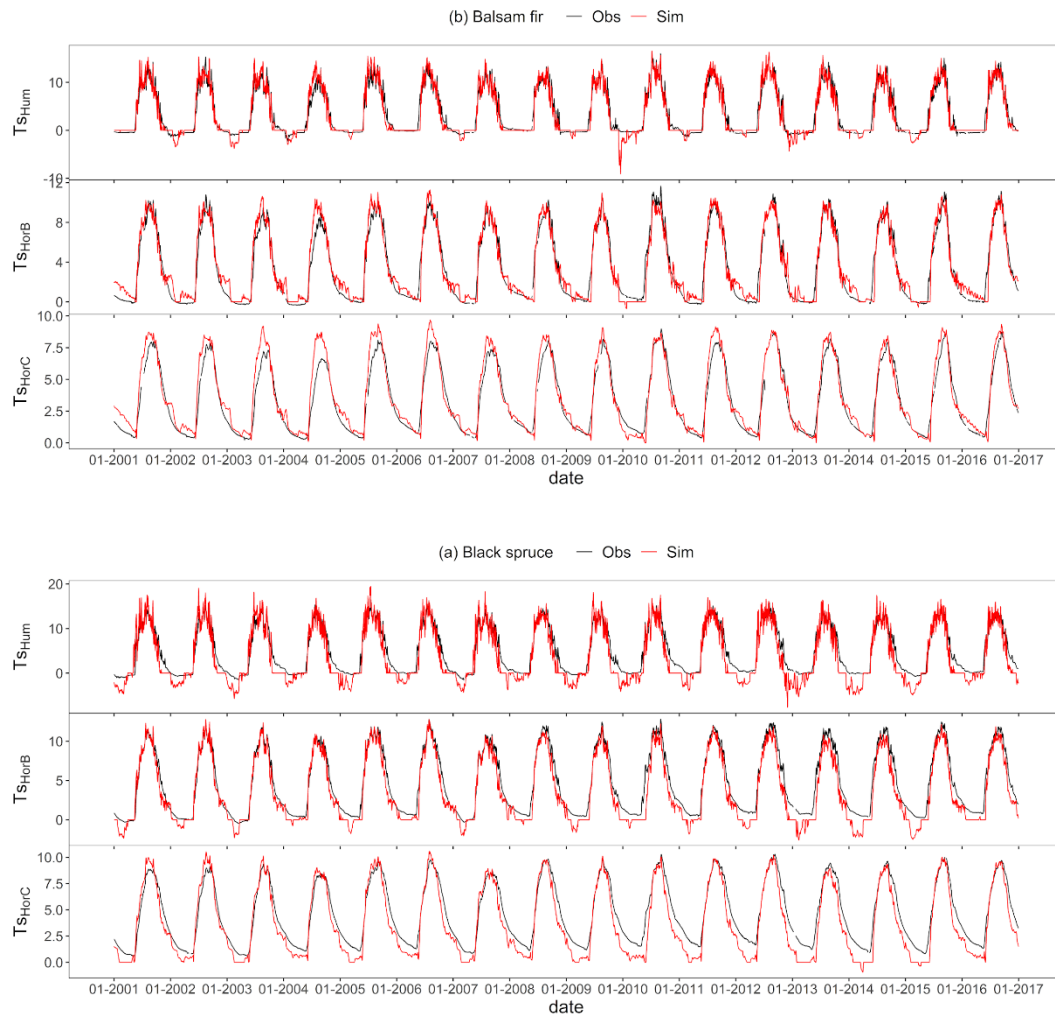


Figure 2.2: Observed and simulated daily soil temperature ( $^{\circ}\text{C}$ ) for the humus layer (top), horizon B (middle) and C (bottom) at black spruce (observed  $T_s$  is mean of 3 soil profiles; a) and balsam fir (observed  $T_s$  is mean of 4 soil profiles; b) sites from 2001 to 2016.

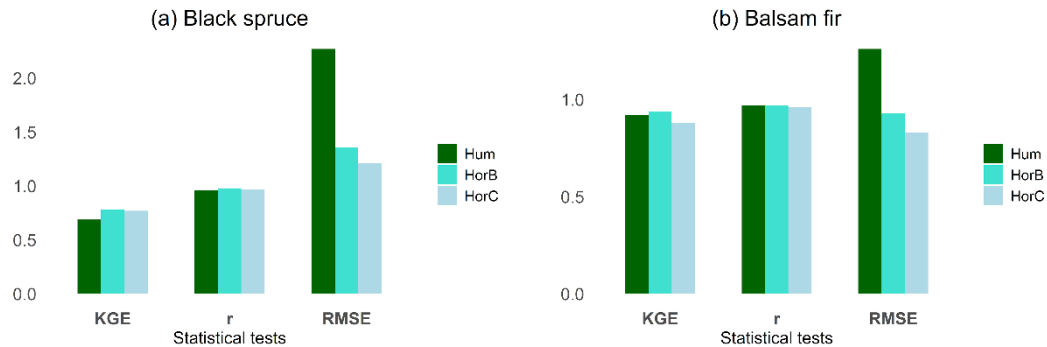


Figure 2.3: Performance metrics of Kling-Gupta Efficiency (KGE), Pearson's correlation ( $r$ ), and root mean square error (RMSE) at black spruce (a) and balsam fir (b) sites for soil temperature for the three soil horizons (Hum, HorB and HorC) for the entire year.

### 2.5.2 Soil water

Figures 2.4a and 2.4b show the observed and simulated soil water content in the two soil layers at the black spruce and the balsam fir sites, respectively. Soil water was underestimated in both soil layers throughout the year at the balsam fir site, but only during winter in the HorB at the black spruce site. In summer, simulated soil water closely matched observations in the HorB, but was slightly overestimated in the HorC at the black spruce site. Based on the KGE values, the model performance appeared to be better at the balsam fir site (positive KGE values) than at the black spruce site (negative KGE values). However, the negative KGE values at the black spruce site were due to the poor model performance during winter (Figure 2.5). On the other hand, Pearson's coefficient ( $r$  values) at the black spruce site was comparable to that at the balsam fir site during winter and better during summer. The model errors (RMSE values) were less than 6.60 at the black spruce site, while it was much higher at the balsam fir site (9.31 to 14.2) in all soil layers for all periods.

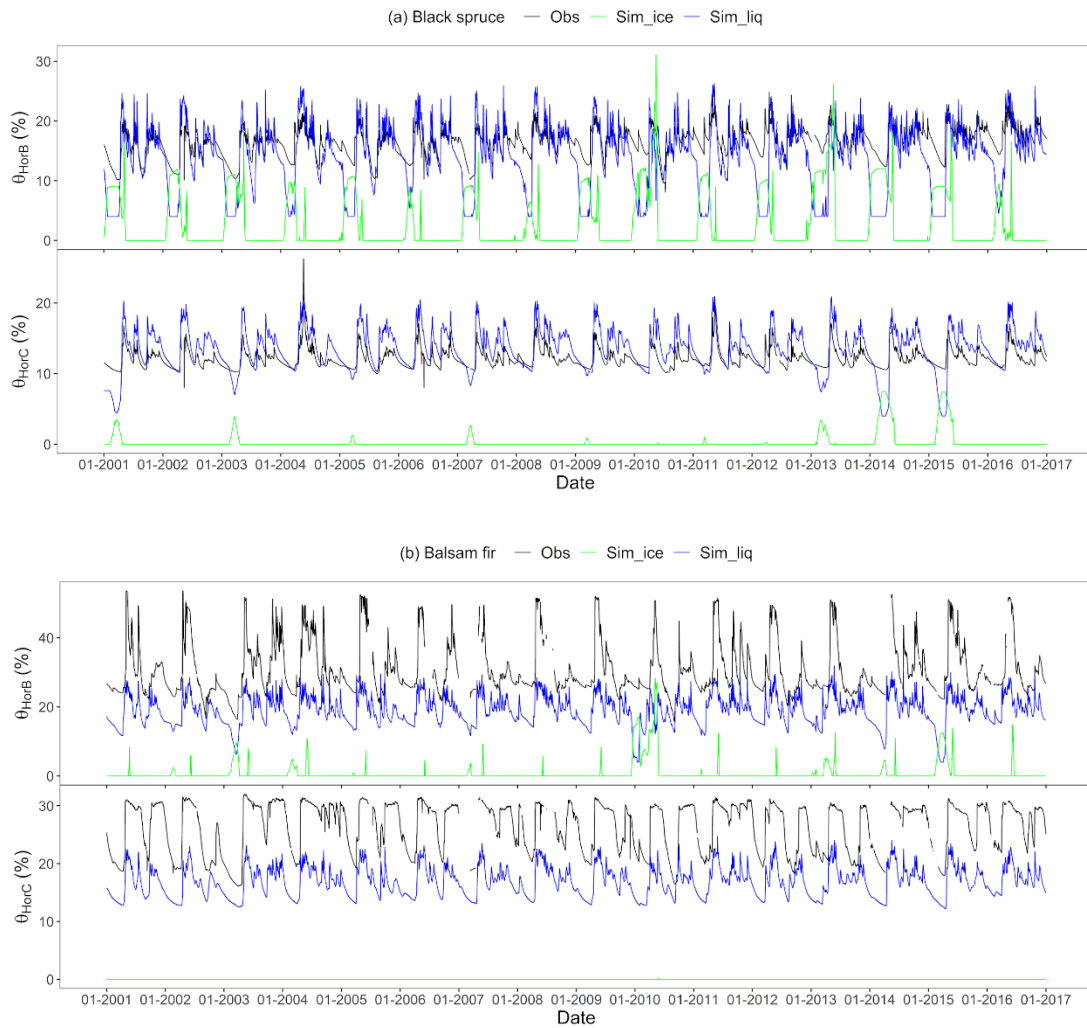


Figure 2.4: Observed and simulated daily soil water (%) for horizons B (top) and C (bottom) at the black spruce (a) and balsam fir (b) sites from 2001 to 2016.

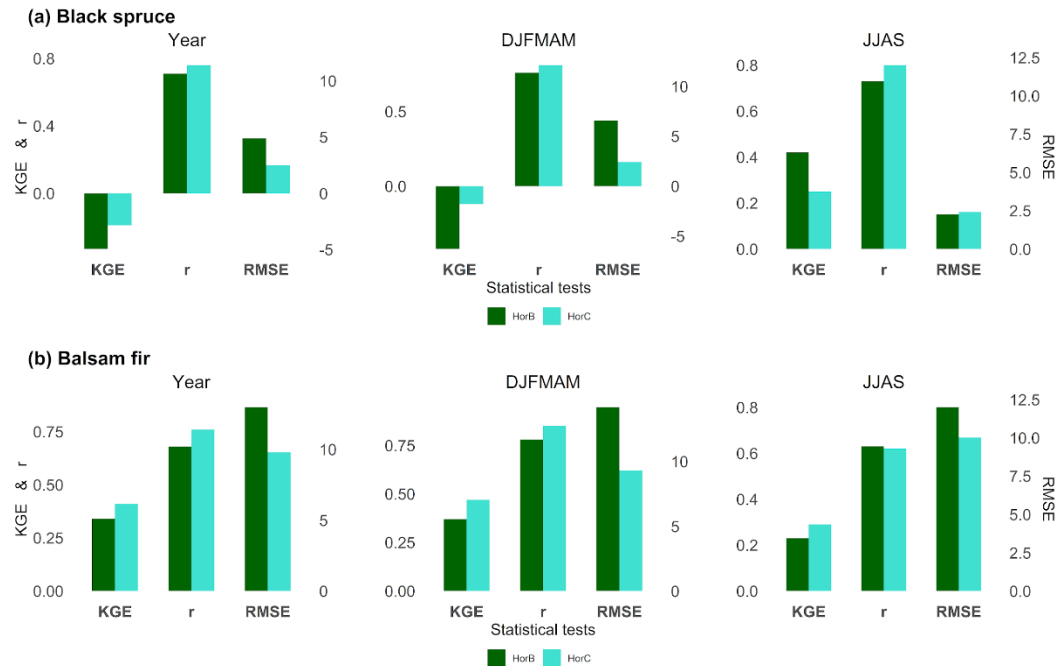


Figure 2.5: Performance metrics of Kling-Gupta Efficiency (KGE), Pearson's correlation ( $r$ ), and root mean square error (RMSE) at black spruce (a) and balsam fir (b) sites for soil liquid water for the two soil horizons (HorB and HorC) for an entire year (Year), winter/spring (DJFMAM) and summer (JJAS) periods.

### 2.5.3 Sensitivity analysis

#### 2.5.3.1 Thickness of the organic layer

Figures 2.6 and 2S.2 (left panel) shows how simulated daily soil temperature and soil water are sensitive to variation in the thickness of the organic layer (TOL) at the balsam fir and black spruce sites, respectively. The results show that the soil temperature decreases in summer while it increases in winter with increasing TOL at both sites. Based on the Taylor diagrams, the base simulation was closest to observations most of the time in horizons B and C, while the thickness of the organic layer simulations (OM26 and OM20) was closest to observations of the humus layer for soil temperature (Figures 2.8 and 2S.4, left).

Soil water increased with increasing TOL during winter and spring in all soil layers at both sites, except in Hum at the black spruce site. During the summer, soil water increased slightly in Hum, but this increase was almost negligible in both the HorB and HorC. The thickest organic layer simulations (OM26 and OM20) usually led to the best model performance in all soil layers at both sites in both seasons and throughout the year (Figures 2.8 right, 2.9, 2S.4 right and 2S.5).

#### 2.5.3.2 Percentage of sand and clay

The effect of % sand (PS) and % clay (PC) on soil temperature was barely noticeable in all soil layers at both sites (Figures 2.6 and 2S.2, top right), with model performance being almost the same among all simulations (Figures 2.8 and 2S.4, left).

As for soil water, the PS & PC effect were negligible in Hum, but substantial in HorB and HorC at both sites throughout the year. Soil water substantially increased with decreasing PS and increasing PC in both HorB and HorC at both sites (Figure 2.6 and 2S.2, bottom right). While there was no clear and consistent pattern in model performance among the simulations at the balsam fir site (Figures 2.8 right and 2.9), the highest PS led to the best model performance at the black spruce site (Figures 2S.4 right and 2S.5).

#### 2.5.3.3 Drainage parameter

Decreasing the drainage parameter (DP) did not impact the soil temperature during the summer at either site, except during the smallest DP simulation where soil temperature increased substantially (DRN0.001; Figures 2.7 and 2S.3; top left). On the other hand, during the winter, all DP simulations had a weak (balsam fir site) to slightly noticeable (black spruce site) impact on soil temperature, which increased with decreasing DP. The model performance of the three DP simulations (base, DRN0.1 and DRN0.01) were almost the same and closer to observations in all soil layers at both sites, while

the smallest DP simulation was further away from observations and had the poorest performance (Figures 2.8 and 2S.4, left).

Soil water increased in general with decreasing DP during both summer and winter at both sites (Figures 2.7 and 2S.3, bottom left). While this increase in soil water was apparent only for the simulation using the smallest DP (DRN0.001) in the Hum layer, it became more pronounced with soil depth for the other DP simulations. Compared to the other DP simulations, DRN0.001 simulated an almost saturated soil water in all three soil layers during the summer. Model performance was lowest in the DRN0.001 simulation in all soil layers, but highest in the base (DRN1) simulation in most cases for all periods at both sites (Figure 2.8 right, 2.9, 2S.4 right and 2S.5).

#### 2.5.3.4 Freezing point

Soil temperature increased throughout the year in all soil layers at both sites as the soil water freezing point (FP) decreased (Figures 2.7 and 2S.3, top right). Furthermore, this increase in soil temperature augmented with soil depth and was more pronounced in summer than in winter. However, the model performance for soil temperature did not change much among the FP simulations in any of the soil layers at both sites, although the base simulation had the best performance in most cases (Figures 2.8 and 2S.4, left).

Soil water decreased slightly with decreasing FP during summer in all soil layers at both sites (Figures 2.7 and 2S.3, bottom right). On the other hand, from fall through winter up to the end of the snowmelt period soil water content increased with decreasing FP in all soil layers at both sites, except in the Hum layer in the winter at black spruce. The model performance for soil water did not differ much among the FP simulations during the summer, but the base simulation was best in the HorB and HorC layers during the winter and throughout the entire year at both sites (Figures 2.8 right, 2.9, 2S.4 right and 2S.5).

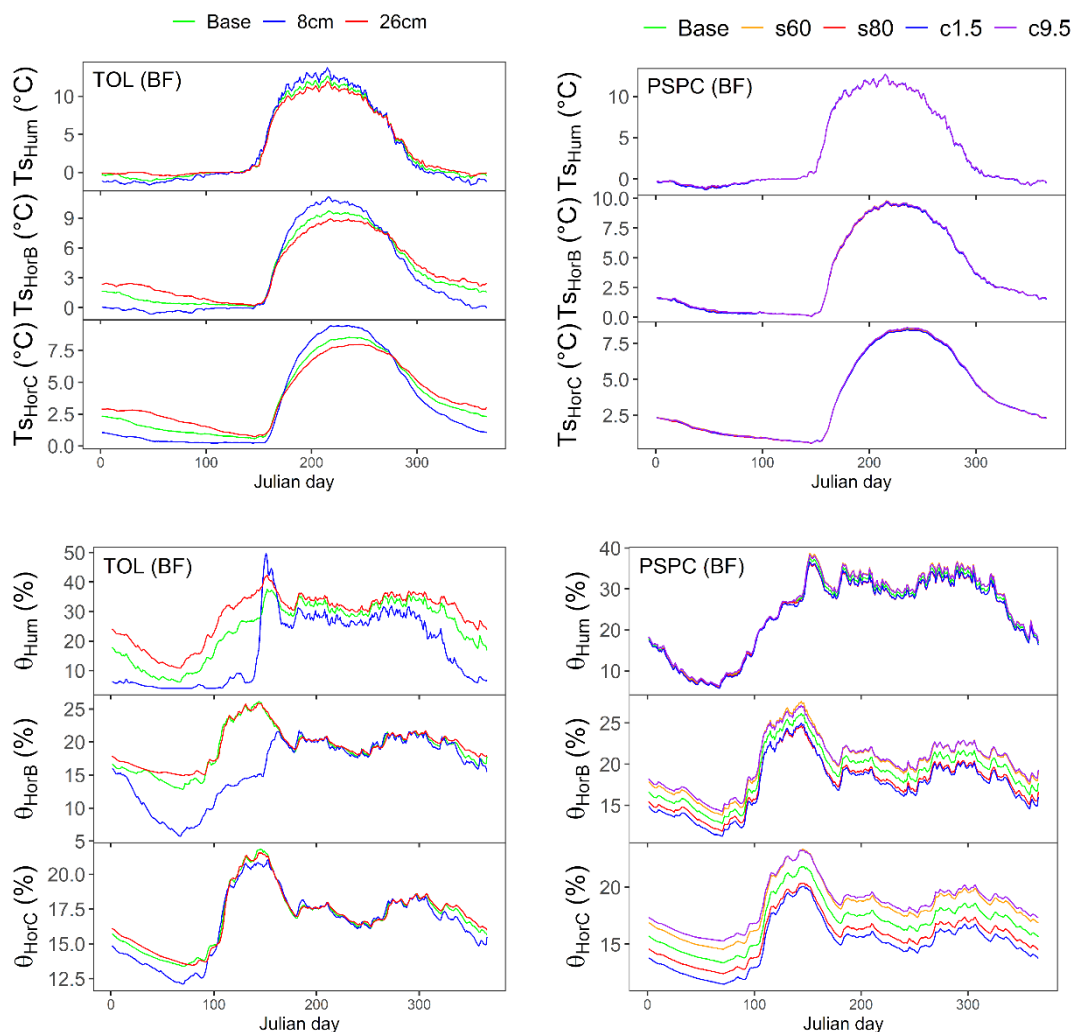


Figure 2.6: Sensitivity analysis of the thickness of the organic layer (TOL; left panel) and of % of sand and % of clay (PSPC; right panel) on multiyear (2001 to 2016) average daily soil temperature (top) and soil liquid water (bottom) at balsam fir (BF) site.

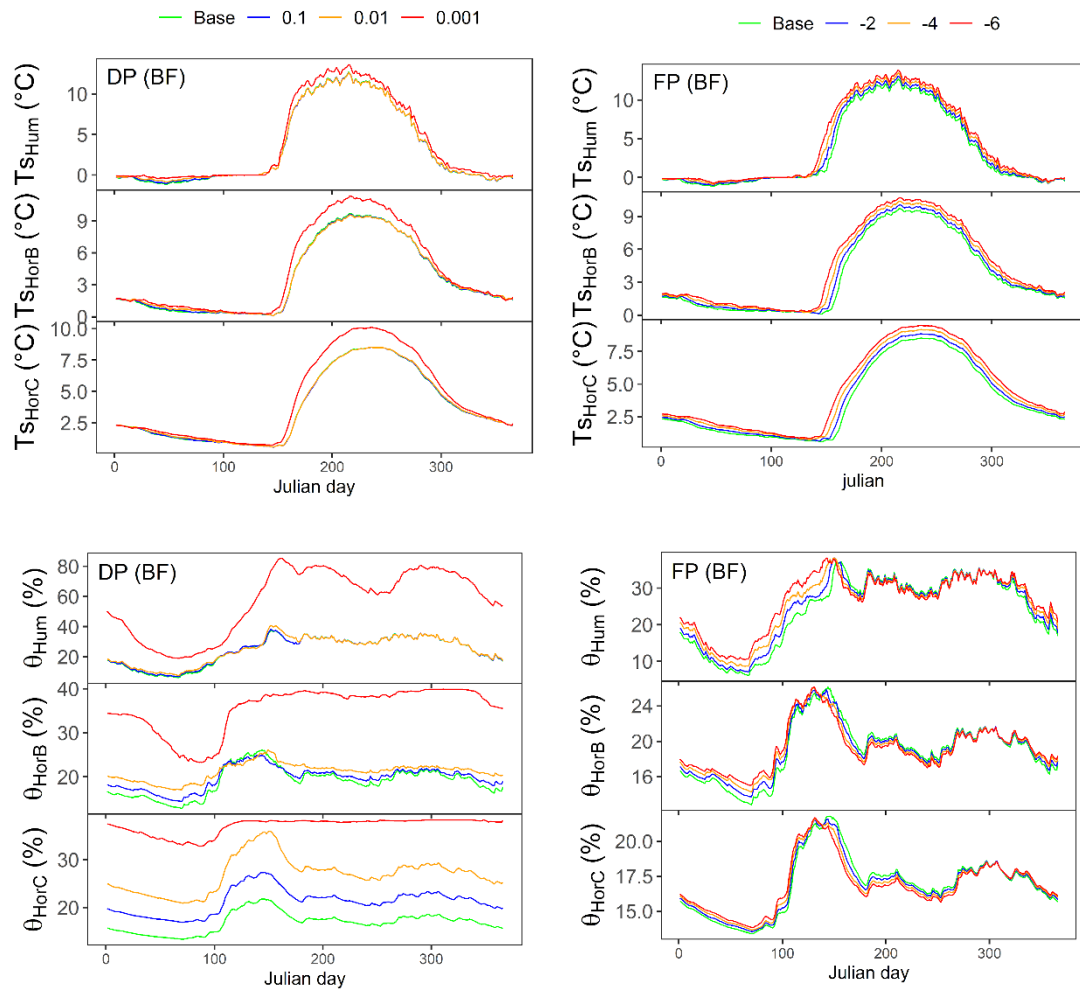


Figure 2.7: Sensitivity analysis of the drainage parameter (DP; left panel) and of freezing point (FP; right panel) for multiyear (2001 to 2016) average daily soil temperature (top) and soil liquid water (bottom) at the balsam fir site.

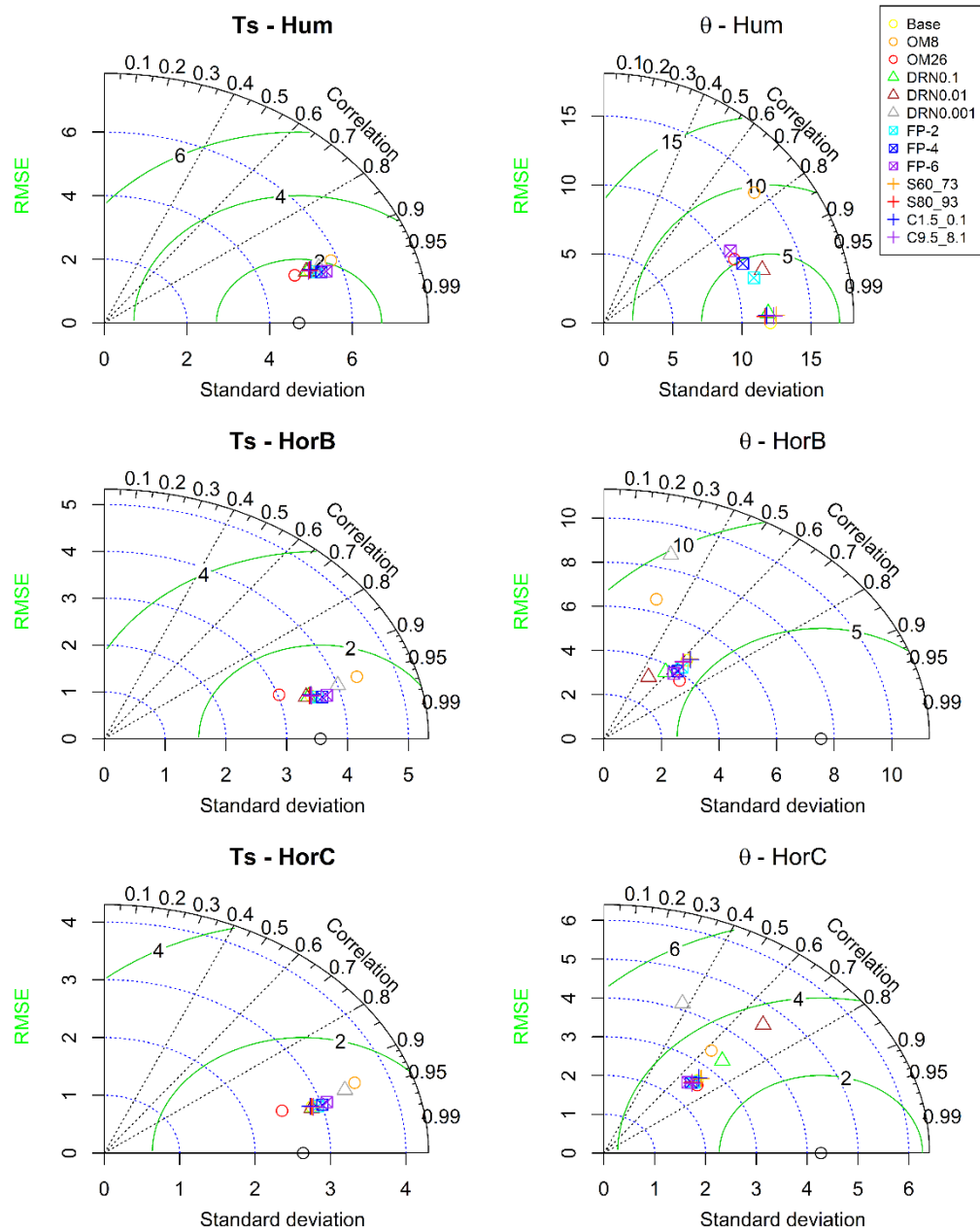


Figure 2.8: Taylor diagrams of observations vs simulations of all sensitivity analyses for soil temperature (Ts; left) and soil liquid water ( $\theta$ ; right) for the three soil horizons (Hum, HorB and HorC) at the balsam fir site. The reference point is the black circle (observations) located on the x-axis for all soil layers, except for soil water in the Hum layer which is represented by a yellow circle (base simulation). Green arcs are RMSE; blue dotted arc are standard deviation; dotted black radial lines are correlation. OM: organic matter; DRN: drainage; FP: freezing point; S: percentage sand; C: percentage clay.

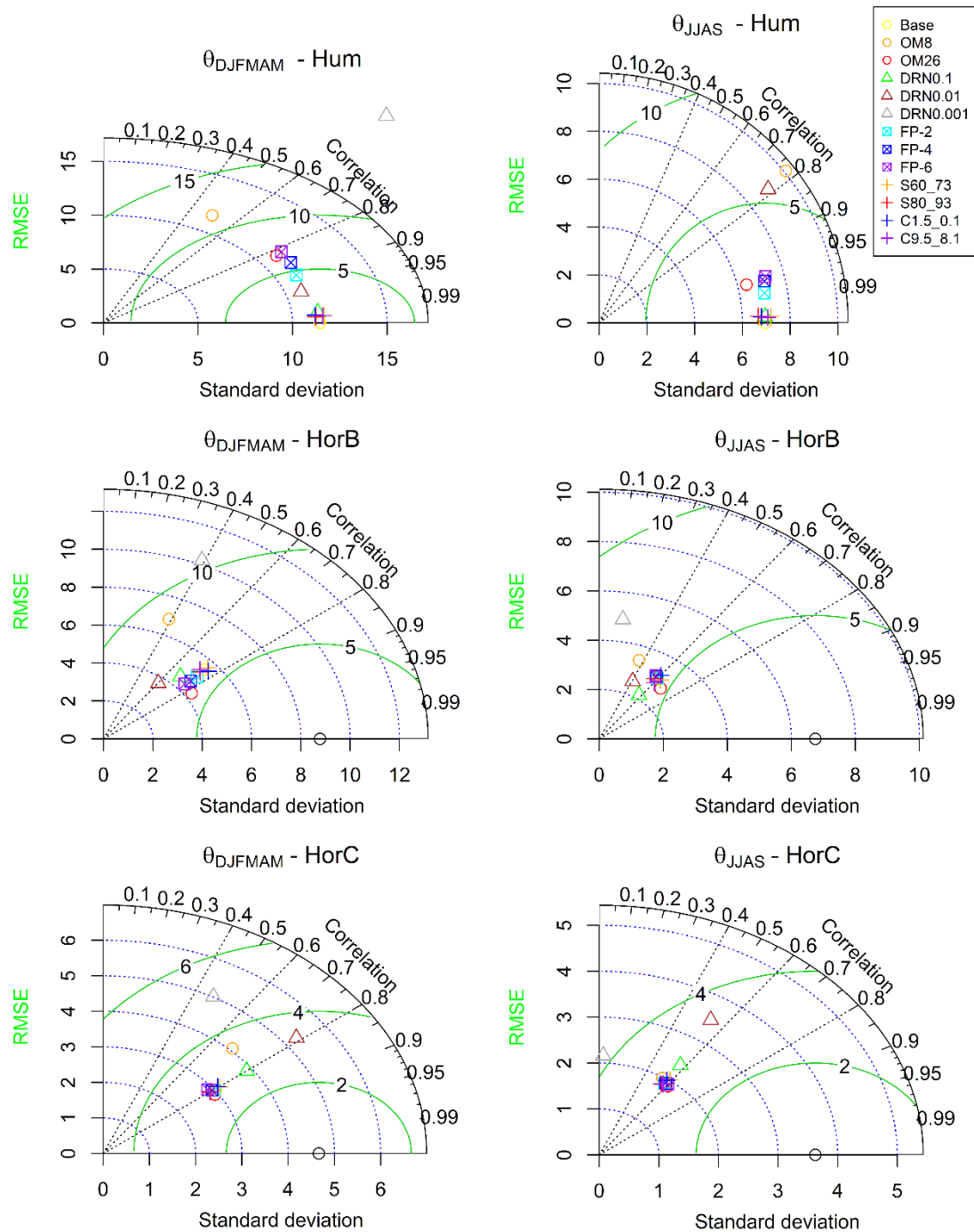


Figure 2.9: Taylor diagrams of observations vs simulations of all sensitivity analyses for soil liquid water ( $\theta$ ) during winter (DJFMAM; left) and summer months (JJAS; right) for the three soil horizons (Hum, HorB and HorC) at the balsam fir site. The reference point is the black circle (observations) located on the x-axis for all soil

layers, except for soil water in the Hum layer (yellow circle – base simulation). Green arcs are RMSE; blue dotted arcs are standard deviation; dotted black radial lines are correlation. OM: organic matter; DRN: drainage; FP: freezing point; S: percentage sand; C: percentage clay.

## 2.6 Discussion

This study is the first to evaluate the performance of CLASS on long-term daily soil temperature and soil water measurements at two sites dominated by two tree species that represent the vast majority of the boreal forest of eastern Canada. Sensitivity analyses were used to further evaluate model behavior and to potentially identify model parameters that could be modified to improve model performance.

### 2.6.1 Soil temperature

During summer, CLASS simulated daily soil temperature was generally excellent for both sites with the small exception that simulated soil temperature was slightly overestimated at one site. A major assumption in CLASS is that there is no vapour and liquid flow in the soil due to temperature gradients (Verseghy, 1991). While soil liquid flow due to temperature gradients is negligible (Philip, 1957; Jackson et al., 1974), soil vapour flow is important especially in the top layer, which normally experiences larger soil temperature fluctuations compared to the deeper soil layers (Jassal et al., 2003). The lack of consideration of soil vapour flow in CLASS may have led to a higher soil temperature in summer with multiple peaks compared to observations which had a lower and smoother curve during summer. During winter, CLASS underestimated soil temperature, particularly at the black spruce site, leading to frequent soil freezing, which might be due to the thinner organic layer at the black spruce site (13 cm) compared to that at the balsam fir site (17 cm). However, at the balsam fir site, the late onset and underestimation of simulated snow depth in winter 2009-2010 (Figure 2S.1) led to very low simulated soil temperatures in the Hum layer (Figure 2.2b). Using the

soil multilayered version of CLASS 2.6, Hejazi and Woodbury (2011) also found cooler simulated soil temperature in winter jack pine forest in Saskatchewan compared to their observations. The simulated soil temperature in CLASS version 2.6w (Letts et al., 2000) was found to lag weekly observations by more than one month at 1 m depth in a mixed-forest wetland in Ontario (Munro et al., 2000) which is a substantially stronger bias than what we observed. In this study, the underestimated modelled soil temperature during winter might be due to the insufficient insulation of the organic layer and/or by snow cover as it is actually defined in the model.

While existing literature mentions the presence of seasonally frozen soil in the northern hemisphere (Zhang et al., 2003), our observations at the two boreal forest sites show that soil temperature rarely drops below 0 °C. While soils may be frozen in the tundra due to lack of trees or thinner snow cover or in temperate regions with little or no snow cover leading to a longer frost period, this is not the case for the boreal forest of eastern Canada where the soil is protected from harsh cold winter temperatures (-14.1 °C and -16.6 °C average January air temperature at the balsam fir and black spruce site, respectively) by a thick snow pack and evergreen trees. The underestimated modelled soil temperature during winter was found to be caused mainly by the insufficient insulation of the ground (organic layer properties) and/or of the snow (snow cover properties) as they are presently defined in the model).

#### 2.6.1.1 Sensitivity analysis on soil temperature

Increased thickness of the organic layer, due to its insulating effect (Hogg and Lieffers, 1991), resulted in a decrease in soil temperature in the summer and an increase in soil temperature in the winter. The increased thickness of the organic layer led to reduced heat fluxes through the entire soil column during the summer, with the decrease being greatest in the Hum layer, while in the winter, the outgoing upward heat fluxes were reduced, especially from deeper soil layers (Figure 2S.6 top left; Lawrence and Slater, 2008). Other studies have also reported a decrease in soil temperature during the

summer due to the presence of organic soil layers (Yoshikawa et al., 2002; Fukui et al., 2008; Lawrence and Slater, 2008; Rinke et al., 2008; Dashtseren et al., 2014).

On the other hand, the impact of percentage sand and percentage clay sensitivity analysis on soil temperature was barely noticeable in either summer or winter. For the drainage parameter sensitivity analysis, only the smallest drainage parameter value (DRN0.001) led to an increase in soil temperature during the summer. Likewise, in winter, soil temperature increased with decreasing drainage parameter, but to a much lesser extent than in the summer. This increase in soil temperature is attributed to the saturated soil water condition modelled in all soil layers (Figure 2.7 bottom left), which is unrealistic for this region, leading to an increase in the heat flux entering the soil column during the summer (Figure 2S.6, top right) and high latent heat of fusion during the winter (Subin et al., 2013). For the freezing point sensitivity analysis, soil temperature increased with decreasing freezing point in both summer and winter. The increase in soil temperature in the winter was caused by an increase in latent heat of fusion (Subin et al., 2013). In the summer, while both soil water and soil heat flux (Figure 2S.6, bottom left) slightly decreased, the energy used for melting ice (Figure 2S.6, bottom right) during the snowmelt period (prior to the growing season) was reduced with decreasing freezing point, which might have contributed to preserving a higher soil temperature once the snow cover has disappeared.

### 2.6.2 Soil water

The performance of CLASS for predicting soil water varies among the sites, seasons and soil horizons, with soil water simulations being slightly better at the black spruce site than at the balsam fir site. Other studies also reported that CLASS generally poorly predicts soil water (Yuan et al., 2007; Dumedah et al., 2011; MacDonald et al., 2016) and that its accuracy varies among sites (Wen et al., 2007), soil texture (Saunders et al., 1999) and soil depth (Wen et al., 1998). While temporal variation in soil water content was relatively well simulated, the absolute soil water content was not, particularly at

the balsam fir site where it was greatly underestimated throughout the year. The simulated CLASS water content is highly sensitive to soil properties and soil depth (Tilley et al., 1997). CLASS determines soil porosity uniquely from the percentage of sand in the soil, excluding percentage of silt, clay, organic matter as well as soil structure and degree of soil compaction that varies with soil depth. Other LSSs also use a fixed porosity and thus have poor simulation of soil water compared to observations (Luo et al., 2003). Moreover, the substantial underestimation of soil water at the balsam fir site compared to the black spruce site could be due to the presence of lateral water movement (caused by the higher precipitation and a steeper slope), which is not simulated by CLASS 3.6.

CLASS underestimated liquid soil water during the winter because water was frozen in the soil in the model compared to observations, especially at the black spruce site (Figure 2.4). Freezing in the soil occurs at 0 °C in CLASS while in reality it may occur at temperature below 0°C due to the presence of impurities in soil water (Verseghy, 1991). Below the freezing point, smaller soil pores are able to retain water in the liquid phase due to a very high freezing point depression compared to larger pores (Johnsson and Lundin, 1991). Thus, liquid water below the freezing point can occur in soil, depending on the quantity of impurities, texture, structure and degree of compaction.

#### 2.6.2.1 Sensitivity analysis on soil water

Overall, soil water increased with increasing TOL (Malhi and O’Sullivan, 1990; Bussière and Cellier, 1994; Schwartz et al., 2010), decreasing PS and increasing PC, i.e. because of their overall increasing water holding capacity. Likewise, soil water increased with decreasing DP as more water was retained in the soil column, eventually leading to a saturated soil condition for the smallest (and unrealistic) DP simulation. On the other hand, soil water increased with decreasing FP during winter as water was kept in a liquid state, but in summer, it decreased slightly, which might have been caused by lower snowmelt water available for replenishing the soil due to the reduced

frozen soil water. However, the much higher insulation at balsam fir site (17 cm organic layer and 1.1 m max. snow cover; Figure 2S.7 middle left) compared to the black spruce site (13 cm organic layer and 0.84 m max. snow cover; Figure 2S.7 middle right) led to much higher increase in liquid soil water and much lower frozen soil water in all soil layers in FP simulations at the balsam fir site (Figure 2S.7 bottom left) compared to black spruce site (Figure 2S.7 bottom right), thus highlighting the importance of degree of insulation despite the decreasing FP. For all sensitivity analyses at the black spruce site, there was no increase in soil water in the Hum layer during winter, which might be due to the modelled sub-freezing soil temperature (Figures 2S.2 and 2S.3). Overall, our sensitivity analyses showed that despite varying model parameters within a realistic range, the simulated soil water did not improve significantly, and thus calibrating the model with existing parameters is not a solution to improve the model output. This underscores that the equations governing soil water in CLASS need to be improved for a better simulation of soil water.

## 2.7 Conclusion

In the context of boreal forest ecosystems, the accurate representation of soil temperature and soil water in LSSs is crucial due to their importance for numerous processes, including transpiration (Ukkola et al., 2016a;2016b), where the latter has a direct feedback on the climate system (Zittis et al., 2014). With increasing soil moisture, evapotranspiration is increased (air temperature is decreased), leading to an increase in precipitation (positive feedback) in most cases, although negative feedback also occurs (Cook et al., 2006; Seneviratne et al., 2010). Inaccurate projection of precipitation and air temperature by climate models (e.g. CRCM) will in turn impact the timing of the beginning of snowmelt, soil temperature, available soil liquid water and eventually the length of the growing season in the boreal forest. Despite some slight underestimation

during winter, daily soil temperature was well simulated by CLASS. While the performance of CLASS for soil water varied among the sites, seasons and soil horizons, the seasonal variation of modeled soil water corresponded well with observations. Sensitivity analyses increased our understanding of CLASS and the processes involved for the computation of both soil temperature and soil water, as well as the model's limitation. TOL had significant impact on both soil temperature and soil water while PSPC had a significant impact on soil water only. The lowest DP (0.001) simulation led to saturated soil water conditions and increased soil temperature in summer. The FP sensitivity analysis did not lead to substantial improvement in either soil temperature or soil water in winter.

CLASS proved to be a model that comprehensively represents the physical system by reproducing well soil temperature and adequately soil water on a daily timescale. However, CLASS needs some improvement in its simulation of soil temperature and soil water during winter in order to provide the CRCM with accurate data for future climate predictions. We recommend increasing the insulation of the humus layer and snow by improving the organic layer and snow cover properties (such as decreasing snow thermal conductivity) in CLASS in order to increase the soil temperature. Also, we recommend varying the freezing point as a function of percentage clay in order to improve soil water content in the winter, as the presence of micropores (% clay) increases the presence of liquid water in the soil. Finally, we recommend implementing a new and more realistic soil porosity equation that incorporates % sand, % clay, % organic matter and degree of soil compaction.

## 2.8 Acknowledgements

This work was supported by a MITACS Cluster grant and the OURANOS organisation. We thank the technicians of the Ministry of Forests, Wildlife, and Parks for the measurement of all data used in this study. We also thank Richard Harvey for his timely advice in CLASS model simulations.

## 2.9 References

- Bartlett, P.A., MacKay, M.D. and Verseghy, D.L., 2006. Modified snow algorithms in the Canadian land surface scheme: Model runs and sensitivity analysis at three boreal forest stands. *Atmosphere-Ocean*, 44(3), pp.207-222.
- Bellisario, L.M., Boudreau, L.D., Verseghy, D.L., Rouse, W.R. and Blanken, P.D., 2000. Comparing the performance of the Canadian land surface scheme (class) for two subarctic terrain types. *Atmosphere-Ocean*, 38 (1), 181-204.
- Bonan, G.B. and Shugart, H.H., 1989. Environmental Factors and Ecological Processes in Boreal Forests. *Annual Review of Ecology and Systematics*, 20, 1-28.
- Brutsaert, W., 1975. On a derivable formula for long-wave radiation from clear skies. *Water Resour. Res.*, 11(5), 742-744.
- Bussière, F. and Cellier, P., 1994. Modification of the soil temperature and water content regimes by a crop residue mulch: experiment and modelling. *Agricultural and Forest Meteorology*, 68 (1), 1-28.
- Campbell, G.S. and Norman, J.M., 2012. *An introduction to environmental biophysics*. Springer Science & Business Media.
- Clapp, R.B. and Hornberger, G.M., 1978. Empirical equations for some soil hydraulic properties. *Water Resour. Res.*, 14, 601-604.
- Cook, B.I., Bonan, G.B. and Levis, S., 2006. Soil moisture feedbacks to precipitation in southern Africa. *Journal of Climate*, 19 (17), 4198-4206.
- Cosgrove, B. A., Lohmann, D., Mitchell, K. E., Houser, P. R., Wood, E. F., Schaake, J. C., Robock, A., Sheffield, J., Duan, Q., Luo, L., Wayne Higgins R.W., Pinker, R.T., Tarpley, J. D., 2003. Land surface model spin-up behavior in the North

- American Land Data Assimilation System (NLDAS). *Journal of Geophysical Research: Atmospheres*, 108(D22).
- Dashtseren, A., Ishikawa, M., Iijima, Y. and Jambaljav, Y., 2014. Temperature Regimes of the Active Layer and Seasonally Frozen Ground under a Forest-Steppe Mosaic, Mongolia. *Permafrost and Periglacial Processes*, 25 (4), 295-306.
- Delpierre, N., Lireux, S., Hartig, F., Camarero, J.J., Cheaib, A., Čufar, K., Cuny, H., Deslauriers, A., Fonti, P., Gričar, J. and Huang, J.G., 2019. Chilling and forcing temperatures interact to predict the onset of wood formation in Northern Hemisphere conifers. *Global change biology*, 25(3), pp.1089-1105.
- D'Orangeville, L., Duchesne, L., Houle, D., Kneeshaw, D., Côté, B. and Pederson, N., 2016. Northeastern North America as a potential refugium for boreal forests in a warming climate. *Science*, 352(6292), pp.1452-1455.
- Dumedah, G., Berg, A.A. and Wineberg, M., 2011. An integrated framework for a joint assimilation of brightness temperature and soil moisture using the nondominated sorting genetic algorithm II. *Journal of hydrometeorology*, 12 (6), 1596-1609.
- Fukui, K., Sone, T., Yamagata, K., Otsuki, Y., Sawada, Y., Vetrova, V. and Vyatkina, M., 2008. Relationships between permafrost distribution and surface organic layers near Esso, central Kamchatka, Russian Far East. *Permafrost and Periglacial Processes*, 19 (1), 85-92.
- Gefler, A., Keitel, C., Nahm, M. and Rennenberg, H., 2004. Water shortage affects the water and nitrogen balance in central European beech forests. *Plant Biology*, 6(3), pp.289-298.
- Gold, L.W., 1963. Influence of snow cover on the average annual ground temperature at Ottawa, Canada. *International Association Scientific Hydrology*, 61 (82-91).
- Gupta, H.V., Kling, H., Yilmaz, K.K. and Martinez, G.F., 2009. Decomposition of the mean squared error and NSE performance criteria: Implications for improving hydrological modelling. *Journal of hydrology*, 377 (1-2), 80-91.
- Hejazi, A. and Woodbury, A.D., 2011. Evaluation of land surface scheme SABAE-HW in simulating snow depth, soil temperature and soil moisture within the BOREAS site, Saskatchewan. *Atmosphere-Ocean*, 49 (4), 408-420.
- Hogg, E.H. and Lieffers, V.J., 1991. The impact of *Calamagrostis canadensis* on soil thermal regimes after logging in northern Alberta. *Canadian Journal of Forest Research*, 21 (3), 387-394.
- Houle, D., Lajoie, G. and Duchesne, L., 2016. Major losses of nutrients following a severe drought in a boreal forest. *Nature plants*, 2(12), pp.1-5.

- Huang, J.G., Ma, Q., Rossi, S., Biondi, F., Deslauriers, A., Fonti, P., Liang, E., Mäkinen, H., Oberhuber, W., Rathgeber, C.B., Tognetti, R., Treml, V., Yang, B., Zhang, J.L., Antonucci, S., Bergeron, Y., Camarero, J.J., Campelo, F., Čufar, K., Cuny, H.E., De Luis, M., Giovannelli, A., Gričar, J., Gruber, A., Gryc, V., Güney, A., Guo, X., Huang, W., Jyske, T., Kašpar, J., King, G., Krause, C., Lemay, A., Liu, F., Lombardi, F., Martinez del Castillo, E., Morin, H., Nabais, C., Nöjd, P., Peters, R.L., Prislán, P., Saracino, A., Swidrak, I., Vavrčik, H., Vieira, J., Yu, B., Zhang, S., Zeng, Q., Zhang, Y., Ziaco, E., 2020. Photoperiod and temperature as dominant environmental drivers triggering secondary growth resumption in Northern Hemisphere conifers. *Proceedings of the National Academy of Sciences*, 117(34), pp.20645-20652.
- Iijima, Y., Fedorov, A.N., Park, H., Suzuki, K., Yabuki, H., Maximov, T.C. and Ohata, T., 2010. Abrupt increases in soil temperatures following increased precipitation in a permafrost region, central Lena River basin, Russia. *Permafrost and Periglacial Processes*, 21 (1), 30-41.
- Jackson, R., Reginato, R., Kimball, B. and Nakayama, F., 1974. Diurnal Soil-Water Evaporation: Comparison of Measured and Calculated Soil-Water Fluxes 1. *Soil Science Society of America Journal*, 38 (6), 861-866.
- Jassal, R.S., Novak, M.D. and Black, T.A., 2003. Effect of surface layer thickness on simultaneous transport of heat and water in a bare soil and its implications for land surface schemes. *Atmosphere-Ocean*, 41 (4), 259-272.
- Johnsson, H. and Lundin, L.C., 1991. Surface runoff and soil water percolation as affected by snow and soil frost. *Journal of Hydrology*, 122 (1-4), 141-159.
- Jungqvist, G., Oni, S.K., Teutschbein, C. and Futter, M.N., 2014. Effect of climate change on soil temperature in Swedish boreal forests. *PLoS One*, 9(4), p.e93957.
- Lawrence, D.M. and Slater, A.G., 2008. Incorporating organic soil into a global climate model. *Climate Dynamics*, 30 (2-3), 145-160.
- Letts, M.G., Roulet, N.T., Comer, N.T., Skarupa, M.R. and Versegny, D.L., 2000. Parametrization of peatland hydraulic properties for the Canadian land surface scheme. *Atmosphere-Ocean*, 38 (1), 141-160.
- Luo, L., Robock, A., Vinnikov, K.Y., Schlosser, C.A., Slater, A.G., Boone, A., Etchevers, P., Habets, F., Noilhan, J., Braden, H. and Cox, P., 2003. Effects of frozen soil on soil temperature, spring infiltration, and runoff: Results from the PILPS 2 (d) experiment at Valdai, Russia. *Journal of Hydrometeorology*, 4 (2), 334-351.
- MacDonald, M.K., Davison, B.J., Mekonnen, M.A. and Pietroniro, A., 2016. Comparison of land surface scheme simulations with field observations versus

- atmospheric model output as forcing. *Hydrological Sciences Journal*, 61 (16), 2860-2871.
- MacKinney, A.L., 1929. Effects of Forest Litter on Soil Temperature and Soil Freezing in Autumn and Winter. *Ecology*, 10 (3), 312-321.
- Malhi, S.S. and O'Sullivan, P.A., 1990. Soil temperature, moisture and penetrometer resistance under zero and conventional tillage in central Alberta. *Soil and Tillage Research*, 17 (1), 167-172.
- Marchand, N., Royer, A., Krinner, G., Roy, A., Langlois, A. and Vargel, C., 2018. Snow-Covered Soil Temperature Retrieval in Canadian Arctic Permafrost Areas, Using a Land Surface Scheme Informed with Satellite Remote Sensing Data. *Remote Sensing*, 10 (11), 1703.
- Milbau, A., Graae, B.J., Shevtsova, A. and Nijs, I., 2009. Effects of a warmer climate on seed germination in the subarctic. *Annals of Botany*, 104(2), pp.287-296.
- Munro, D.S., Bellisario, L.M. and Versegny, D.L., 2000. Measuring and modelling the seasonal climatic regime of a temperate wooded wetland. *Atmosphere-Ocean*, 38 (1), 227-249.
- Napoly, A., Boone, A., Samuelsson, P., Gollvik, S., Martin, E., Seferian, R., Carrer, D., Decharme, B. and Jarlan, L., 2017. The interactions between soil–biosphere–atmosphere (ISBA) land surface model multi-energy balance (MEB) option in SURFEXv8 – Part 2: Introduction of a litter formulation and model evaluation for local-scale forest sites. *Geosci. Model Dev.*, 10 (4), 1621-1644.
- Ouimet, R., & Duchesne, L., 2005. Base cation mineral weathering and total release rates from soils in three calibrated forest watersheds on the Canadian Boreal Shield. *Canadian Journal of Soil Science*, 85(2), 245-260.
- Paquin, J.P. and Sushama, L., 2015. On the Arctic near-surface permafrost and climate sensitivities to soil and snow model formulations in climate models. *Climate Dynamics*, 44 (1), 203-228.
- Philip, J.R., 1957. Evaporation, and moisture and heat fields in the soil. *Journal of meteorology*, 14 (4), 354-366.
- Rennenberg, H., Loreto, F., Polle, A., Brilli, F., Fares, S., Beniwal, R.S. and Gessler, A.J.P.B., 2006. Physiological responses of forest trees to heat and drought. *Plant Biology*, 8(5), pp.556-571.
- Rinke, A., Kuhry, P. and Dethloff, K., 2008. Importance of a soil organic layer for Arctic climate: A sensitivity study with an Arctic RCM. *Geophysical Research Letters*, 35 (13).
- Rossi, S., Deslauriers, A., Griçar, J., Seo, J.W., Rathgeber, C.B., Anfodillo, T., Morin, H., Levanic, T., Oven, P. and Jalkanen, R., 2008. Critical temperatures for

- xylogenesis in conifers of cold climates. *Global Ecology and Biogeography*, 17(6), pp.696-707.
- Saunders, I., Bowers, J., Huo, Z., Bailey, W. and Verseghy, D., 1999. Simulation of alpine tundra surface microclimates using the Canadian Land Surface Scheme: II. Energy balance and surface microclimatology. *International Journal of Climatology: A Journal of the Royal Meteorological Society*, 19 (10), 1131-1143.
- Schwartz, R.C., Baumhardt, R.L. and Evett, S.R., 2010. Tillage effects on soil water redistribution and bare soil evaporation throughout a season. *Soil and Tillage Research*, 110 (2), 221-229.
- Seneviratne, S.I., Corti, T., Davin, E.L., Hirschi, M., Jaeger, E.B., Lehner, I., Orlowsky, B. and Teuling, A.J., 2010. Investigating soil moisture–climate interactions in a changing climate: A review. *Earth-Science Reviews*, 99 (3–4), 125-161.
- Subin, Z.M., Koven, C.D., Riley, W.J., Torn, M.S., Lawrence, D.M. and Swenson, S.C., 2013. Effects of Soil Moisture on the Responses of Soil Temperatures to Climate Change in Cold Regions. *Journal of Climate*, 26 (10), 3139-3158.
- Sugita, M. and Brutsaert, W., 1993. Cloud effect in the estimation of instantaneous downward longwave radiation. *Water Resources Research*, 29 (3), 599-605.
- Tilley, J.S., Chapman, W.L. and Wu, W., 1997. Sensitivity tests of the Canadian land surface scheme (CLASS) for arctic tundra. *Annals of Glaciology*, 25, 46-50.
- Ukkola, A.M., Kauwe, M.G.D., Pitman, A.J., Best, M.J., Abramowitz, G., Haverd, V., Decker, M. and Haughton, N., 2016b. Land surface models systematically overestimate the intensity, duration and magnitude of seasonal-scale evaporative droughts. *Environmental Research Letters*, 11 (10), 104012.
- Ukkola, A.M., Pitman, A.J., Decker, M., De Kauwe, M.G., Abramowitz, G., Kala, J. and Wang, Y.P., 2016a. Modelling evapotranspiration during precipitation deficits: identifying critical processes in a land surface model. *Hydrology and Earth System Sciences*, 20 (6), 2403-2419.
- Verseghy, Diana, 2012. CLASS—The Canadian land surface scheme (version 3.6). *Environment Canada Science and Technology Branch Tech. Rep.*
- Verseghy, D.L., 1991. Class—A Canadian land surface scheme for GCMS. I. Soil model. *International Journal of Climatology*, 11 (2), 111-133.
- Verseghy, D.L., McFarlane, N.A. and Lazare, M., 1993. Class—A Canadian land surface scheme for GCMS, II. Vegetation model and coupled runs. *International Journal of Climatology*, 13 (4), 347-370.

- Wang, S., Grant, R.F., Verseghy, D.L. and Black, T.A., 2001. Modelling plant carbon and nitrogen dynamics of a boreal aspen forest in CLASS—the Canadian Land Surface Scheme. *Ecological Modelling*, 142(1-2), pp.135-154.
- Wang, L., Cole, J. N., Bartlett, P., Verseghy, D., Derksen, C., Brown, R., & von Salzen, K., 2016. Investigating the spread in surface albedo for snow-covered forests in CMIP5 models. *Journal of Geophysical Research: Atmospheres*, 121(3), 1104-1119.
- Wen, L., Gallichand, J., Viau, A., Delage, Y. and Benoit, R., 1998. Calibration of the CLASS model and its improvement under agricultural conditions. *Transactions of the ASAE*, 41 (5), 1345.
- Wen, L., Wu, Z., Lu, G., Lin, C.A., Zhang, J. and Yang, Y., 2007. Analysis and improvement of runoff generation in the land surface scheme CLASS and comparison with field measurements from China. *Journal of hydrology*, 345 (1-2), 1-15.
- Williams, P.J. and Smith, M.W., 1989. *The frozen earth : fundamentals of geocryology*. Cambridge University Press: Cambridge; New York.
- Yang, Z. L., Dickinson, R. E., Henderson-Sellers, A., & Pitman, A. J., 1995. Preliminary study of spin-up processes in land surface models with the first stage data of Project for Intercomparison of Land Surface Parameterization Schemes Phase 1 (a). *Journal of Geophysical Research: Atmospheres*, 100(D8), 16553-16578.
- Yoshikawa, K., Bolton, W.R., Romanovsky, V.E., Fukuda, M. and Hinzman, L.D., 2002. Impacts of wildfire on the permafrost in the boreal forests of Interior Alaska. *Journal of Geophysical Research: Atmospheres*, 107 (D1), FFR 4-1-FFR 4-14.
- Yuan, F., Arain, M.A., Black, T.A. and Morgenstern, K., 2007. Energy and water exchanges modulated by soil–plant nitrogen cycling in a temperate Pacific Northwest conifer forest. *ecological modelling*, 201 (3-4), 331-347.
- Zadra, A., Caya, D., Côté, J., Dugas, B., Jones, C., Laprise, R., Winger, K. and Caron, L.P., 2008. The next Canadian regional climate model. *Phys Can*, 64(2), pp.75-83.
- Zhang, T., Barry, R.G., Knowles, K., Ling, F. and Armstrong, R.L., 2003, July. Distribution of seasonally and perennially frozen ground in the Northern Hemisphere. In *Proceedings of the 8th International Conference on Permafrost* (Vol. 2, pp. 1289-1294). Zürich, Switzerland: AA Balkema Publishers.

Zittis, G., Hadjinicolaou, P. and Lelieveld, J., 2014. Role of soil moisture in the amplification of climate warming in the Eastern Mediterranean and the Middle East. *Climate Research*, 59 (1), 27-37.

## 2.10 Supplementary materials

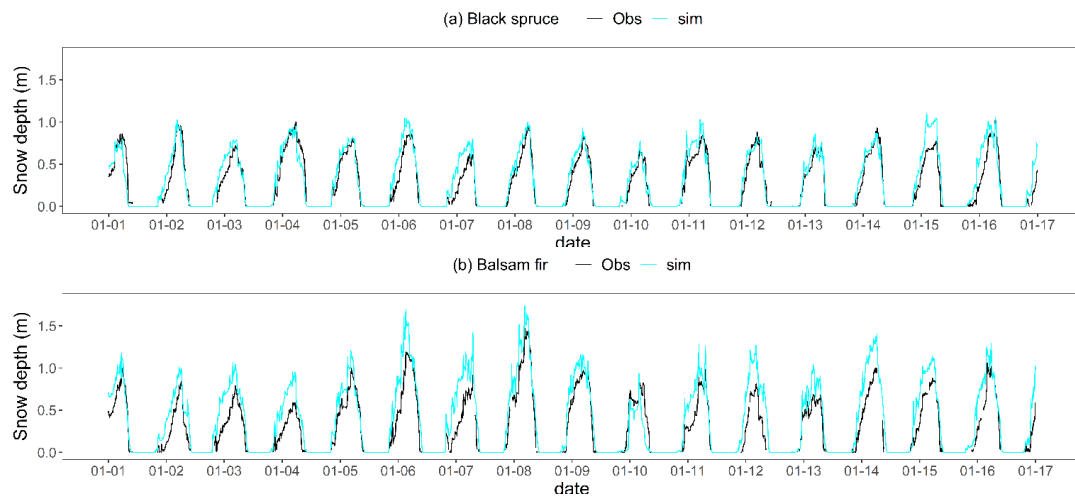


Figure 2S.1: Observed and simulated daily snow depth (m) at black spruce (a) and balsam fir (b) sites from 2001 to 2016.

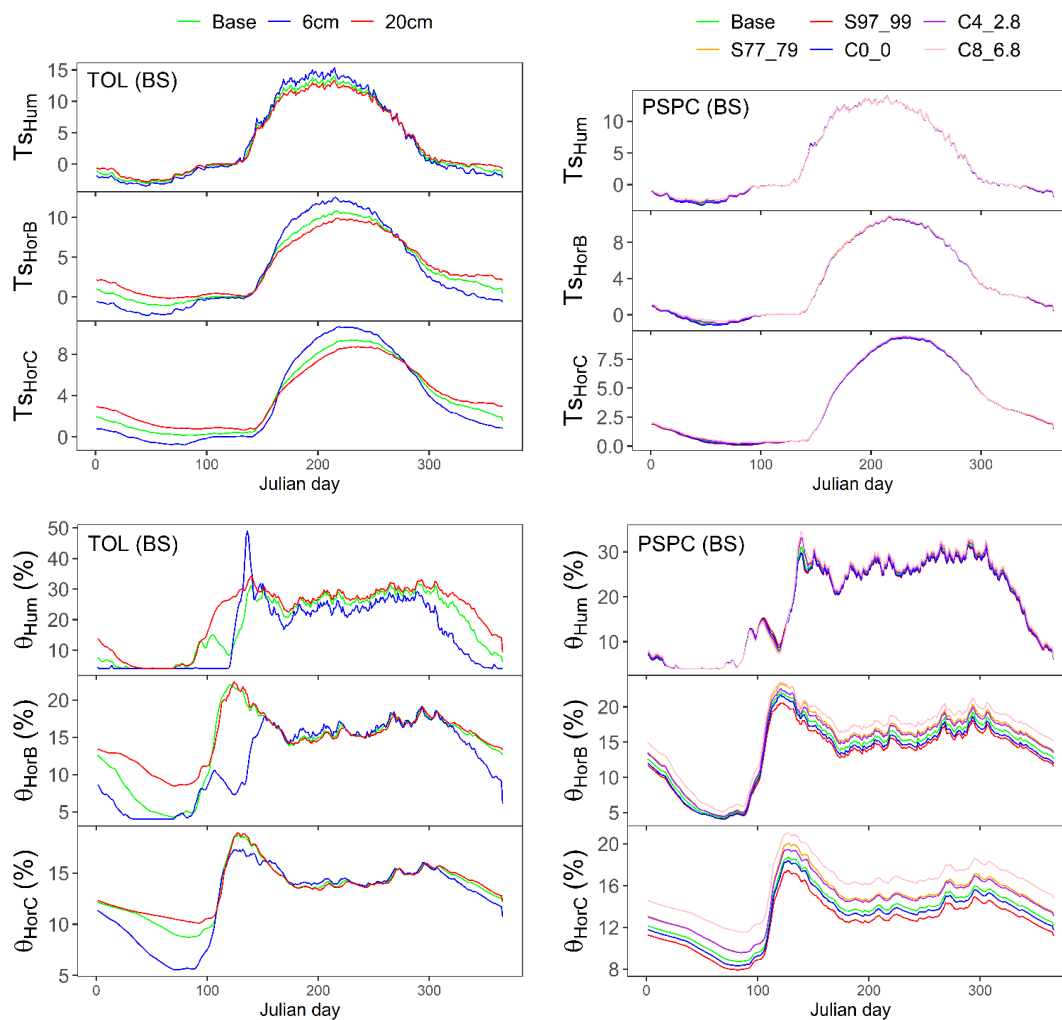


Figure 2S.2: Sensitivity analysis of thickness of organic matter (TOL; left panel) and of % sand and % clay (PSPC; right panel) on multiyear (2001 to 2016) average daily soil temperature ( $^{\circ}\text{C}$ ; top) and soil liquid water ( $\%$ ; bottom) at black spruce (BS) site.

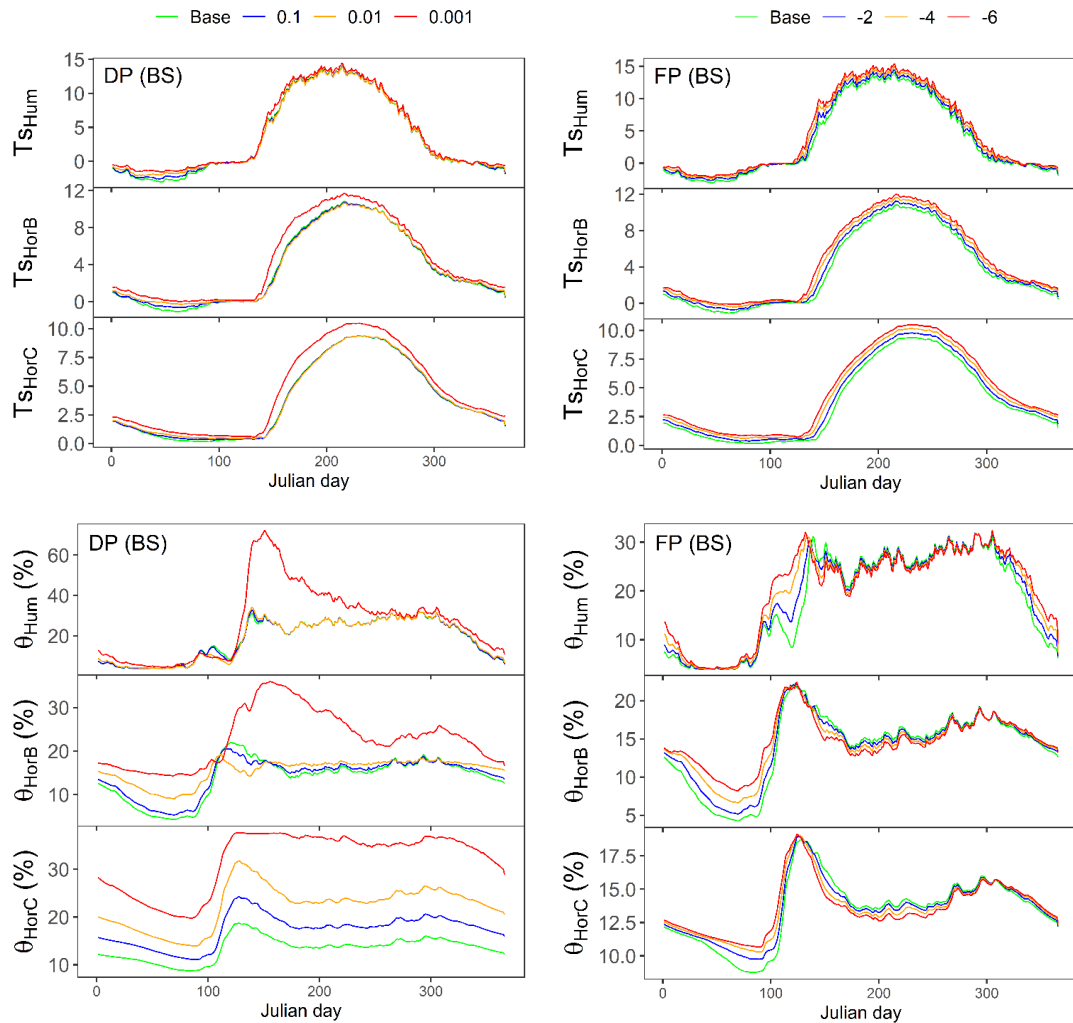


Figure 2S.3: Sensitivity analysis of drainage parameter (DP; left panel) and of freezing point (FP; right panel) on multiyear (2001 to 2016) average daily soil temperature (°C; top) and soil liquid water (%; bottom) at black spruce (BS) site.

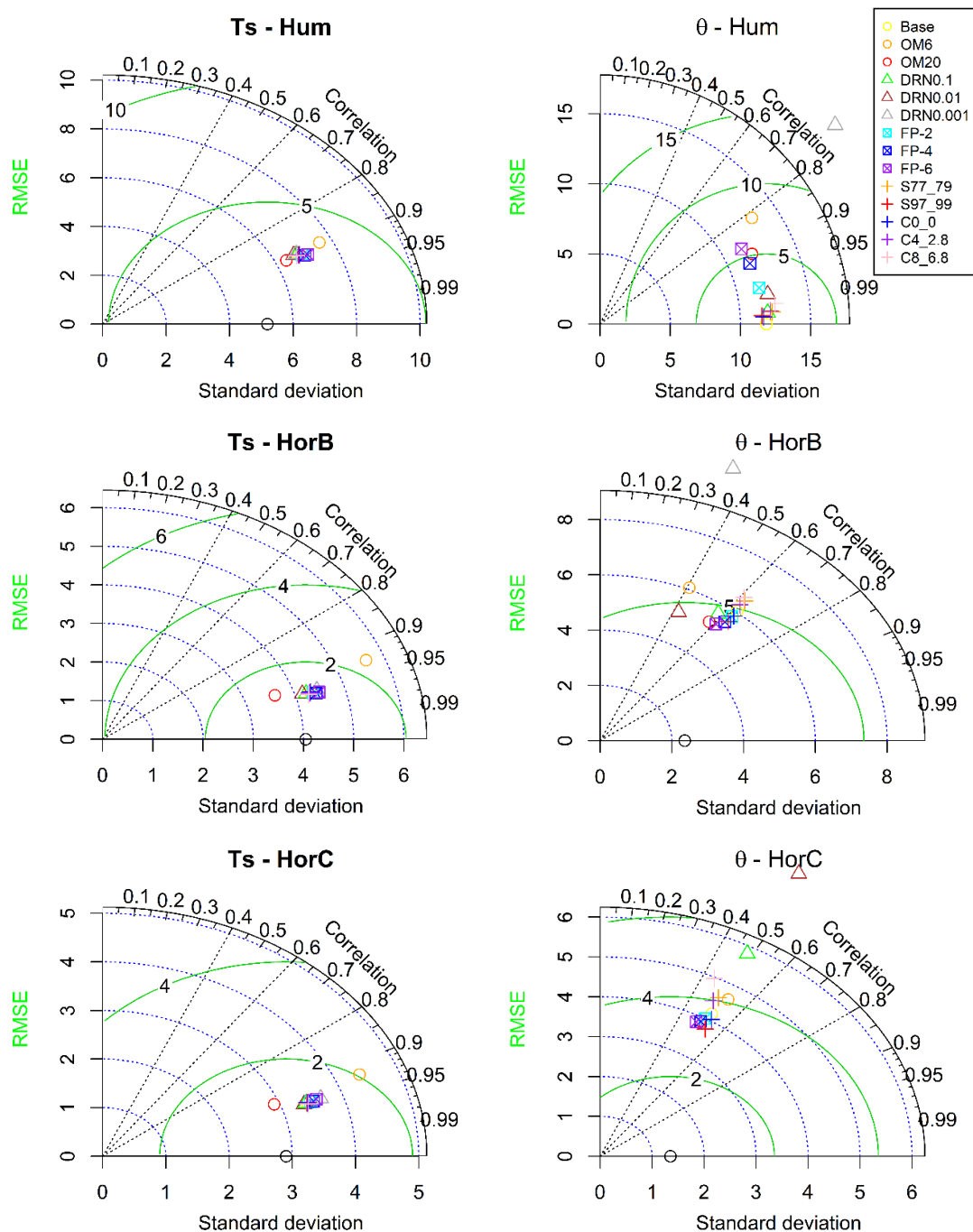


Figure 2S.4: Taylor diagrams of observations vs simulations of all sensitivity analyses for soil temperature (Ts; left) and soil liquid water ( $\theta$ ; right) for the three soil horizons (Hum, HorB and HorC) at the black spruce site. The reference point is the black circle (observations) located on the x-axis for all soil layers, except for soil water in the Hum layer which is represented by a yellow circle (base simulation).

Green arcs are RMSE; blue dotted arcs are standard deviation; dotted black radial lines are correlation.

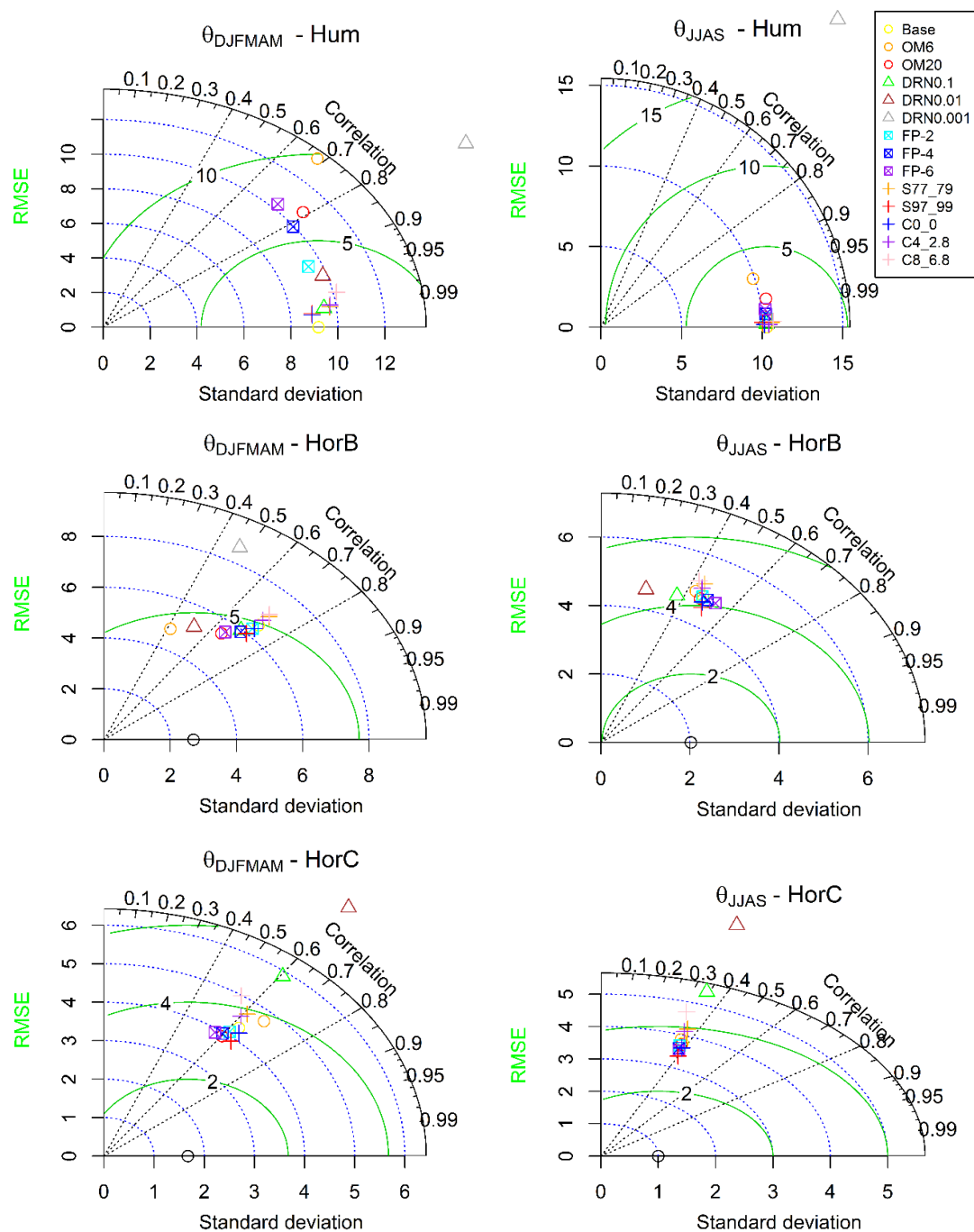


Figure 2S.5: Taylor diagrams of observations vs simulations of all sensitivity analyses for soil liquid water ( $\theta$ ) during winter (DJFMAM; left) and summer (JJAS;

right) months for the three soil horizons (Hum, HorB and HorC) at the black spruce site. The reference point is the black circle (observations) located on the x-axis for all soil layers, except for soil water in the Hum layer which is represented by a yellow circle (base simulation). Green arcs are RMSE; blue dotted arcs are standard deviation; dotted black radial lines are correlation.

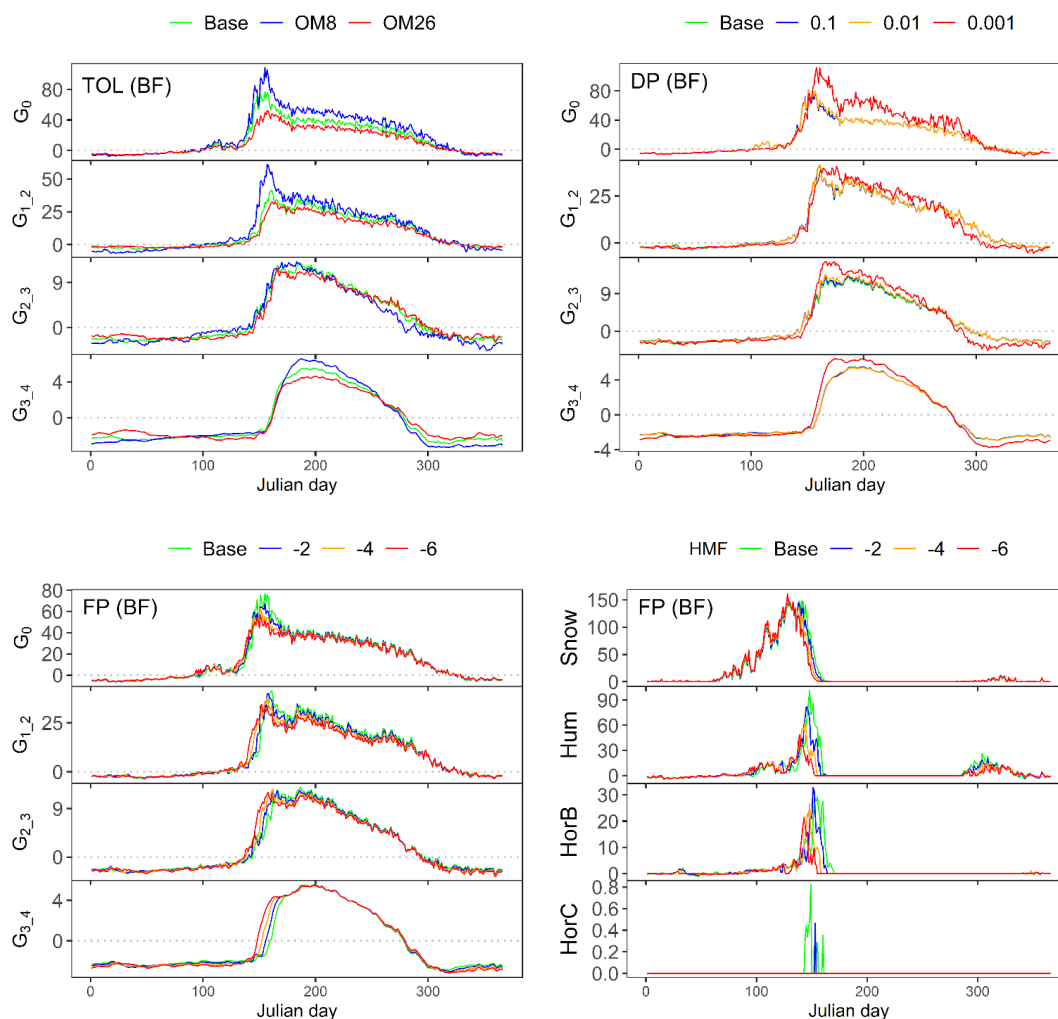
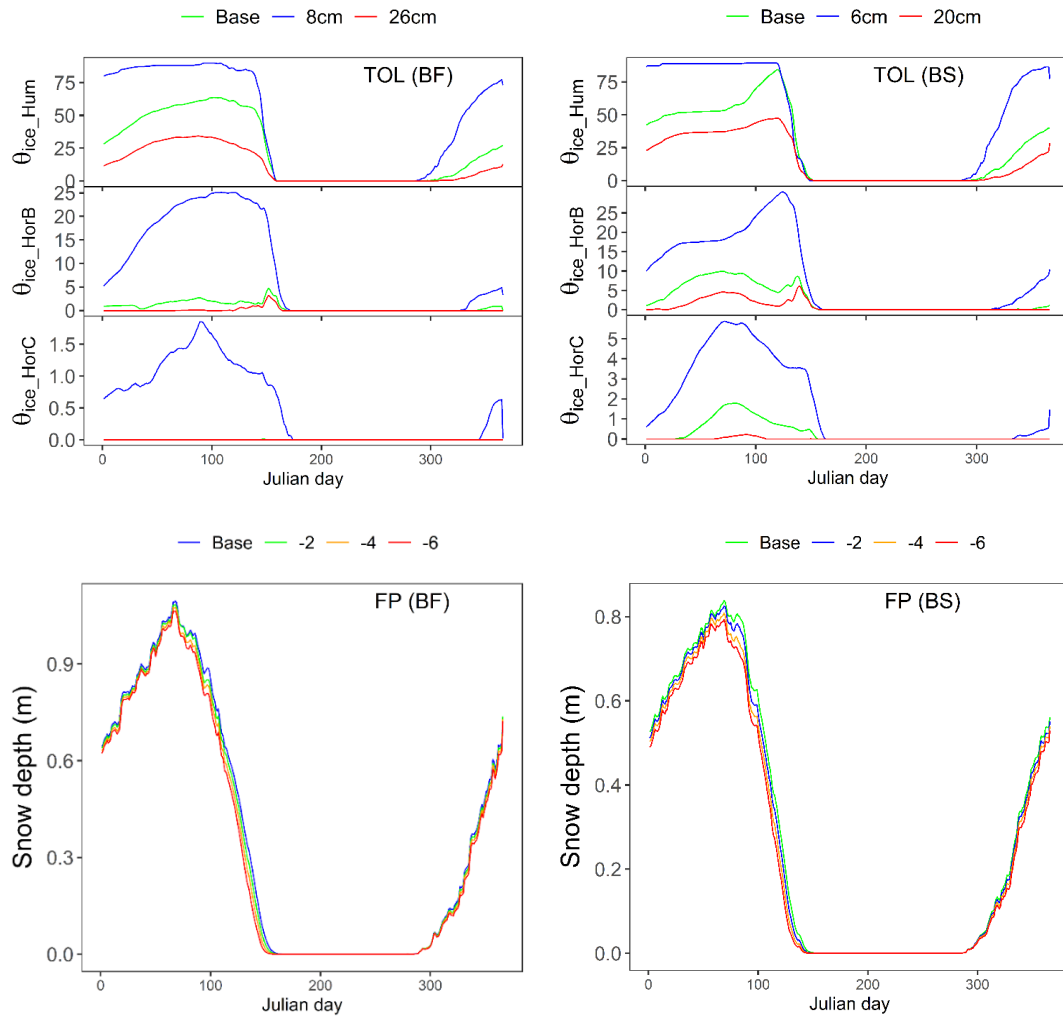


Figure 2S.6: Multiyear (2001 to 2016) average daily soil heat fluxes ( $\text{W m}^{-2}$ ) entering (positive) & leaving (negative) by thickness of organic layer (TOL; top left), drainage parameter (DP; top right), and freezing point (FP; bottom left) sensitivity analyses at balsam fir (BF) site; multiyear (2001 to 2016) average daily energy used in melting of ice ( $\text{W m}^{-2}$ ) in snow and soil layers for freezing point

sensitivity analysis at balsam fir (bottom right).  $G$  is soil heat flux on surface ( $G_0$ ), Hum ( $G_1$ ), HorB ( $G_2$ ), HorC ( $G_3$ ), and beneath HorC ( $G_4$ ).



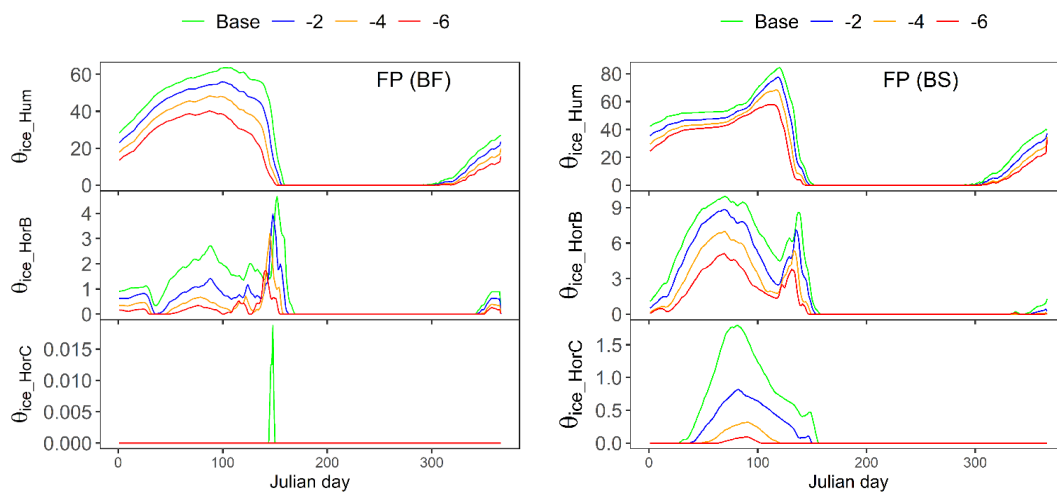


Figure 2S.7: Multiyear (2001 to 2016) average frozen soil water (%) by thickness of organic layer (TOL) and freezing point (FP) sensitivity analyses at balsam (BF) fir site (top and bottom left) and black spruce site (top and bottom right); multiyear (2001 to 2016) average daily snow depth (m) for freezing point sensitivity analysis at balsam fir (middle left) and black spruce (middle right) sites.

## CHAPITRE III

### VAPOUR PRESSURE DEFICIT AND SOLAR RADIATION ARE THE MAJOR DRIVERS OF TRANSPIRATION OF BALSAM FIR AND BLACK SPRUCE TREE SPECIES IN HUMID BOREAL REGIONS, EVEN DURING A SHORT-TERM DROUGHT

Article écrit par Shalini Oogathoo <sup>1</sup>

et révisé par Daniel Houle <sup>2,3</sup>, Louis Duchesne <sup>2</sup>, Daniel Kneeshaw <sup>1</sup>.

<sup>1</sup> Centre d'Étude de la Forêt, Université du Québec à Montréal, Case Postale 8888,  
Succursale Centre-Ville, Montréal, Quebec H3C 3P8, Canada.

<sup>2</sup> Direction de la Recherche Forestière, Ministère des Forêts, de la Faune et des Parcs du  
Québec, 2700 Einstein, Quebec City, Quebec G1P 3W8, Canada.

<sup>3</sup> Consortium sur la Climatologie Régionale et l'Adaptation aux Changements  
Climatiques (Ouranos), 550 Sherbrooke W, Montréal, Quebec H3A 1B9, Canada.

### 3.1 Résumé

Sur les surfaces terrestres couvertes de végétation, la transpiration des arbres, comparée à l'évaporation du sol et de la canopée, est un processus majeur qui renvoie de grandes quantités d'eau dans l'atmosphère. Bien que les forces motrices de la transpiration des arbres aient été étudiées sur une gamme d'espèces d'arbres dans un éventail d'écosystèmes, aucun travail n'a été effectué sur le sapin baumier et l'épinette noire dans la forêt boréale humide de l'est du Canada, particulièrement en utilisant une longue série temporelle des mesures de flux de sèves comprenant des événements extrêmes (sécheresses). J'ai ainsi étudié les relations entre les variables environnementales et la vitesse de flux de sève à une échelle temporelle quotidienne pour ces deux espèces d'arbres boréaux situés sur deux sites forestiers au Québec, au Canada sur plusieurs saisons de croissance (2004 à 2013 pour le sapin baumier et 2006 à 2009 pour épinette noire). Le flux de sève quotidien avait une forte relation non linéaire avec le déficit de pression de vapeur (VPD) pour les deux espèces. Le flux de sève était également fortement corrélé au radiation solaire (Rad) pour les deux espèces, bien qu'avec des relations légèrement plus faibles que pour le VPD. D'autres variables quotidiennes telles que la température de l'air maximale et les précipitations expliquent une plus petite partie de la variance du flux de sève (statistiquement significatif), tandis que le contenu en eau du sol (SWC), la température de l'air minimale et la vitesse du vent n'ont pratiquement aucun effet (statistiquement non-significatif). Une analyse des relations entre le flux de sève et le VPD / Rad sur une base horaire sur plusieurs années a montré une forte hystérésis diurne pour les deux espèces. Contrairement à ce qui a été proposé précédemment, l'ampleur de cette hystérésis ne semble pas être liée au degré d'iso/anisohydricité. Finalement, notre étude des relations entre les flux de sève et les variables environnementales pendant une sécheresse intense sur le site dominé par le sapin baumier a montré que le flux de sève n'était que légèrement réduit malgré une diminution significative du SWC. D'autre part, VPD et Rad sont restés les

principaux moteurs du flux de sève. Cette étude souligne que VPD et Rad sont en effet les principaux moteurs de la transpiration pendant la saison de croissance ainsi que pendant les périodes de sécheresse dans la région boréale humide.

### 3.2 Abstract

Compared to soil and canopy evaporation, tree transpiration is a major process that sends large amounts of water back to the atmosphere on vegetation-covered land surfaces. While the driving forces of tree transpiration have been studied over a range of tree species across an array of ecosystems, no work has been done on balsam fir and black spruce in the humid boreal forest of eastern Canada, especially by using an exceptionally long timeseries of sapflow measurements and focussing on a humid boreal forest's drought as well. We thus studied the relationships between environmental variables and sap flow velocity (as a proxy for transpiration) on a daily temporal scale for these two boreal tree species located at two forest sites in Quebec, Canada over multiple growing seasons (2004 to 2013 for balsam fir and 2006 to 2009 for black spruce). Daily sap flow had a strong non-linear relationship with vapour pressure deficit (VPD) for both species. Sap flow was also strongly correlated to solar radiation (Rad) for both species although with slightly weaker relationships than for VPD. Other daily variables such as maximum air temperature and precipitation explain a smaller but statistically significant portion of the variance in sap flow while soil water content (SWC), minimum air temperature and wind speed had almost no effect (statistically non-significant based on p-value). An analysis of the relationships between sap flow and VPD/Rad on an hourly basis over multiple years showed strong diel hysteresis for both species. Contrary to what has been previously proposed, the magnitude of this hysteresis does not seem to relate to the degree of anisohydricity. Finally, our investigation of sap flow relationships to environmental variables during a

drought period at the balsam fir site showed that sap flow was only slightly reduced despite a significant decrease in SWC. On the other hand, VPD and Rad remained the main drivers of sap flow. This study emphasizes that VPD and Rad are indeed the major drivers of transpiration during the growing season as well as during drought in humid boreal region.

### 3.3 Introduction

Boreal forests cover about 11% of the earth's surface (Bonan and Shugart, 1989) and the Canadian boreal forest represents about 28% of the global boreal forest (Brandt et al., 2013). Forests interact with the atmosphere primarily via two processes: photosynthesis and transpiration. While trees use photosynthesis to sequester atmospheric carbon, transpiration releases large amounts of water to the atmosphere having major feedbacks on surface temperature and precipitation regimes (Seneviratne et al., 2006). Consequently, the boreal forest plays a major role in carbon sequestration and in evaporative cooling (Bonan, 2008) and it is one of the nine major tipping elements in the climate system (Lenton et al., 2008). The coupling of land-atmosphere is carried out mainly by soil/canopy evaporation and tree transpiration, the latter being quantitatively much more important in forests (Ward and Trimble, 2004).

Evapotranspiration can be measured by terrestrial/atmospheric water balance at the watershed level or by eddy covariance techniques on small footprint areas (Seneviratne et al., 2010). Transpiration at the tree level can be measured with sap flow techniques with a high temporal resolution. This type of measurement allows understanding the fine control of hydroclimatic variables on transpiration as well as its influence on radial growth during the course of the growing season when combined with dendrometer measurements.

In our study, sap flow was measured as a proxy of transpiration rate in individual trees to evaluate the impact of environmental variables on sap flow velocity. Many sap flow studies have focused on transpiration and canopy conductance (Saugier et al., 1997; Köstner et al., 1998; Granier et al., 2000; Daley and Phillips, 2006; Macfarlane et al., 2010; Jung et al., 2011). Others have directly assessed the relationships between environmental variables and sap flow in natural environments (Hogg and Hurdle, 1997; Wullschleger et al., 2000; Lagergren and Lindroth, 2002; Bovard et al., 2005; Chen et al., 2011; Jonard et al., 2011; Wang et al., 2017) or in experimental-field set-ups (Juice et al., 2016; Wang et al., 2005; Collins et al., 2018). From these studies, sap flow has been found to be controlled by environmental variables, such as vapour pressure deficit (VPD), solar radiation (Rad), air temperature, wind speed, soil water and soil temperature. However, the impact of each variable on sap flow varied with climatic region, species, and age of trees. VPD and Rad were found to be the most important driving variables for transpiration in *Pinus sylvestris* in Scotland (Wang et al. 2017). On the other hand, soil water was reported as being important during periods of low rainfall (Gartner et al., 2009; Mitchell et al., 2012; da Silva Sallo et al., 2017; Wang et al., 2017), such that transpiration was reduced when 80% of the plant's available water in the soil was depleted (Lagergren and Lindroth, 2002).

Only a few studies have been carried out on sap flow for black spruce (Van Herk et al., 2011; Patankar et al., 2015; Pappas et al., 2018) despite its critical importance in the Canadian boreal forest. However, these studies were conducted in dry regions (Van Herk et al., 2011; Pappas et al., 2018) or in boreal peatlands exhibiting rapid permafrost thaw (Patankar et al., 2015). Regarding balsam fir, there is one study for a temperate forest of the USA (Ewers et al., 2002). To our knowledge, no long term studies have been carried out in black spruce or balsam fir on the relationship between sap flow and environmental variables in cold-humid boreal forests such as those found in eastern Canada. In our study, the relationships between sap flow and environmental variables were studied over 10 and 4 growing seasons at two intensively monitored sites,

respectively dominated by balsam fir and black spruce in eastern Canada. The balsam fir site was affected by a drought during the growing season (July 2012) which caused large losses of nutrients from the tree canopies through leaching in throughfall as well as large litterfall losses (Houle et al. 2016). These long-term sap flow measurements are also used to evaluate the link between iso/anisohydricity and diel hysteresis in the two study species.

In this study, we hypothesized that (1) VPD and Rad will be the main drivers of sap flow during the growing season for both species. We also hypothesize that during the 2012 drought at the balsam fir site, (2) sap flow will be reduced and that its control will shift from atmospheric variables (VPD and Rad) to soil water availability. Thus, the objectives of this study are to evaluate the relationship between environmental variables and daily sap flow (1) during the growing season and (2) during a drought. As a third objective, we also verified the link between diel hysteresis of sap flow velocity vs VPD/Rad and anisohydricity.

### 3.4 Materials and methods

#### 3.4.1 Site description

The two study sites, dominated respectively by balsam fir and black spruce forests, are located in the province of Quebec, Canada. The Laflamme (balsam fir) site is situated at 47° 19' 41'' N and 71° 07' 37'' W, at an elevation of 784 m above sea level with an average slope of 8%. The forest is dominated by even-aged balsam fir (*Abies balsamea* (L.) Mill.), constituting 88% of the basal area (Duchesne et al., 2012). Other tree species that are present in lower abundance are white spruce (*Picea glauca* (Moench) Voss) and paper birch (*Betula papyrifera* Marsh.). The mean annual temperature at the site was 1.3 °C while the mean annual precipitation is 1300 mm for the period 2001-

2016. The Tirasse site (black spruce) is located at 49°12'45' N and 73°39'00' W, in the Ashuapmushuan wildlife reserve at an elevation of 411 m above sea level. The forest at this site is dominated by even-aged black spruce (*Picea mariana* (Mill) BSP) with basal area being 66.4%, accompanied by jack pine (*Pinus banksiana* Lamb.). The mean annual temperature was 1.3 °C and the mean annual precipitation is 941 mm for the period 2001 to 2016. Detailed characteristics of the forest stands, instrumented trees and soil is summarized in Tables 3.1 and 3S.1.

#### 3.4.2 Meteorological and soil measurements

A weather station, to measure atmospheric weather variables as per standard protocols, was located in a clearing approximately 600 m from the forest plot at the balsam fir site and 250 m from the forest plot at the black spruce site. Climate variables were measured continuously and recorded hourly since 1999 at Laflamme and 1996 at Tirasse, this includes solar radiation (Rad, LI190SB, Campbell Scientific, Logan, UT, light spectrum 400–700 nm), air temperature (minimum: T<sub>min</sub>, maximum: T<sub>max</sub>, mean: T<sub>mean</sub>), relative humidity (RH, HMP35CF, Campbell Scientific, Logan, UT), precipitation (PCP, 35-1558, Fisher and Porter, Albany, NY) and wind speed (WS, Met-One 013A, Campbell Scientific, Logan, UT). Both air temperature and relative humidity were measured at a height of 3.3 m while solar radiation and wind speed were recorded at a height of 14 m. Vapour pressure deficit (VPD, Pa) was calculated using daily relative humidity and saturated vapour pressure (Ward and Trimble, 2004), in which the latter was determined using daily average air temperature (Murray, 1967).

In an intensively studied forest plot site (0.25 ha) at both sites, soil water content (SWC) was measured around the study trees using time-domain reflectometry (CS615, Campbell Scientific, Logan, UT) at four and three locations at the balsam fir and black spruce site respectively. SWC was measured at three depths in the soil: within the humus layer (2 cm above the mineral horizon), and in the mineral soil (22 cm below the mineral soil surface) and subsoil layers (81 cm). Only data from the B horizon (22

cm; mean of four soil profiles) were used in the regression analysis because it is the depth at both sites where most of the roots are located, as shown in Table 3.1.

Table 3.1: Description of forest stand characteristics for trees with a DBH > 9.1 cm and the three instrumented trees at the two sites (Mean  $\pm$  one standard deviation)

	Balsam fir	Black spruce
<i>Stand characteristics<sup>1</sup></i>		
Number of trees per hectare	2252	3008
Average age of dominant & co-dominant trees (yr)	49 $\pm$ 6	61 $\pm$ 6
Basal area (m <sup>2</sup> /ha)	56.4	37.3
Average height (m)	16.4 $\pm$ 4.9	12.4 $\pm$ 2.5
Average DBH (mm)	169 $\pm$ 55	123 $\pm$ 23
Rooting depth (cm)		
- Peak Abundance	28	19
- Maximum	59	32
Depth of humus layer (cm)	16.8	12.7
<i>Instrumented trees characteristics<sup>2</sup></i>		
Average height (m)	19.1 $\pm$ 1.3	15.6 $\pm$ 0.2
Average DBH (mm)	183.5 $\pm$ 11.5	170.3 $\pm$ 6.1

<sup>1</sup> Forest stand characteristics were measured in 2018 for balsam fir and 2016 for black spruce; <sup>2</sup> Instrumented trees characteristics were measured in 2019 for both sites.

### 3.4.3 Sap flow & dendrometric data

At both study sites, sap flow was measured in three co-dominant trees of the main tree species (one measurement on the north and one measurement on the south side for each tree in order to allow the observation of sap flow variation on different sides of the stem) using a 30 mm thermal dissipation probe (TDP-30, Dynamax, Houston, TX).

Instruments were positioned at approximately 1.3 m above ground level. Trees were instrumented in 2003 for balsam fir and 2006 for black spruce. The same three trees at both sites were also instrumented with electronic strain gauge dendrometers for stem diameter variation measurements (SDV, DEX70, Dynamax Inc., Houston, TX). Instrumented trees had well-developed crowns with no apparent lesions on the trunk. Sap flow and stem diameter variation were measured every 30-min throughout the day. Sap flow velocity ( $\text{cm s}^{-1}$ ) was calculated based on the procedure explained in Granier (1987; Eq. 3.1), where  $T$  is temperature difference every 30 mins ( $^{\circ}\text{C}$ ) and  $\Delta T$  is the maximum temperature difference from midnight (0h00) to early morning (10h00).

$$SF_v = 0.0119[(\Delta T - T)/T]^{1.231} \quad \text{Eq. 3.1}$$

Though a large number of sampled trees for measurements of sap flow are normally used for the quantification of total stand transpiration, such large numbers are not the case in studies that aim to evaluate the impact of climate variables on sap flow velocity in individual trees. Other studies have used fewer than 4 trees per species and this often with measurements only on one side of the tree for the purpose of establishing relationships between environmental variables and sap flow (O'Brien et al., 2004; Bovard et al., 2005; Wang et al., 2005) or for determining canopy conductance (Wang et al., 2014). Moreover, in our study, hourly and daily variations in sap flow are highly correlated between sun-side and shade-side probes of each tree and between trees (Tables 3S.2 and 3S.3).

In our study, we did not measure sapwood area for the studied years at both sites, as we were interested in sap flow velocity (whereby its variations correspond exactly to variations in sap flow volume) on an hourly basis rather than on stand level transpiration. We further note that the relationship between sap volume and ascending sap speed with climatic variables will be the same, except for the coefficient values of the equations. In our study, the sap flow probes were not re-installed every year. The

hourly and daily variation of sap flow were checked at the beginning of each season to ensure that the signal was clear. Though sap flow probes are commonly re-installed every year to avoid wounding, Peters et al. (2018) found the dampening of signal to occur only in the second year of measurement while the signal remains stable for the following years. On the other hand, re-installing the probes on the same tree every year might lead to problems of circumferential variability (Peters et al., 2018). Also, while fast-growing species might require installation of sap flow probes more often (due to burying of needles in the heartwood; Peters et al., 2018), this may not be the case for slow-growing species like balsam fir and black spruce. For this study, the data were analysed from the years 2004 to 2013 and 2006 to 2009 for balsam fir and for black spruce respectively i.e. the years where continuous monitoring of sap flow and climate variables were available for each site. At each site, the same three instrumented trees were followed throughout the study.

#### 3.4.4 Analyses

##### 3.4.4.1 Relationship of sap flow with environmental variables during the growing season

The relationship of daily sap flow to climatic variables was evaluated separately for each year (2004 to 2013 for balsam fir and 2006 to 2009 for black spruce) to avoid confounding between-year variations in climate and timing of the growing season. The period studied was not fixed since the data were analysed from the beginning of radial growth (mean of the three trees) till the end of August. The 4-parameter Gompertz model was fitted to the daily averaged dendrometer data from May to September for each year separately and the beginning of radial growth was determined when the modelled daily growth was above  $5 \mu\text{m d}^{-1}$  (Duchesne et al., 2012). The end of the growing season was taken as the end of August in order to avoid the freeze/thaw events that occurred in September. The relationship between environmental variables and daily cumulated sap flow (SF) was analysed for each probe separately as sap flow

varied in magnitude between the north and south sides of a tree, although synchronicity between the two sides (and between trees) is very high at both sites (Tables 3S.2 and 3S.3). SF variations were assessed with regards to variations in VPD, Rad, Tmax, Tmin, SWC, PCP and WS. Many different models were tested to fit the data, but only the best models (i.e. linear, sigmoidal and Gompertz) were retained for each environmental variable vs sap flow relationship (based on the highest  $R^2$  value obtained). The Gompertz (3 parameters) equation was used for VPD whereas the sigmoidal (3 parameters) equation was used for Rad. For the other variables, simple linear regressions were carried out. For all the regression analyses, the original sap flow (i.e. no data transformation) and environmental variable data were used. Second, the variation in mean hourly sap flow velocity ( $SF_v$ ) for the period determined by the beginning of the growing season to the end of August is presented to show the diel hysteresis with Rad and VPD, respectively using standardized data (i.e. each hourly observation is divided by the daily maximum) in order to compare the two species as explained in Pappas et al. (2018). Only days with no rain were selected for the diel hysteresis analysis.

#### 3.4.4.2 Analysis of a drought in the summer of 2012

In July 2012, a meteorological drought occurred at the balsam fir site (Houle et al., 2016). Between July 1<sup>st</sup> and August 4<sup>th</sup>, only 23 mm of rain was recorded while the average amount for this time period is 150 mm. This led to very low soil moisture as compared to the long-term average at the site (Figure 3.1). Figure 3S.1 (top panel) shows the total monthly precipitation and its anomaly as well as daily soil moisture anomaly (bottom panel) from 2001 to 2016. Although year 2010 was also characterised by strong negative soil moisture anomalies, 2012 was chosen because of combined very low precipitation and soil moisture anomalies and because the precipitation anomalies occurred in July as compared to August (2010), i.e. during the period of stem growth, the latter generally levelling off after August 1 (Duchesne and Houle, 2011).

Tree species have been shown to be very sensitive to the timing of drought (D'Orangeville et al., 2018). Besides, the summer 2012 had the highest needle fall, with the July 2012 drought leading to large losses of nutrients at the balsam fir site (Houle et al., 2016). While the permanent wilting point might not have been reached in both HorB and HorC during this drought based on the soil texture, the soil water content was quite low (23.9 % in HorB and below 20 % in HorC). Soil texture varies greatly spatially and soil porosity is not only influenced by soil texture, but also by the presence of organic matter, degree of soil compaction and soil depth. Thus, the permanent wilting point and the actual soil water content are subject to great variation within the site. During this drought period, the impact of the main environmental variables (VPD, Rad and SWC) on SF was analysed via a 15-day moving average of the coefficient of determination. The Gompertz (3 parameters) equation was used for VPD, sigmoidal (3 parameters) for Rad, and a simple linear regression for SWC.

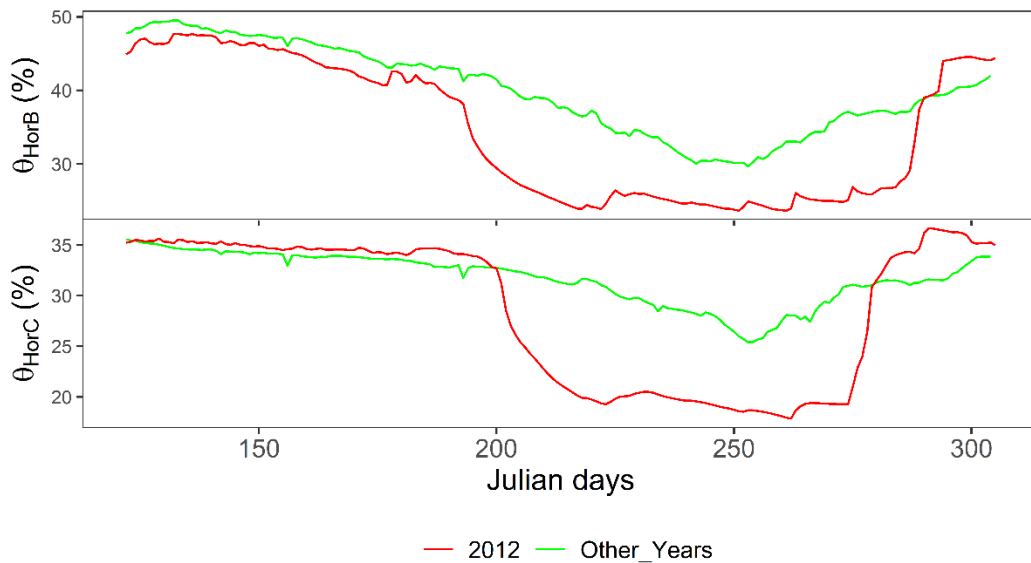


Figure 3.1: Daily soil water content from 1<sup>st</sup> May (Julian day 122) to 31<sup>st</sup> October (Julian day 305) in soil horizons B ( $\theta_{HorB}$ ) and C ( $\theta_{HorC}$ ) at the balsam fir site for the year 2012 (red) and for the average of years 1999 to 2016 (excluding 2012).

## 3.5 Results

### 3.5.1 Impact of environmental variables on sap flow during the growing season

Figure 3.2 (left panel) shows an example of the average diurnal SFv for each tree obtained for a typical week in June 2007 for both balsam fir (top) and black spruce (bottom). Julian day 171 of 2007 at the balsam fir site shows the impact of a rainy day, in which 29 mm of rain fell, leading to a very low diurnal SFv. On the other hand, although there was no rainfall on Julian day 174, there was low radiation ( $\sim 162 \text{ W m}^{-2}$ ) which led to slightly lower SFv. On the other days of that week, no rain fell and we observed significant diurnal SFv of up to about 3 cm/h. The results also show that diurnal solar radiation was synchronised with diurnal SFv, with the peak solar radiation aligning with peak SFv most of the time. However, this is not observed for vapour pressure deficit, where there is a lag between the peak SFv and peak vapour pressure deficit, especially on non-rainy days. The right panel of Figure 3.2 shows the hourly mean (mean over one week period) SFv and Rad for one week in June 2007 and one week in August 2007 for both balsam fir (top) and black spruce (bottom). The result shows that the hourly mean SFv starts much earlier and ends later during the day in the month of June as compared to August due to day length.

#### 3.5.1.1 Relationship of sap flow to environmental variables

Two variables (VPD and Rad) consistently had the strongest relationships to daily SF (Figure 3.3) over all the years studied. Figures 3.4 and 3.5 show examples of these relationships for one year. The strong non-linear relationship between daily SF and VPD was best described using the Gompertz equation (Figure 3.4) with an average coefficient of determination value of  $0.73 \pm 0.11$  for balsam fir for the six probes for the entire study period (2004-2013; Figure 3.3 - left). For black spruce, an average

coefficient of determination of  $0.67 \pm 0.13$  was obtained for the six probes for the period 2006 to 2009 (Figure 3.3 – right).

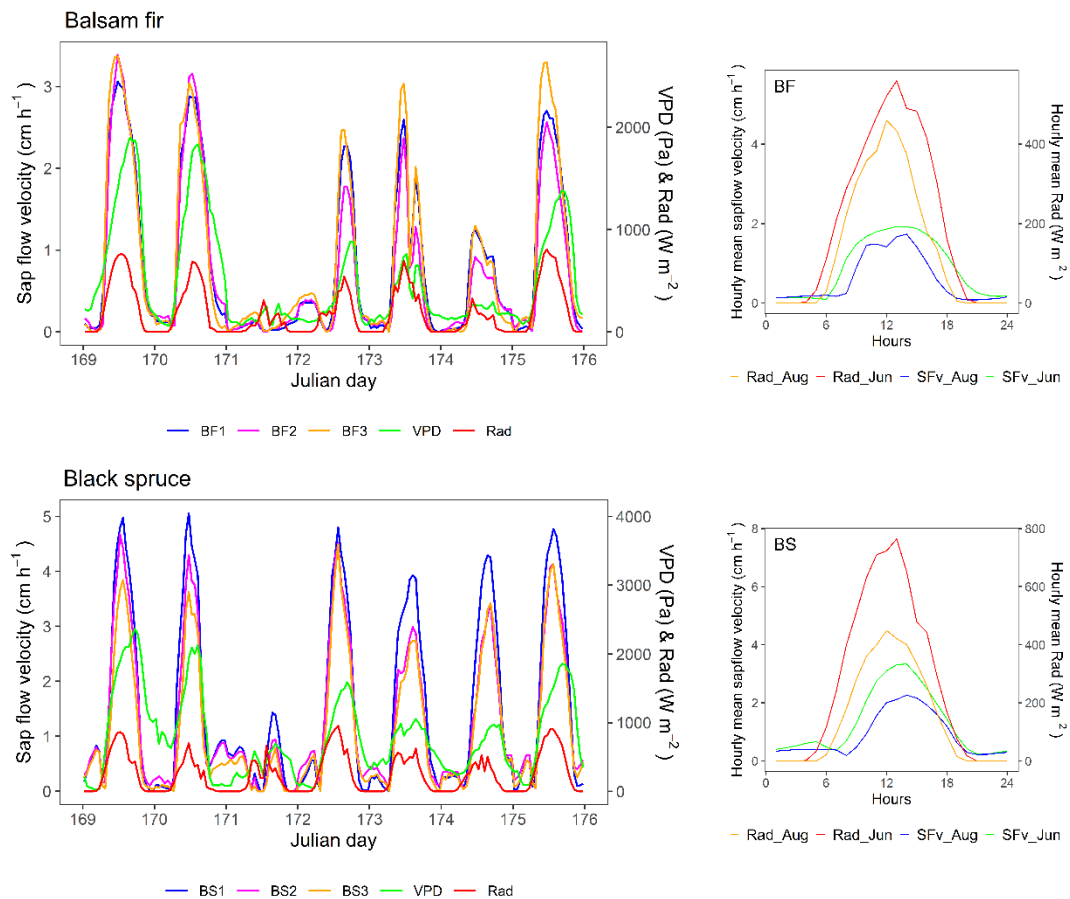


Figure 3.2: An example of sap flow velocity ( $\text{cm h}^{-1}$ ; mean of sun-side and shade-side of each tree) for balsam fir (BF1, BF2 and BF3; top left) and black spruce (BS1, BS2 and BS3; bottom left) together with vapour pressure deficit (VPD, Pa) and solar radiation (Rad,  $\text{W m}^{-2}$ ) for one week in June (peak transpiration period) 2007; hourly mean sap flow velocity (average of the six probes) and hourly mean solar radiation for one-week in June 2007 and one-week in August 2007 for balsam fir (BF; top right) and black spruce (BS; bottom right).

A sigmoidal equation best described the relationship between Rad and daily SF (Figure 3.5) with an average coefficient of determination of  $0.63 \pm 0.14$  for balsam fir (Figure 3.3 – left). As for black spruce, the average coefficient of determination was  $0.59 \pm$

0.11. The other climatic variables had a much smaller impact on SF and a simple linear regression described this relationship (Figure 3.3). The coefficient of determination together with the direction of correlation (positive or negative) for each variable and each year are shown in Table 3S.4 for both species. For balsam fir, Tmax had an average coefficient of determination of  $0.32 \pm 0.13$ , followed by PCP with a value of  $0.26 \pm 0.09$ , then both SWC and Tmin having values of  $0.04 \pm 0.04$ , and finally WS having the lowest values of  $0.01 \pm 0.01$ . As for black spruce, the average coefficient of determination was  $0.34 \pm 0.11$  for Tmax,  $0.17 \pm 0.07$  for PCP,  $0.02 \pm 0.02$  for Tmin,  $0.03 \pm 0.03$  for SWC, and finally  $0.01 \pm 0.02$  for WS.

Strong diel hysteresis (clockwise) was observed for both species for the relationship SF-VPD. The hysteresis was counter clockwise for Rad, but not as strong as for VPD, especially for balsam fir (Figure 3.6). The SF-VPD and SF-Rad hysteresis for the other studied years at both sites are given in Figures 3S.2, 3S.3 and 3S.4.

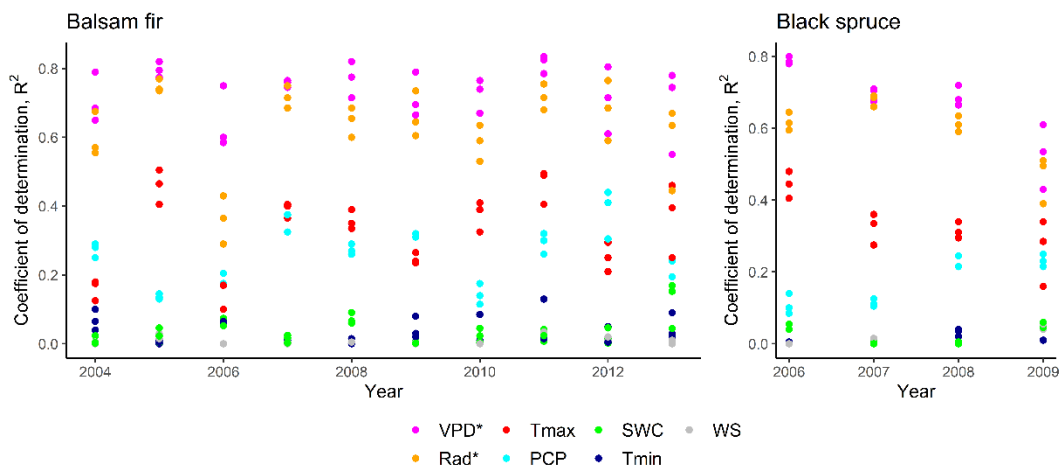


Figure 3.3: Coefficient of determination ( $R^2$ ) between daily sap flow and each environmental variable of the three sample trees at both balsam fir (left) and black spruce (right) site for each studied year. The \* indicate non-linear regressions (Gompertz for VPD and sigmoidal for Rad) as described in the text and in Figures 3.4 and 3.5.

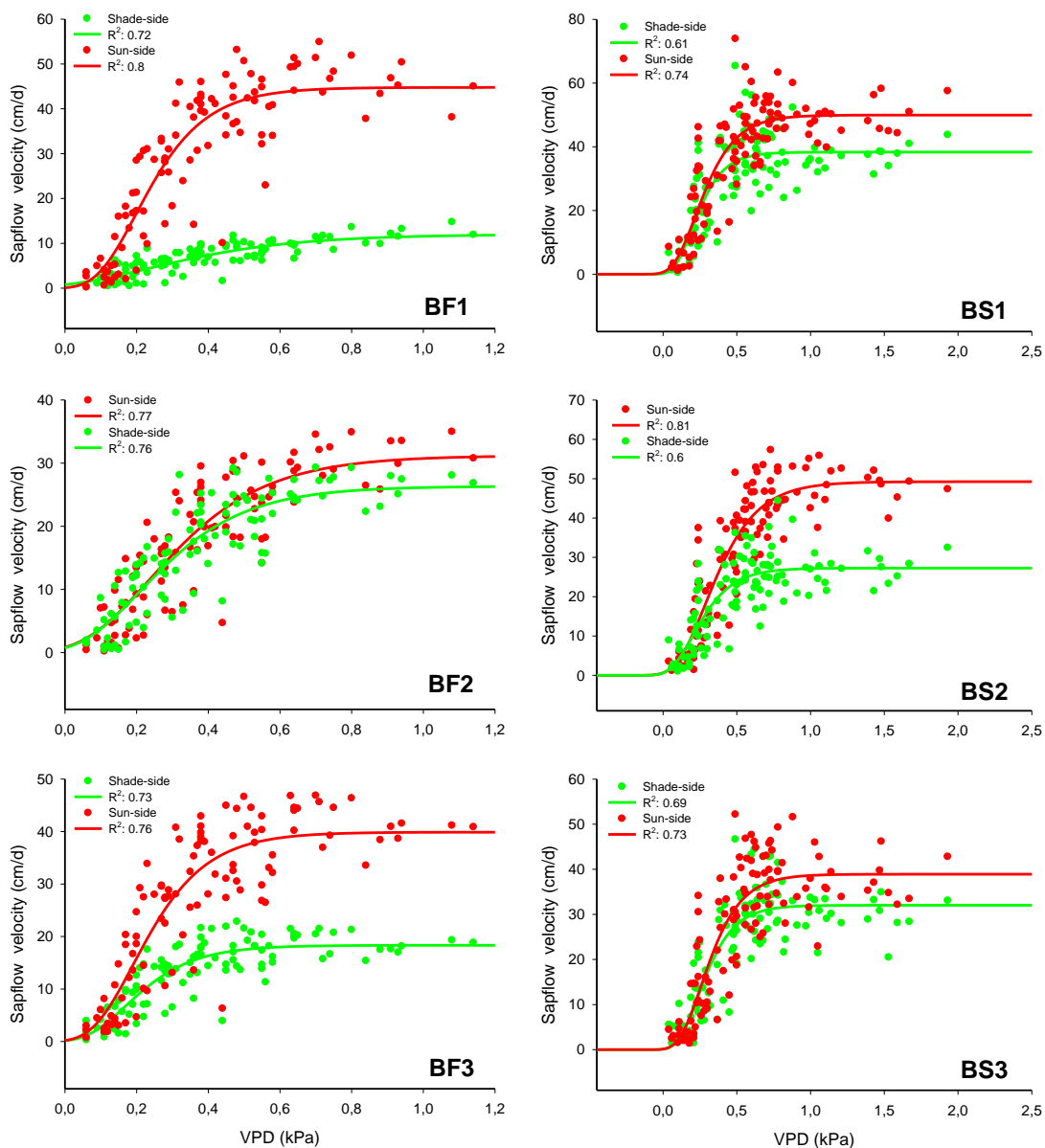


Figure 3.4: Example of the relationship between daily sap flow (cm/d) and vapour pressure deficit (VPD; kPa) for each probe (sun and shade sides) for balsam fir (BF1 to BF3) and black spruce trees (BS1 to BS3) for the year 2007 using the Gompertz (3 parameters) equation. The year 2007 was selected as its  $R^2$  value for the relationships between sap flow and VPD is representative of the average  $R^2$  of all years.

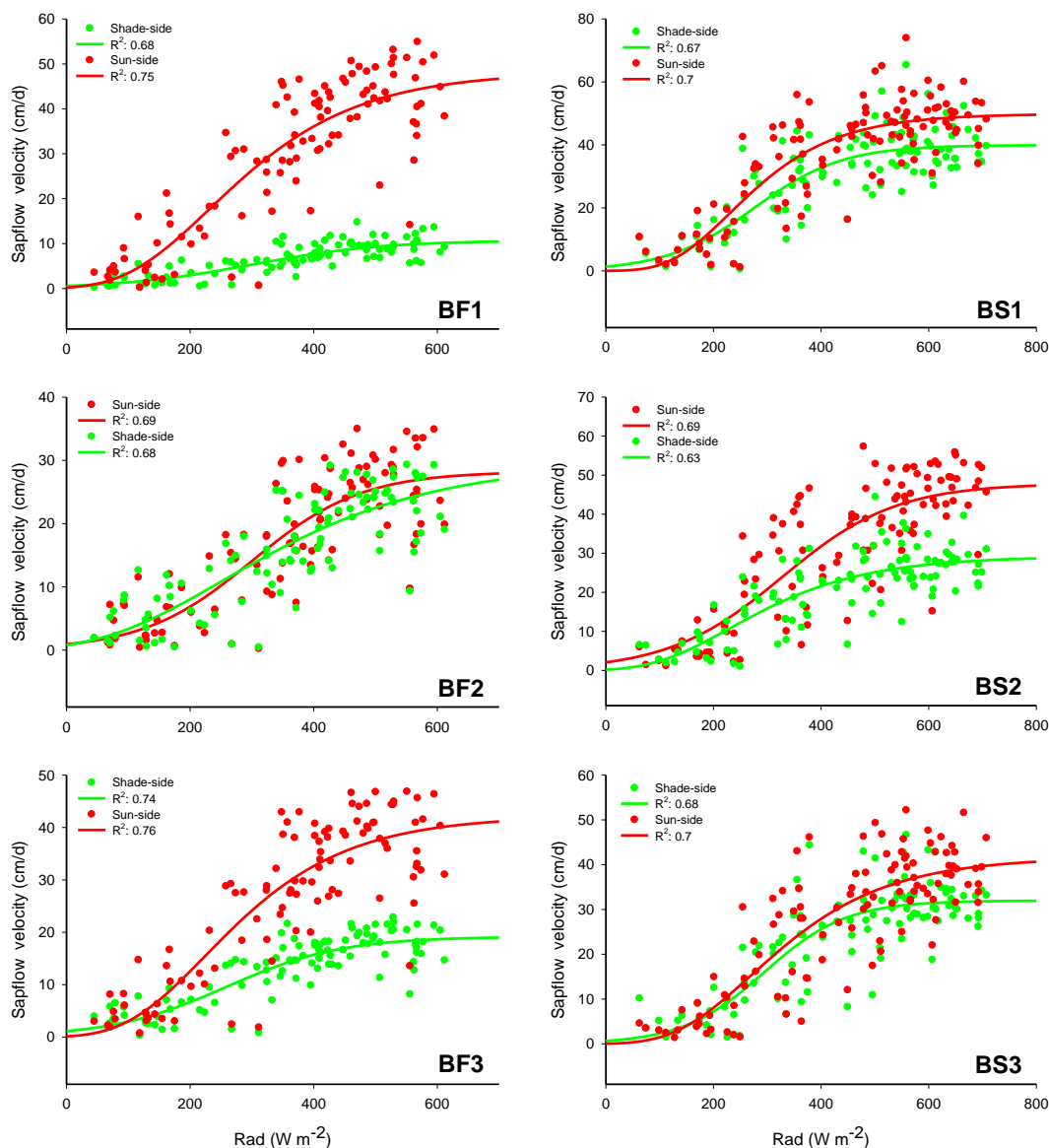


Figure 3.5: Example of the relationship between daily sap flow (cm/d) and solar radiation (Rad;  $W m^{-2}$ ) for each probe (sun and shade sides) for balsam fir (BF1 to BF3) and black spruce (BS1 to BS3) for the year 2007 using the sigmoidal (3 parameters) equation. The year 2007 was selected as its  $R^2$  value for the relationship between sap flow and Rad is representative of the average  $R^2$  of all years.

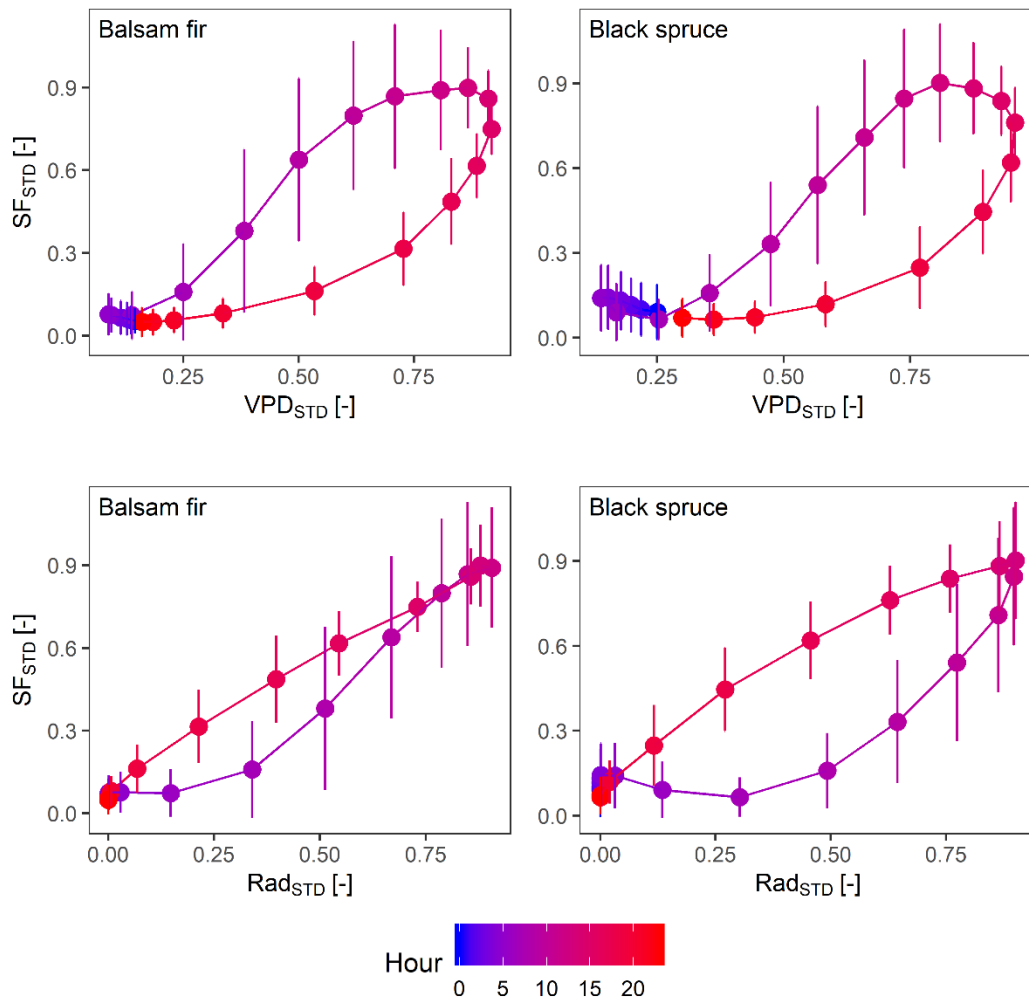


Figure 3.6. Typical hysteresis loop of standardized sap flow velocity ( $SF_{STD}$ ) data with standardized VPD and Rad on an hourly basis for 2007 for the period from the beginning of the growing season to the end of August. Error bars are  $\pm$  standard deviation based on the six probes. The diel hysteresis for other years are shown in the supplementary material (Figures 3S.2, 3S.3 and 3S.4).

### 3.5.2 Impact of an extreme drought on sap flow in the summer 2012 at the balsam fir site

Figure 3.7 shows the daily time series from May to September in the extreme drought year 2012 for  $T_{max}$ ,  $T_{min}$ , VPD, stem diameter variation (SDV) for the three sample

balsam fir trees, daily SF for the six probes, and PCP and SWC for the B horizon at the balsam fir site. SWC gradually decreased during the drought in the B horizon. The daily SF seemed to decrease slightly during the second half of the drought but remains similar to other moments throughout the year.

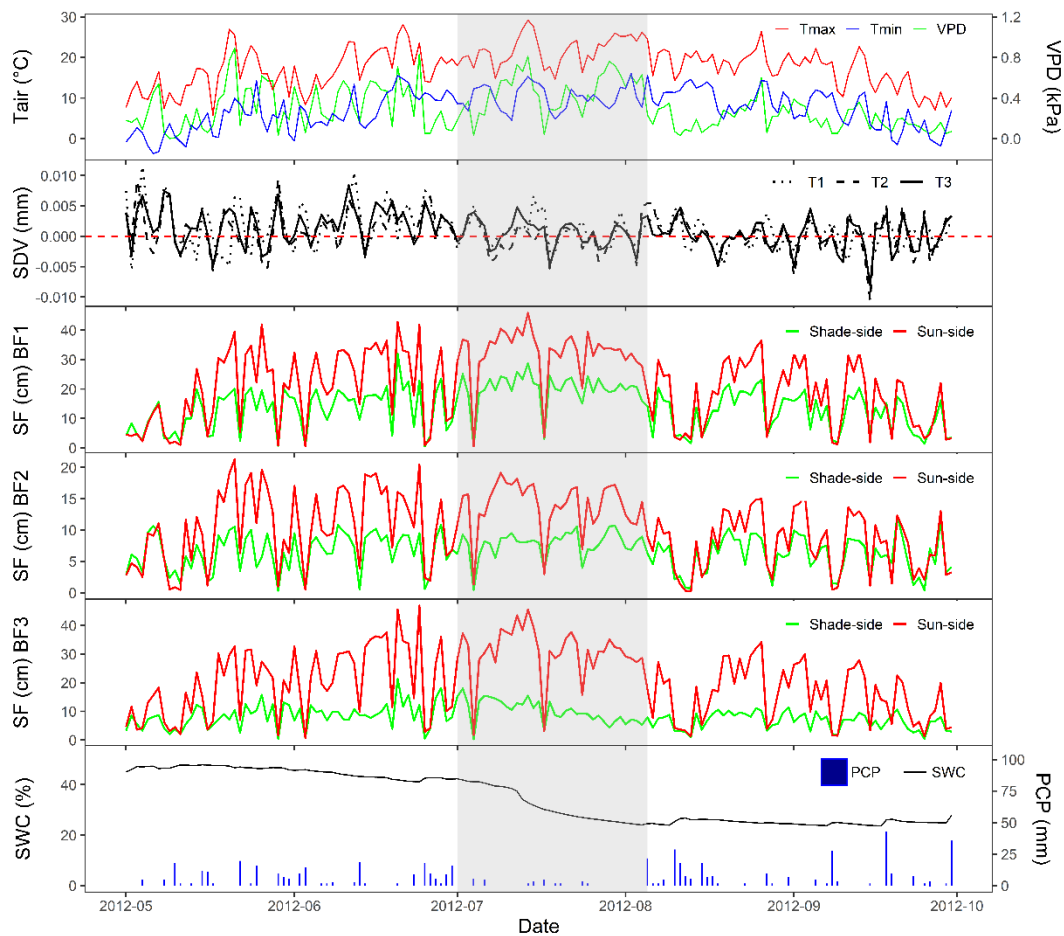


Figure 3.7: Daily sap flow (SF, cm) with stem diameter variation (SDV, mm) for the three balsam fir trees during the growing season (May-Sep) over a year (2012), together with variations in vapour pressure deficit (VPD, kPa), minimum and maximum air temperature (Tmin and Tmax, °C), soil water content (SWC, %) in the B horizon and precipitation (PCP, mm).

Figure 3.8 shows the 15-day moving average coefficient of determination of daily SF versus the main environmental variables (VPD, Rad and SWC) for the drought period

and one week prior and after it. Both VPD and Rad had a very high coefficient of determination from the beginning, but dropped at the end of the drought period. However, the high value resumed a few days after the drought. As for SWC, it had a low coefficient of determination, much below either VPD or Rad, throughout the drought period. This shows that even during the drought period Rad and VPD still had the greatest impact on SF.

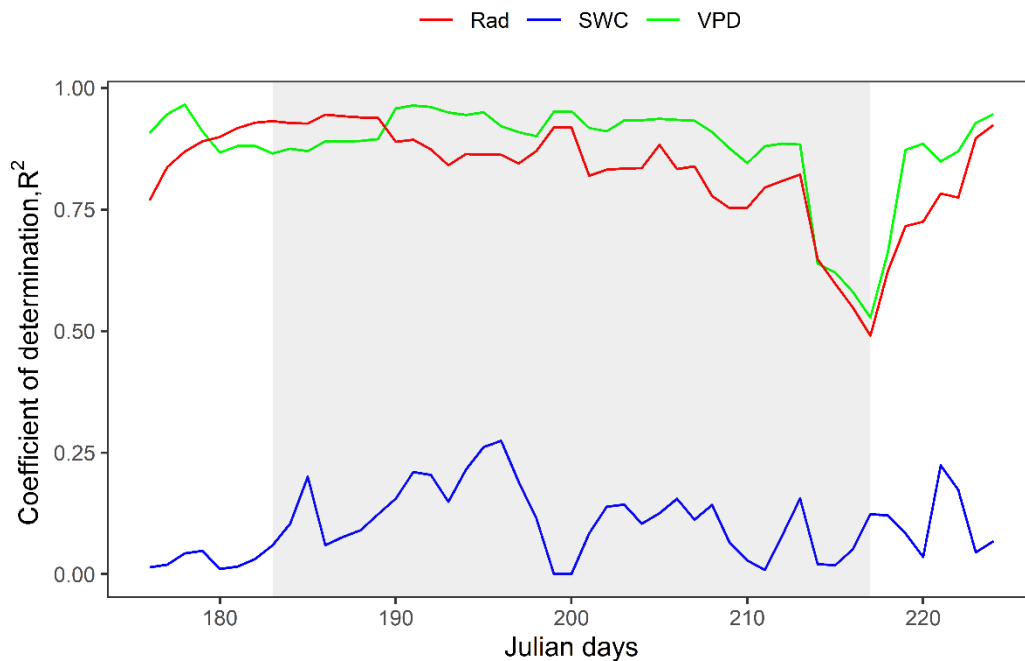


Figure 3.8: Moving average (15-day) of coefficient of determination ( $R^2$ ; average of the six probes) for the regression between daily sap flow and the main environmental variables (VPD, Rad and SWC) for balsam fir during and one week prior and after the drought (1<sup>st</sup> Jul to 4<sup>th</sup> Aug 2012; highlighted in grey).

## 3.6 Discussion

### 3.6.1 Control of sap flow during the growing season

Based on the dendrometer data, the beginning of the growing season occurs mostly from the 2<sup>nd</sup> week of May (day 128) to the end of May (day 149) for balsam fir, while it ranges from mid May (day 133) to the 2<sup>nd</sup> week of June (day 159) for black spruce (see Table 3S.5). This is more or less in agreement with the data of Rossi et al. (2008) for two sites in eastern Canada, in which they showed that wood formation begins between May 17<sup>th</sup> (day 137) and June 6<sup>th</sup> (day 157) for balsam fir.

In our multiple year study, SF in both species was strongly non-linearly related to VPD, with the former rising quickly before attaining a plateau for each year of observation. Such non-linear relationships (with large variance explanation) were reported for instance, in trembling aspen in Saskatchewan (Hogg and Hurdle, 1997), in balsam fir in Wisconsin, US (Ewers et al., 2002), in Loblolly pine in Georgia, USA (Ford et al., 2004), in black spruce in western Canada (Van Herk et al., 2011; Patankar et al., 2015; Pappas et al. 2018), and in subtropical coniferous/broadleaf evergreen forests in China (Liu et al., 2014). Likewise, SF also had a strong non-linear relationship with Rad. The impact of Rad on SF has been studied by others as well, for example in red maple in the US (Wullschleger et al., 2000), in Scots pine in Scotland (Wang et al., 2017) and Qinghai spruce in China (Chang et al. 2014), but the relationship varied from linear to slightly non-linear. The study of Patankar et al. (2015) suggested that Rad alone was a better determinant of daily SF than VPD, however, we found that VPD was consistently a better (although sometimes only slightly) predictor of SF than Rad over all years and across both sites (Figure 3.3).

Our data show that soil water is not an important driving variable for transpiration which may be due to the humid conditions encountered at our study sites. In drier

environments, soil water has been found to be an important variable controlling transpiration in Scots pine (Wang et al., 2017). Daily SF was also correlated with other climate variables but much more weakly (Tmax, PCP, Tmin and WS; Figure 3.3). The smaller influence of Tmax on SF (as compared to VPD and Rad) is in agreement with the results of Wang et al. (2017). PCP explains relatively little variance and had a negative relationship with SF as the precipitation intercepted in the canopy reduces transpiration and also because Rad is usually low on rainy days. While day length was not an environmental variable considered in the regression analysis, we observed it to have an important effect on the duration of daily SF. Longer day lengths led to a higher total amount of transpiration when comparing days in June to those in August (shown as average duration of solar radiation in a day in Figure 3.2 right panel), which is in agreement with the findings of Lagergren and Lindroth (2002) and reflects the greater photosynthesis in anisohydric species around the summer solstice. Overall, our first hypothesis was verified whereby SF was mainly controlled by VPD and Rad during the growing season while SWC had nearly no impact on a daily time scale. However, these results might differ on a coarser (weekly or monthly) timescale.

#### 3.6.1.1 Sap flow hysteresis in relation to VPD and Rad

Hourly variation of SFv with VPD and Rad were studied for both species. The SFv standardized curves showed strong hysteresis (clockwise direction) with VPD for both species. Such hysteresis with VPD has been reported for evapotranspiration measured with tower fluxes (Zhang et al. 2014; Zheng et al. 2014) and for sap flow measurements for different species in various ecosystems (O'Brien et al. 2004; Zeppel et al. 2004; Pappas et al. 2018). However, the strength of the hysteresis varies as a function of species and environmental variables and these relationships are still not clearly understood. Meinzer et al. (1997) suggested that the out of phase diurnal variation of VPD and Rad, found mostly on clear days, was responsible for this hysteresis effect. Similarly, Zhang et al. (2014) found the magnitude of the evapotranspiration-VPD

hysteresis depended on the time lag between evapotranspiration and VPD (the latter peaking later in the day, see Figure 3.2 left), and also on plant water status, with high water potential in plant tissues (due to high soil water content) associated with more pronounced hysteresis. An interesting hysteresis characteristic of the hourly SF with VPD is the higher between day variability in the ascending phase than in the descending phase that could be due to variability in the predawn water potential of the tree. Based on one summer of observations for a dry site in the southern portion of the boreal forest in central Canada, Pappas et al. (2018) suggested that larch, because of a much more pronounced hysteresis than black spruce, has stomatal regulation strategies employing isohydric behaviour as compared to the anisohydric black spruce. Contrary to the weak SF-VPD hysteresis observed by Pappas et al. (2018) for black spruce, we observed a much stronger hysteresis for this same species and for balsam fir as well although both species are known to be anisohydric. Therefore, our results are not in agreement with Pappas et al. (2018) regarding the link between the magnitude of the hysteresis and the iso/anisohydric behaviour of tree species. Our results also differ from theirs, since they observed stronger hysteresis with Rad than with VPD for larch and black spruce while our results show the opposite for both black spruce and balsam fir. Our results are more consistent with Zeppel et al. (2004) who observed a higher degree of hysteresis for VPD than for Rad for two native Australian species. O'Brien et al. (2004) also observed much stronger hysteresis with VPD than with Rad for 10 different species in a wet tropical forest in Costa Rica.

Conciliating these contrasting observations for black spruce would require more research but they could at least potentially be attributed to contrasted precipitation between the studied sites as well as different genotypes of black spruce. Precipitation averaged 69 mm for the months of June to August at the Pappas et al. (2018) site, while our sites were moister as precipitation averaged 314 mm and 356 mm respectively at the black spruce and the balsam fir site for the same period. On the other hand, while an absence of diel hysteresis was reported during cloudy days for both VPD and Rad

as the Rad-VPD are more in phase (Meinzer et al. 1997), the magnitude of hysteresis was found to increase with increasing soil water potential and leaf water potential (Zhang et al., 2014), thus resulting in greater hysteresis for our studied humid site populations. In contrast with both, our findings and those of Pappas et al. (2018), O'Grady et al. (1999) found the magnitude of hysteresis to be more pronounced during the dry season compared to the wet season in Eucalyptus species in Australian savannas. While the finding of the latter study contradicts other studies carried out in the same region, the authors concluded that in the presence of a strong coupling between open forests (less than 50% forest cover) and the atmosphere and the availability of unlimited soil water supply in the deeper soil horizon, the continued transpiration in the dry season was mostly driven by the increased VPD, thus leading to stronger hysteresis. Henceforth, the varying responses of these species in regards to hysteresis in different climatic conditions further underlines the necessity for a more profound study on this subject across species but also within a species as a function of fluctuations in environmental variables.

### 3.6.2 The analysis of the 2012 summer drought at the balsam fir site

During July 2012, the total amount of rain that fell at the balsam fir site was much below the long-term average (Houle et al., 2016) leading to the worst drought observed at the site since the beginning of meteorological measurements in 1966. The absence of rain in July led to a progressive decline in SWC that was apparent after mid-July in the B horizon (Figure 3.7). In contrast with other studies on the impact of drought (Lu et al., 1995; Cavender-Bares et al. 2007), SF did not substantially decline during this drought period. Granier et al. (2007) found that water vapour fluxes were reduced across a range of forest ecosystems and climates in Europe when soil water dropped below 40% during a severe long duration (six months) drought. Lagergren and Lindroth (2002) recorded a decrease in transpiration when the relative extractable water dropped

below 20%. da Silva Sallo et al. (2017) found soil water to influence transpiration during dry months, while VPD controlled transpiration during wet months in a seasonally flooded forest in Brazil. Likewise, Gartner et al. (2009) found SF to be controlled by SWC in both Norway spruce and birch trees during a drought in Austria, but was a function of atmospheric demand (i.e. potential evapotranspiration) during the other months. As noted by Pataki and Oren (2003), transpiration from trees during a drought was species-specific. At our study site, the short duration of the drought period could be a plausible explanation for the maintained sap flow.

While sap flow was not substantially reduced during the drought period, the relationships between the former and VPD/Rad differed slightly at the end of the drought (Figure 3.8). Both VPD and Rad maintained their high coefficient of determination throughout the drought period except at the end, where the coefficient of determination dropped. On the other hand, SWC had a low coefficient of determination throughout the drought period. Both VPD and Rad were still the main environmental variables controlling sap flow during the 2012 drought. Thus, our second hypothesis stating that soil water would control sap flow during a drought is rejected.

The first precipitation events after the drought of July 2012 were accompanied by large nutrient losses (particularly potassium) in throughfall (Houle et al. 2016) while needle fall in the summer 2012 was the highest in 14 years. Such a loss of nutrients probably had a strong impact on tree reserves which compounded the drought effect itself. Despite these impacts, growth in 2012 was comparable to the average annual growth (14 year average) at this site (Table 3S.5), because most tree rings are formed in July. Drought impacts on growth often occur in the years following the event (this is often observed in dendrochronology studies; Itter et al. 2019) and as shown for balsam fir at this site after an experimental throughfall exclusion simulating drought (D'Orangeville et al. 2013). Indeed, growth in 2013 and 2014 was lower than preceding years (Table

3S.5). July 2013 was in fact the second driest July after 2012 which may have further impacted the 2014 growth. It is difficult to precisely identify the cause of the strongly reduced growth in 2013 and 2014 but our results suggest the combination of multiple factors.

### 3.7 Conclusion

This study focused on the relationship between SF and environmental variables in the growing season for two boreal tree species. It also assessed the influence of environmental variables during a drought period. As per our first hypothesis, SF was under the control of VPD and Rad for both balsam fir and black spruce. SF had a significant non-linear relationship with both VPD and Rad and much weaker linear relationships with Tmax and PCP while other studied variables had marginal effects. While the above findings of the regression analyses between SF and environmental variables are based on a daily timescale, the results might be different at coarser time scales. Concurrently, our study also found a strong diel hysteresis of  $SF_v$  vs VPD and Rad for both species. The magnitude of the hysteresis does not seem to relate to the degree of iso/anisohydricity as previously proposed (Pappas et al. 2018).

Contrary to our second hypothesis, soil water did not become the dominant factor influencing SF during the drought encountered at the balsam fir site, since VPD and Rad remained the most important variables. Indeed, we observed a barely noticeable decrease in SF in the second half of the drought. Our study emphasized that VPD drives transpiration followed by solar radiation in this energy-limited system. However, under much more frequent and intense longer-duration droughts in the future as well as earlier snowmelt (and longer growing seasons), there may be a shift from an energy-limited system to water-limited system in these humid boreal forests. Thus, in order to identify

the threshold SWC at which the driving forces of transpiration shifts from VPD/Rad to SWC in this humid boreal forest, I recommend conducting an experimental field study of longer-duration droughts (via exclusion of rainwater) and to measure the soil water content/soil water potential and sapflow to determine this threshold SWC value.

### 3.8 Acknowledgements

This work was supported by a MITACS Cluster grant and the OURANOS organisation. We thank the technicians of the Ministry of Forests, Wildlife, and Parks for the measurement of all data used in this study.

### 3.9 References

- Bonan, G. B., 2008. Forests and Climate Change: Forcings, Feedbacks, and the Climate Benefits of Forests. *Science*, 320(5882), 1444-1449.
- Bonan, G. B., & Shugart, H. H., 1989. Environmental Factors and Ecological Processes in Boreal Forests. *Annual Review of Ecology and Systematics*, 20, 1-28.
- Bovard, B. D., Curtis, P. S., Vogel, C. S., Su, H. B., & Schmid, H. P., 2005. Environmental controls on sap flow in a northern hardwood forest. *Tree Physiology*, 25(1), 31-38. doi: 10.1093/treephys/25.1.31
- Brandt, J., Flannigan, M., Maynard, D., Thompson, I., & Volney, W., 2013. An introduction to Canada's boreal zone: ecosystem processes, health, sustainability, and environmental issues. *Environmental Reviews*, 21(4), 207-226.
- Cavender-Bares, J., Sack, L., & Savage, J., 2007. Atmospheric and soil drought reduce nocturnal conductance in live oaks. *Tree Physiol*, 27(4), 611-620.
- Chang, X., Zhao, W., & He, Z., 2014. Radial pattern of sap flow and response to microclimate and soil moisture in Qinghai spruce (*Picea crassifolia*) in the

- upper Heihe River Basin of arid northwestern China. *Agricultural and Forest Meteorology*, 187, 14-21.
- Chen, L., Zhang, Z., Li, Z., Tang, J., Caldwell, P., & Zhang, W., 2011. Biophysical control of whole tree transpiration under an urban environment in Northern China. *Journal of Hydrology*, 402(3-4), 388-400. <https://doi.org/10.1016/j.jhydrol.2011.03.034>
- Collins, A. R., Burton, A. J., & Cavaleri, M. A., 2018. Effects of Experimental Soil Warming and Water Addition on the Transpiration of Mature Sugar Maple. *Ecosystems*, 21(1), 98-111. doi: 10.1007/s10021-017-0137-9
- da Silva Sallo, F., Sanches, L., de Moraes Dias, V. R., da Silva Palácios, R., & de Souza Nogueira, J., 2017. Stem water storage dynamics of *Vochysia divergens* in a seasonally flooded environment. *Agricultural and Forest Meteorology*, 232, 566-575.
- Daley, M. J., & Phillips, N. G., 2006. Interspecific variation in nighttime transpiration and stomatal conductance in a mixed New England deciduous forest. *Tree Physiol*, 26(4), 411-419.
- D'Orangeville, L., Côté, B., Houle, D., & Morin, H., 2013. The effects of throughfall exclusion on xylogenesis of balsam fir. *Tree Physiology*, 33(5), 516-526.
- D'Orangeville, L., Maxwell, J., Kneeshaw, D., Pederson, N., Duchesne, L., Logan, T., Houle, D., Arseneault, D., Beier, C.M., Bishop, D.A. and Druckenbrod, D., 2018. Drought timing and local climate determine the sensitivity of eastern temperate forests to drought. *Global change biology*, 24(6), pp.2339-2351.
- Duchesne, L., & Houle, D., 2011. Modelling day-to-day stem diameter variation and annual growth of balsam fir (*Abies balsamea* (L.) Mill.) from daily climate. *Forest Ecology and Management*, 262(5), 863-872. doi: <https://doi.org/10.1016/j.foreco.2011.05.027>
- Duchesne, L., Houle, D., & D'Orangeville, L., 2012. Influence of climate on seasonal patterns of stem increment of balsam fir in a boreal forest of Québec, Canada. *Agricultural and Forest Meteorology*, 162, 108-114.
- Ewers, B., Mackay, D., Gower, S., Ahl, D., Burrows, S., & Samanta, S., 2002. Tree species effects on stand transpiration in northern Wisconsin. *WATER RESOURCES RESEARCH*, 38(7), 8-1-8-11.
- Ford, C. R., Goranson, C. E., Mitchell, R. J., Will, R. E., & Teskey, R. O., 2004. Diurnal and seasonal variability in the radial distribution of sap flow: predicting total stem flow in *Pinus taeda* trees. *Tree Physiology*, 24(9), 951-960.
- Gartner, K., Nadezhdina, N., Englisch, M., Čermak, J., & Leitgeb, E., 2009. Sap flow of birch and Norway spruce during the European heat and drought in summer

2003. *Forest Ecology and Management*, 258(5), 590-599. doi:<https://doi.org/10.1016/j.foreco.2009.04.028>
- Granier, A., 1987. Evaluation of transpiration in a Douglas-fir stand by means of sap flow measurements. *Tree Physiology*, 3, 309-320. doi: 10.1093/treephys/3.4.309
- Granier, A., Biron, P., & Lemoine, D., 2000. Water balance, transpiration and canopy conductance in two beech stands. *Agricultural and Forest Meteorology*, 100(4), 291-308.
- Granier, A., Reichstein, M., Bréda, N., Janssens, I. A., Falge, E., Ciais, P., Grünwald, T., Aubinet, M., Berbigier, P., Bernhofer, C., Buchmann, N., Facini, O., Grassi, G., Heinesch, B., Ilvesniemi, H., Keronen, P., Knohl, A., Köstner, B., Lagergren, F., Lindroth, A., Longdoz, B., Loustau, D., Mateus, J., Montagnani, L., Nys, C., Moors, E., Papale, D., Peiffer, M., Pilegaard, K., Pita, G., Pumpanen, J., Rambal, S., Rebmann, C., Rodrigues, A., Seufert, G., Tenhunen, J., Vesala, T., Wang, Q., 2007. Evidence for soil water control on carbon and water dynamics in European forests during the extremely dry year: 2003. *Agricultural and Forest Meteorology*, 143(1-2), 123-145. doi:<http://dx.doi.org/10.1016/j.agrformet.2006.12.004>
- Hogg, E. H., & Hurdle, P. A., 1997. Sap flow in trembling aspen: implications for stomatal responses to vapor pressure deficit. *Tree Physiology*, 17(8-9), 501-509. doi: 10.1093/treephys/17.8-9.501
- Houle, D., Lajoie, G., & Duchesne, L., 2016. Major losses of nutrients following a severe drought in a boreal forest. *Nature Plants*, 2, 16187. doi: 10.1038/nplants.2016.187. <http://www.nature.com/articles/nplants2016187#supplementary-information>
- Itter, M. S., D'Orangeville, L., Dawson, A., Kneeshaw, D., Duchesne, L., & Finley, A. O., 2019. Boreal tree growth exhibits decadal-scale ecological memory to drought and insect defoliation, but no negative response to their interaction. *Journal of Ecology*, 107(3), 1288-1301.
- Jonard, F., André, F., Ponette, Q., Vincke, C., & Jonard, M., 2011. Sap flux density and stomatal conductance of European beech and common oak trees in pure and mixed stands during the summer drought of 2003. *Journal of Hydrology*, 409(1-2), 371-381.
- Juice, S. M., Templer, P. H., Phillips, N. G., Ellison, A. M., & Pelini, S. L., 2016. Ecosystem warming increases sap flow rates of northern red oak trees. *Ecosphere*, 7(3), e01221-n/a. doi: 10.1002/ecs2.1221
- Jung, E. Y., Otieno, D., Lee, B., Lim, J. H., Kang, S. K., Schmidt, M. W. T., & Tenhunen, J., 2011. Up-scaling to stand transpiration of an Asian temperate

- mixed-deciduous forest from single tree sapflow measurements. *Plant Ecology*, 212(3), 383-395. doi: 10.1007/s11258-010-9829-3
- Köstner, B., Falge, E., M., Alsheimer, M., Geyer, R., & Tenhunen, J., D., 1998. Estimating tree canopy water use via xylem sapflow in an old Norway spruce forest and a comparison with simulation-based canopy transpiration estimates. *Ann. For. Sci.*, 55(1-2), 125-139.
- Lagergren, F., & Lindroth, A., 2002. Transpiration response to soil moisture in pine and spruce trees in Sweden. *Agricultural and Forest Meteorology*, 112(2), 67-85. doi: [https://doi.org/10.1016/S0168-1923\(02\)00060-6](https://doi.org/10.1016/S0168-1923(02)00060-6)
- Lenton, T. M., Held, H., Kriegler, E., Hall, J. W., Lucht, W., Rahmstorf, S., & Schellnhuber, H. J., 2008. Tipping elements in the Earth's climate system. *Proceedings of the National Academy of Sciences*, 105(6), 1786-1793. doi: 10.1073/pnas.0705414105
- Liu, X., Li, Y., Chen, X., Zhou, G., Cheng, J., Zhang, D., Meng, Z., Zhang, Q., 2014. Partitioning evapotranspiration in an intact forested watershed in southern China. *Ecohydrology*, 8(6), 1037-1047.
- Lu, P., Biron, P., Breda, N., & Granier, A., 1995. Water relations of adult Norway spruce (*Picea abies* (L) Karst) under soil drought in the Vosges mountains: water potential, stomatal conductance and transpiration. Paper presented at the *Annales des Sciences Forestieres*.
- Macfarlane, C., Bond, C., White, D. A., Grigg, A. H., Ogden, G. N., & Silberstein, R., 2010. Transpiration and hydraulic traits of old and regrowth eucalypt forest in southwestern Australia. *Forest Ecology and Management*, 260(1), 96-105.
- Meinzer, F., Hinckley, T., & Ceulemans, R., 1997. Apparent responses of stomata to transpiration and humidity in a hybrid poplar canopy. *Plant, Cell & Environment*, 20(10), 1301-1308.
- Mitchell, P. J., Benyon, R. G., & Lane, P. N. J., 2012. Responses of evapotranspiration at different topographic positions and catchment water balance following a pronounced drought in a mixed species eucalypt forest, Australia. *Journal of Hydrology*, 440-441, 62-74. doi: <https://doi.org/10.1016/j.jhydrol.2012.03.026>
- Murray, F.W., 1967. On the Computation of Saturation Vapor Pressure. *Journal of Applied Meteorology*, 6, 203-204.
- O'Brien, J. J., Oberbauer, S. F., & Clark, D. B., 2004. Whole tree xylem sap flow responses to multiple environmental variables in a wet tropical forest. *Plant, Cell & Environment*, 27(5), 551-567.
- O'Grady, A., Eamus, D., & Hutley, L., 1999. Transpiration increases during the dry season: patterns of tree water use in eucalypt open-forests of northern Australia. *Tree Physiology*, 19(9), 591-597.

- Pappas, C., Matheny, A. M., Baltzer, J. L., Barr, A. G., Black, T. A., Bohrer, G., Detto, M., Maillet, J., Roy, A., Sonnentag, O., 2018. Boreal tree hydrodynamics: asynchronous, diverging, yet complementary. *Tree Physiology*, 38(7), 953-964.
- Pataki, D. E., & Oren, R., 2003. Species differences in stomatal control of water loss at the canopy scale in a mature bottomland deciduous forest. *Advances in Water Resources*, 26(12), 1267-1278.  
doi:<https://doi.org/10.1016/j.advwatres.2003.08.001>
- Patankar, R., Quinton, W. L., Hayashi, M., & Baltzer, J. L., 2015. Sap flow responses to seasonal thaw and permafrost degradation in a subarctic boreal peatland. *Trees*, 29(1), 129-142.
- Peters, R.L., Fonti, P., Frank, D.C., Poyatos, R., Pappas, C., Kahmen, A., Carraro, V., Prendin, A.L., Schneider, L., Baltzer, J.L. and Baron-Gafford, G.A., 2018. Quantification of uncertainties in conifer sap flow measured with the thermal dissipation method. *New Phytologist*, 219(4), pp.1283-1299.
- Rossi, S., Deslauriers, A., Gričar, J., Seo, J.-W., Rathgeber, C. B. K., Anfodillo, T., Morin, H., Levanic, T., Oven, P., Jalkanen, R., 2008. Critical temperatures for xylogenesis in conifers of cold climates. *Global Ecology and Biogeography*, 17(6), 696-707. doi:10.1111/j.1466-8238.2008.00417.x
- Saugier, B., Granier, A., Pontailier, J. Y., Dufrene, E., & Baldocchi, D. D., 1997. Transpiration of a boreal pine forest measured by branch bag, sap flow and micrometeorological methods. *Tree Physiol*, 17(8\_9), 511-519.
- Seneviratne, S. I., Corti, T., Davin, E. L., Hirschi, M., Jaeger, E. B., Lehner, I., Orlowsky, B., Teuling, A. J., 2010. Investigating soil moisture–climate interactions in a changing climate: A review. *Earth-Science Reviews*, 99(3–4), 125-161. doi:<http://dx.doi.org/10.1016/j.earscirev.2010.02.004>
- Seneviratne, S. I., Luthi, D., Litschi, M., & Schar, C., 2006. Land-atmosphere coupling and climate change in Europe. *Nature*, 443(7108), 205-209. doi:[http://www.nature.com/nature/journal/v443/n7108/supinfo/nature05095\\_S1.html](http://www.nature.com/nature/journal/v443/n7108/supinfo/nature05095_S1.html)
- Van Herk, I. G., Gower, S. T., Bronson, D. R., & Tanner, M. S., 2011. Effects of climate warming on canopy water dynamics of a boreal black spruce plantation. *Canadian Journal of Forest Research*, 41(2), 217-227.
- Wang, H., Guan, H., Deng, Z., & Simmons, C. T., 2014. Optimization of canopy conductance models from concurrent measurements of sap flow and stem water potential on Drooping Sheoak in South Australia. *WATER RESOURCES RESEARCH*, 50(7), 6154-6167. doi:10.1002/2013WR014818

- Wang, K.-Y., Kellomäki, S., Zha, T., & Peltola, H., 2005. Annual and seasonal variation of sap flow and conductance of pine trees grown in elevated carbon dioxide and temperature. *Journal of Experimental Botany*, 56(409), 155-165.
- Wang, H., Tetzlaff, D., Dick, J. J., & Soulsby, C., 2017. Assessing the environmental controls on Scots pine transpiration and the implications for water partitioning in a boreal headwater catchment. *Agricultural and Forest Meteorology*, 240-241, 58-66. doi: 10.1016/j.agrformet.2017.04.002
- Ward, A. D., & Trimble, S. W., 2004. *Environmental Hydrology* (second ed.): Lewis publishers.
- Wullschleger, S. D., Wilson, K. B., & Hanson, P. J., 2000. Environmental control of whole-plant transpiration, canopy conductance and estimates of the decoupling coefficient for large red maple trees. *Agricultural and Forest Meteorology*, 104(2), 157-168. doi: [http://dx.doi.org/10.1016/S0168-1923\(00\)00152-0](http://dx.doi.org/10.1016/S0168-1923(00)00152-0)
- Zeppel, M. J., Murray, B. R., Barton, C., & Eamus, D., 2004. Seasonal responses of xylem sap velocity to VPD and solar radiation during drought in a stand of native trees in temperate Australia. *Functional Plant Biology*, 31(5), 461-470.
- Zhang, Q., Manzoni, S., Katul, G., Porporato, A., & Yang, D., 2014. The hysteretic evapotranspiration—Vapor pressure deficit relation. *Journal of Geophysical Research: Biogeosciences*, 119(2), 125-140.
- Zheng, H., Wang, Q., Zhu, X., Li, Y., & Yu, G., 2014. Hysteresis responses of evapotranspiration to meteorological factors at a diel timescale: patterns and causes. *PLOS ONE*, 9(6), e98857.

## 3.10 Supplementary materials

Table 3S.1: Description of soil characteristics at the two sites.

	<b>Balsam fir</b>							<b>Black spruce</b>				
	Ae	Bhf	Bf1	Bf2	Bf3	BC	C	Ae	Bhf	Bf	BC	C
<i>Soil profile 1</i>												
Thickness (cm)	6	10	20	18	5	-	41	10	5	11	10	64
Sand	66	-	81	79	74	-	82	80	90	92	80	76
Loam	28	-	17	18	22	-	14	18	8	7	19	22
Clay	6	-	2	3	4	-	4	2	2	1	1	2
<i>Soil profile 2</i>												
Thickness (cm)	7	17	20	18	25	-	23	4	4	20	20	52
Sand	81	-	85	90	-	83	89	84	86	92	94	78
Loam	13	-	10	6	-	12	7	12	12	7	6	21
Clay	6	-	5	4	-	5	4	4	2	1	0	1
<i>Soil profile 3</i>												
Thickness (cm)	10	9	10	15	15	20	21	8	10	18	20	44
Sand	66	-	-	75	91	93	83	82	86	96	74	80
Loam	28	-	-	19	6	4	12	16	11	4	24	20
Clay	6	-	-	6	3	3	5	2	3	0	2	0
<i>Soil profile 4</i>												
Thickness (cm)	6	10	15	15	25	20	9	8	10	20	15	47
Sand	66	-	64	75	89	95	94	79	82	94	95	96
Loam	30	-	29	21	8	3	3	18	16	4	3	4
Clay	4	-	7	4	3	2	3	3	2	2	2	0

Table 3S.2: Regression coefficients of sap flow (daily and half-hourly) between the sun-side and the shade side of the same tree and between trees from the beginning of the growing season to the end of August for each year at the balsam fir site. T1, T2 and T3 are the three instrumented trees.

Year	<i>R</i> <sup>2</sup> between <i>sun-side and shade-side</i>			<i>Trees</i>		
	T1	T2	T3	T1-T2	T1-T3	T2-T3
<i>Daily sap flow</i>						
2004	0.88	0.95	0.97	0.84	0.9	0.9
2005	0.88	0.94	0.88	0.79	0.9	0.89
2006	0.86	0.9	0.69	0.83	0.89	0.78
2007	0.76	0.95	0.97	0.95	0.97	0.91
2008	0.78	0.95	0.96	0.94	0.97	0.92
2009	0.91	0.93	0.92	0.9	0.96	0.85
2010	0.89	0.89	0.79	0.88	0.92	0.87
2011	0.95	0.81	0.86	0.81	0.98	0.76
2012	0.91	0.76	0.49	0.81	0.94	0.8
2013	0.93	0.78	0.51	0.78	0.94	0.67
<i>Half-hourly sap flow</i>						
2004	0.94	0.97	0.98	0.87	0.95	0.87
2005	0.94	0.94	0.95	0.84	0.94	0.86
2006	0.83	0.94	0.86	0.89	0.92	0.88
2007	0.69	0.97	0.98	0.96	0.97	0.94
2008	0.65	0.96	0.97	0.94	0.97	0.92
2009	0.88	0.94	0.94	0.93	0.96	0.88
2010	0.96	0.93	0.87	0.92	0.96	0.89
2011	0.98	0.85	0.87	0.84	0.97	0.8
2012	0.97	0.66	0.68	0.76	0.95	0.79
2013	0.96	0.5	0.63	0.68	0.94	0.62

Table 3S.3: Regression coefficients of sap flow (daily and half-hourly) between sun-side and shade side of the same tree and between trees from the beginning of the growing season to the end of August for each year at the black spruce site. T1, T2 and T3 are the three instrumented trees.

Year	<i>R<sup>2</sup> between sun-side and shade-side</i>			<i>trees</i>		
	P12	P34	P56	T12	T13	T23
<i>Daily sap flow</i>						
2006	0.94	0.84	0.93	0.95	0.96	0.97
2007	0.88	0.77	0.91	0.92	0.93	0.93
2008	0.99	0.92	0.96	0.97	0.96	0.98
2009	0.8	0.62	0.87	0.95	0.88	0.9
<i>Half-hourly sap flow</i>						
2006	0.98	0.89	0.96	0.97	0.96	0.98
2007	0.93	0.74	0.94	0.96	0.95	0.96
2008	0.99	0.95	0.98	0.98	0.97	0.99
2009	0.9	0.73	0.91	0.96	0.92	0.95

Table 3S.4: Mean seasonal regression coefficients (direction of correlation: positive or negative) between daily sap flow and environmental variables for the six probes at the balsam fir and black spruce sites. The Gompertz (3 parameters) equation was used for VPD; and a Sigmoidal (3 parameters) equation was used for Rad; simple linear regression was used for the other variables.

Year	VPD	Rad	Tmax	PCP	SWC	Tmin	WS
<i>Balsam fir</i>							
2004	0.71 (+) ***	0.60 (+) ***	0.16 (+) ***	0.27 (-) ***	0.01 (+) NS	0.07 (-) **	0.00 (-) NS
2005	0.80 (+) ***	0.75 (+) ***	0.46 (+) ***	0.14 (-) ***	0.02 (-) NS	0.01 (+) NS	0.02 (-) NS
2006	0.65 (+) ***	0.36 (+) ***	0.12 (+) **	0.20 (-) ***	0.06 (+) ***	0.06 (-) **	0.00 (-) NS
2007	0.76 (+) ***	0.72 (+) ***	0.39 (+) ***	0.36 (-) ***	0.01 (+) NS	0.00 (-) NS	0.00 (-) NS
2008	0.77 (+) ***	0.65 (+) ***	0.36 (+) ***	0.27 (-) ***	0.07 (-) NS	0.01 (-) NS	0.01 (+) NS
2009	0.72 (+) ***	0.66 (+) ***	0.25 (+) ***	0.31 (-) ***	0.00 (-) NS	0.04 (-) *	0.00 (+) NS
2010	0.73 (+) ***	0.59 (+) ***	0.38 (+) ***	0.14 (-) ***	0.02 (-) NS	0.05 (+) **	0.00 (-) NS
2011	0.82 (+) ***	0.72 (+) ***	0.46 (+) ***	0.29 (-) ***	0.02 (-) NS	0.06 (-) **	0.03 (-) NS
2012	0.71 (+) ***	0.68 (+) ***	0.25 (+) ***	0.39 (-) ***	0.02 (+) NS	0.02 (-) NS	0.01 (+) NS
2013	0.69 (+) ***	0.58 (+) ***	0.37 (+) ***	0.23 (-) ***	0.12 (-) ***	0.05 (+) **	0.01 (-) NS
<i>Black spruce</i>							
2006	0.79 (+) ***	0.62 (+) ***	0.44 (+) ***	0.11 (-) ***	0.05 (+) **	0.00 (+) NS	0.00 (+) NS
2007	0.70 (+) ***	0.68 (+) ***	0.32 (+) ***	0.11 (-) ***	0.01 (+) NS	0.01 (-) NS	0.01 (-) NS
2008	0.69 (+) ***	0.61 (+) ***	0.32 (+) ***	0.23 (-) ***	0.00 (-) NS	0.03 (-) NS	0.00 (-) NS
2009	0.53 (+) ***	0.47 (+) ***	0.26 (+) ***	0.23 (-) ***	0.05 (+) **	0.04 (-) **	0.05 (-) *

\*\*\* < 0.001; \*\* < 0.05; \* < 0.1; NS: not significant

Table 3S.5: Characterization of average seasonal radial growth patterns for balsam fir and black spruce for their respective years. Numbers in parentheses represent inter-tree variability (+1 SE). DOY: day of year.

Year	<i>Balsam fir</i>		<i>Black spruce</i>	
	Seasonal growth (mm)	Timing of growth initiation (DOY)	Seasonal growth (mm)	Timing of growth initiation (DOY)
2004	2.0 (0.1)	148 (2.0)	-	-
2005	2.0 (0.3)	137 (2.8)	-	-
2006	1.1 (0.1)	149 (3.6)	0.8(0.2)	145(3.2)
2007	2.9 (0.5)	133 (3.3)	1.3(0.2)	133(1.2)
2008	2.6 (0.4)	140 (2.4)	1.1(0.2)	148(1.7)
2009	2.3 (0.3)	146 (0.7)	1.1(0.2)	159(4.5)
2010	2.6 (0.4)	128 (4.0)	-	-
2011	1.7 (0.2)	148 (1.3)	-	-
2012	1.9 (0.4)	144 (4.7)	-	-
2013	1.4 (0.2)	138 (0.9)	-	-
2014	1.0 (0.2)	148 (6.1)	-	-

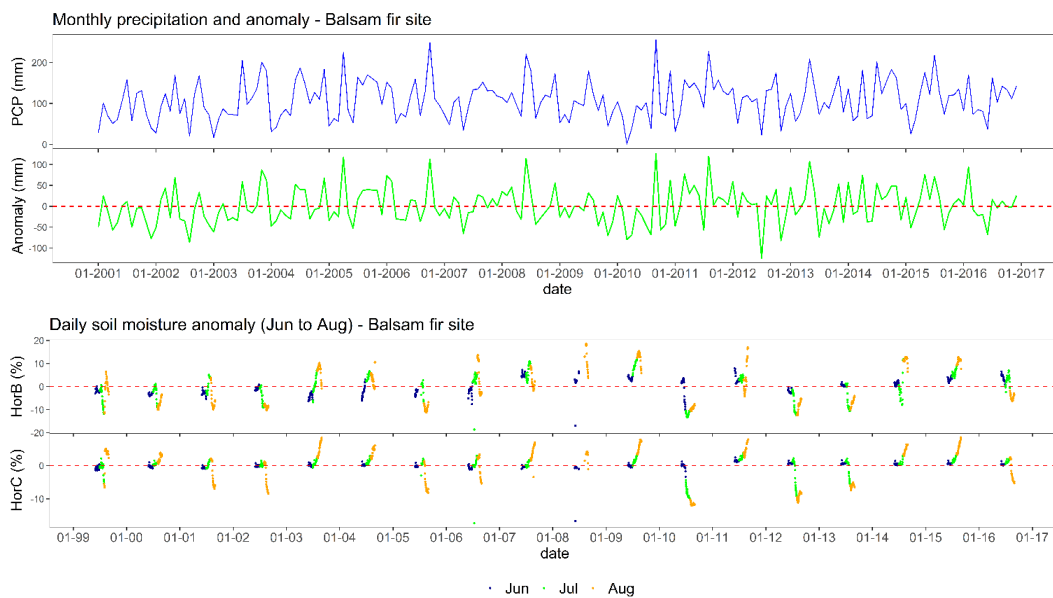


Figure 3S.1: Total monthly precipitation and its anomalies from 2001 to 2016 (top panel) and daily soil moisture anomalies during growing season (Jun to Aug) from 1999 to 2016 (bottom panel) at the balsam fir site.

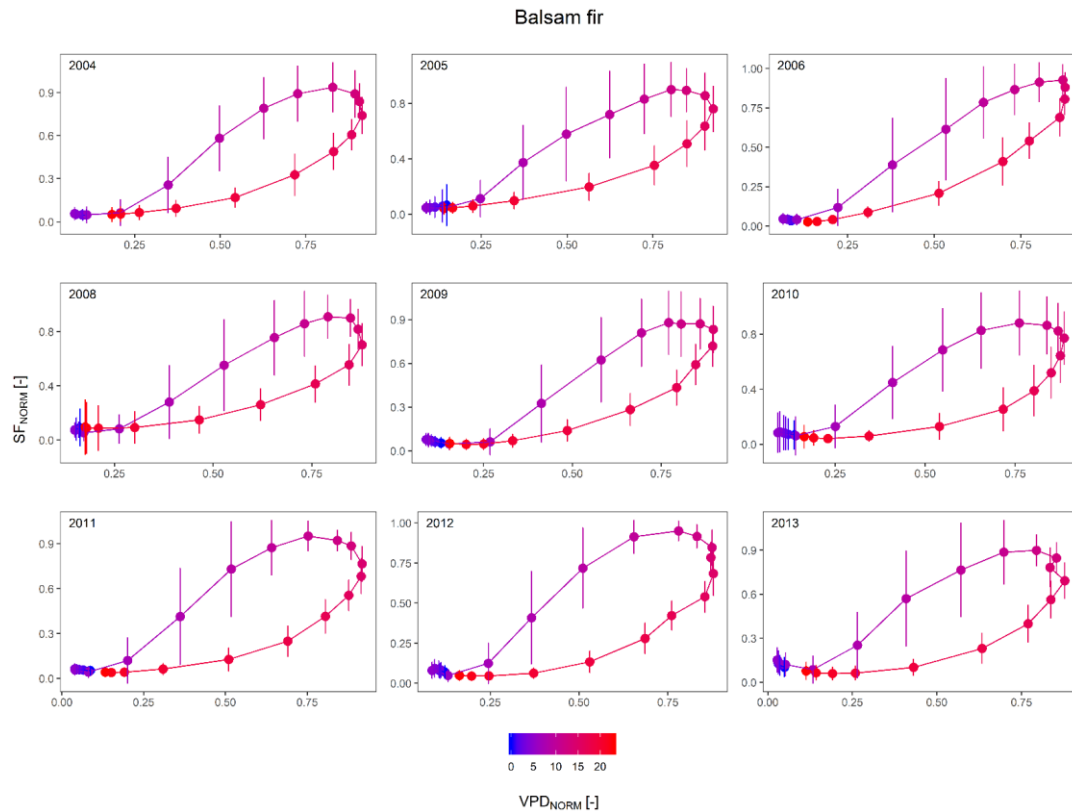


Figure 3S.2: Diel hysteresis of standardized sap flow velocity ( $SF_{NORM}$ ) with standardized VPD from 2001 to 2013 (excluding 2007 which is shown in the main text) for balsam fir for the period from the beginning of the growing season to the end of August at the balsam fir site. Vertical bars are  $1 \pm$  standard deviation.

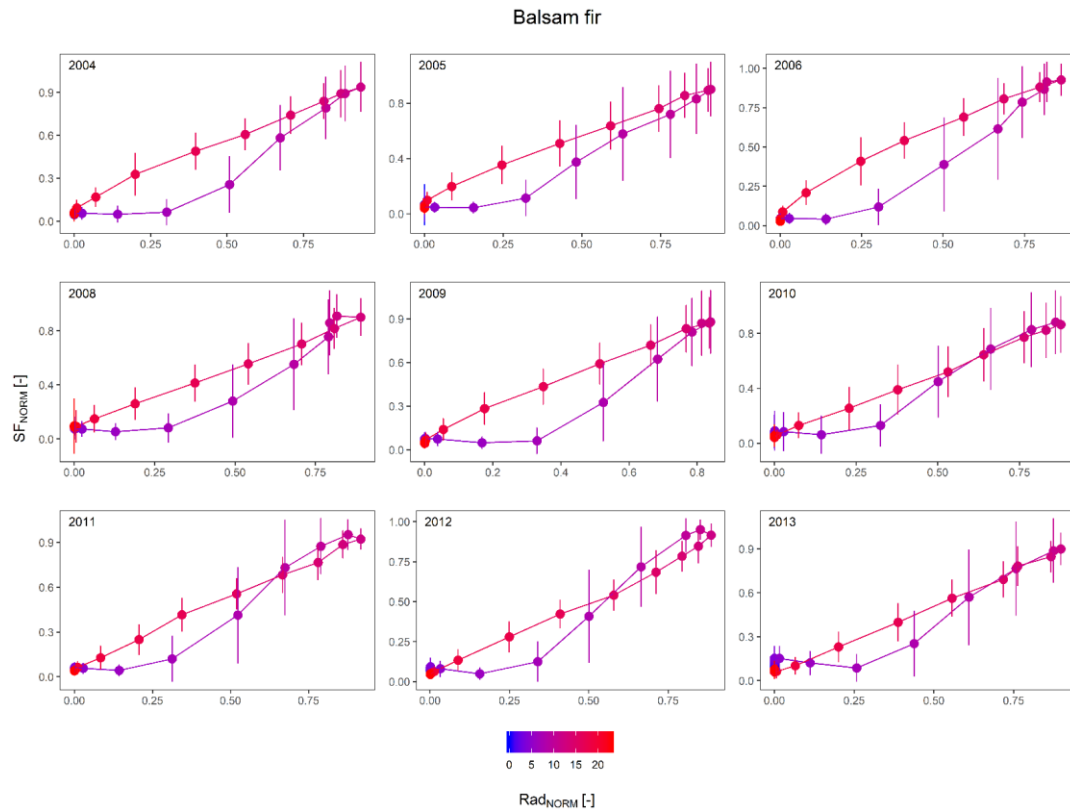


Figure 3S.3: Diel hysteresis of standardized sap flow velocity ( $SF_{NORM}$ ) with standardized Rad from 2001 to 2013 (excluding 2007 which is shown in the main text) for the period from the beginning of the growing season to the end of August at the balsam fir site. Vertical bars are  $1 \pm$  standard deviation.

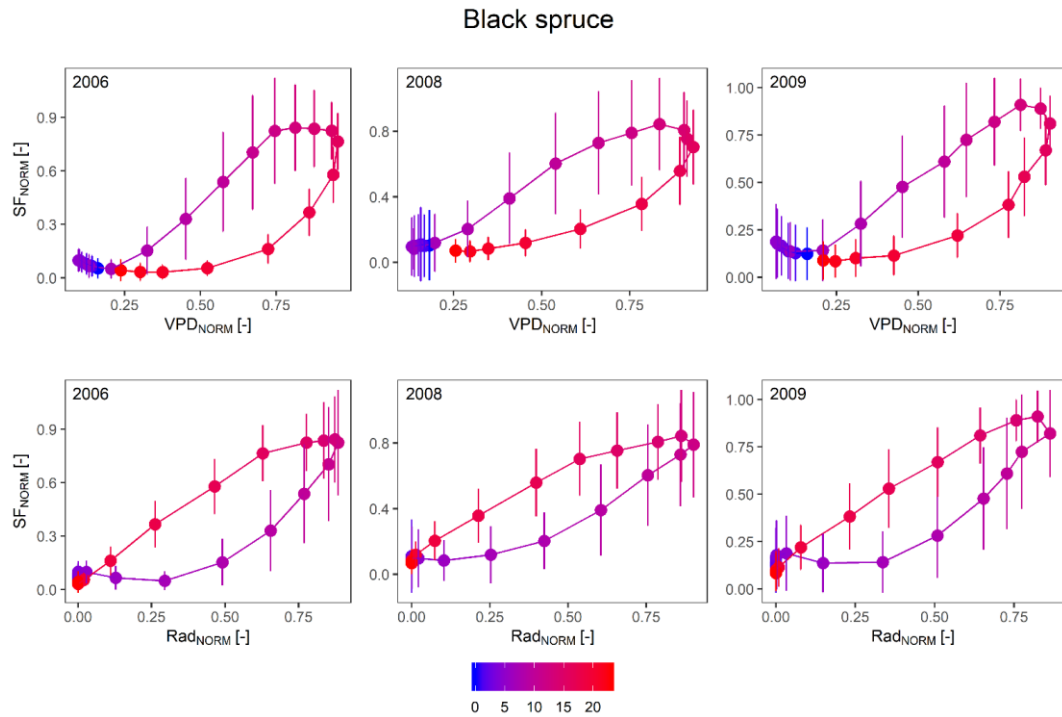


Figure 3S.4: Diel hysteresis of standardized sap flow velocity ( $SF_{NORM}$ ) with standardized VPD (top panel) and Rad (bottom panel) from 2006 to 2009 (excluding 2007 which is shown in the main text) for the period from the beginning of the growing season to the end of August at the black spruce site. Vertical bars are  $1 \pm$  standard deviation.

## CHAPITRE IV

### TREE TRANSPIRATION WELL SIMULATED BY THE CANADIAN LAND SURFACE SCHEME (CLASS) BUT NOT DURING DROUGHT

Article écrit par Shalini Oogathoo <sup>1</sup>

et révisé par Daniel Houle <sup>2,3</sup>, Louis Duchesne <sup>2</sup>, Daniel Kneeshaw <sup>1</sup>.

<sup>1</sup> Centre d'Étude de la Forêt, Université du Québec à Montréal, Case Postale 8888,  
Succursale Centre-Ville, Montréal, Quebec H3C 3P8, Canada.

<sup>2</sup> Direction de la Recherche Forestière, Ministère des Forêts, de la Faune et des Parcs du  
Québec, 2700 Einstein, Quebec City, Quebec G1P 3W8, Canada.

<sup>3</sup> Consortium sur la Climatologie Régionale et l'Adaptation aux Changements  
Climatiques (Ouranos), 550 Sherbrooke W, Montréal, Quebec H3A 1B9, Canada.

#### 4.1 Résumé

La transpiration, un élément clé du cycle hydrologique, contribue grandement au système climatique en transférant une grande quantité d'eau des sols vers l'atmosphère. La représentation adéquate de la transpiration dans les schémas de surface des modèles climatiques est cruciale pour obtenir des projections climatiques fiables et précises. Dans cette étude, la transpiration simulée par le Canadian Land Surface Scheme (CLASS) a été évaluée avec le flux de sève mesuré à long-terme dans deux peuplements boréaux, situés dans l'est de Canada et dominés respectivement par le sapin baumier et l'épinette noire. En général, CLASS modélise adéquatement la transpiration quotidienne pendant la saison de croissance pour la plupart des années sur les deux sites. Durant la période de réhydratation (avant le début de la croissance), la transpiration simulée a été grandement sous-estimée dû à la surestimation de la durée de la présence de neige, ce dernier limitant la transpiration. De plus, CLASS n'a pas capturé l'impact des événements extrêmes sur la physiologie des arbres et a maintenu une transpiration élevée pendant un coup de chaleur et une sécheresse. Pendant les épisodes de sécheresse observés et simulés, la transpiration modélisée a été surestimée, dû à l'insensibilité de CLASS à la diminution de contenu en eau du sol, la transpiration modélisée étant strictement contrôlée par les variables atmosphériques (déficit de pression de vapeur et radiation solaire). La simulation inexacte de la transpiration par CLASS pendant les stress hydriques entraînera une sous-estimation des sécheresses intenses dans les projections climatiques futures du modèle régional climatique Canadien.

## 4.2 Abstract

Transpiration, a key component of the hydrological cycle, contributes greatly to the climate system by transferring large amount of water from soils to the atmosphere. Its correct representation within Land Surface Schemes in climate models is crucial to provide accurate and reliable climate projections. In this study, transpiration simulated by the Canadian Land Surface Scheme (CLASS) was compared to long-term observations of sap flow measurements in two boreal forest sites of eastern Canada dominated by balsam fir and black spruce. In general, CLASS adequately models daily transpiration during the growing season for most of the years at both sites. During the tree rehydration period (preceding the growing season), modeled transpiration was greatly underestimated because of overestimating the duration of the snowpack, the latter restricting transpiration. Moreover, CLASS did not capture the impact of extreme events on tree physiology and maintained high transpiration rates during a heat stress and a drought. During both observed and simulated drought events, transpiration modeled using CLASS was overestimated, due to insensitivity to substantial decreases in soil water content; modeled transpiration being strictly controlled by atmospheric variables (vapour pressure deficit and radiations). The inaccurate simulation of transpiration by CLASS during dry periods will lead to an underestimation of severe droughts in future climate projections by the Canadian Regional Climate Model.

## 4.3 Introduction

Evapotranspiration is the combined process of transpiration and evaporation occurring on a vegetation-covered land surface. As per Kramer (1983), transpiration is defined as the “loss of water in the form of vapour from plants” (Ward and Trimble 2004) while

evaporation is the loss of water from the soil surface and vegetation canopy (following interception of water from precipitation). The partitioning of evapotranspiration into soil evaporation, canopy evaporation and tree transpiration over a land surface depends on the type of vegetation (Baldocchi, et al. 2004) and percentage of vegetation cover (Wang, et al. 2010). Studies have shown transpiration to vary from 48 to 52 %, soil evaporation from 15 to 36 %, and canopy evaporation from 16 to 20 % of the total evapotranspiration of land surfaces on a global-scale using process-based models (Choudhury and DiGirolamo 1998, Choudhury, et al. 1998, Dirmeyer, et al. 2005). In a boreal forest, evaporation from the canopy and the forest floor were respectively 20 % and 15 % of the total forest evapotranspiration, while tree transpiration accounted for 65 % (Grelle, et al. 1997).

Transpiration is a function of many environmental factors, such as solar radiation, vapour pressure deficit, air temperature and soil water (Bovard, et al. 2005; Gartner, et al. 2009; Lagergren and Lindroth 2002; Wang, et al. 2017; Wullschleger, et al. 2000). Transpiration can be measured via different approaches or modeled at regional to global scales with Land Surface Models (Seneviratne, et al. 2010). The latter, also known as Land Surface Schemes (LSS), have been used in many modeling studies to simulate evapotranspiration. This includes, for example, the Simple Biosphere Model (Lei et al. 2011), the Community Land Model (Gayler et al. 2013, Li et al. 2013), the Noah Land Surface model (Jaksa and Sridhar 2015; Ma et al. 2017; Malik et al. 2014; Wang et al. 2018), the Community Atmosphere Biosphere Land Exchange model (Ukkola et al. 2016a, Zhang et al. 2016) or multiple Land Surface Schemes (Chen et al. 2013; Grippa et al. 2011; Ukkola et al. 2016b).

While transpiration is an important component of the hydrological cycle, it also has a crucial role in regulating climate as supported by both observations and modelling studies (Bala et al. 2007; Seneviratne, et al. 2012; Swann, et al. 2010). Modelling

studies of complete deforestation or conversion to grassland of the amazon forests using a General Circulation Model or Earth System Model have shown a decrease in evapotranspiration and an increase in surface temperature (Brovkin, et al. 2009; Dickinson and Henderson-Sellers 1988 in Garratt 1993). In temperate forests, excessive evapotranspiration was identified as the cause of the extreme 2003 drought in Europe (Seneviratne, et al. 2012). Among all biomes, the boreal forest has the most important biogeophysical impact on global mean annual temperature (Bonan, 2008). Its expansion towards the arctic for instance, would increase air temperature (Bonan, 2008) via increased transpiration (Swann et al., 2010) and decreased surface albedo (Betts, 2000).

The Canadian Land Surface Scheme (CLASS; Verseghy 1991, Verseghy, et al. 1993), developed by the Canadian Climate Centre, is an LSS that was specifically designed to be used within the Canadian Regional Climate Model (CRCM; Zadra et al., 2008). Brochu and Laprise (2007) showed that simulated summer evapotranspiration in the CRCM was greatly improved when CLASS was used instead of the simple Manabe bucket model (Manabe, 1969), emphasizing the importance of proper representation of transpiration within LSSs. To date, a few studies have used CLASS to quantitatively assess how it simulates evapotranspiration from forests. These were conducted on a daily basis in the boreal forest in Saskatchewan (Wang et al., 2002), Manitoba (Bartlett et al., 2003) and Quebec (Isabelle et al., 2018), in temperate forests in British Columbia (Yuan et al., 2007) and Ontario (Huang et al., 2011), and in a sub-alpine forest in western Canada (MacDonald et al., 2016). All of these studies used observations based on eddy covariance measurements to validate their findings. None of these studies have, however, focused on the temporal evolution of simulated transpiration compared to observations of daily transpiration derived from sap flow velocity data measured on a daily time-scale in various conditions. While sap flow and eddy covariance techniques are comparable qualitatively, eddy covariance techniques measure evapotranspiration

over a large footprint area that varies with time, making measurements highly unstable (Hogg et al., 1997; Wilson et al., 2001). Moreover, the eddy covariance technique is applicable only in homogenous and flat terrain, and is subject to errors when interpreting results during times of low turbulence (Wilson et al., 2001). On the other hand, sap flow techniques allows for the assessment of environmental and physiological controls on transpiration at the tree level and are considered more stable due to the fixed location of the sensor in the tree (Hogg et al., 1997). Furthermore, sap flow techniques enable the study of intra- and inter-specific differences in tree transpiration, even in heterogeneous and complex terrain where edaphic and microclimatic variation is greater (Wilson et al., 2001).

In our study, the temporal evolution of transpiration modeled by CLASS is evaluated using sap flow velocity data. The latter was measured in two tree species, namely balsam fir and black spruce, which are the most important conifers in the boreal forest region of central and eastern Canada. Sap flow was measured over multiple growing seasons (10 for balsam fir and 4 for black spruce), allowing us to validate the CLASS model in many contrasting environmental conditions.

The period prior to the growing season is important for tree species in the boreal region, as winter dehydrated trees must recharge during spring prior to the onset of tree growth (Turcotte et al. 2009). However, tree water uptake during this period is not well known. Important questions also remain regarding how trees regulate water uptake during droughts. Isohydic tree species normally reduce (or even stop) their transpiration as soil water decreases but anisohydric trees maintain transpiration rates during dry periods. In this study, we evaluate how well CLASS represents tree transpiration during normal conditions, during the rehydration period and during drought.

## 4.4 Materials & methods

### 4.4.1 Description of study area

The two studied sites are in a balsam fir forest (47° 19' 41'' N and 71° 07' 37'' W) and a black spruce forest (49°12'45' N and 73°39'00' W), located in the province of Quebec in Canada. Their elevations are 784 m and 411 m above sea level, respectively. The balsam fir site had an average slope of 8 %. The mean annual temperature is 1.3 °C at both the balsam fir and black spruce sites for the period from 2001 to 2016. Mean annual precipitation is 1300 mm at the balsam fir site and 941 mm at the black spruce site for the period 2001 to 2016. The vegetation rests on Precambrian charnockitic gneiss covered by loamy sand to sandy loam till.

### 4.4.2 Measured data

Climate variables were measured on an hourly basis at both forest sites, and were used as inputs for CLASS. These climate variables are photosynthetic active radiation (solar radiation in the visible range (400 to 700 nm wavelength) used for photosynthesis) and wind speed measured in a flux tower at 14 m height; air temperature and relative humidity measured at a height of 3.3 m; and precipitation measured at ground level. All climate data were available from 1999 to 2016 at the balsam fir site and from 1997 to 2016 at the black spruce site. Air temperature within the canopy was measured by a shield-protected temperature probe, placed in the top quarter portion of the canopy of three co-dominant trees (one probe on each tree, approximately 10 m distance between the probes) at both sites. The depth of snow cover was measured close to the instrumented trees with ultrasonic sensors (SR50 type sonic distance sensor, Campbell Scientific inc.).

Soil water content (CS615, Campbell Scientific, Logan, UT) and soil temperature (Thermometric DC95F232V and YSI 401) were measured daily in 3 and 4 pedons at

the black spruce and balsam fir sites, respectively, in the B horizon (22 cm below the mineral soil surface). Both soil water and soil temperature were measured since 1997 at the black spruce site and since 1999 at the balsam fir site. The mean values of the pedons were used to characterize both soil water and soil temperature.

At both study sites, sap flow was measured in three co-dominant trees of the main tree species (two measurements; one on the north and the other on the south side for each tree) using 30 mm thermal dissipation probes (TDP-30, Dynamax, Houston, TX). Instruments were positioned at breast height, approximately 1.3 m above ground level. Trees were instrumented in 2003 for balsam fir and 2006 for black spruce. Sap flow was measured every 30-min throughout the day and was calculated based on the procedure explained in Granier (1987). While only three trees per species were measured in our study, there were two measurements per tree (two probes per tree on opposite sides to follow sap flow variation around the stem). In this study, sapwood area was not measured at either site. While sapwood depth is generally assumed to be positively correlated with stem diameter, there seems to be no relationship at all between sapwood area and stem diameter for some species (Ewers, et al. 2002). Thus, for this study, stand transpiration was not calculated. Instead, the standardized sap flow velocity was used to evaluate the temporal variation of sap flow against standardized modeled transpiration. The standardized sap flow velocity and standardized modeled transpiration were obtained by dividing the absolute values by their respective maximum value during the growing season in each year separately. Sap flow velocity was available from 2004 to 2013 and 2006 to 2009 for balsam fir and for black spruce respectively, and thus these long-term observations were used to evaluate the performance of CLASS for transpiration. Stem diameter variation was also measured at both sites in the same three trees with electronic strain gauge dendrometers (DEX70, Dynamax Inc., Houston, TX). These measurements were used to define rehydration

periods and growing season. Further information on forest stand characteristics at both sites are presented in Oogathoo et al. (2020).

#### 4.4.3 Canadian Land Surface Scheme (CLASS)

CLASS enables the exchange of water and energy with the atmospheric component of the CRCM. It models the hydrological cycle in a one-dimensional column, at a time step of 30 mins. The model is comprised of a vegetation layer, a snow layer of variable depth and multiple soil layers with varying thicknesses. The vegetation in the model is grouped into four categories: broadleaf, conifer, crops, and grass. Each model grid is divided into four sub-grids based on land cover types, which are: 1) bare soil; 2) soil covered with snow; 3) soil covered with vegetation; 4) and vegetation over snow-covered soil. The energy and mass balances are calculated for each sub-grid and composite energy and mass balance are determined for each grid using a weighted average based on the area occupied by each land cover type (Verseghy 1991, Verseghy, et al. 1993).

##### 4.4.3.1 Mathematical representation of transpiration within CLASS

Latent heat and sensible heat fluxes are determined based on gradient turbulent diffusion theory. Transpiration is calculated for each vegetation type, where canopy is treated as a single big leaf with no differentiation between sunlit and shaded leaves. Transpiration is calculated using Eq. 4.1, Where,  $L_v$  is latent heat of vaporization,  $\rho_a$  is air density,  $q_a$  is the actual specific humidity,  $q_{sat}(\bar{T}_c)$  is the saturation specific humidity at effective canopy temperature ( $\bar{T}_c$ ),  $r_a$  is aerodynamic resistance, and  $r_c$  is canopy resistance.

$$Q_{E,c,dry} = \frac{L_v \rho_a [q_a - q_{sat}(\bar{T}_c)]}{r_a + r_c} \quad \text{Eq. 4.1}$$

Modeled transpiration occurs when water is present in the soil layers, and it is controlled by the specific humidity deficit, aerodynamic resistance and canopy resistance. Unstressed canopy resistance depends on the minimum stomatal resistance for each vegetation type, incoming visible shortwave radiation, and leaf area index. The stressed canopy resistance ( $r_{c,i}$ ) is a function of the unstressed canopy resistance ( $r_{c,u,i}$ ) and environmental stresses such as vapour pressure deficit ( $f(\Delta e)$ ), soil water potential ( $f(\varphi_s)$ ) as a surrogate for leaf water potential and air temperature ( $f(T_a)$ ) as a surrogate for canopy temperature, as shown in Eq. 4.2 to 4.5.  $C_{v1}$ ,  $C_{v2}$ ,  $C_{\varphi1}$  and  $C_{\varphi2}$  are parameters that depend on vegetation categories. Composite canopy resistance is the weighted average of canopy resistance of the vegetation categories present in each model grid. In the model, transpiration ceases under two conditions: 1) snow is present beneath the canopy; and 2) incoming visible radiation is  $< 2 \text{ W/m}^2$ , whereby in all cases, a very high canopy resistance is used in the model. (Verseghy, et al. 1993, Verseghy 2012).

$$r_{c,i} = f(T_a)f(\Delta e)f(\varphi_s)r_{c,u,i} \quad \text{Eq. 4.2}$$

$$f(T_a) = 1 \quad (5 < T_a < 40 \text{ }^\circ\text{C}) \quad \text{or} \quad f(T_a) = 250 \quad (5 > T_a > 40 \text{ }^\circ\text{C}) \quad \text{Eq.4.3}$$

$$f(\Delta e) = (\Delta e/10)^{C_{v1}/C_{v2}} \quad \text{or} \quad f(\Delta e) = 1/\exp(-C_{v1} \Delta e/10) \quad \text{Eq. 4.4}$$

$$f(\varphi_s) = 1 + (\varphi_s/C_{\varphi1})^{C_{\varphi2}} \quad \text{Eq. 4.5}$$

#### 4.4.3.2 Model inputs for CLASS offline

##### 4.4.3.2.1 Climate data

The climate variables required by CLASS are incoming shortwave radiation ( $\text{W m}^{-2}$ ), downwelling longwave radiation ( $\text{W m}^{-2}$ ), precipitation ( $\text{mm s}^{-1}$ ), air temperature ( $^\circ\text{C}$ ), specific humidity ( $\text{kg kg}^{-1}$ ), wind speed ( $\text{m s}^{-1}$ ), and atmospheric pressure (Pa) at 30-

min intervals. The measured data available for this study were incoming shortwave radiation, precipitation, air temperature, and wind speed at one-hour intervals. These data were assumed not to vary greatly within an hour, thus they were duplicated when splitting each hour into two 30-min intervals.

Downwelling longwave radiation ( $R_{ldc}$ ) was estimated using Eq. 4.6 (Sugita and Brutsaert, 1993), where  $\varepsilon_{ac}$  is atmospheric emissivity under clear skies,  $\sigma$  is the Stefan-Boltzmann constant,  $T_a$  is air temperature in kelvin near the ground.  $\varepsilon_{ac}$  was determined using Eq. 4.7 (Brutsaert 1975), where  $\rho_a$  is ambient vapour pressure (hPa),  $a_3$  is 0.98 and  $b_3$  is 0.0687 (Sugita and Brutsaert 1993).

$$R_{ldc} = \varepsilon_{ac}\sigma T_a^4 \quad \text{Eq. 4.6}$$

$$\varepsilon_{ac} = a_3(\rho_a/T_a)^{b_3} \quad \text{Eq. 4.7}$$

Atmospheric pressure ( $P_h$ ) was estimated using the barometric formula (Eq. 4.8), where  $P_0$  is atmospheric pressure at sea level (101.3 kPa),  $m$  is the mass of one molecule (0.02896 kg mol<sup>-1</sup>),  $g$  is acceleration due to gravity (9.807 m s<sup>-2</sup>),  $h$  is altitude above sea level (m),  $R$  is the universal gas constant (8.3143 J mol<sup>-1</sup>k<sup>-1</sup>),  $T$  is air temperature in kelvin.

$$P_h = P_0 \exp^{-mgh/RT} \quad \text{Eq. 4.8}$$

Specific humidity ( $q$ ) was calculated using Eq. 4.9, where  $MR$  is the mixing ratio. The latter was determined using Eq. 4.10, where  $\varepsilon$  is the ratio of the molecular weight of water and dry air (0.62198),  $\rho_a$  is the actual vapour pressure (Pa) and  $P_h$  is atmospheric pressure (Pa). Actual vapour pressure was calculated using Eq. 4.11, where  $RelHum$  is

the relative humidity. The saturated vapour pressure ( $\rho_s$ ) was determined using Eq. 4.12, where T is air temperature in degrees Celsius (Campbell and Norman 2012).

$$q = MR / (MR + 1) \quad \text{Eq. 4.9}$$

$$MR = \varepsilon(\rho_a / (P_h - \rho_a)) \quad \text{Eq. 4.10}$$

$$\rho_a = \rho_s (\text{RelHum} / 100) \quad \text{Eq. 4.11}$$

$$\rho_s = 611 e^{(17.502T / (T + 240.97))} \quad \text{Eq. 4.12}$$

#### 4.4.3.2.2 Initialization parameters

Initialization parameters are required to describe vegetation and soil properties. For most of the parameters, default values (Appendix A) in the model were used except for certain parameters where measured values were used (Table 4.1). The top layer (humus layer) was configured as a peat layer of fibric type.

Table 4.1: Initialisation parameters used in the model

Parameters	Balsam fir	Black spruce
<i>Vegetation properties</i>		
For plant functional type 1 (needleleaf):		
- Log of roughness length (m)	0.438	0.182
- Above-ground canopy mass (kg m <sup>-2</sup> )	18.5	14.6
- Maximum rooting depth (m)	0.81	0.52
<i>Soil properties</i>		
- Soil permeable depth (m)	1	1
- Sand (%) : horB / horC	69.8 / 83.0	86.9 / 89.0
- Clay (%) : horB / horC	5.5 / 4.1	2.0 / 0.8
- Organic matter (%) * : horB / horC	3.2 / 0.5	1.7 / 0.3
- Soil layer thickness (m) : hum / horB / horC	0.17 / 0.30 / 0.60	0.13 / 0.30 / 0.60

\* Ouimet and Duchesne, 2005

#### 4.4.4 Analyses

The performance of the CLASS model for the simulation of transpiration was tested against sap flow velocity of balsam fir and black spruce for the rehydration period and during the growing season. The beginning of the growing season for each year was calculated based on dendrometer data while the end was fixed to August 31<sup>st</sup>. The 4-parameter Gompertz model was fitted to the daily average dendrometer data from May to September for each year separately. The beginning of radial growth was determined when the modelled daily growth was above  $5 \mu\text{m d}^{-1}$  (Duchesne et al., 2012). The end of the growing season was considered to be the end of August in order to avoid the freeze/thaw events that occurred in September. For the rehydration period, a fixed period of 21 days prior to the onset of the growing season was used to assess modeled transpiration. We also tested the model during a short-term drought that occurred during July 2012 at the balsam fir site, where only 23 mm of rain fell compared to the long-term average of 150 mm for this period (Houle, et al. 2016). Moreover, a forced zero-precipitation simulation was also carried out in CLASS, starting from October 2006 and ending on September 2008 at the balsam fir site to test model behaviour in an extreme situation. For comparison between modelled transpiration and sap flow velocity, both were standardized by dividing by their maximum values during the growing season for each year separately, where the beginning and the end of growing season was calculated based on dendrometer data.

Since standardized values were used instead of absolute values for transpiration and sap flow velocity, the performance of all model simulations was evaluated using regression coefficient ( $R^2$ ) and slope of the simple linear regression of model simulations vs observations, Euclidean distance (ED) and dynamic time warping (DTW). DTW computes the optimal match between two time series (Sakoe and Chiba, 1978). The symmetric form of the DTW was used and the DTW standardized distance

was calculated. Both for ED and DTW, the smaller the values are, the greater the match between the simulated and observed time series.

## 4.5 Results and discussion

### 4.5.1 Transpiration during the rehydration period (prior to growing season)

In the boreal forest, spring is an important time prior to the growing season, where water in the soil is fully replenished from snowmelt, keeping the soil much above the permanent wilting point and thus allowing tree rehydration prior to the onset of tree growth (Turcotte et al. 2009). Our simulations in CLASS show that the standardized modeled transpiration ( $T_{SIM}$ ) underestimated the measured standardized sap flow velocity ( $SF_{OBS}$ ) during the rehydration period at both sites for most years (Figures 4.1a, 4S.1 and 4S.2). While  $R^2$  values were high and significant in some of the years, slopes (b values) of their respective simple linear regression equations were quite small and far from unity during the rehydration period at both sites, except in 2010 at the balsam fir site ( $b = 0.96$ ), indicating a poor match between the model simulations and observations (Table 4.2). Similarly, the ED was above 1 in all years at both sites, except for 2010 at the balsam fir site. The DTW also indicates poor agreement between simulations and observations except for the rehydration period in balsam fir which was well simulated in 2010 (Figure 4.1b), the only year for which the simulated snowpack disappeared in advance of observations (Figure 4.2). Indeed, the relatively weak performance of the model during the rehydration period is due to its poor simulation of snow cover depth and duration, which are generally much greater than observations at both sites (Figure 4.2). In CLASS, the presence of a snow pack restrains transpiration. When the simulated snow depth is less than 0.1 m, the percent snow cover over the model grid is less than 100%, allowing transpiration to begin.

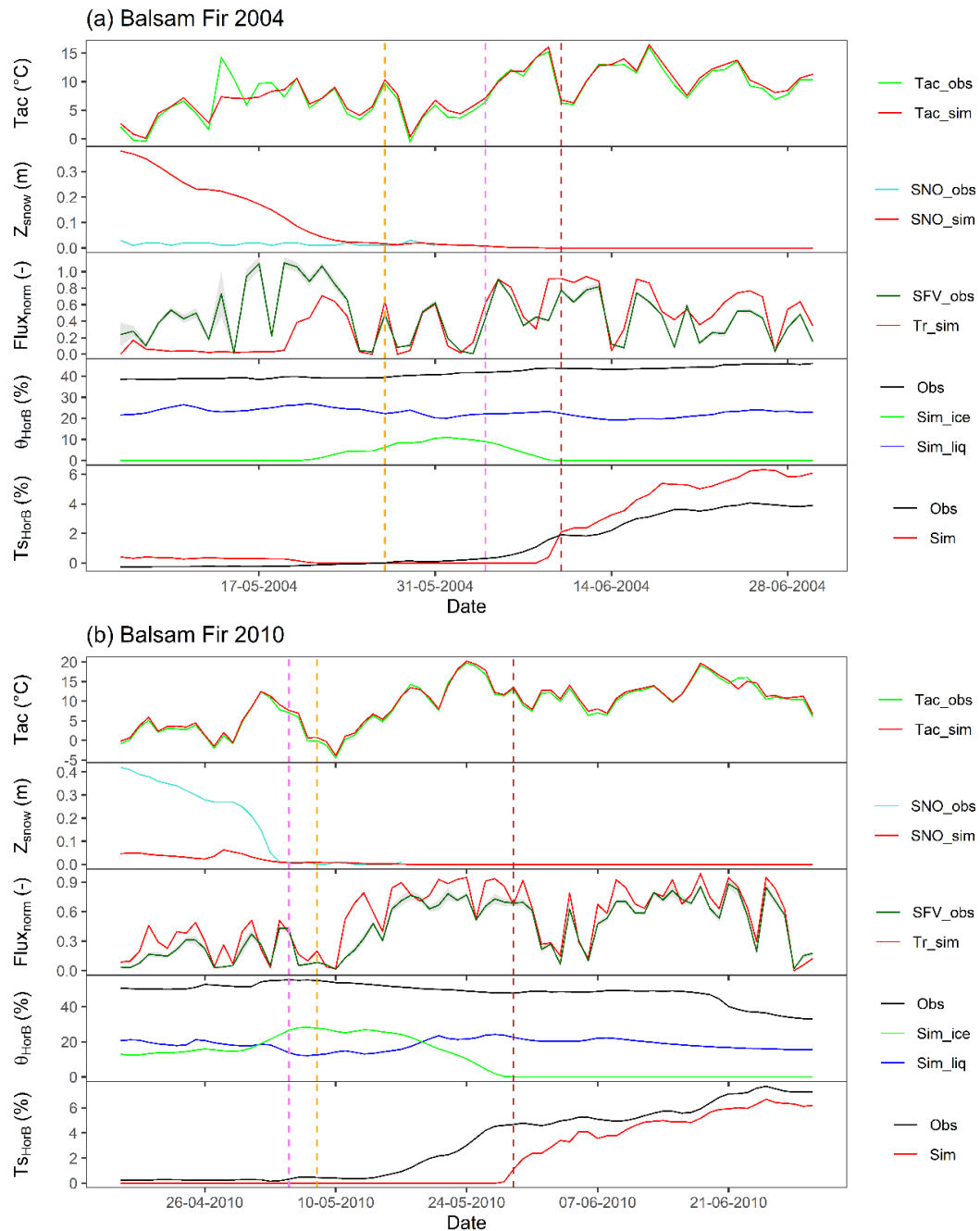


Figure 4.1: Simulated and observed air temperature within the canopy ( $T_{ac}$  - °C; top panel); simulated and observed snow depth (m; 2<sup>nd</sup> panel); standardized modeled transpiration and standardized observed sapflow velocity (mean  $\pm$  1 SE [grey zone] of three trees; 3<sup>rd</sup> panel); simulated (liquid and ice) and observed (mean of four pedons) soil water content in the B horizon (%; 4<sup>th</sup> panel); and simulated and observed (mean of four pedons) soil temperature in the B horizon (°C; bottom panel)

at the balsam fir site in 2004 (a) and 2010 (b). Vertical dashed lines are the beginning of the growing season (orange), the end of the simulated snowmelt period (purple), and the end of simulated frozen soil water presence in the soil (brown).

Table 4.2: Regression coefficients ( $R^2$ ) and slopes (b) of simple linear regressions, Euclidean Distances (ED) and Dynamic Time Warping (DTW) between standardized transpiration and standardized sap flow velocity for multiple years during the rehydration period of balsam fir and black spruce

Year	2004	2005	2006	2007	2008	2009	2010	2011	2012	2013
<i>Balsam Fir</i>										
$R^2$	0.21	0.0	0.88*	0.30*	0.49*	0.19	0.71*	0.14	0.70*	0.60*
b	0.28	0.01	0.06	0.22	0.19	0.24	0.96	0.04	0.12	0.13
ED	2.44	1.34	1.90	1.01	1.46	1.69	0.57	1.51	1.81	1.82
DTW	0.141	0.152	0.225	0.055	0.124	0.078	0.052	0.185	0.161	0.181
<i>Black Spruce</i>										
$R^2$			0.41*	0.42*	0.54*	0.09				
b	-	-	0.33	0.72	0.49	0.22	-	-	-	-
ED	-	-	1.98	1.04	1.74	1.62	-	-	-	-
DTW	-	-	0.128	0.096	0.174	0.155	-	-	-	-

\* p-value < 0.01

Similar to our results, MacDonald, et al. (2016), and Munro et al. (2000) also found the duration of snow cover to be greater in CLASS compared to observations. This may be due to higher surface albedo and upward shortwave radiation modeled by CLASS, leading to a prolonged presence of snow cover compared to the other snow albedo parameterizations (Malik et al. 2014) suggesting that one possibility to improve the simulation of snow depth in CLASS could be to adjust its surface albedo algorithm.

While it could be argued that the presence of frozen water in the soil in addition to snow on the ground could contribute to the low transpiration modeled, this is not the

case as long as there is still liquid water in the soil. Our results show that in 2010,  $Tr_{SIM}$  was not different from observed values at the balsam fir site despite the presence of simulated soil frozen water prior to the growing season (Figure 4.1b, 4<sup>th</sup> panel).

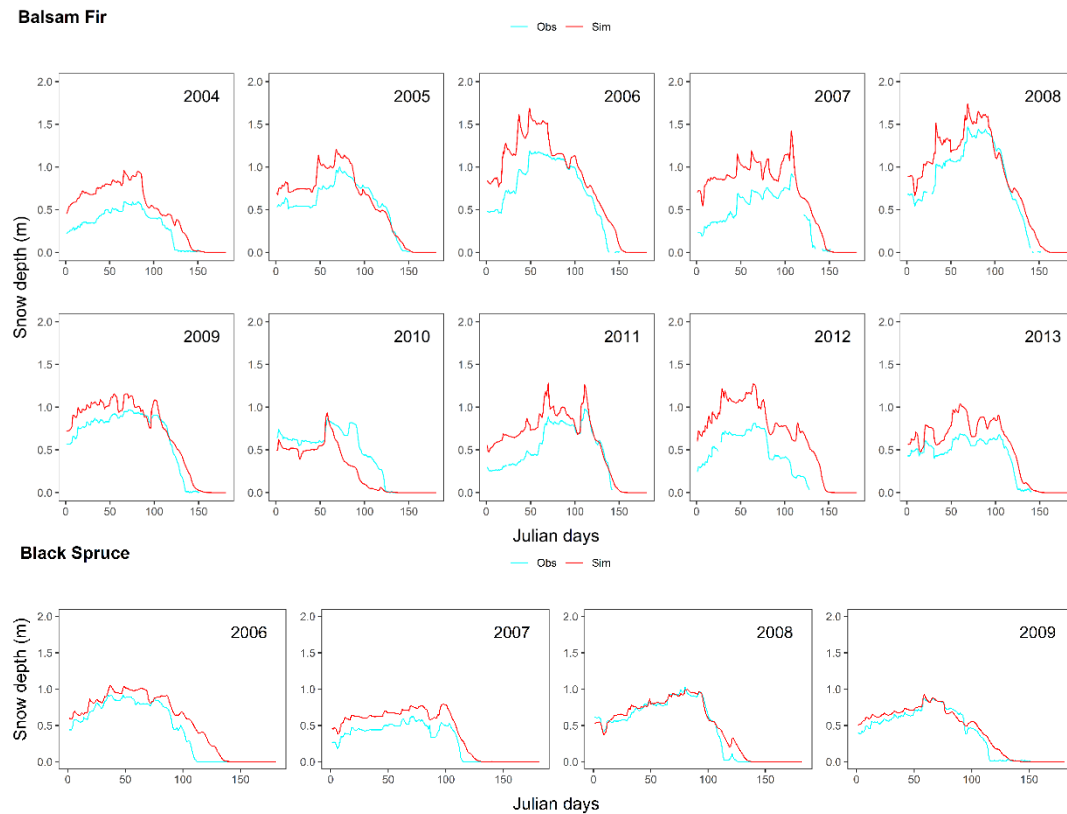


Figure 4.2: Simulated and observed snow depth (m) from 2004 to 2013 at the balsam fir site (top) and from 2006 to 2009 at the black spruce site (bottom).

#### 4.5.2 Transpiration during the growing season

Despite the fact that other studies have used CLASS to quantitatively assess the simulation of transpiration on a daily basis in many ecosystems (Bartlett et al., 2003; Huang et al., 2011; Isabelle et al., 2018; MacDonald et al., 2016; Wang et al., 2002; Yuan et al., 2007), none of them have focused on the temporal evolution of transpiration based on sap flow velocity data on a daily time-scale. As mentioned above,

sap flow techniques are more stable, enabling us to assess not only tree transpiration but also the influence of species, environmental and physiological factors on transpiration. This is not possible with eddy covariance techniques since they provide measures of evapotranspiration for an entire footprint area (Hogg et al., 1997; Wilson et al. 2001). In this study, during the growing season, the temporal evolution of  $Tr_{SIM}$  corresponded closely to the  $SF_{OBS}$  for all years analysed (2006 to 2009 for black spruce and 2004 to 2013 for balsam fir; Figures 4.3, 4S.1 and 4S.2). The  $R^2$  values were high and significant during the growing season in most years at both sites, with  $b$  values being very close to unity which supports a good performance of the model in all years except 2006 which had a slope much greater than unity ( $b = 1.91$ ) (Table 4.3). Likewise, low ED (less than 2) and DTW values (below 0.1) in most years at both sites demonstrate the good performance of the model, again except in 2006 at the balsam fir site which had highest values (3.16 for ED and 0.161 for DTW).

The beginning of the growing season in 2007 at the balsam fir site fell outside of the best fit line of the simple linear regression of  $Tr_{SIM}$  vs  $SF_{OBS}$  (empty triangle) compared to other years at both sites (Figures 4.4). This discrepancy at the beginning of the growing season in 2007 is due to snow on the ground in the model that restrained the modeled transpiration as explained above for the rehydration period (Figure 4S.3). In 2006 at the balsam fir site, the model performance was poor with high ED and DTW values. While 2006 did not undergo a drought, there was a short-duration heat stress and tree growth ceased around July 1<sup>st</sup> which is at least one month earlier than normal (Duchesne and Houle, 2011). The observations showed a reduced transpiration rate (Figure 4S.1 – 2006) that began around mid-June 2006 with a marked decrease around the first of July up to the end of the growing season while modeled transpiration was maintained at high values. Indeed, the large discrepancy between simulated and observed transpiration values for the year 2006 is likely due to the fact that CLASS did not capture the impact of the heat stress on tree physiology and transpiration.

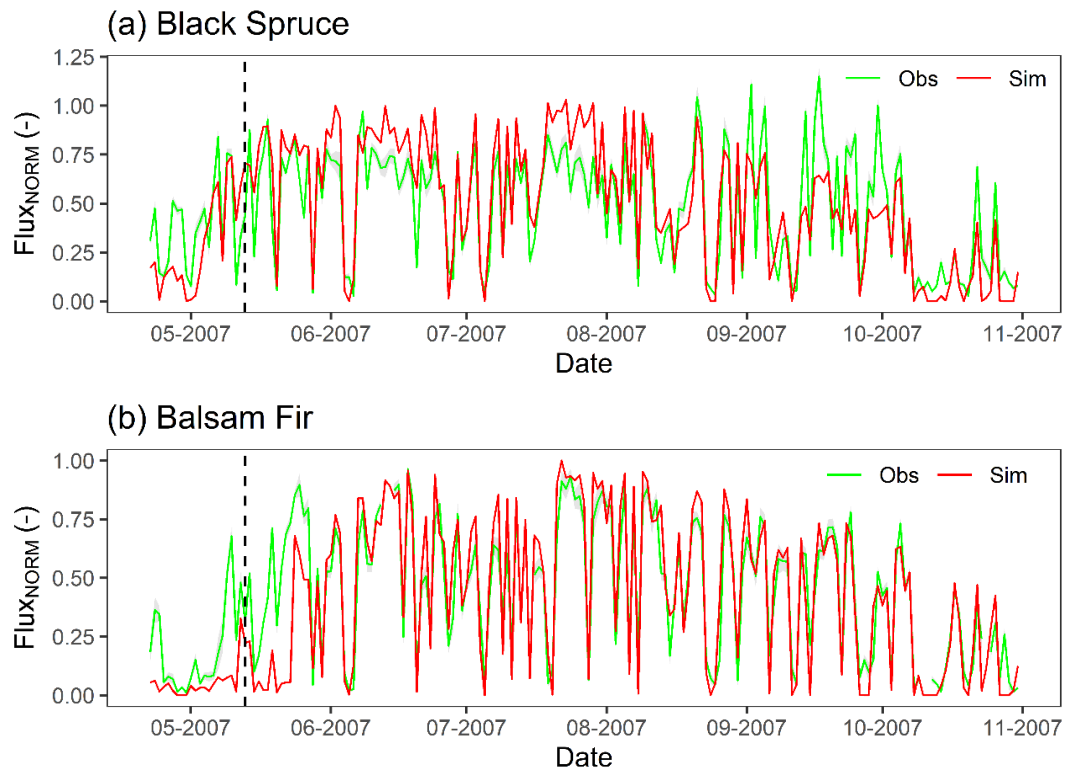


Figure 4.3: Daily standardized modeled transpiration [unitless] and standardized sap flow velocity [-; mean  $\pm$  1 SE (grey zone) of six probes] at the black spruce (a) and balsam fir sites (b) in 2007. The vertical dashed line shows the beginning of the growing season as determined from dendrometers.

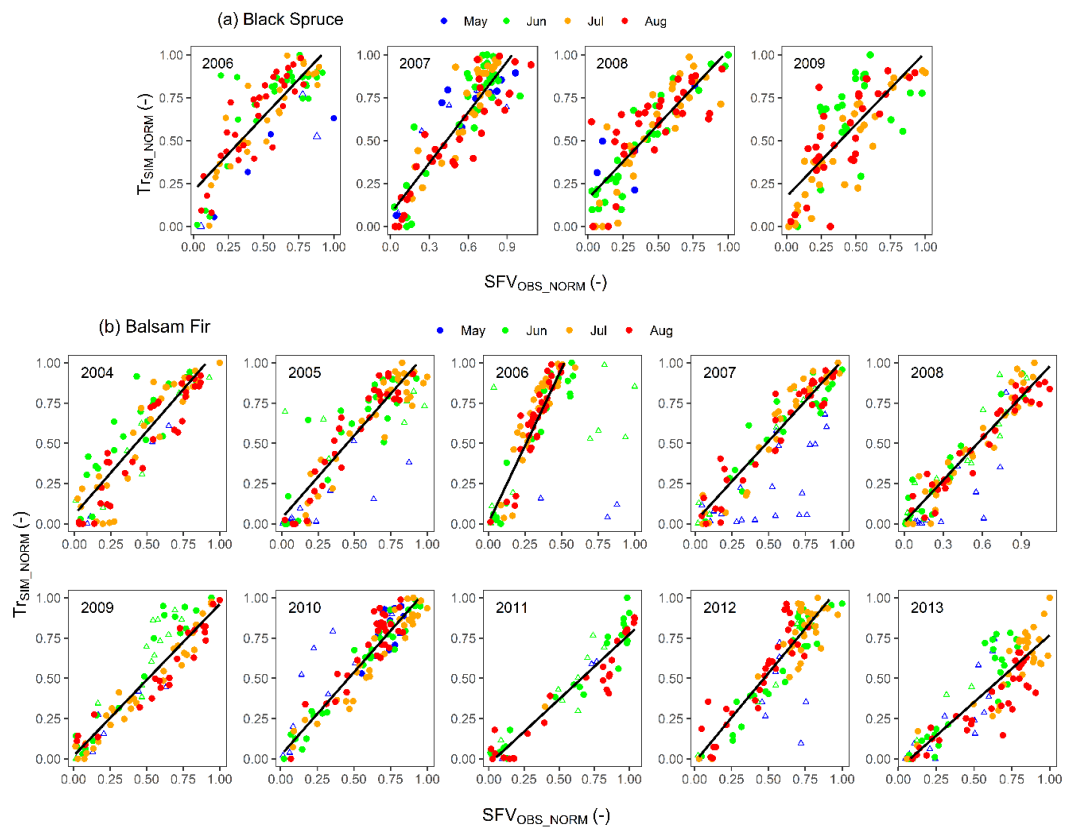


Figure 4.4: Simple linear regressions of standardized modeled transpiration ( $T_{SIM\_NORM}$ ) vs standardized observed sap flow velocity ( $SFV_{OBS\_NORM}$ , mean of three trees) during the growing period at black spruce (a; 2006 to 2009) and balsam fir (b; 2004 to 2013) sites. Filled circles: no modeled snow on the ground; empty triangles: modeled snow on the ground. Best lines of fit are during the period with no modeled snow on the ground (filled circles).

Table 4.3: Regression coefficients ( $R^2$ ) and slopes (b) of simple linear regressions, Euclidean Distances (ED) and Dynamic Time Warping (DTW) between standardized transpiration and standardized sap flow velocity for multiple years during the period without snow from the beginning of the growing season to the end of August of balsam fir and black spruce

Year	2004	2005	2006	2007	2008	2009	2010	2011	2012	2013
<i>Balsam Fir</i>										
$R^2$	0.80*	0.85*	0.84*	0.89*	0.91*	0.89*	0.88*	0.91*	0.84*	0.76*
b	1.04	1.03	1.91	1.00	0.86	0.94	1.03	0.81	1.11	0.83
ED	1.45	1.22	3.16	0.91	1.02	0.89	1.03	1.36	1.19	2.04
DTW	0.095	0.085	0.161	0.069	0.075	0.068	0.062	0.121	0.072	0.101
<i>Black Spruce</i>										
$R^2$			0.70*	0.79*	0.72*	0.57*				
b	-	-	0.88	1.00	0.88	0.84	-	-	-	-
ED	-	-	2.02	1.58	1.77	1.97	-	-	-	-
DTW	-	-	0.094	0.081	0.088	0.095	-	-	-	-

\* p-value < 0.001

#### 4.5.3 Transpiration during observed and simulated drought at the balsam fir site

##### 4.5.3.1 Drought of July 2012

In the summer of 2012, there was a drought that began on July 1<sup>st</sup> and ended on August 4<sup>th</sup> at the balsam fir site (Houle et al., 2016). The normal average precipitation during this period at this site is about 150 mm, but in 2012 it was only 23 mm. The low amount of precipitation led to a marked decrease in the soil water content in the B and C layers (Figure 4.5). Observed transpiration decreased during the second half of the drought period, where there is a divergence between simulated and observed transpiration leading to decrease  $R^2$  (Figure 4.5, bottom panel). Unlike the field measurements, CLASS maintained transpiration throughout the entire drought period. This shows that CLASS was primarily driven by VPD and Rad during the drought and unresponsive to

the decreased soil water content. However, the 2012 drought had a strong impact on tree physiology and not only on transpiration, such that important nutrient losses (nutrient base cations, phosphorus and dissolved organic carbon) occurred via both canopy throughfall and litterfall (Houle et al., 2016). Delage et al. (1999) found that the discretization of soil layers in CLASS has an important impact on transpiration, the latter being overestimated when even a small portion of roots has access to water in deeper soil layers in the model. The authors proposed that the rooting layer should coincide with the soil layers in the model in order to ensure that the roots occupy the entire model layer. In this study, roots (with maximum rooting depth of 0.98 m) coincides with the total depth of the three top soil layers in the model (1.07 m; Appendix A). Moreover, the permeable soil depth defined in the model is 1 m, thus water cannot be extracted beyond 1 m depth. Henceforth, the overestimation of transpiration during the drought period could not be due to the soil layer discretization in the model as the roots covers all the three top soil layers.

#### 4.5.3.2 Simulated forced zero-precipitation during the hydrological year 2006-2007

The apparent absence of an impact on simulated transpiration during July 2012 drought led us to further investigate CLASS's sensitivity to drought conditions. This was done by artificially stopping precipitation inputs starting in October 2006 (i.e. to ensure that the summer drought was total and that there was no groundwater recharge from melting snowpack in the spring 2007). The simulation showed that  $Tr_{SIM}$  was maintained during the whole 2007 growing season (Figure 4.6 bottom panel) due in part to the amount of water stored in the soils as frozen water that melts at the beginning of the growing season. This is an artefact due to the absence of the insulating effect of the snowpack in the simulation. This amount of water was in fact relatively small. Transpiration finally dropped to zero on September 11<sup>th</sup> 2007 when the simulated soil liquid water content reached 4.5 % in Hum, 5.7 % in HorB, and 5 % in HorC (Figure 4.6, middle panel), thus very close to the soil water threshold of 4 % assigned in CLASS at which

transpiration ceases (horizontal black dashed line in Figure 4.6 middle panel; Verseghy, 2012). Our results further show the unrealistic control of transpiration by atmospheric variables in CLASS to the detriment of soil water content even when the latter reaches critically low values which normally affects both canopy conductance and transpiration (Granier et al., 2000; Lagergren and Lindroth, 2002). In coupled simulations with the CRCM, CLASS will feed greater amounts of water into the atmosphere during drought thus resulting in greater precipitation. As a consequence, the CRCM will subsequently underestimate drought projections. This thus exposes a weakness of CLASS to accurately model the effect of water-stressed conditions on transpiration and its feedback process (precipitation). Indirectly, the increased modelled precipitation might decrease air temperature via evaporative cooling (due to the presence of higher amount water in the soil) and reduced solar radiation under overcast conditions.

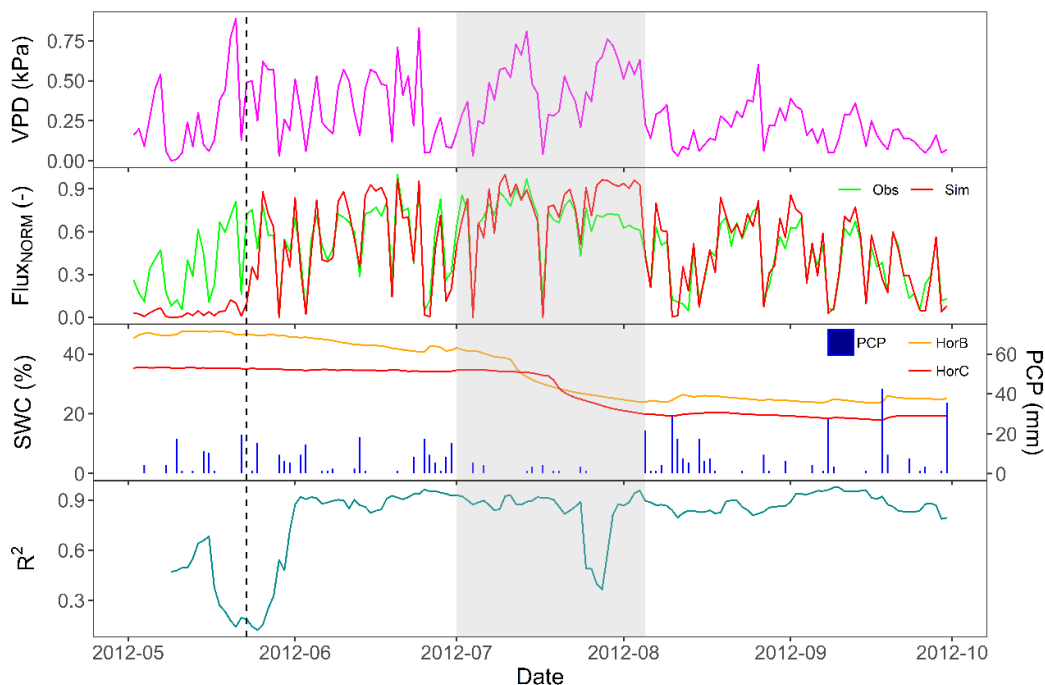


Figure 4.5: Vapour pressure deficit (VPD, kPa; top panel); standardized modeled transpiration (Sim) and standardized observed sap flow velocity (Obs, mean of six probes; 2<sup>nd</sup> panel); observed soil water content (%) in the B and C Horizons and

precipitation (mm, PCP; 3<sup>rd</sup> panel); 15-day moving average of regression coefficients between simulated and observed data ( $R^2$ ; bottom panel) at the balsam fir site during the drought (grey shaded area) of 2012. Vertical black dashed line shows the beginning of the growing season.

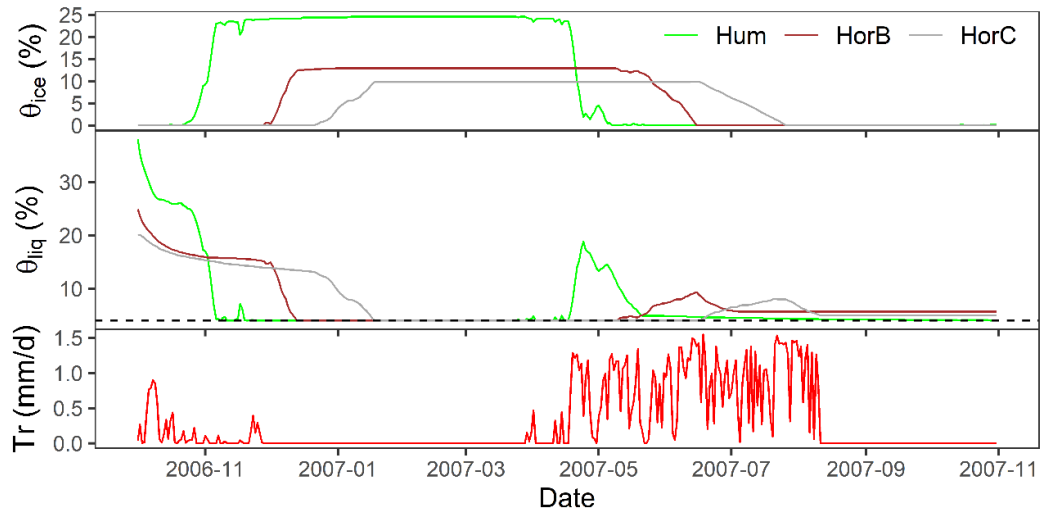


Figure 4.6: Simulated ice (top panel) and liquid (middle panel) soil water content for the three soil layers (Hum, HorB, HorC) and simulated transpiration (bottom panel) for the first hydrological year of the forced zero-precipitation simulation. The horizontal dashed black line is the threshold soil liquid water content at 4 % assigned in CLASS.

Other studies have found most land surface schemes to underestimate evapotranspiration that would result in an overestimation of drought intensity and duration (De Kauwe, et al. 2015; Ukkola, et al. 2016b). However, our study showed that CLASS overestimates transpiration during drought periods, nevertheless, evaporation was not included in our analysis which might lead to a different conclusion for modelled evapotranspiration. Ukkola, et al. (2016b) evaluated the performance of eight land surface schemes (excluding CLASS) under water stress conditions across six sites which were evergreen needleleaf/broadleaf, deciduous broadleaf and grassland. Their study showed that all the land surface schemes underestimated

evapotranspiration and thereby greatly overestimated drought in terms of both magnitude and frequency. Ukkola et al. (2016b) concluded that the proper representation of vertical soil water fluxes (via the use of validated soil hydraulic properties) and plant water stress within LSS are critical for modelling transpiration during drought. This plant water stress function itself depends solely on the plant available water in the soil (Verhoef and Egea, 2014). Our results suggest that, while the presence of a threshold value to cease transpiration in CLASS is important to represent soil residual water that is not available for transpiration/evaporation, the fixed 4 % value is too low and unrealistic. CLASS should thus incorporate an equation that determines the soil water threshold based on soil properties instead of using a fixed threshold value for all mineral soil. Moreover, CLASS should also include an equation similar to the plant water stress function (Verhoef and Egea, 2014) that will slow down transpiration when soil water decreases from field capacity to the permanent wilting point in order to increase the realism of the transpiration process in the LSS. Sun and Versegby (2019) used the same soil moisture suction function in CLASS, but used the soil moisture suction for the top soil layer only instead of the minimum liquid moisture suction in soil layers (currently used in CLASS) in order to increase the sensitivity of CLASS to decreasing soil water. In this study, we propose to slightly modify the soil moisture suction function ( $f(\varphi_s)$ ; Eq. 4.13) by varying it with actual soil moisture suction ( $\varphi_s$ ) and soil moisture suction at permanent wilting point ( $\varphi_{PWP}$ ) in order to increase the stomatal resistance as the actual soil moisture suction approaches the permanent wilting point ( $\alpha$  is a multiplying factor for the exponential increase).

$$f(\varphi_s) = 1 \quad (\varphi_s \geq \text{field capacity}),$$

$$f(\varphi_s) = 1 + \alpha \text{EXP}^{(\varphi_{PWP} - \varphi_s)} \quad (\text{PWP} < \varphi_s < \text{FC}),$$

$$f(\varphi_s) = 250 \quad (\varphi_s \leq \text{permanent wilting point}) \quad \text{Eq. 4.13}$$

#### 4.6 Conclusion

Due to long-term *in situ* sap flow measurements, we were able to evaluate the performance of CLASS for modeled transpiration during many contrasting climatic conditions for two boreal forests. Overall, our study showed that CLASS modeled transpiration adequately during the growing season, but not during the tree rehydration period where the modeled transpiration greatly underestimated the observations. The poor performance of CLASS during the latter period is due to its overestimation of snow pack depth and duration, the presence of which artificially restrains transpiration. CLASS also overestimates transpiration during extreme events such as heat-waves or droughts. Its poor performance during drought is due to its unrealistic sensitivity to low soil water content. Though the underestimation of transpiration during tree rehydration might not contribute substantially to the inaccuracy of the feedback process (i.e. underestimation of precipitation) when coupled with the CRCM, the overestimation of transpiration during heat stressed and water-stressed conditions will lead to overestimation of precipitation, and consequently, to the underestimation of drought events in future climate projections. This will also affect air temperature projections. Our results strongly suggest that the improvement of CLASS during the rehydration period and drought will lead to more realistic climate projections in the future.

#### 4.7 Acknowledgements

This work was supported by a MITACS Cluster grant and the OURANOS organisation. We thank the technicians of the Ministry of Forests, Wildlife, and Parks for the measurement of all data used in this study. We also thank Richard Harvey for his timely advice in CLASS model simulations.

## 4.8 References

- Bala, G., Caldeira, K., Wickett, M., Phillips, T., Lobell, D., Delire, C. and Mirin, A., 2007. Combined climate and carbon-cycle effects of large-scale deforestation. *Proceedings of the National Academy of Sciences*, 104 (16), 6550-6555.
- Baldocchi, D.D., Xu, L. and Kiang, N., 2004. How plant functional-type, weather, seasonal drought, and soil physical properties alter water and energy fluxes of an oak–grass savanna and an annual grassland. *Agricultural and Forest Meteorology*, 123 (1-2), 13-39.
- Bartlett, P.A., McCaughey, J.H., Lafleur, P.M. and Verseghy, D.L. 2003. Modelling evapotranspiration at three boreal forest stands using the CLASS: tests of parameterizations for canopy conductance and soil evaporation. *International Journal of Climatology*, 23 (4), 427-451.
- Betts, R.A., 2000. Offset of the potential carbon sink from boreal forestation by decreases in surface albedo. *Nature*, 408(6809), pp.187-190.
- Bonan, G.B., 2008. Forests and Climate Change: Forcings, Feedbacks, and the Climate Benefits of Forests. *Science*, 320 (5882), 1444-1449.
- Bovard, B.D., Curtis, P.S., Vogel, C.S., Su, H.B. and Schmid, H.P., 2005. Environmental controls on sap flow in a northern hardwood forest. *Tree Physiology*, 25 (1), 31-38.
- Brochu, R. and Laprise, R., 2007. Surface water and energy budgets over the Mississippi and Columbia river basins as simulated by two generations of the Canadian Regional Climate Model. *Atmosphere-ocean*, 45 (1), 19-35.
- Brovkin, V., Raddatz, T., Reick, C.H., Claussen, M. and Gayler, V., 2009. Global biogeophysical interactions between forest and climate. *Geophysical Research Letters*, 36 (7).
- Brutsaert, W., 1975. On a derivable formula for long-wave radiation from clear skies. *Water Resour. Res.*, 11(5), 742-744.
- Campbell, G.S. and Norman, J.M., 2012. *An introduction to environmental biophysics*. Springer Science & Business Media.
- Chen, J., Chen, B., Black, T.A., Innes, J.L., Wang, G., Kiely, G., Hirano, T., and Wohlfahrt, G., 2013. Comparison of terrestrial evapotranspiration estimates using the mass transfer and Penman-Monteith equations in land surface models. *Journal of Geophysical Research: Biogeosciences*, 118 (4), 1715-1731.
- Choudhury, B.J. and DiGirolamo, N.E., 1998. A biophysical process-based estimate of global land surface evaporation using satellite and ancillary data I. Model

- description and comparison with observations. *Journal of Hydrology*, 205 (3-4), 164-185.
- Choudhury, B.J., DiGirolamo, N.E., Susskind, J., Darnell, W.L., Gupta, S.K. and Asrar, G., 1998. A biophysical process-based estimate of global land surface evaporation using satellite and ancillary data II. Regional and global patterns of seasonal and annual variations. *Journal of Hydrology*, 205 (3-4), 186-204.
- De Kauwe, M.G., Zhou, S., Medlyn, B.E., Pitman, A.J., Wang, Y., Duursma, R.A. and Prentice, I.C., 2015. Do land surface models need to include differential plant species responses to drought? Examining model predictions across a mesic-xeric gradient in Europe.
- Delage, Yves, Lei Wen, and Jean-Marc Bélanger, 1999. Aggregation of parameters for the land surface model CLASS. *Atmosphere-Ocean* 37.2: 157-178.
- Dickinson, R.E. and Henderson-Sellers, A., 1988. Modelling tropical deforestation: A study of GCM land-surface parametrizations. *Quarterly Journal of the Royal Meteorological Society*, 114 (480), 439-462.
- Dirmeyer, P.A., Gao, X., Zhao, M., Guo, Z., Oki, T. and Hanasaki, N., 2005. The second Global Soil Wetness Project (GSWP-2): Multi-model analysis and implications for our perception of the land surface. *Bull. Amer. Meteor. Soc.*
- Duchesne, L., & Houle, D., 2011. Modelling day-to-day stem diameter variation and annual growth of balsam fir (*Abies balsamea* (L.) Mill.) from daily climate. *Forest Ecology and Management*, 262(5), 863-872. doi:<https://doi.org/10.1016/j.foreco.2011.05.027>
- Duchesne, L., Houle, D. and D'Orangeville, L., 2012. Influence of climate on seasonal patterns of stem increment of balsam fir in a boreal forest of Québec, Canada. *Agricultural and forest meteorology*, 162, pp.108-114.
- Ewers, B., Mackay, D., Gower, S., Ahl, D., Burrows, S. and Samanta, S., 2002. Tree species effects on stand transpiration in northern Wisconsin. *Water resources research*, 38 (7), 8-1-8-11.
- Garratt, J.R., 1993. Sensitivity of Climate Simulations to Land-Surface and Atmospheric Boundary-Layer Treatments-A Review. *Journal of Climate*, 6 (3), 419-448.
- Gartner, K., Nadezhdina, N., Englisch, M., Čermak, J. and Leitgeb, E., 2009. Sap flow of birch and Norway spruce during the European heat and drought in summer 2003. *Forest Ecology and Management*, 258 (5), 590-599.
- Gayler, S., Ingwersen, J., Priesack, E., Wöhling, T., Wulfmeyer, V. and Streck, T., 2013. Assessing the relevance of subsurface processes for the simulation of evapotranspiration and soil moisture dynamics with CLM3. 5: comparison with

- field data and crop model simulations. *Environmental earth sciences*, 69 (2), 415-427.
- Granier, A., 1987. Evaluation of transpiration in a Douglas-fir stand by means of sap flow measurements. *Tree Physiology*, 3, 309-320.
- Granier, A., Loustau, D. and Bréda, N., 2000. A generic model of forest canopy conductance dependent on climate, soil water availability and leaf area index. *Annals of Forest Science*, 57(8), pp.755-765.
- Grelle, A., Lundberg, A., Lindroth, A., Morén, A.-S., & Cienciala, E., 1997. Evaporation components of a boreal forest: variations during the growing season. *Journal of Hydrology*, 197(1-4), 70-87.
- Grippa, M., Kergoat, L., Frappart, F., Araud, Q., Boone, A., De Rosnay, P., Lemoine, J.M., Gascoin, S., Balsamo, G., Oettle, C. and Decharme, B., 2011. Land water storage variability over West Africa estimated by Gravity Recovery and Climate Experiment (GRACE) and land surface models. *Water Resources Research*, 47 (5).
- Hogg, E.H., Black, T.A., den Hartog, G., Neumann, H.H., Zimmermann, R., Hurdle, P.A., Blanken, P.D., Nesic, Z., Yang, P.C., Staebler, R.M. and McDonald, K.C., 1997. A comparison of sap flow and eddy fluxes of water vapor from a boreal deciduous forest. *Journal of Geophysical Research: Atmospheres*, 102(D24), pp.28929-28937.
- Houle, D., Lajoie, G. and Duchesne, L., 2016. Major losses of nutrients following a severe drought in a boreal forest. *Nature Plants*, 2, 16187.
- Huang, S., Arain, M.A., Arora, V.K., Yuan, F., Brodeur, J. and Peichl, M., 2011. Analysis of nitrogen controls on carbon and water exchanges in a conifer forest using the CLASS-CTEMN+ model. *Ecological modelling*, 222 (20-22), 3743-3760.
- Isabelle, P.-E., Nadeau, D.F., Asselin, M.-H., Harvey, R., Musselman, K.N., Rousseau, A.N. and Anctil, F., 2018. Solar radiation transmittance of a boreal balsam fir canopy: Spatiotemporal variability and impacts on growing season hydrology. *Agricultural and forest meteorology*, 263, 1-14.
- Jaksa, W.T. and Sridhar, V., 2015. Effect of irrigation in simulating long-term evapotranspiration climatology in a human-dominated river basin system. *Agricultural and Forest Meteorology*, 200, 109-118.
- Kramer, P.J., 1983. *Water Relations of Plants*: Academic Press, Inc. Orlando, FL.
- Lagergren, F. and Lindroth, A., 2002. Transpiration response to soil moisture in pine and spruce trees in Sweden. *Agricultural and Forest Meteorology*, 112 (2), 67-85.

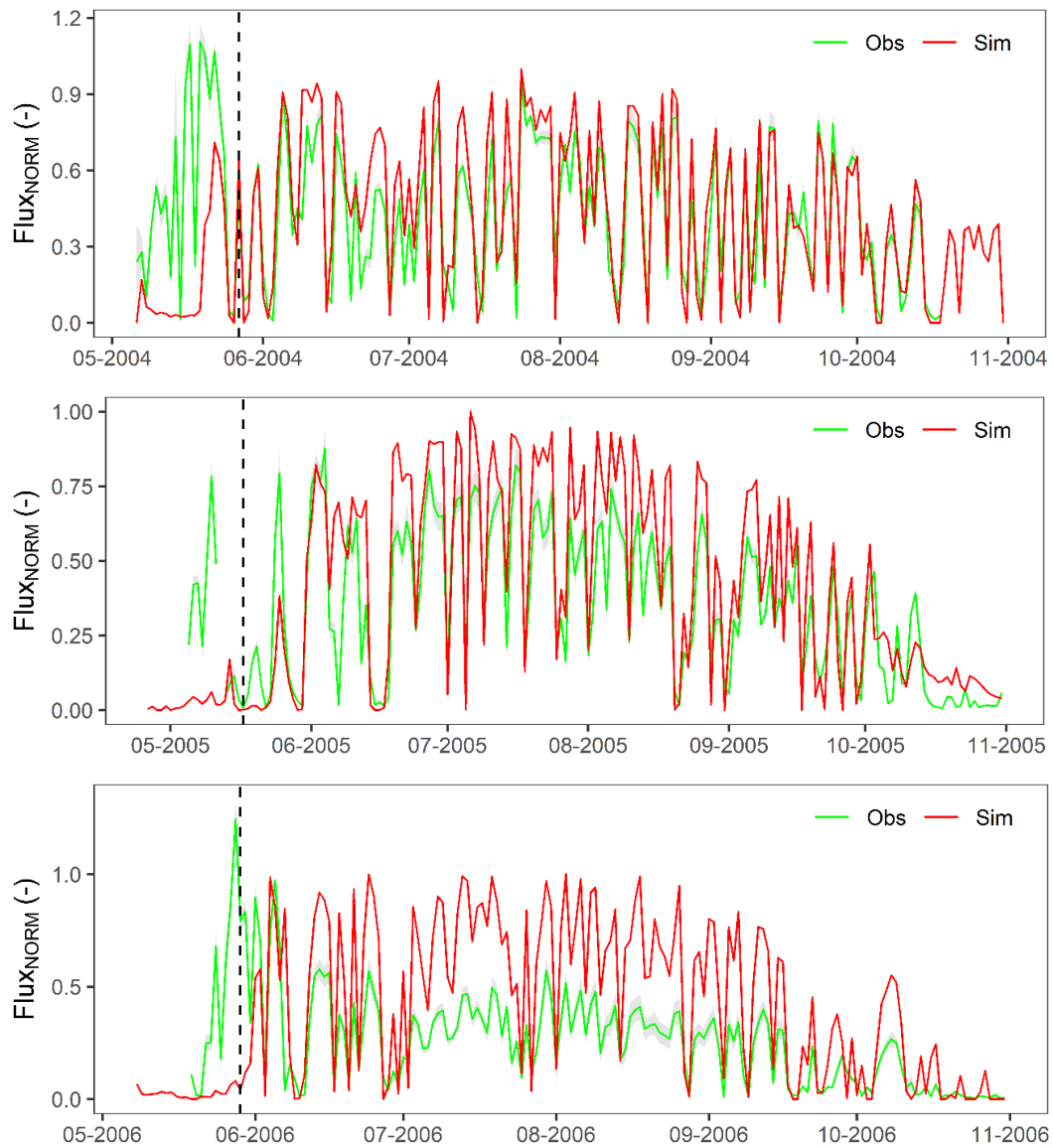
- Lei, H., Yang, D., Shen, Y., Liu, Y. and Zhang, Y., 2011. Simulation of evapotranspiration and carbon dioxide flux in the wheat-maize rotation croplands of the North China Plain using the Simple Biosphere Model. *Hydrological Processes*, 25 (20), 3107-3120.
- Li, L., Van der Tol, C., Chen, X., Jing, C., Su, B., Luo, G. and Tian, X., 2013. Representing the root water uptake process in the Common Land Model for better simulating the energy and water vapour fluxes in a Central Asian desert ecosystem. *Journal of hydrology*, 502, 145-155.
- Ma, N., Niu, G.Y., Xia, Y., Cai, X., Zhang, Y., Ma, Y., and Fang, Y., 2017 A systematic evaluation of Noah-MP in simulating land-atmosphere energy, water, and carbon exchanges over the continental United States. *Journal of Geophysical Research: Atmospheres*, 122 (22), 12,245-212,268.
- MacDonald, M.K., Davison, B.J., Mekonnen, M.A. and Pietroniro, A., 2016. Comparison of land surface scheme simulations with field observations versus atmospheric model output as forcing. *Hydrological Sciences Journal*, 61 (16), 2860-2871.
- Malik, M.J., van der Velde, R., Vekerdy, Z. and Su, Z., 2014. Improving modeled snow albedo estimates during the spring melt season. *Journal of geophysical research: Atmospheres*, 119 (12), 7311-7331.
- Manabe, S., 1969. Climate and the ocean circulation: I. The atmospheric circulation and the hydrology of the earth's surface. *Monthly Weather Review*, 97(11), pp.739-774.
- Munro, D.S., Bellisario, L.M. and Versegny, D.L., 2000. Measuring and modelling the seasonal climatic regime of a temperate wooded wetland. *Atmosphere-Ocean*, 38 (1), 227-249.
- Oogathoo, S., Houle, D., Duchesne, L. and Kneeshaw, D., 2020. Vapour pressure deficit and solar radiation are the major drivers of transpiration of balsam fir and black spruce tree species in humid boreal regions, even during a short-term drought. *Agricultural and Forest Meteorology*, 291, p.108063.
- Ouimet, R. and Duchesne, L., 2005. Base cation mineral weathering and total release rates from soils in three calibrated forest watersheds on the Canadian Boreal Shield. *Canadian Journal of Soil Science*, 85 (2), 245-260.
- Sakoe, H. and Chiba, S., 1978. Dynamic programming algorithm optimization for spoken word recognition. *IEEE transactions on acoustics, speech, and signal processing*, 26(1), pp.43-49.

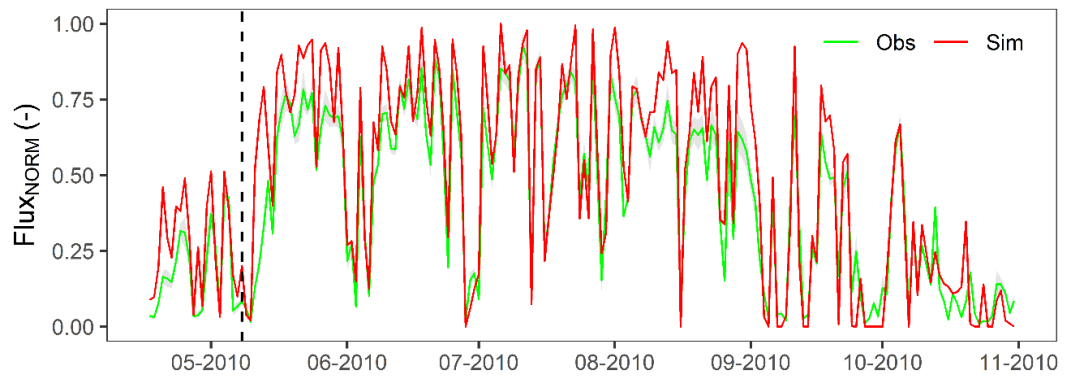
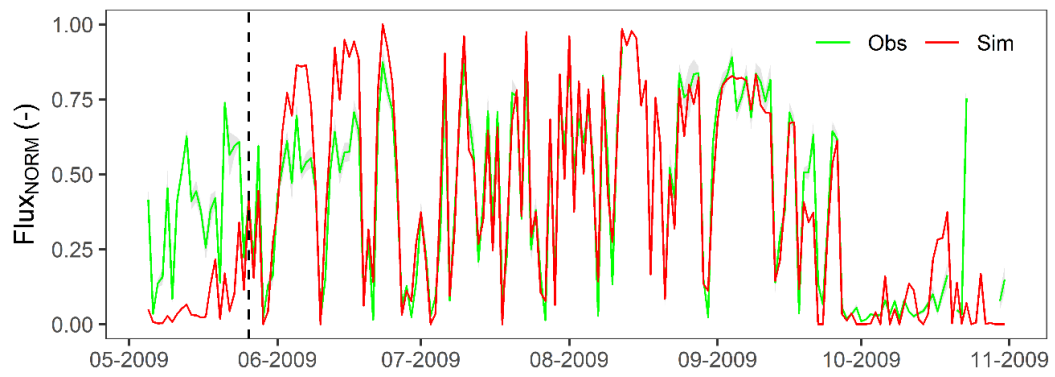
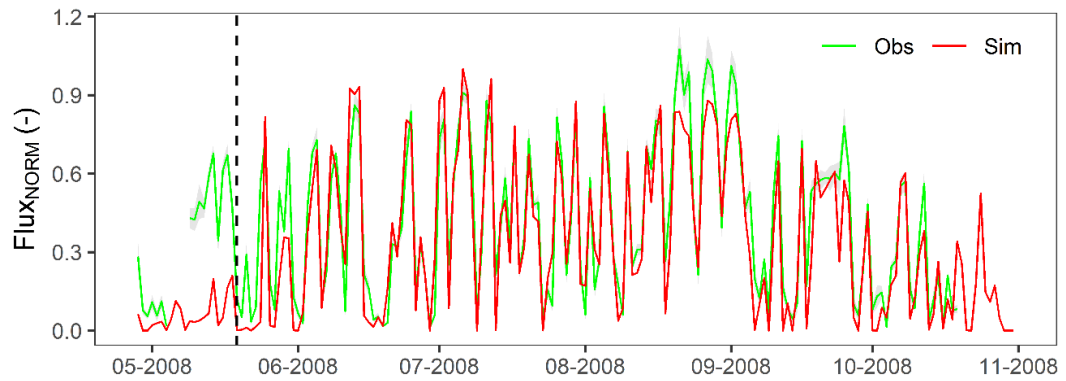
- Seneviratne, S.I., Corti, T., Davin, E.L., Hirschi, M., Jaeger, E.B., Lehner, I., Orlowsky, B. and Teuling, A.J., 2010. Investigating soil moisture–climate interactions in a changing climate: A review. *Earth-Science Reviews*, 99 (3–4), 125-161.
- Seneviratne, S.I., Lehner, I., Gurtz, J., Teuling, A.J., Lang, H., Moser, U., Grebner, D., Menzel, L., Schroff, K., Vitvar, T. and Zappa, M., 2012 Swiss prealpine Rietholzbach research catchment and lysimeter: 32 year time series and 2003 drought event. *Water Resources Research*, 48 (6).
- Sugita, M. and Brutsaert, W., 1993. Cloud effect in the estimation of instantaneous downward longwave radiation. *Water Resources Research*, 29 (3), 599-605.
- Sun, S. and Verseghy, D., 2019. Introducing water-stressed shrubland into the Canadian Land Surface Scheme. *Journal of Hydrology*, 579, p.124157.
- Swann, A.L., Fung, I.Y., Levis, S., Bonan, G.B. and Doney, S.C., 2010. Changes in Arctic vegetation amplify high-latitude warming through the greenhouse effect. *Proceedings of the National Academy of Sciences*, 107 (4), 1295-1300.
- Turcotte, A., Morin, H., Krause, C., Deslauriers, A. and Thibeault-Martel, M., 2009. The timing of spring rehydration and its relation with the onset of wood formation in black spruce. *Agricultural and Forest Meteorology*, 149(9), pp.1403-1409.
- Ukkola, A.M., Kauwe, M.G.D., Pitman, A.J., Best, M.J., Abramowitz, G., Haverd, V., Decker, M. and Haughton, N., 2016b. Land surface models systematically overestimate the intensity, duration and magnitude of seasonal-scale evaporative droughts. *Environmental Research Letters*, 11 (10), 104012.
- Ukkola, A.M., Pitman, A.J., Decker, M., De Kauwe, M.G., Abramowitz, G., Kala, J. and Wang, Y.P., 2016a. Modelling evapotranspiration during precipitation deficits: identifying critical processes in a land surface model. *Hydrology and Earth System Sciences*, 20 (6), 2403-2419.
- Verhoef, A., & Egea, G., 2014. Modeling plant transpiration under limited soil water: Comparison of different plant and soil hydraulic parameterizations and preliminary implications for their use in land surface models. *Agricultural and Forest Meteorology*, 191, 22-32.  
doi:<https://doi.org/10.1016/j.agrformet.2014.02.009>
- Verseghy, D., 2012. CLASS – THE CANADIAN LAND SURFACE SCHEME (VERSION 3.6) Technical Documentation. E. CANADA and S.A.T.B. CLIMATE RESEARCH DIVISION (eds.).
- Verseghy, D.L., 1991. Class—A Canadian land surface scheme for GCMS. I. Soil model. *International Journal of Climatology*, 11 (2), 111-133.

- Verseghy, D.L., McFarlane, N.A. and Lazare, M., 1993. Class - A Canadian land surface scheme for GCMs, II. Vegetation model and coupled runs. *International Journal of Climatology*, 13 (4), 347-370.
- Wang, H., Tetzlaff, D., Dick, J.J. and Soulsby, C., 2017. Assessing the environmental controls on Scots pine transpiration and the implications for water partitioning in a boreal headwater catchment. *Agricultural and Forest Meteorology*, 240-241, 58-66.
- Wang, L., Caylor, K.K., Villegas, J.C., Barron-Gafford, G.A., Breshears, D.D. and Huxman, T.E., 2010. Partitioning evapotranspiration across gradients of woody plant cover: Assessment of a stable isotope technique. *Geophysical Research Letters*, 37 (9).
- Wang, P., Niu, G.Y., Fang, Y.H., Wu, R.J., Yu, J.J., Yuan, G.F., Pozdniakov, S.P. and Scott, R.L., 2018. Implementing dynamic root optimization in Noah-MP for simulating phreatophytic root water uptake. *Water Resources Research*, 54 (3), 1560-1575.
- Wang, S., Grant, R.F., Verseghy, D.L. and Andrew Black, T., 2002. Modelling carbon-coupled energy and water dynamics of a boreal aspen forest in a general circulation model land surface scheme. *International Journal of Climatology: A Journal of the Royal Meteorological Society*, 22 (10), 1249-1265.
- Ward, A.D. and Trimble, S.W., 2004. *Environmental Hydrology*. second edn. Lewis publishers.
- Wilson, K.B., Hanson, P.J., Mulholland, P.J., Baldocchi, D.D. and Wullschleger, S.D., 2001. A comparison of methods for determining forest evapotranspiration and its components: sap-flow, soil water budget, eddy covariance and catchment water balance. *Agricultural and Forest Meteorology*, 106(2), pp.153-168.
- Wullschleger, S.D., Wilson, K.B. and Hanson, P.J., 2000. Environmental control of whole-plant transpiration, canopy conductance and estimates of the decoupling coefficient for large red maple trees. *Agricultural and Forest Meteorology*, 104 (2), 157-168.
- Yuan, F., Arain, M.A., Black, T.A. and Morgenstern, K., 2007. Energy and water exchanges modulated by soil-plant nitrogen cycling in a temperate Pacific Northwest conifer forest. *ecological modelling*, 201 (3-4), 331-347.
- Zadra, A., Caya, D., Côté, J., Dugas, B., Jones, C., Laprise, R., Winger, K. and Caron, L.P., 2008. The next Canadian regional climate model. *Phys Can*, 64(2), pp.75-83.
- Zhang, Y., Zheng, H., Chiew, F.H., Arancibia, J.P. and Zhou, X., 2016. Evaluating regional and global hydrological models against streamflow and

evapotranspiration measurements. *Journal of Hydrometeorology*, 17 (3), 995-1010.

#### 4.9 Supplementary materials





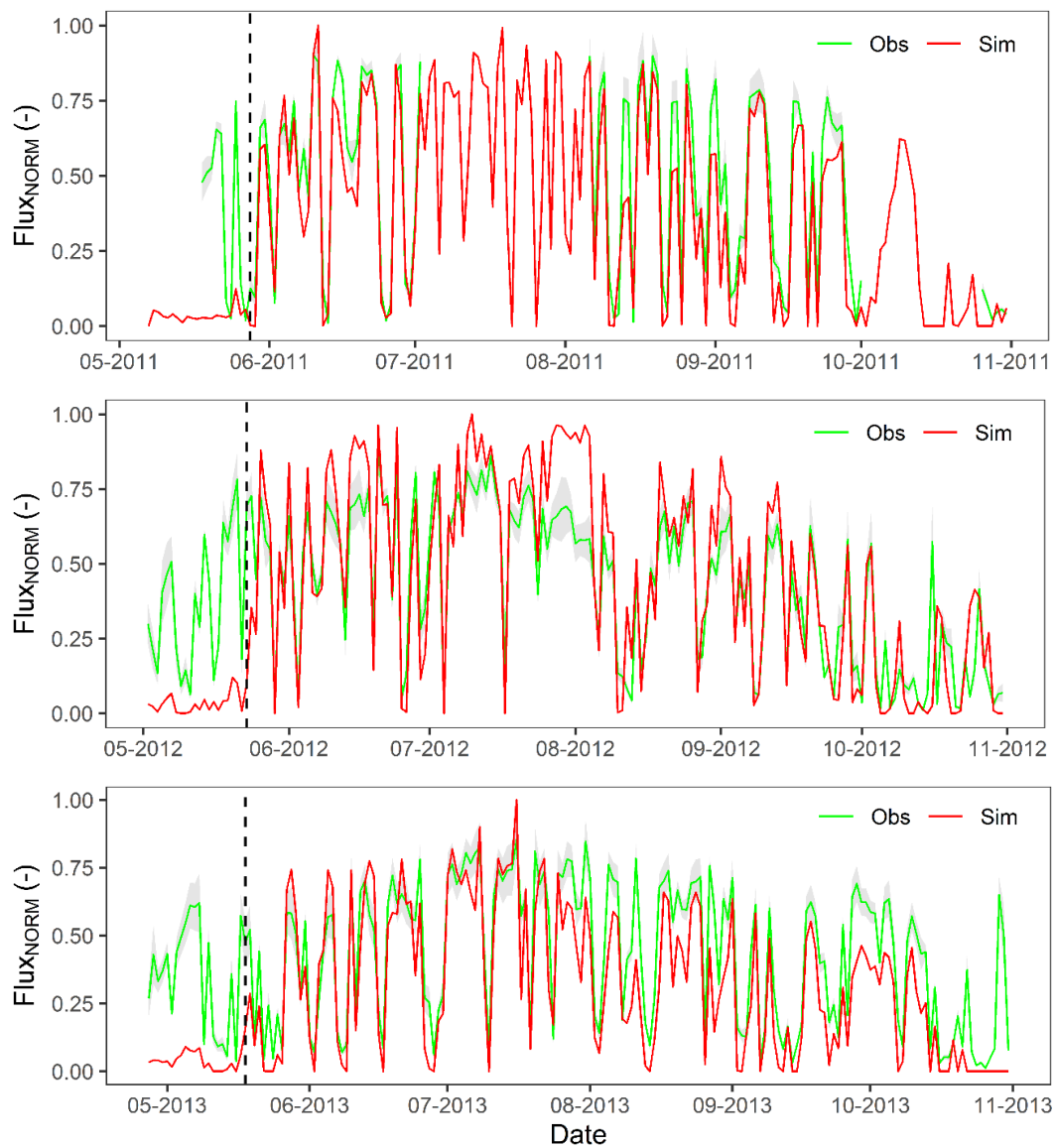


Figure 4S.1: Daily standardized modeled transpiration [-] and daily standardized sapflow velocity [-; mean  $\pm 1$  SE (grey zone) of six probes] at the balsam fir site from 2004 to 2013 (excluding 2007). The vertical dashed black line shows the beginning of the growing season as determined from dendrometers.

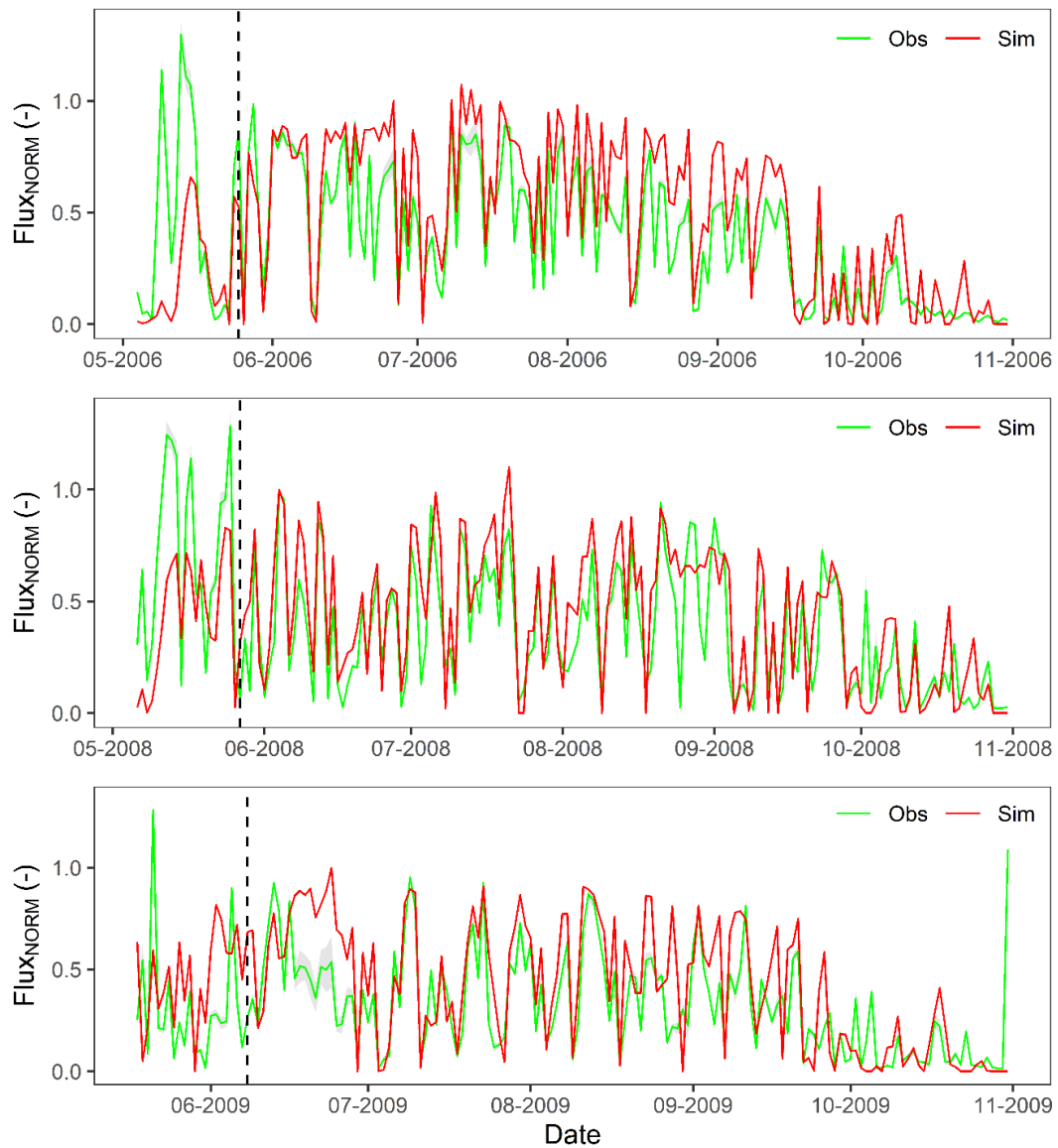


Figure 4S.2: Daily standardized modeled transpiration [-] and daily standardized sapflow velocity [-; mean  $\pm$  1 SE (grey zone) of six probes] at the black spruce site. The vertical dashed black line shows the beginning of the growing season as determined from dendrometers.

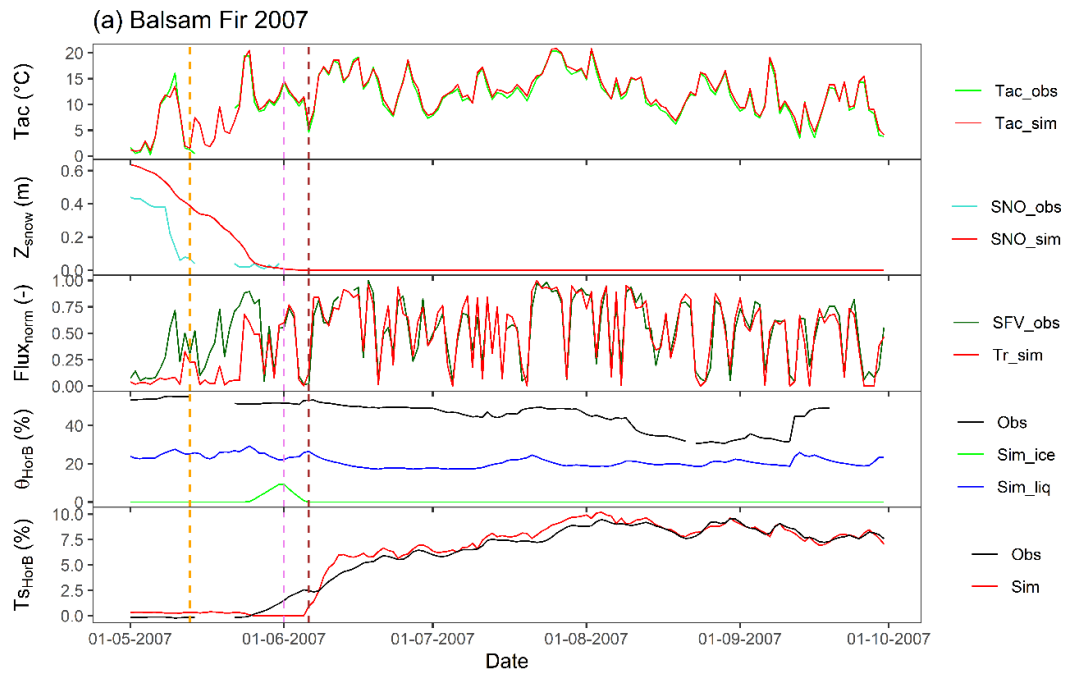


Figure 4S.3: Simulated and observed air temperature within the canopy ( $T_{ac}$  -  $^{\circ}\text{C}$ ; 1<sup>st</sup> panel); simulated and observed snow depth (m; 2<sup>nd</sup> panel); standardized modeled transpiration and standardized observed sapflow velocity (mean of six probes; 3<sup>rd</sup> panel); simulated (liquid and ice) and observed soil water content in the B horizon (%) (4<sup>th</sup> panel); and simulated and observed soil temperature in the B horizon ( $^{\circ}\text{C}$ ; bottom panel) at balsam fir in 2007. Vertical dashed lines are the beginning of the growing season (orange), the simulated end of the snowmelt period (purple), and the simulated end of frozen soil water (brown).

## CHAPITRE V

### GENERAL CONCLUSION

#### 5.1 Summary of findings

Rising air temperature and increasing drought occurrence in the past few decades across the globe have led to an increasing interest in investigating the land surface processes, their interactions with the atmosphere, and their impacts on future climate projections (Andrys et al., 2017; Bala et al., 2007; Brovkin, et al. 2009; Dickinson and Henderson-Sellers 1988; Laprise et al., 2013; Matthes et al., 2012; Swann et al., 2010). Transpiration is an important land surface process and the only component in the hydrological cycle that links soil-vegetation-atmosphere, via the transport of water from the soil, through the plant, to the atmosphere. Accurate projection of future precipitation and air temperature by climate models depends on the accurate simulation of transpiration by land surface schemes integrated within climate models. In addition to climatic variables (vapour pressure deficit, solar radiation, air temperature, and wind speed), land surface variables (soil water and soil temperature) also have an important impact on transpiration. Soil water has a direct impact while soil temperature has an indirect impact through its impact on liquid soil water, particularly in the boreal region. In my PhD research project I first studied the underlying land surface variables (soil water and soil temperature) in the Canadian Land Surface Scheme (CLASS), and then, the land surface process of transpiration in a natural system and in CLASS, focusing on the humid boreal forest of eastern Canada (Chapters II, III and IV). In the first part

of the study, the performance of CLASS is evaluated together with sensitivity analyses for the simulation of both soil water and soil temperature using long-term measured daily soil water and soil temperature (Chapter II). In the second part of the study, the environmental control on transpiration was investigated during multiple growing seasons including a drought period using long-term sap flow data measured at two forest sites (dominated by balsam fir and black spruce trees species each; Chapter III). In the third part of the study, the performance of the Canadian Land Surface Scheme (CLASS) for the simulation of transpiration was evaluated using these same long-term sap flow measurements (Chapter IV).

The novelty of my project is that I studied transpiration both in a natural system and in a Land Surface Scheme concurrently. Moreover, no studies have used long-term daily measurements of sap flow, soil water and soil temperature to validate the Canadian Land Surface Scheme. This is unique in that it permitted me to capture the effect of extreme but infrequent events that are projected to increase in the future. This is critical for testing the behaviour of the model, but has never previously been done. Besides, no previous study has investigated the environmental control on transpiration on balsam fir and black spruce tree species in the humid boreal forest of eastern Canada despite the critical importance of the boreal forest on the climate system.

#### 5.1.1 Performance and sensitivity analyses of CLASS for the simulation of soil water and soil temperature

In chapter II, CLASS was run for more than a decade in the two forest sites (1999 to 2016 at the balsam fir site and 1997 to 2016 at the black spruce site), and its performance in simulating both soil water and soil temperature was evaluated from 2001 to 2016 using daily measurements. In addition, several analyses were carried out to evaluate the sensitivity of modelled soil water and soil temperature to thickness of the organic layer (TOL), soil texture via percentage sand and percentage clay (PSPC),

drainage using a drainage parameter (DP), and freezing point (FP). Soil temperature was well simulated by CLASS. Though the performance of modelled soil water varied by site, season (an important underestimation was observed during winter) and soil horizons, the seasonal variations produced by the model closely matched observations. Thickness of the organic layer impacted both soil temperature and soil water, but up to a threshold thickness, beyond which the effect was negligible. Soil texture had no effect on soil temperature, but had a substantial effect on soil water. Decreasing drainage increased soil water (and even led to unrealistic saturated soil conditions) and consequently increased soil temperature due to the increasing incoming soil heat fluxes. Depressing the freezing point increased soil temperature throughout the year, but increased (liquid) soil water only during the winter. A depressed freezing point in soil is observed in many fine textured soils due to greater percentage of micropores and presence of particles (as impurities) in water. Our sensitivity analyses showed that CLASS can be calibrated to improve simulated soil water in all seasons, though this process might be more complex due to the extensive nature of land surface schemes compared to hydrological models. Improvements would however be relatively modest in their effect on results.

#### 5.1.2 Environmental drivers of transpiration in humid boreal region during growing season and a drought period

In chapter III, the impact of environmental variables on sap flow velocity (as a proxy of transpiration) was evaluated during multiple growing seasons (ten years for balsam fir: 2004 to 2013 and four years for black spruce: 2006 to 2009). Both vapour pressure deficit and solar radiation were found to be major drivers of transpiration during the growing season. During the measurement period, a short-term drought occurred at the balsam fir site in July 2012. Contrary to our expectation, soil water did not influence transpiration during this drought period as compared to dryer environments (da Silva Sallo et al., 2017). Instead vapour pressure deficit and solar radiation remained the

main drivers in this boreal region. This result could be due to the presence of a threshold soil water content, beyond which, the effect of the latter on transpiration becomes negligible. Our findings highlight that the broad generalisation that soil moisture is a limitation, based on research from dry environments, cannot be applied uniformly in other regions, in particular humid ones. Additionally, both of the tree species I studied exhibited diel hysteresis relationships between sap flow velocity and vapour pressure deficit/solar radiation in all growing seasons. Similar to the findings of other studies (O'Brien et al., 2004; Zeppel et al., 2004; Zheng et al., 2014), the diel hysteresis was clockwise and more pronounced with vapour pressure deficit and anticlockwise and less pronounced with solar radiation indicating the afternoon lag in VPD response (might be due to higher VPD or decreasing Rad in the afternoon) and the morning lag in Rad response (might be due to stem water capacitance or leaf wetness in the morning), respectively (O'Brien et al., 2004). However, Pappas et al. (2018) did not find a hysteresis relationship between sap flow and vapour pressure deficit in black spruce and suggested that this was due to the anisohydric behaviour of the species. However, our results showed strong hysteresis between sap flow and vapour pressure deficit for the black spruce despite it being anisohydric, and I thus conclude that there is an absence of a link between the magnitudes of diel hysteresis and the degree of iso/anisohydric properties of boreal tree species. The presence of a diel hysteresis relationship between sap flow and environmental variables (e.g. vapour pressure deficit, solar radiation) implies that the relationship between the two are not straightforward and thus that these environmental variables should not be used individually to model diurnal sap flow as this could lead to high uncertainties (Zheng et al., 2014).

### 5.1.3 Performance of CLASS for the simulation of transpiration during the rehydration period, the growing season and a drought period

In CLASS, transpiration is a function of specific humidity deficit, aerodynamic resistance and canopy resistance, the latter being further controlled by solar radiation,

vapour pressure deficit, soil moisture potential, and air temperature. In chapter IV, CLASS was run for more than a decade at the two forest sites (from 1999 to 2016 at the balsam fir site and from 1997 to 2016 at the black spruce site), the output was compared to observed values, based on the availability of measured sap flow data, from 2004 to 2013 at the balsam fir site and 2006 to 2009 at the black spruce site. This long-term measured sap flow data enabled me to evaluate the performance of CLASS over multiple growing seasons as well as during the July 2012 drought. The temporal variation in transpiration was well represented by CLASS during the multiple growing seasons. However, modelled transpiration was greatly underestimated during the rehydration period (prior to the growing season) and overestimated during the drought. During the rehydration period, this underestimated modelled transpiration was caused by overestimated modelled snow cover depth and duration. On the other hand, during the short-term drought in July 2012 and a simulated long-term drought, modelled transpiration did not decrease gradually with decreasing soil water, it ceased only when soil water reached an unrealistic threshold value of 0.04 that is the default value used in CLASS. In addition, a high transpiration rate was maintained in CLASS compared to observations during the heat stress period in 2006. The overall results showed that CLASS did not reproduce the eco-physiological behavior of trees during extreme events. The prolonged presence of snow on the ground and delayed snowmelt modelled by CLASS delayed the beginning of modelled transpiration compared to observations. This result highlights that CLASS needs to model adequately both, snow cover and timing of snowmelt, in order to accurately simulate transpiration during the rehydration period. Furthermore, the relation between transpiration and soil water in the model need to be redefined as modelled transpiration at present is insensitive to decreasing soil water. Despite very low soil water content, optimum transpiration is maintained in CLASS which does not allow the correct representation of water stress conditions. These shortcomings of CLASS will have a direct impact on climate models due to its feedback on precipitation. Though the underestimation of transpiration during

rehydration period might not be significant to the climate system, the overestimation of transpiration during drought will have important impact on the climate system, resulting in overestimation of precipitation and cooling of the atmospheric air temperature in climate model projections and consequently in an underestimation of drought severity.

## 5.2 Limitations and future works

Several limitations were encountered in both field measurements and the land surface scheme CLASS. In the field measurements, the sample size and sapwood depth (or sapwood area) greatly restricted the possibilities in our analyses to quantitatively assess CLASS transpiration values. Default and fixed values in CLASS and documentation of these parameters and their choice also limited my exploration, as some of these were not apparent (i.e. for sensitivity analyses) and were only uncovered at the end of the project.

### 5.2.1 Field measurement limitations

#### 5.2.1.1 Representativeness of number of sampled trees

A limitation of the study is the measurement of only three trees per species. Normally, 5-10 trees are used to scale up from the tree to the stand level (Granier et al., 1996). While measurement of 3 trees is low, other studies also have used fewer than 4 trees (O'Brien et al., 2004; Bovard et al., 2005; Wang et al., 2005). However, the number of sampled trees depends hugely on stand structure, such as the distribution of tree species, tree size, tree social position (dominant, co-dominant, intermediate, and suppressed trees), and soil properties (Köstner et al., 1998). Due to the small number of measured trees, we could not up-scale to quantify stand transpiration. Besides comparing

modelled transpiration with stand transpiration, the latter could have been used to verify the water balance of the watershed at both sites given that watershed discharge data were available. However, as I wanted to make the most of these long-term sap flow measurement data, the study was thus limited to individual tree transpiration only. Nevertheless, in the future, measurements of more than five trees per stand (depending on the stand structure) at multiple study sites would permit not only validation of the generalisability of our results but also permit results to be up-scaled to the stand scale.

#### 5.2.1.2 Use of tree transpiration vs sap flow velocity

Despite the long-term measurements of sap flow velocity, which was the strength of this study, the absence of sapwood area (or depth of sapwood) measurements of the two studied species over the measurement years unfortunately meant that our sap flow velocity data could not be converted into tree transpiration. This limited our work in evaluating the CLASS modelled transpiration with absolute measured transpiration which would have yielded a stronger assessment of CLASS. Quantitative LSS transpiration fluxes have often been compared to observations from flux towers in the past rather than to sap flow data. However, by standardizing both our modelled transpiration and sap flow velocity by dividing with the maximum value obtained during the growing period of each year, this enabled us to evaluate the underestimation of modelled transpiration during the rehydration period and the optimum transpiration modelled during the July 2012 drought. In future, I recommend carrying concurrent measurements of sapwood depth and tree diameter at breast height (DBH) for these two species across different tree sizes and ages, in order to build a relationship between sapwood depth and DBH. This new empirical equation will enable the determination of sapwood depth based on DBH data only and thus will avoid the need to perforate holes in stems of trees every year. However, if no relationship is found between sapwood depth and DBH for the two tree species, more efficient techniques (e.g. SF3 probes; East 30 sensors, 2021) could be used that measure the sap flow radially (i.e. at

different depths in the xylem) and that determine tree transpiration directly from the measurements.

## 5.2.2 Shortcomings of CLASS

### 5.2.2.1 Modelled transpiration insensitivity to decreasing soil water content

During the July 2012 drought, observed transpiration decreased with decreasing soil water in the second half of the month, however modelled transpiration was maintained throughout this period. The sensitivity of CLASS was tested by simulating an artificial drought of more than one year (zero precipitation). The modelled transpiration did not decrease gradually with soil water, but instead ceased completely when soil water reached about 4 %, which is the residual soil liquid water remaining after freezing or evaporation in the model. In CLASS, this residual soil water has been fixed for the mineral soil layer, whereas in reality, it changes with soil texture, structure and soil depth. Moreover, transpiration declines gradually from field capacity to permanent wilting (Granier et al., 2000). Thus, to improve model sensitivity to decreasing soil water content in order to better simulate drought events in future, I recommend improving the soil moisture suction function in CLASS in order to increase the sensitivity of transpiration to decreasing soil water. Currently, the soil moisture suction function depends on the actual soil moisture suction and two vegetation parameters. I suggest improving this equation by incorporating the actual soil moisture suction and the soil moisture suction at permanent wilting point. Also, I recommend varying the residual soil water as a function of percentage clay as the latter mainly controls the amount of hygroscopic water in the soil (Wuddivira et al., 2012).

### 5.2.2.2 Snow cover depth and duration are overestimated

At present, CLASS overestimates snow depth and its duration. The prolonged presence of snow on the ground in spring delays the beginning of transpiration during the rehydration period. Although this was not under the scope of our study, this would have

strong impact in hydrological studies because snowmelt is also strongly delayed. CLASS was found to have high snow albedo, leading to very high upward shortwave radiation (Malik et al., 2014), which subsequently preserves the snowpack longer on the ground. At present, the snow albedo refreshment threshold set in CLASS is 0.1 mm (Verseghy, 2012). Whenever snowfall on snowpack is equal to or greater than 0.1 mm in a given time step, snow albedo is reset to the fresh snow albedo value (i.e. 0.84). Thus, I recommend increasing the snow albedo refreshment threshold in order to reduce the snow albedo.

#### 5.2.2.3 Soil porosity

The soil porosity in CLASS is a function of percentage sand only, based on an empirical relationship (Cosby et al., 1984). In reality, soil porosity is a function of soil texture (percentage sand, silt, clay and organic matter), soil structure and degree of compaction with soil depth. My work shows that CLASS could be improved further by modifying the porosity equation by adding percentage clay, organic matter and degree of compaction in order to have more realistic soil porosity values. I propose adding a new set of measurements in the future: soil porosity and soil texture (% sand, % clay and % organic matter) at different soil depths and at multiple sites in order to build a new equation that relates soil porosity with soil texture and soil depth. The addition of soil depth in the same equation is crucial in order to incorporate the effect of increasing soil compaction with soil depth on the soil porosity.

### 5.3 Concluding remarks

This PhD project has led to the in-depth investigation of the environmental control on transpiration in both field measured data and the Canadian Land Surface Scheme. This

study enables us to understand the main variables that drive transpiration in this humid boreal forest, and the mathematical representation of the transpiration process together with soil water and soil temperature land surface variables in the Canadian Land Surface Scheme. By assessing CLASS' performance to reproduce observed responses and through sensitivity analyses, I identified drawbacks inherent in the model and proposed solutions for improving the model. Currently, CLASS needs to improve its simulation of transpiration during both tree rehydration and drought, and its representation of both soil water and soil temperature during winter. I have made recommendations for all the identified model limitations in order to improve model output. These suggested improvements will permit CLASS to better simulate the effect of extreme events such as drought, especially in the boreal forest, and thus ultimately better model the extreme events projections in the future when coupled with the Canadian Regional Climate model.

#### 5.4 References

- Andrys, J., Kala, J. and Lyons, T.J., 2017. Regional climate projections of mean and extreme climate for the southwest of Western Australia (1970–1999 compared to 2030–2059). *Climate Dynamics*, 48(5-6), pp.1723-1747.
- Bala, G., Caldeira, K., Wickett, M., Phillips, T.J., Lobell, D.B., Delire, C. and Mirin, A., 2007. Combined climate and carbon-cycle effects of large-scale deforestation. *Proceedings of the National Academy of Sciences*, 104(16), pp.6550-6555.
- Bovard, B.D., Curtis, P.S., Vogel, C.S., Su, H.B. and Schmid, H.P., 2005. Environmental controls on sap flow in a northern hardwood forest. *Tree physiology*, 25(1), pp.31-38.
- Brovkin, V., Raddatz, T., Reick, C.H., Claussen, M. and Gayler, V., 2009. Global biogeophysical interactions between forest and climate. *Geophysical research letters*, 36(7).

- Cosby, B.J., Hornberger, G.M., Clapp, R.B. and Ginn, T., 1984. A statistical exploration of the relationships of soil moisture characteristics to the physical properties of soils. *Water resources research*, 20(6), pp.682-690.
- da Silva Sallo, F., Sanches, L., de Moraes Dias, V.R., da Silva Palácios, R., de Souza Nogueira, J., 2017. Stem water storage dynamics of *Vochysia divergens* in a seasonally flooded environment. *Agric. For. Meteorol.* 232, 566–575.
- Dickinson, R.E. and Henderson-Sellers, A., 1988. Modelling tropical deforestation: A study of GCM land-surface parametrizations. *Quarterly Journal of the Royal Meteorological Society*, 114(480), pp.439-462.
- East 30 sensors, 2021. East 30 Sapflow sensors. Available at <[Sap Flow Sensors \(east30sensors.com\)](http://Sap Flow Sensors (east30sensors.com))> [Accessed 12 February 2021].
- Granier, A., Biron, P., Breda, N., Pontailleur, J.Y. and Saugier, B., 1996. Transpiration of trees and forest stands: Short and long-term monitoring using sapflow methods. *Global Change Biology*, 2(3), pp.265-274.
- Granier, A., Loustau, D. and Bréda, N., 2000. A generic model of forest canopy conductance dependent on climate, soil water availability and leaf area index. *Annals of forest science*, 57(8), pp.755-765.
- Köstner, B., Granier, A. and Cermák, J., 1998. Sapflow measurements in forest stands: methods and uncertainties. In *Annales des sciences forestières* (Vol. 55, No. 1-2, pp. 13-27). EDP Sciences.
- Laprise, R., Hernández-Díaz, L., Tete, K., Sushama, L., Šeparović, L., Martynov, A., Winger, K. and Valin, M., 2013. Climate projections over CORDEX Africa domain using the fifth-generation Canadian Regional Climate Model (CRCM5). *Climate Dynamics*, 41(11), pp.3219-3246.
- Malik, M.J., van der Velde, R., Vekerdy, Z. and Su, Z., 2014. Improving modeled snow albedo estimates during the spring melt season. *Journal of geophysical research: Atmospheres*, 119(12), pp.7311-7331.
- Matthes, H., Rinke, A., Miller, P.A., Kuhry, P., Dethloff, K. and Wolf, A., 2012. Sensitivity of high-resolution Arctic regional climate model projections to different implementations of land surface processes. *Climatic Change*, 111(2), pp.197-214.
- O'Brien, J.J., Oberbauer, S.F., Clark, D.B., 2004. Whole tree xylem sap flow responses to multiple environmental variables in a wet tropical forest. *Plant Cell Environ.* 27 (5), 551–567.
- Pappas, C., Matheny, A.M., Baltzer, J.L., Barr, A.G., Black, T.A., Bohrer, G., Detto, M., Maillet, J., Roy, A., Sonnentag, O., 2018. Boreal tree hydrodynamics: asynchronous, diverging, yet complementary. *Tree Physiol.* 38 (7), 953–964.

- Swann, A.L., Fung, I.Y., Levis, S., Bonan, G.B. and Doney, S.C., 2010. Changes in Arctic vegetation amplify high-latitude warming through the greenhouse effect. *Proceedings of the National Academy of Sciences*, 107(4), pp.1295-1300.
- Verseghy, Diana, 2012. CLASS–The Canadian land surface scheme (version 3.6). *Environment Canada Science and Technology Branch Tech. Rep.*
- Wang, K.-Y., Kellomäki, S., Zha, T., & Peltola, H., 2005. Annual and seasonal variation of sap flow and conductance of pine trees grown in elevated carbon dioxide and temperature. *Journal of Experimental Botany*, 56(409), 155-165.
- Wuddivira, M.N., Robinson, D.A., Lebron, I., Bréchet, L., Atwell, M., De Caires, S., Oatham, M., Jones, S.B., Abdu, H., Verma, A.K. and Tuller, M., 2012. Estimation of soil clay content from hygroscopic water content measurements. *Soil Science Society of America Journal*, 76(5), pp.1529-1535.
- Zeppel, M.J., Murray, B.R., Barton, C., Eamus, D., 2004. Seasonal responses of xylem sap velocity to VPD and solar radiation during drought in a stand of native trees in temperate Australia. *Funct. Plant Biol.* 31 (5), 461–470.
- Zheng, H., Wang, Q., Zhu, X., Li, Y., Yu, G., 2014. Hysteresis responses of evapotranspiration to meteorological factors at a diel timescale: patterns and causes. *PLoS ONE* 9 (6), e98857.

APPENDIX A

CLASS INITIALISATION PARAMETERS

Table A.1: Initialisation parameters for CLASS simulation at balsam fir site

DegLat	DegLon	RefHeight momentum	RefHeight heat	Blending height	Land/sea cover	Num grid	Num mosaic		
47.33	288.87	14	14	14	-1	1	1		
PFT1: needle leaf; PFT2: broadleaf; PFT3: crops; PFT4: grass; PFT5: urban									
1	2	3	4	5	1	2	3	4	
Fractional coverage of PFTs (FCAN)					Max. leaf area index (PAMX)				
0.999	0	0	0	0	2	0	0	0	
Log of roughness length (LNZO)					Min. leaf area index (PAMN)				
0.438	0	0	0	0	1.6	0	0	0	
Visible albedo (ALVC)					Above-ground canopy mass (CMAS)				
0.03	0	0	0	0	18.5	0	0	0	
Near-infrared albedo (ALIC)					Rooting depth (m)				
0.19	0	0	0	0	0.98	0	0	0	
Minimum stomatal resistance (RSMN)					Ref. value for SW radiation (QA50)				
200	0	0	0	0	30	0	0	0	
Vapour pressure deficit coefficients									
VPDA					VPDB				
0.65	0	0	0	0	1.05	0	0	0	
Soil moisture suction coefficients									
PSGA					PSGB				
100	0	0	0	0	5	0	0	0	
Drainage	Soil permea ble depth	Fractional coverage of mosaic							
1	1	1							
Soil layers:									
1	2	3							
% SAND									
-2.0	69.80	83							
% CLAY									
0	5.5	4.1							
% ORGM									

2	3.2	0.5						
Temperature of Soil layers			Veg Canopy temp.	Snow temp.	Ponded water temp.			
TBAR1	TBAR2	TBAR3	TCAN	TSNO	TPND			
14.65	11.03	7.98	15.58	0	0			
Liquid water in soil layers			Frozen water in soil layers			Depth Ponded water		
THLQ1	THLQ2	THLQ3	THIC1	THIC2	THIC3	ZPND		
0.385	0.258	0.252	0	0	0	0		
Canopy water	Canopy snow	Ground snow	Snow albedo	Snow density	Plant growth index			
0	0	0	0	0	1			
Soil thickness (m)	Soil depth (m)							
0.17	0.17							
0.3	0.47							
0.6	1.07							
0.93	2							
1	3							
1	4							
1	5							
1	6							
1	7							
1	8							
1	9							
1	10							
1	11							
1	12							
1	13							
1	14							
1	15							
5	20							
5	25							
5	30							
5	35							
5	40							
5	45							
5	50							
5	55							
5	60							
Half-hourly output		Daily output						
From day	To day	From day	To day					
1	366	1	366					

From year	To year	From year	To year					
1999	2017	1999	2017					

Table A.2: Initialisation parameters for CLASS simulation at black spruce site

DegLat	DegLon	RefHeight momentum	RefHeight heat	Blending height	Land/sea cover	Num grid	Num mosaic	
49.21	286.35	14	14	14	-1	1	1	
PFT1: needle leaf; PFT2: broadleaf; PFT3: crops; PFT4: grass; PFT5: urban								
1	2	3	4	5	1	2	3	4
Fractional coverage of PFTs (FCAN)					Max. leaf area index (PAMX)			
0.999	0	0	0	0	2	0	0	0
Log of roughness length (LNZO)					Min. leaf area index (PAMN)			
0.182	0	0	0	0	1.6	0	0	0
Visible albedo (ALVC)					Above-ground canopy masss (CMAS)			
0.03	0	0	0	0	14.6	0	0	0
Near-infrared albedo (ALIC)					Rooting depth (m)			
0.19	0	0	0	0	0.65	0	0	0
Minimum stomatal resistance (RSMN)					Ref. value for SW radiation (QA50)			
200	0	0	0	0	30	0	0	0
Vapour pressure deficit coefficients								
VPDA					VPDB			
0.65	0	0	0	0	1.05	0	0	0
Soil moisture suction coefficients								
PSGA					PSGB			
100	0	0	0	0	5	0	0	0
Drainage	Soil permeable depth	Fractional coverage of mosaic						
1	1	1						
Soil layers:								
1	2	3						
% SAND								
-2.0	86.9	89						
% CLAY								
0	2	0.8						
% ORGM								
2	1.7	0.3						
Temperature of Soil layers			Veg Canopy temp.	Snow temp.	Ponded water temp.			
TBAR1	TBAR2	TBAR3	TCAN	TSNO	TPND			
16.34	15.69	9.72	15.54	0	0			

Liquid water in soil layers			Frozen water in soil layers			Depth Poned water		
THLQ1	THLQ2	THLQ3	THIC1	THIC2	THIC3	ZPND		
0.240	0.246	0.029	0	0	0	0		
Canopy water	Canopy snow	Ground snow	Snow albedo	Snow density	Plant growth index			
0	0	0	0	0	1			
Soil thickness (m)	Soil depth (m)							
0.13	0.13							
0.3	0.43							
0.6	1.03							
0.97	2							
1	3							
1	4							
1	5							
1	6							
1	7							
1	8							
1	9							
1	10							
1	11							
1	12							
1	13							
1	14							
3	17							
3	20							
5	25							
5	30							
5	35							
5	40							
5	45							
5	50							
5	55							
5	60							
Half-hourly output		Daily output						
From day	To day	From day	To day					
1	366	1	366					
From year	To year	From year	To year					
1997	2017	1997	2017					

## BIBLIOGRAPHY

- Allen, C. D., A. K. Macalady, H. Chenchouni, D. Bachelet, N. McDowell, M. Vennetier, T. Kitzberger, A. Rigling, D. D. Breshears, E. H. Hogg, P. Gonzalez, R. Fensham, Z. Zhang, J. Castro, N. Demidova, J.-H. Lim, G. Allard, S. W. Running, A. Semerci and N. Cobb, 2010. "A global overview of drought and heat induced tree mortality reveals emerging climate change risks for forests." *Forest Ecology and Management* 259(4): 660-684.
- Andrys, J., Kala, J. and Lyons, T.J., 2017. Regional climate projections of mean and extreme climate for the southwest of Western Australia (1970–1999 compared to 2030–2059). *Climate Dynamics*, 48(5-6), pp.1723-1747.
- Arora, V.K., 2003. Simulating energy and carbon fluxes over winter wheat using coupled land surface and terrestrial ecosystem models. *Agricultural and Forest Meteorology*, 118(1-2), pp.21-47.
- Bala, G., Caldeira, K., Wickett, M., Phillips, T., Lobell, D., Delire, C. and Mirin, A., 2007. Combined climate and carbon-cycle effects of large-scale deforestation. *Proceedings of the National Academy of Sciences*, 104 (16), 6550-6555.
- Baldocchi, D.D., Xu, L. and Kiang, N., 2004. How plant functional-type, weather, seasonal drought, and soil physical properties alter water and energy fluxes of an oak–grass savanna and an annual grassland. *Agricultural and Forest Meteorology*, 123 (1-2), 13-39.
- Bartlett, P.A., MacKay, M.D. and Verseghy, D.L., 2006. Modified snow algorithms in the Canadian land surface scheme: Model runs and sensitivity analysis at three boreal forest stands. *Atmosphere-Ocean*, 44(3), pp.207-222.
- Bartlett, P.A., McCaughey, J.H., Lafleur, P.M. and Verseghy, D.L. 2003. Modelling evapotranspiration at three boreal forest stands using the CLASS: tests of parameterizations for canopy conductance and soil evaporation. *International Journal of Climatology*, 23 (4), 427-451.
- Bellisario, L.M., Boudreau, L.D., Verseghy, D.L., Rouse, W.R. and Blanken, P.D., 2000. Comparing the performance of the Canadian land surface scheme (class) for two subarctic terrain types. *Atmosphere-Ocean*, 38 (1), 181-204.

- Best, M.J., Pryor, M., Clark, D.B., Rooney, G.G., Essery, R.L.H., Ménard, C.B., Edwards, J.M., Hendry, M.A., Porson, A., Gedney, N. and Mercado, L.M., 2011. The Joint UK Land Environment Simulator (JULES), model description– Part 1: energy and water fluxes. *Geoscientific Model Development*, 4(1), pp.677-699.
- Betts, R.A., 2000. Offset of the potential carbon sink from boreal forestation by decreases in surface albedo. *Nature*, 408(6809), pp.187-190.
- Bonan, G. B., & Shugart, H. H., 1989. Environmental Factors and Ecological Processes in Boreal Forests. *Annual Review of Ecology and Systematics*, 20, 1-28.
- Bonan, G. B., 2008. Forests and Climate Change: Forcings, Feedbacks, and the Climate Benefits of Forests. *Science*, 320(5882), 1444-1449.
- Bovard, B. D., Curtis, P. S., Vogel, C. S., Su, H. B., & Schmid, H. P., 2005. Environmental controls on sap flow in a northern hardwood forest. *Tree Physiology*, 25(1), 31-38. doi: 10.1093/treephys/25.1.31
- Brandt, J., Flannigan, M., Maynard, D., Thompson, I., & Volney, W., 2013. An introduction to Canada's boreal zone: ecosystem processes, health, sustainability, and environmental issues. *Environmental Reviews*, 21(4), 207-226.
- Brochu, R. and Laprise, R., 2007. Surface water and energy budgets over the Mississippi and Columbia river basins as simulated by two generations of the Canadian Regional Climate Model. *Atmosphere-ocean*, 45(1), pp.19-35.
- Brovkin, V., Raddatz, T., Reick, C.H., Claussen, M. and Gayler, V., 2009. Global biogeophysical interactions between forest and climate. *Geophysical Research Letters*, 36(7).
- Brutsaert, W., 1975. On a derivable formula for long-wave radiation from clear skies. *Water Resour. Res.*, 11(5), 742-744.
- Burgess, S.S.O. and Bleby, T.M., 2006. Redistribution of soil water by lateral roots mediated by stem tissues. *Journal of Experimental Botany*, 57(12), pp.3283-3291.
- Bussièrè, F. and Cellier, P., 1994. Modification of the soil temperature and water content regimes by a crop residue mulch: experiment and modelling. *Agricultural and Forest Meteorology*, 68 (1), 1-28.
- Campbell, G.S. and Norman, J.M., 2012. *An introduction to environmental biophysics*. Springer Science & Business Media.
- Cavender-Bares, J., Sack, L., & Savage, J., 2007. Atmospheric and soil drought reduce nocturnal conductance in live oaks. *Tree Physiol*, 27(4), 611-620.

- Chang, X., Zhao, W., & He, Z., 2014. Radial pattern of sap flow and response to microclimate and soil moisture in Qinghai spruce (*Picea crassifolia*) in the upper Heihe River Basin of arid northwestern China. *Agricultural and Forest Meteorology*, 187, 14-21.
- Chapin iii, F. S., McGuire, A. D., Randerson, J., Pielke Sr, R., Baldocchi, D., Hobbie, S. E., Roulet N., Eugster W., Kasischke E., Rastetter E.B., Zimov S.A., Running, S. W., 2000. Arctic and boreal ecosystems of western North America as components of the climate system. *Global Change Biology*, 6(SUPPLEMENT 1), 211-223. doi: 10.1046/j.1365-2486.2000.06022.x
- Chen, J., Chen, B., Black, T.A., Innes, J.L., Wang, G., Kiely, G., Hirano, T., and Wohlfahrt, G., 2013. Comparison of terrestrial evapotranspiration estimates using the mass transfer and Penman-Monteith equations in land surface models. *Journal of Geophysical Research: Biogeosciences*, 118 (4), 1715-1731.
- Chen, L., Zhang, Z., Li, Z., Tang, J., Caldwell, P., & Zhang, W., 2011. Biophysical control of whole tree transpiration under an urban environment in Northern China. *Journal of Hydrology*, 402(3-4), 388-400. <https://doi.org/10.1016/j.jhydrol.2011.03.034>
- Choudhury, B.J. and DiGirolamo, N.E., 1998. A biophysical process-based estimate of global land surface evaporation using satellite and ancillary data I. Model description and comparison with observations. *Journal of Hydrology*, 205 (3-4), 164-185.
- Choudhury, B.J., DiGirolamo, N.E., Susskind, J., Darnell, W.L., Gupta, S.K. and Asrar, G., 1998. A biophysical process-based estimate of global land surface evaporation using satellite and ancillary data II. Regional and global patterns of seasonal and annual variations. *Journal of Hydrology*, 205 (3-4), 186-204.
- Clapp, R.B. and Hornberger, G.M., 1978. Empirical equations for some soil hydraulic properties. *Water Resour. Res.*, 14, 601-604.
- Collatz GJ, Ball JT, Grivet C, Berry JA. 1991. Physiological and environmental regulation of stomatal conductance, photosynthesis and transpiration: a model that includes a laminar boundary layer. *Agricultural and Forest Meteorology* 54: 107-136.
- Collins, A. R., Burton, A. J., & Cavaleri, M. A., 2018. Effects of Experimental Soil Warming and Water Addition on the Transpiration of Mature Sugar Maple. *Ecosystems*, 21(1), 98-111. doi: 10.1007/s10021-017-0137-9
- Cook, B.I., Bonan, G.B. and Levis, S., 2006. Soil moisture feedbacks to precipitation in southern Africa. *Journal of Climate*, 19 (17), 4198-4206.

- Cosby, B.J., Hornberger, G.M., Clapp, R.B. and Ginn, T., 1984. A statistical exploration of the relationships of soil moisture characteristics to the physical properties of soils. *Water resources research*, 20(6), pp.682-690.
- Cosgrove, B. A., Lohmann, D., Mitchell, K. E., Houser, P. R., Wood, E. F., Schaake, J. C., Robock, A., Sheffield, J., Duan, Q., Luo, L., Wayne Higgins R.W., Pinker, R.T., Tarpley, J. D., 2003. Land surface model spin-up behavior in the North American Land Data Assimilation System (NLDAS). *Journal of Geophysical Research: Atmospheres*, 108(D22).
- D'Orangeville, L., Côté, B., Houle, D., & Morin, H., 2013. The effects of throughfall exclusion on xylogenesis of balsam fir. *Tree Physiology*, 33(5), 516-526.
- D'Orangeville, L., Duchesne, L., Houle, D., Kneeshaw, D., Côté, B. and Pederson, N., 2016. Northeastern North America as a potential refugium for boreal forests in a warming climate. *Science*, 352(6292), pp.1452-1455.
- D'Orangeville, L., Maxwell, J., Kneeshaw, D., Pederson, N., Duchesne, L., Logan, T., Houle, D., Arseneault, D., Beier, C.M., Bishop, D.A. and Druckenbrod, D., 2018. Drought timing and local climate determine the sensitivity of eastern temperate forests to drought. *Global change biology*, 24(6), pp.2339-2351.
- da Silva Sallo, F., Sanches, L., de Morais Dias, V. R., da Silva Palácios, R., & de Souza Nogueira, J., 2017. Stem water storage dynamics of *Vochysia divergens* in a seasonally flooded environment. *Agricultural and Forest Meteorology*, 232, 566-575.
- Dai, A., 2011. Characteristics and trends in various forms of the Palmer Drought Severity Index during 1900–2008. *Journal of Geophysical Research: Atmospheres*, 116(D12).
- Daley, M. J., & Phillips, N. G., 2006. Interspecific variation in nighttime transpiration and stomatal conductance in a mixed New England deciduous forest. *Tree Physiol*, 26(4), 411-419.
- Dashtseren, A., Ishikawa, M., Iijima, Y. and Jambaljav, Y., 2014. Temperature Regimes of the Active Layer and Seasonally Frozen Ground under a Forest-Steppe Mosaic, Mongolia. *Permafrost and Periglacial Processes*, 25 (4), 295-306.
- De Kauwe, M.G., Zhou, S., Medlyn, B.E., Pitman, A.J., Wang, Y., Duursma, R.A. and Prentice, I.C., 2015. Do land surface models need to include differential plant species responses to drought? Examining model predictions across a mesic-xeric gradient in Europe.
- Delage, Yves, Lei Wen, and Jean-Marc Bélanger, 1999. Aggregation of parameters for the land surface model CLASS." *Atmosphere-Ocean* 37.2: 157-178.

- Delpierre, N., Lireux, S., Hartig, F., Camarero, J.J., Cheaib, A., Čufar, K., Cuny, H., Deslauriers, A., Fonti, P., Gričar, J. and Huang, J.G., 2019. Chilling and forcing temperatures interact to predict the onset of wood formation in Northern Hemisphere conifers. *Global change biology*, 25(3), pp.1089-1105.
- Delzon, S. and Loustau, D., 2005. Age-related decline in stand water use: sap flow and transpiration in a pine forest chronosequence. *Agricultural and Forest Meteorology*, 129(3-4), pp.105-119.
- Dickinson, R. E., A. Henderson-Sellers, P. J. Kennedy, M.F. Wilson., 1986. Biosphere-atmosphere transfer scheme (BATS) for the NCAR community climate model Tech Note/TN-275+STR. Nat. Cent. for Atmos.Res., Boulder, Colo.
- Dickinson, R.E. and Henderson-Sellers, A., 1988. Modelling tropical deforestation: A study of GCM land-surface parametrizations. *Quarterly Journal of the Royal Meteorological Society*, 114(480), pp.439-462.
- Dirmeyer, P.A., Gao, X., Zhao, M., Guo, Z., Oki, T. and Hanasaki, N., 2005. The second Global Soil Wetness Project (GSWP-2): Multi-model analysis and implications for our perception of the land surface. *Bull. Amer. Meteor. Soc.*
- Duchesne, L. and D. Houle, 2006. Base cation cycling in a pristine watershed of the Canadian boreal forest. *Biogeochemistry* 78(2): 195-216.
- Duchesne, L., & Houle, D., 2011. Modelling day-to-day stem diameter variation and annual growth of balsam fir (*Abies balsamea* (L.) Mill.) from daily climate. *Forest Ecology and Management*, 262(5), 863-872. doi: <https://doi.org/10.1016/j.foreco.2011.05.027>
- Duchesne, L., Houle, D. and D'Orangeville, L., 2012. Influence of climate on seasonal patterns of stem increment of balsam fir in a boreal forest of Québec, Canada. *Agricultural and forest meteorology*, 162, pp.108-114.
- Dumedah, G., Berg, A.A. and Wineberg, M., 2011. An integrated framework for a joint assimilation of brightness temperature and soil moisture using the nondominated sorting genetic algorithm II. *Journal of hydrometeorology*, 12 (6), 1596-1609.
- Dutrieux, P., 2016. Évaluation de simulations du Modèle Régional Canadien du Climat (MRCC5) au-dessus de l'Atlantique Nord. Maîtrise, Université du Québec à Montréal.
- East 30 sensors, 2021. East 30 Sapflow sensors. Available at <[Sap Flow Sensors \(east30sensors.com\)](http://SapFlowSensors.com)> [Accessed 12 February 2021].
- Ewers, B., Mackay, D., Gower, S., Ahl, D., Burrows, S. and Samanta, S., 2002. Tree species effects on stand transpiration in northern Wisconsin. *Water resources research*, 38 (7), 8-1-8-11.

- Ewers, B.E., Gower, S.T., Bond-Lamberty, B. and Wang, C.K., 2005. Effects of stand age and tree species on canopy transpiration and average stomatal conductance of boreal forests. *Plant, Cell & Environment*, 28(5), pp.660-678.
- Ford, C. R., Goranson, C. E., Mitchell, R. J., Will, R. E., & Teskey, R. O., 2004. Diurnal and seasonal variability in the radial distribution of sap flow: predicting total stem flow in *Pinus taeda* trees. *Tree Physiology*, 24(9), 951-960.
- Forster, M.A., 2014. How significant is nocturnal sap flow?. *Tree physiology*, 34(7), pp.757-765.
- Fukui, K., Sone, T., Yamagata, K., Otsuki, Y., Sawada, Y., Vetrova, V. and Vyatkina, M., 2008. Relationships between permafrost distribution and surface organic layers near Esso, central Kamchatka, Russian Far East. *Permafrost and Periglacial Processes*, 19 (1), 85-92.
- Garratt, J.R., 1993. Sensitivity of Climate Simulations to Land-Surface and Atmospheric Boundary-Layer Treatments-A Review. *Journal of Climate*, 6 (3), 419-448.
- Gartner, K., Nadezhdina, N., Englisch, M., Čermak, J. and Leitgeb, E., 2009. Sap flow of birch and Norway spruce during the European heat and drought in summer 2003. *Forest Ecology and Management*, 258(5), pp.590-599.
- Gayler, S., Ingwersen, J., Priesack, E., Wöhling, T., Wulfmeyer, V. and Streck, T., 2013. Assessing the relevance of subsurface processes for the simulation of evapotranspiration and soil moisture dynamics with CLM3. 5: comparison with field data and crop model simulations. *Environmental earth sciences*, 69 (2), 415-427.
- Geßler, A., Keitel, C., Nahm, M. and Rennenberg, H., 2004. Water shortage affects the water and nitrogen balance in central European beech forests. *Plant Biology*, 6(3), pp.289-298.
- Gold, L.W., 1963. Influence of snow cover on the average annual ground temperature at Ottawa, Canada. *International Association Scientific Hydrology*, 61 (82-91).
- Goldstein, G., J. L. Andrade, F. C. Meinzer, N. M. Holbrook, J. Cavelier, P. Jackson and A. Celis, 1998. Stem water storage and diurnal patterns of water use in tropical forest canopy trees. *Plant, Cell & Environment* 21(4): 397-406.
- Granier, A., 1987. Evaluation of transpiration in a Douglas-fir stand by means of sap flow measurements. *Tree Physiology*, 3, 309-320. doi: 10.1093/treephys/3.4.309
- Granier, A., Biron, P., & Lemoine, D., 2000. Water balance, transpiration and canopy conductance in two beech stands. *Agricultural and Forest Meteorology*, 100(4), 291-308.

- Granier, A., Biron, P., Bréda, N., Pontailier, J. Y., & Saugier, B., 1996. Transpiration of trees and forest stands: short and long-term monitoring using sapflow methods. *Global Change Biology*, 2(3), 265-274.
- Granier, A., Loustau, D. and Bréda, N., 2000. A generic model of forest canopy conductance dependent on climate, soil water availability and leaf area index. *Annals of Forest Science*, 57(8), pp.755-765.
- Granier, A., Reichstein, M., Bréda, N., Janssens, I. A., Falge, E., Ciais, P., Grünwald, T., Aubinet, M., Berbigier, P., Bernhofer, C., Buchmann, N., Facini, O., Grassi, G., Heinesch, B., Ilvesniemi, H., Keronen, P., Knohl, A., Köstner, B., Lagergren, F., Lindroth, A., Longdoz, B., Loustau, D., Mateus, J., Montagnani, L., Nys, C., Moors, E., Papale, D., Peiffer, M., Pilegaard, K., Pita, G., Pumpanen, J., Rambal, S., Rebmann, C., Rodrigues, A., Seufert, G., Tenhunen, J., Vesala, T., Wang, Q., 2007. Evidence for soil water control on carbon and water dynamics in European forests during the extremely dry year: 2003. *Agricultural and Forest Meteorology*, 143(1-2), 123-145. doi:<http://dx.doi.org/10.1016/j.agrformet.2006.12.004>
- Grelle, A., Lundberg, A., Lindroth, A., Morén, A.S. and Cienciala, E., 1997. Evaporation components of a boreal forest: variations during the growing season. *Journal of Hydrology*, 197(1-4), pp.70-87.
- Grippa, M., Kergoat, L., Frappart, F., Araud, Q., Boone, A., De Rosnay, P., Lemoine, J.M., Gascoin, S., Balsamo, G., Otle, C. and Decharme, B., 2011. Land water storage variability over West Africa estimated by Gravity Recovery and Climate Experiment (GRACE) and land surface models. *Water Resources Research*, 47 (5).
- Gupta, H.V., Kling, H., Yilmaz, K.K. and Martinez, G.F., 2009. Decomposition of the mean squared error and NSE performance criteria: Implications for improving hydrological modelling. *Journal of hydrology*, 377 (1-2), 80-91.
- Hejazi, A. and Woodbury, A.D., 2011. Evaluation of land surface scheme SABAE-HW in simulating snow depth, soil temperature and soil moisture within the BOREAS site, Saskatchewan. *Atmosphere-Ocean*, 49 (4), 408-420.
- Hogg, E. H., & Hurdle, P. A., 1997. Sap flow in trembling aspen: implications for stomatal responses to vapor pressure deficit. *Tree Physiology*, 17(8-9), 501-509. doi: 10.1093/treephys/17.8-9.501
- Hogg, E.H. and Lieffers, V.J., 1991. The impact of *Calamagrostis canadensis* on soil thermal regimes after logging in northern Alberta. *Canadian Journal of Forest Research*, 21 (3), 387-394.
- Hogg, E.H., Black, T.A., den Hartog, G., Neumann, H.H., Zimmermann, R., Hurdle, P.A., Blanken, P.D., Nesic, Z., Yang, P.C., Staebler, R.M. and McDonald, K.C.,

1997. A comparison of sap flow and eddy fluxes of water vapor from a boreal deciduous forest. *Journal of Geophysical Research: Atmospheres*, 102(D24), pp.28929-28937.
- Houle, D. and J.-D. Moore, 2008. Soil solution, foliar concentrations and tree growth response to 3-year of ammonium-nitrate addition in two boreal forests of Québec, Canada. *Forest Ecology and Management* 255(7): 2049-2060.
- Houle, D., Lajoie, G., & Duchesne, L., 2016. Major losses of nutrients following a severe drought in a boreal forest. *Nature Plants*, 2, 16187. doi: 10.1038/nplants.2016.187.  
<http://www.nature.com/articles/nplants2016187#supplementary-information>
- Huang, J.G., Ma, Q., Rossi, S., Biondi, F., Deslauriers, A., Fonti, P., Liang, E., Mäkinen, H., Oberhuber, W., Rathgeber, C.B., Tognetti, R., Treml, V., Yang, B., Zhang, J.L., Antonucci, S., Bergeron, Y., Camarero, J.J., Campelo, F., Čufar, K., Cuny, H.E., De Luis, M., Giovannelli, A., Gričar, J., Gruber, A., Gryc, V., Güney, A., Guo, X., Huang, W., Jyske, T., Kašpar, J., King, G., Krause, C., Lemay, A., Liu, F., Lombardi, F., Martinez del Castillo, E., Morin, H., Nabais, C., Nöjd, P., Peters, R.L., Prislán, P., Saracino, A., Swidrak, I., Vavrčík, H., Vieira, J., Yu, B., Zhang, S., Zeng, Q., Zhang, Y., Ziaco, E., 2020. Photoperiod and temperature as dominant environmental drivers triggering secondary growth resumption in Northern Hemisphere conifers. *Proceedings of the National Academy of Sciences*, 117(34), pp.20645-20652.
- Huang, S., Arain, M.A., Arora, V.K., Yuan, F., Brodeur, J. and Peichl, M., 2011. Analysis of nitrogen controls on carbon and water exchanges in a conifer forest using the CLASS-CTEMN+ model. *Ecological modelling*, 222 (20-22), 3743-3760.
- Iijima, Y., Fedorov, A.N., Park, H., Suzuki, K., Yabuki, H., Maximov, T.C. and Ohata, T., 2010. Abrupt increases in soil temperatures following increased precipitation in a permafrost region, central Lena River basin, Russia. *Permafrost and Periglacial Processes*, 21 (1), 30-41.
- Isabelle, P.-E., Nadeau, D.F., Asselin, M.-H., Harvey, R., Musselman, K.N., Rousseau, A.N. and Anctil, F., 2018. Solar radiation transmittance of a boreal balsam fir canopy: Spatiotemporal variability and impacts on growing season hydrology. *Agricultural and forest meteorology*, 263, 1-14.
- Itter, M. S., D'Orangeville, L., Dawson, A., Kneeshaw, D., Duchesne, L., & Finley, A. O., 2019. Boreal tree growth exhibits decadal-scale ecological memory to drought and insect defoliation, but no negative response to their interaction. *Journal of Ecology*, 107(3), 1288-1301.

- Jackson, R., Reginato, R., Kimball, B. and Nakayama, F., 1974. Diurnal Soil-Water Evaporation: Comparison of Measured and Calculated Soil-Water Fluxes 1. *Soil Science Society of America Journal*, 38 (6), 861-866.
- Jaksa, W.T. and Sridhar, V., 2015. Effect of irrigation in simulating long-term evapotranspiration climatology in a human-dominated river basin system. *Agricultural and Forest Meteorology*, 200, 109-118.
- Jarvis, P.G., 1976. The interpretation of the variations in leaf water potential and stomatal conductance found in canopies in the field. *Philosophical Transactions of the Royal Society of London. B, Biological Sciences*, 273(927), pp.593-610.
- Jassal, R.S., Novak, M.D. and Black, T.A., 2003. Effect of surface layer thickness on simultaneous transport of heat and water in a bare soil and its implications for land surface schemes. *Atmosphere-Ocean*, 41 (4), 259-272.
- Johnsson, H. and Lundin, L.C., 1991. Surface runoff and soil water percolation as affected by snow and soil frost. *Journal of Hydrology*, 122 (1-4), 141-159.
- Johnston, M., 2009. *Vulnerability of Canada's tree species to climate change and management options for adaptation: An overview for policy makers and practitioners*. Canadian Council of Forest Ministers.
- Jonard, F., André, F., Ponette, Q., Vincke, C., & Jonard, M., 2011. Sap flux density and stomatal conductance of European beech and common oak trees in pure and mixed stands during the summer drought of 2003. *Journal of Hydrology*, 409(1-2), 371-381.
- Juice, S. M., Templer, P. H., Phillips, N. G., Ellison, A. M., & Pelini, S. L., 2016. Ecosystem warming increases sap flow rates of northern red oak trees. *Ecosphere*, 7(3), e01221-n/a. doi: 10.1002/ecs2.1221
- Jung, E.Y., Otieno, D., Lee, B., Lim, J.H., Kang, S.K., Schmidt, M.W.T., Tenhunen, J., 2011. Up-scaling to stand transpiration of an Asian temperate mixed-deciduous forest from single tree sapflow measurements. *Plant Ecol.* 212 (3), 383–395. <https://doi.org/10.1007/s11258-010-9829-3>.
- Jungqvist, G., Oni, S.K., Teutschbein, C. and Futter, M.N., 2014. Effect of climate change on soil temperature in Swedish boreal forests. *PLoS One*, 9(4), p.e93957.
- Jyske, T., & Hölttä, T., 2015. Comparison of phloem and xylem hydraulic architecture in *Picea abies* stems. *New phytologist*, 205(1), 102-115.
- Kavanagh, K. L., R. Pangle and A. D. Schotzko, 2007. Nocturnal transpiration causing disequilibrium between soil and stem predawn water potential in mixed conifer forests of Idaho. *Tree Physiol* 27(4): 621-629.

- Klein, T., 2014. The variability of stomatal sensitivity to leaf water potential across tree species indicates a continuum between isohydric and anisohydric behaviours. *Functional ecology*, 28(6), pp.1313-1320.
- Konarska, J., J. Uddling, B. Holmer, M. Lutz, F. Lindberg, H. Pleijel and S. Thorsson, 2016. Transpiration of urban trees and its cooling effect in a high latitude city. *Int J Biometeorol* 60(1): 159-172.
- Köstner, B., Falge, E., M., Alsheimer, M., Geyer, R., & Tenhunen, J., D., 1998. Estimating tree canopy water use via xylem sapflow in an old Norway spruce forest and a comparison with simulation-based canopy transpiration estimates. *Ann. For. Sci.*, 55(1-2), 125-139.
- Köstner, B., Granier, A. and Cermák, J., 1998. Sapflow measurements in forest stands: methods and uncertainties. In *Annales des sciences forestières* (Vol. 55, No. 1-2, pp. 13-27). EDP Sciences.
- Kowalczyk, E.A., Wang, Y.P., Law, R.M., Davies, H.L., McGregor, J.L. and Abramowitz, G., 2006. The CSIRO Atmosphere Biosphere Land Exchange (CABLE) model for use in climate models and as an offline model. *CSIRO Marine and Atmospheric Research Paper*, 13, p.42.
- Kramer, P. J., 1983. *Water Relations of Plants*. Academic Press, Inc. Orlando, FL.
- Lagergren, F. and A. Lindroth, 2002. Transpiration response to soil moisture in pine and spruce trees in Sweden. *Agricultural and Forest Meteorology* 112(2): 67-85.
- Laprise, R., 2008. Regional climate modelling. *J. Comput. Phys.* 227(7): 3641-3666.
- Laprise, R., Hernández-Díaz, L., Tete, K., Sushama, L., Šeparović, L., Martynov, A., Winger, K. and Valin, M., 2013. Climate projections over CORDEX Africa domain using the fifth-generation Canadian Regional Climate Model (CRCM5). *Climate Dynamics*, 41(11), pp.3219-3246.
- Lawrence, D.M. and Slater, A.G., 2008. Incorporating organic soil into a global climate model. *Climate Dynamics*, 30 (2-3), 145-160.
- Lei, H., Yang, D., Shen, Y., Liu, Y. and Zhang, Y., 2011. Simulation of evapotranspiration and carbon dioxide flux in the wheat-maize rotation croplands of the North China Plain using the Simple Biosphere Model. *Hydrological Processes*, 25 (20), 3107-3120.
- Lenton, T. M., Held, H., Kriegler, E., Hall, J. W., Lucht, W., Rahmstorf, S., & Schellnhuber, H. J., 2008. Tipping elements in the Earth's climate system. *Proceedings of the National Academy of Sciences*, 105(6), 1786-1793. doi: 10.1073/pnas.0705414105

- Letts, M.G., Roulet, N.T., Comer, N.T., Skarupa, M.R. and Versegny, D.L., 2000. Parametrization of peatland hydraulic properties for the Canadian land surface scheme. *Atmosphere-Ocean*, 38 (1), 141-160.
- Li, L., Van der Tol, C., Chen, X., Jing, C., Su, B., Luo, G. and Tian, X., 2013. Representing the root water uptake process in the Common Land Model for better simulating the energy and water vapour fluxes in a Central Asian desert ecosystem. *Journal of hydrology*, 502, 145-155.
- Liu, X., Li, Y., Chen, X., Zhou, G., Cheng, J., Zhang, D., Meng, Z., Zhang, Q., 2014. Partitioning evapotranspiration in an intact forested watershed in southern China. *Ecohydrology*, 8(6), 1037-1047.
- Lu, P., Biron, P., Breda, N., & Granier, A., 1995. Water relations of adult Norway spruce (*Picea abies* (L) Karst) under soil drought in the Vosges mountains: water potential, stomatal conductance and transpiration. Paper presented at the Annales des Sciences Forestieres.
- Luo, L., Robock, A., Vinnikov, K.Y., Schlosser, C.A., Slater, A.G., Boone, A., Etchevers, P., Habets, F., Noilhan, J., Braden, H. and Cox, P., 2003. Effects of frozen soil on soil temperature, spring infiltration, and runoff: Results from the PILPS 2 (d) experiment at Valdai, Russia. *Journal of Hydrometeorology*, 4 (2), 334-351.
- Lupi, C., Morin, H., Deslauriers, A., & Rossi, S., 2012. Xylogenesis in black spruce: Does soil temperature matter? *Tree Physiology*, 32(1), 74-82. doi: 10.1093/treephys/tpr132
- Ma, N., Niu, G.Y., Xia, Y., Cai, X., Zhang, Y., Ma, Y., and Fang, Y., 2017 A systematic evaluation of Noah-MP in simulating land-atmosphere energy, water, and carbon exchanges over the continental United States. *Journal of Geophysical Research: Atmospheres*, 122 (22), 12,245-212,268.
- MacDonald, M.K., Davison, B.J., Mekonnen, M.A. and Pietroniro, A., 2016. Comparison of land surface scheme simulations with field observations versus atmospheric model output as forcing. *Hydrological Sciences Journal*, 61 (16), 2860-2871.
- Macfarlane, C., Bond, C., White, D. A., Grigg, A. H., Ogden, G. N., & Silberstein, R., 2010. Transpiration and hydraulic traits of old and regrowth eucalypt forest in southwestern Australia. *Forest Ecology and Management*, 260(1), 96-105.
- MacKinney, A.L., 1929. Effects of Forest Litter on Soil Temperature and Soil Freezing in Autumn and Winter. *Ecology*, 10 (3), 312-321.

- Mäkinen, H., P. Nöjd and P. Saranpää, 2003. "Seasonal changes in stem radius and production of new tracheids in Norway spruce." *Tree Physiology* 23(14): 959-968.
- Malhi, S.S. and O'Sullivan, P.A., 1990. Soil temperature, moisture and penetrometer resistance under zero and conventional tillage in central Alberta. *Soil and Tillage Research*, 17 (1), 167-172.
- Malik, M.J., van der Velde, R., Vekerdy, Z. and Su, Z., 2014. Improving modeled snow albedo estimates during the spring melt season. *Journal of geophysical research: Atmospheres*, 119 (12), 7311-7331.
- Manabe S. 1969. Climate and the ocean circulation: 1, the atmospheric circulation and the hydrology of the Earth's surface. *Monthly Weather Review* 97: 739–805.
- Marchand, N., Royer, A., Krinner, G., Roy, A., Langlois, A. and Vargel, C., 2018. Snow-Covered Soil Temperature Retrieval in Canadian Arctic Permafrost Areas, Using a Land Surface Scheme Informed with Satellite Remote Sensing Data. *Remote Sensing*, 10 (11), 1703.
- Matthes, H., Rinke, A., Miller, P.A., Kuhry, P., Dethloff, K. and Wolf, A., 2012. Sensitivity of high-resolution Arctic regional climate model projections to different implementations of land surface processes. *Climatic Change*, 111(2), pp.197-214.
- McDowell, N., Pockman, W.T., Allen, C.D., Breshears, D.D., Cobb, N., Kolb, T., Plaut, J., Sperry, J., West, A., Williams, D.G. and Yezzer, E.A., 2008. Mechanisms of plant survival and mortality during drought: why do some plants survive while others succumb to drought?. *New phytologist*, 178(4), pp.719-739.
- Meinzer, F., Hinckley, T., & Ceulemans, R., 1997. Apparent responses of stomata to transpiration and humidity in a hybrid poplar canopy. *Plant, Cell & Environment*, 20(10), 1301-1308.
- Michaelian, M., Hogg, E.H., Hall, R.J. and Arsenault, E., 2011. Massive mortality of aspen following severe drought along the southern edge of the Canadian boreal forest. *Global Change Biology*, 17(6), pp.2084-2094.
- Milbau, A., Graae, B.J., Shevtsova, A. and Nijs, I., 2009. Effects of a warmer climate on seed germination in the subarctic. *Annals of Botany*, 104(2), pp.287-296.
- Mitchell, P. J., Benyon, R. G., & Lane, P. N. J., 2012. Responses of evapotranspiration at different topographic positions and catchment water balance following a pronounced drought in a mixed species eucalypt forest, Australia. *Journal of Hydrology*, 440–441, 62-74. doi: <https://doi.org/10.1016/j.jhydrol.2012.03.026>

- Munro, D.S., Bellisario, L.M. and Verseghy, D.L., 2000. Measuring and modelling the seasonal climatic regime of a temperate wooded wetland. *Atmosphere-Ocean*, 38 (1), 227-249.
- Murray, F.W., 1967. On the Computation of Saturation Vapor Pressure. *Journal of Applied Meteorology*, 6, 203-204.
- Napoly, A., Boone, A., Samuelsson, P., Gollvik, S., Martin, E., Seferian, R., Carrer, D., Decharme, B. and Jarlan, L., 2017. The interactions between soil–biosphere–atmosphere (ISBA) land surface model multi-energy balance (MEB) option in SURFEXv8 – Part 2: Introduction of a litter formulation and model evaluation for local-scale forest sites. *Geosci. Model Dev.*, 10 (4), 1621-1644.
- O'Brien, J. J., Oberbauer, S. F., & Clark, D. B., 2004. Whole tree xylem sap flow responses to multiple environmental variables in a wet tropical forest. *Plant, Cell & Environment*, 27(5), 551-567.
- O'Grady, A., Eamus, D., & Hutley, L., 1999. Transpiration increases during the dry season: patterns of tree water use in eucalypt open-forests of northern Australia. *Tree Physiology*, 19(9), 591-597.
- Oleson, K.W., Lawrence, D.M., Bonan, G.B., Drewniak, B., Huang, M., Koven, C.D., Levis, S., Li, F., Riley, W.J., Subin, Z.M. and Swenson, S.C., 2013. Technical description of version 4.5 of the Community Land Model (CLM), NCAR Technical Note: NCAR/TN-503+ STR. *National Center for Atmospheric Research (NCAR), Boulder, CO, USA*, <https://doi.org/10.5065/D6RR1W7M>.
- Oogathoo, S., Houle, D., Duchesne, L. and Kneeshaw, D., 2020. Vapour pressure deficit and solar radiation are the major drivers of transpiration of balsam fir and black spruce tree species in humid boreal regions, even during a short-term drought. *Agricultural and Forest Meteorology*, 291, p.108063.
- Ouimet, R. and Duchesne, L., 2005. Base cation mineral weathering and total release rates from soils in three calibrated forest watersheds on the Canadian Boreal Shield. *Canadian Journal of Soil Science*, 85 (2), 245-260.
- Pappas, C., Matheny, A. M., Baltzer, J. L., Barr, A. G., Black, T. A., Bohrer, G., Detto, M., Maillet, J., Roy, A., Sonnentag, O., 2018. Boreal tree hydrodynamics: asynchronous, diverging, yet complementary. *Tree Physiology*, 38(7), 953-964.
- Paquin, J.P. and Sushama, L., 2015. On the Arctic near-surface permafrost and climate sensitivities to soil and snow model formulations in climate models. *Climate Dynamics*, 44 (1), 203-228.
- Pataki, D. E., & Oren, R., 2003. Species differences in stomatal control of water loss at the canopy scale in a mature bottomland deciduous forest. *Advances in Water*

Resources, 26(12), 1267-1278.

doi:<https://doi.org/10.1016/j.advwatres.2003.08.001>

- Patankar, R., Quinton, W. L., Hayashi, M., & Baltzer, J. L., 2015. Sap flow responses to seasonal thaw and permafrost degradation in a subarctic boreal peatland. *Trees*, 29(1), 129-142.
- Peters, R.L., Fonti, P., Frank, D.C., Poyatos, R., Pappas, C., Kahmen, A., Carraro, V., Prendin, A.L., Schneider, L., Baltzer, J.L. and Baron-Gafford, G.A., 2018. Quantification of uncertainties in conifer sap flow measured with the thermal dissipation method. *New Phytologist*, 219(4), pp.1283-1299.
- Philip, J.R., 1957. Evaporation, and moisture and heat fields in the soil. *Journal of meteorology*, 14 (4), 354-366.
- Phillips, N. G., M. G. Ryan, B. J. Bond, N. G. McDowell, T. M. Hinckley and J. Čermák, 2003. Reliance on stored water increases with tree size in three species in the Pacific Northwest. *Tree Physiology* 23(4): 237-245.
- Pitman, A. J., 2003. The evolution of, and revolution in, land surface schemes designed for climate models. *International Journal of Climatology*, 23(5), 479-510. doi: 10.1002/joc.893
- Qian, B., Gregorich, E.G., Gameda, S., Hopkins, D.W. and Wang, X.L., 2011. Observed soil temperature trends associated with climate change in Canada. *Journal of Geophysical Research: Atmospheres*, 116(D2).
- Rennenberg, H., Loreto, F., Polle, A., Brilli, F., Fares, S., Beniwal, R.S. and Gessler, A.J.P.B., 2006. Physiological responses of forest trees to heat and drought. *Plant Biology*, 8(5), pp.556-571.
- Rinke, A., Kuhry, P. and Dethloff, K., 2008. Importance of a soil organic layer for Arctic climate: A sensitivity study with an Arctic RCM. *Geophysical Research Letters*, 35 (13).
- Rossi, S., A. Deslauriers, J. Gričar, J.-W. Seo, C. B. K. Rathgeber, T. Anfodillo, H. Morin, T. Levanic, P. Oven and R. Jalkanen, 2008. Critical temperatures for xylogenesis in conifers of cold climates. *Global Ecology and Biogeography* 17(6): 696-707.
- Roy, P., Gachon, P. and Laprise, R., 2012. Assessment of summer extremes and climate variability over the north-east of North America as simulated by the Canadian Regional Climate Model. *International journal of climatology*, 32(11), pp.1615-1627.
- Sakoe, H. and Chiba, S., 1978. Dynamic programming algorithm optimization for spoken word recognition. *IEEE transactions on acoustics, speech, and signal processing*, 26(1), pp.43-49.

- Sánchez-Costa, E., R. Poyatos and S. Sabaté, 2015. Contrasting growth and water use strategies in four co-occurring Mediterranean tree species revealed by concurrent measurements of sap flow and stem diameter variations. *Agricultural and Forest Meteorology* 207: 24-37.
- Saugier, B., Granier, A., Pontailler, J. Y., Dufrene, E., & Baldocchi, D. D., 1997. Transpiration of a boreal pine forest measured by branch bag, sap flow and micrometeorological methods. *Tree Physiol*, 17(8\_9), 511-519.
- Saunders, I., Bowers, J., Huo, Z., Bailey, W. and Verseghy, D., 1999. Simulation of alpine tundra surface microclimates using the Canadian Land Surface Scheme: II. Energy balance and surface microclimatology. *International Journal of Climatology: A Journal of the Royal Meteorological Society*, 19 (10), 1131-1143.
- Schär, C., Lüthi, D., Beyerle, U. and Heise, E., 1999. The soil–precipitation feedback: A process study with a regional climate model. *Journal of Climate*, 12(3), pp.722-741.
- Schwartz, R.C., Baumhardt, R.L. and Evett, S.R., 2010. Tillage effects on soil water redistribution and bare soil evaporation throughout a season. *Soil and Tillage Research*, 110 (2), 221-229.
- Sellers PJ, Mintz Y, Sud YC, Dalcher A. 1986. A Simple Biosphere model (SiB) for use within general circulation models. *Journal of the Atmospheric Sciences* 43: 505–531.
- Sellers W.D., 1965. *Physical Climatology*. The University of Chicago Press, 272 pp.
- Seneviratne, S. I., Corti, T., Davin, E. L., Hirschi, M., Jaeger, E. B., Lehner, I., Orlowsky, B., Teuling, A. J., 2010. Investigating soil moisture–climate interactions in a changing climate: A review. *Earth-Science Reviews*, 99(3–4), 125-161. doi:<http://dx.doi.org/10.1016/j.earscirev.2010.02.004>
- Seneviratne, S. I., Luthi, D., Litschi, M., & Schar, C., 2006. Land-atmosphere coupling and climate change in Europe. *Nature*, 443(7108), 205-209. doi:[http://www.nature.com/nature/journal/v443/n7108/supinfo/nature05095\\_S1.html](http://www.nature.com/nature/journal/v443/n7108/supinfo/nature05095_S1.html)
- Seneviratne, S.I., Lehner, I., Gurtz, J., Teuling, A.J., Lang, H., Moser, U., Grebner, D., Menzel, L., Schroff, K., Vitvar, T. and Zappa, M., 2012. Swiss prealpine Rietholzbach research catchment and lysimeter: 32 year time series and 2003 drought event. *Water Resources Research*, 48 (6).
- Steppe, K., De Pauw, D.J., Doody, T.M. and Teskey, R.O., 2010. A comparison of sap flux density using thermal dissipation, heat pulse velocity and heat field

- deformation methods. *Agricultural and Forest Meteorology*, 150(7-8), pp.1046-1056.
- Subin, Z.M., Koven, C.D., Riley, W.J., Torn, M.S., Lawrence, D.M. and Swenson, S.C., 2013. Effects of Soil Moisture on the Responses of Soil Temperatures to Climate Change in Cold Regions. *Journal of Climate*, 26 (10), 3139-3158.
- Sugita, M. and Brutsaert, W., 1993. Cloud effect in the estimation of instantaneous downward longwave radiation. *Water Resources Research*, 29 (3), 599-605.
- Sun, S. and Verseghy, D., 2019. Introducing water-stressed shrubland into the Canadian Land Surface Scheme. *Journal of Hydrology*, 579, p.124157.
- Swann, A.L., Fung, I.Y., Levis, S., Bonan, G.B. and Doney, S.C., 2010. Changes in Arctic vegetation amplify high-latitude warming through the greenhouse effect. *Proceedings of the National Academy of Sciences*, 107(4), pp.1295-1300.
- Tardieu, F., & Simonneau, T. (1998). Variability among species of stomatal control under fluctuating soil water status and evaporative demand: modelling isohydric and anisohydric behaviours. *Journal of Experimental Botany*, 419-432.
- Tilley, J.S., Chapman, W.L. and Wu, W., 1997. Sensitivity tests of the Canadian land surface scheme (CLASS) for arctic tundra. *Annals of Glaciology*, 25, 46-50.
- Tsuruta, K., Kosugi, Y., Takanashi, S., & Tani, M., 2016. Inter-annual variations and factors controlling evapotranspiration in a temperate Japanese cypress forest. *Hydrological Processes*, 30(26), 5012-5026. doi: 10.1002/hyp.10977
- Turcotte, A., H. Morin, C. Krause, A. Deslauriers and M. Thibeault-Martel, 2009. The timing of spring rehydration and its relation with the onset of wood formation in black spruce. *Agricultural and Forest Meteorology* 149(9): 1403-1409.
- Tyrrell, M., 2020. *Boreal Forest Ecology | Global Forest Atlas*. [online] Globalforestatlas.yale.edu. Available at: <<https://globalforestatlas.yale.edu/boreal-forest/boreal-ecoregions-ecology/boreal-forest-ecology>> [Accessed 28 March 2020].
- Ukkola, A.M., Kauwe, M.G.D., Pitman, A.J., Best, M.J., Abramowitz, G., Haverd, V., Decker, M. and Haughton, N., 2016b. Land surface models systematically overestimate the intensity, duration and magnitude of seasonal-scale evaporative droughts. *Environmental Research Letters*, 11 (10), 104012.
- Ukkola, A.M., Pitman, A.J., Decker, M., De Kauwe, M.G., Abramowitz, G., Kala, J. and Wang, Y.P., 2016a. Modelling evapotranspiration during precipitation deficits: identifying critical processes in a land surface model. *Hydrology and Earth System Sciences*, 20(6), pp.2403-2419.

- Vaganov, E. A., M. K. Hughes, A. V. Kirilyanov, F. H. Schweingruber and P. P. Silkin, 1999. Influence of snowfall and melt timing on tree growth in subarctic Eurasia. *Nature* 400(6740): 149-151.
- Van Herk, I. G., Gower, S. T., Bronson, D. R., & Tanner, M. S., 2011. Effects of climate warming on canopy water dynamics of a boreal black spruce plantation. *Canadian Journal of Forest Research*, 41(2), 217-227.
- Vandegehuchte, M.W. and Steppe, K., 2013. Corrigendum to: Sap-flux density measurement methods: working principles and applicability. *Functional Plant Biology*, 40(10), pp.1088-1088.
- Verhoef, A., & Egea, G., 2014. Modeling plant transpiration under limited soil water: Comparison of different plant and soil hydraulic parameterizations and preliminary implications for their use in land surface models. *Agricultural and Forest Meteorology*, 191, 22-32.  
doi:<https://doi.org/10.1016/j.agrformet.2014.02.009>
- Verseghy, D. L., 1991. Class—A Canadian land surface scheme for GCMS. I. Soil model. *International Journal of Climatology* 11(2): 111-133.
- Verseghy, D. L., N. A. McFarlane and M. Lazare, 1993. Class—A Canadian land surface scheme for GCMS, II. Vegetation model and coupled runs. *International Journal of Climatology* 13(4): 347-370.
- Verseghy, D., 2012. CLASS – THE CANADIAN LAND SURFACE SCHEME (VERSION 3.6) Technical Documentation. E. CANADA and S.A.T.B. CLIMATE RESEARCH DIVISION (eds.).
- Verstraete, M. M., & Dickinson, R. E., 1986. Modeling surface processes in atmospheric general circulation models. *Annales Geophysicae, Series B*, 4 B(4), 357-364.
- Wang, H., Guan, H., Deng, Z., & Simmons, C. T., 2014. Optimization of canopy conductance models from concurrent measurements of sap flow and stem water potential on Drooping Sheoak in South Australia. *WATER RESOURCES RESEARCH*, 50(7), 6154-6167. doi:10.1002/2013WR014818
- Wang, H., Tetzlaff, D., Dick, J. J., & Soulsby, C., 2017. Assessing the environmental controls on Scots pine transpiration and the implications for water partitioning in a boreal headwater catchment. *Agricultural and Forest Meteorology*, 240-241, 58-66. doi: 10.1016/j.agrformet.2017.04.002
- Wang, K.-Y., Kellomäki, S., Zha, T., Peltola, H., 2005. Annual and seasonal variation of sap flow and conductance of pine trees grown in elevated carbon dioxide and temperature. *J. Exp. Bot.* 56 (409), 155–165.

- Wang, L., Caylor, K.K., Villegas, J.C., Barron-Gafford, G.A., Breshears, D.D. and Huxman, T.E., 2010. Partitioning evapotranspiration across gradients of woody plant cover: Assessment of a stable isotope technique. *Geophysical Research Letters*, 37 (9).
- Wang, L., Cole, J. N., Bartlett, P., Verseghy, D., Derksen, C., Brown, R., & von Salzen, K., 2016. Investigating the spread in surface albedo for snow-covered forests in CMIP5 models. *Journal of Geophysical Research: Atmospheres*, 121(3), 1104-1119.
- Wang, P., Niu, G.Y., Fang, Y.H., Wu, R.J., Yu, J.J., Yuan, G.F., Pozdniakov, S.P. and Scott, R.L., 2018. Implementing dynamic root optimization in Noah-MP for simulating phreatophytic root water uptake. *Water Resources Research*, 54 (3), 1560-1575.
- Wang, S., Grant, R.F., Verseghy, D.L. and Andrew Black, T., 2002. Modelling carbon-coupled energy and water dynamics of a boreal aspen forest in a general circulation model land surface scheme. *International Journal of Climatology: A Journal of the Royal Meteorological Society*, 22 (10), 1249-1265.
- Wang, S., Grant, R.F., Verseghy, D.L. and Black, T.A., 2001. Modelling plant carbon and nitrogen dynamics of a boreal aspen forest in CLASS—the Canadian Land Surface Scheme. *Ecological Modelling*, 142(1-2), pp.135-154.
- Ward, A.D. and Trimble, S.W., 2004. *Environmental Hydrology*. second edn. Lewis publishers.
- Waring, R. H., D. Whitehead and P. G. Jarvis, 1979. "The contribution of stored water to transpiration in Scots pine." *Plant, Cell & Environment* 2(4): 309-317.
- Wen, L., Gallichand, J., Viau, A., Delage, Y. and Benoit, R., 1998. Calibration of the CLASS model and its improvement under agricultural conditions. *Transactions of the ASAE*, 41 (5), 1345.
- Wen, L., Wu, Z., Lu, G., Lin, C.A., Zhang, J. and Yang, Y., 2007. Analysis and improvement of runoff generation in the land surface scheme CLASS and comparison with field measurements from China. *Journal of hydrology*, 345 (1-2), 1-15.
- Williams, P.J. and Smith, M.W., 1989. *The frozen earth: fundamentals of geocryology*. Cambridge University Press: Cambridge; New York.
- Wilson, K.B., Hanson, P.J., Mulholland, P.J., Baldocchi, D.D. and Wullschleger, S.D., 2001. A comparison of methods for determining forest evapotranspiration and its components: sap-flow, soil water budget, eddy covariance and catchment water balance. *Agricultural and forest Meteorology*, 106(2), pp.153-168.

- Wuddivira, M.N., Robinson, D.A., Lebron, I., Bréchet, L., Atwell, M., De Caires, S., Oatham, M., Jones, S.B., Abdu, H., Verma, A.K. and Tuller, M., 2012. Estimation of soil clay content from hygroscopic water content measurements. *Soil Science Society of America Journal*, 76(5), pp.1529-1535.
- Wullschleger, S. D., Wilson, K. B., & Hanson, P. J., 2000. Environmental control of whole-plant transpiration, canopy conductance and estimates of the decoupling coefficient for large red maple trees. *Agricultural and Forest Meteorology*, 104(2), 157-168. doi: [http://dx.doi.org/10.1016/S0168-1923\(00\)00152-0](http://dx.doi.org/10.1016/S0168-1923(00)00152-0)
- Yang, Z. L., Dickinson, R. E., Henderson-Sellers, A., & Pitman, A. J., 1995. Preliminary study of spin-up processes in land surface models with the first stage data of Project for Intercomparison of Land Surface Parameterization Schemes Phase 1 (a). *Journal of Geophysical Research: Atmospheres*, 100(D8), 16553-16578.
- Yoshikawa, K., Bolton, W.R., Romanovsky, V.E., Fukuda, M. and Hinzman, L.D., 2002. Impacts of wildfire on the permafrost in the boreal forests of Interior Alaska. *Journal of Geophysical Research: Atmospheres*, 107 (D1), FFR 4-1-FFR 4-14.
- Yuan, F., Arain, M.A., Black, T.A. and Morgenstern, K., 2007. Energy and water exchanges modulated by soil–plant nitrogen cycling in a temperate Pacific Northwest conifer forest. *ecological modelling*, 201 (3-4), 331-347.
- Zadra, A., Caya, D., Côté, J., Dugas, B., Jones, C., Laprise, R., Winger, K. and Caron, L.P., 2008. The next Canadian regional climate model. *Phys Can*, 64(2), pp.75-83.
- Zeppel, M. J., Murray, B. R., Barton, C., & Eamus, D., 2004. Seasonal responses of xylem sap velocity to VPD and solar radiation during drought in a stand of native trees in temperate Australia. *Functional Plant Biology*, 31(5), 461-470.
- Zhang, Q., Manzoni, S., Katul, G., Porporato, A., & Yang, D., 2014. The hysteretic evapotranspiration—Vapor pressure deficit relation. *Journal of Geophysical Research: Biogeosciences*, 119(2), 125-140.
- Zhang, T., Barry, R.G., Knowles, K., Ling, F. and Armstrong, R.L., 2003, July. Distribution of seasonally and perennially frozen ground in the Northern Hemisphere. In *Proceedings of the 8th International Conference on Permafrost* (Vol. 2, pp. 1289-1294). Zürich, Switzerland: AA Balkema Publishers.
- Zhang, Y., Zheng, H., Chiew, F.H., Arancibia, J.P. and Zhou, X., 2016. Evaluating regional and global hydrological models against streamflow and evapotranspiration measurements. *Journal of Hydrometeorology*, 17 (3), 995-1010.

- Zheng, H., Wang, Q., Zhu, X., Li, Y., & Yu, G., 2014. Hysteresis responses of evapotranspiration to meteorological factors at a diel timescale: patterns and causes. *PLOS ONE*, 9(6), e98857.
- Ziaco, E., Biondi, F., Rossi, S. and Deslauriers, A., 2016. Environmental drivers of cambial phenology in Great Basin bristlecone pine. *Tree Physiology*, 36 (7), 818-831.
- Zittis, G., Hadjinicolaou, P. and Lelieveld, J., 2014. Role of soil moisture in the amplification of climate warming in the Eastern Mediterranean and the Middle East. *Climate Research*, 59 (1), 27-37.
- Zweifel, R. and Häsler, R., 2000. Frost-induced reversible shrinkage of bark of mature subalpine conifers. *Agricultural and Forest Meteorology*, 102(4), pp.213-222.